THE DEVELOPMENT OF HIGH-THROUGHPUT MASS SPECTROMETRIC METHODS FOR THE QUALITATIVE AND QUANTITATIVE ANALYSIS OF DIQUATERNARY AMMONIUM GEMINI SURFACTANTS

A Thesis Submitted to the College of

Graduate Studies and Research

In Partial Fulfillment of the Requirements

For the Degree of Doctor of Philosophy

In the College of Pharmacy and Nutrition

University of Saskatchewan

Saskatoon, SK, Canada

By

JOSHUA DAVID BUSE

PERMISSION TO USE

In presenting this dissertation in partial fulfilment of the requirements for a Postgraduate degree from the University of Saskatchewan, I agree that the Libraries of this University may make it freely available for inspection. I further agree that permission for copying of this thesis in any manner, in whole or in part, for scholarly purposes may be granted by the professor or professors who supervised my thesis work or, in their absence, by the Head of the Department or the Dean of the College in which my thesis work was done. It is understood that any copying or publication or use of this thesis or parts thereof for financial gain shall not be allowed without my written permission. It is also understood that due recognition shall be given to me and to the University of Saskatchewan in any scholarly use which may be made of any material in my thesis.

Requests for permission to copy or to make other use of material in this dissertation in whole or part should be addressed to:

Dean of the College of Pharmacy and Nutrition
University of Saskatchewan
Saskatoon, Saskatchewan S7N 5C9
Canada

OR

Dean of the College of Graduate Studies and Research
University of Saskatchewan
Saskatoon, Saskatchewan S7N 5A2
Canada

ABSTRACT

For over a decade, diquaternary ammonium gemini surfactants have shown promise as non-viral gene delivery agents in both *in vitro* and *in vivo* systems. Their continued development, however, requires an understanding of their biological fate. The absence of identification and quantification methods that can achieve that goal is what drove the development of simple and rapid mass spectrometry (MS)-based methods; the focus of my Ph.D. dissertation.

Prior to the development of these MS-based methods, an understanding of the gas phase behavior of diquaternary ammonium gemini surfactants is required. The development of a universal fragmentation pathway for gemini surfactants was achieved using low resolution and high resolution MS instruments. Single stage (MS), tandem stage (MS/MS and quasi-multi-stage (quasi MS^3) mass spectrometry analysis allowed for the confirmation of the molecular composition and structure of each gemini surfactant through the identification of common and unique mass to charge values. Understanding the fragmentation behavior allowed for the specific identification and/or quantification of gemini surfactants by MS-based methods; including liquid chromatography low resolution tandem mass spectrometry (LC-LR-MS/MS), fast chromatography low resolution tandem mass spectrometry, fast chromatography high resolution mass spectrometry, desorption electrospray ionization low resolution mass spectrometry and matrix assisted laser desorption ionization high resolution mass spectrometry.

We hypothesized that a LC-LR-MS/MS method would be the most effective quantitative method for the quantification of *N*,*N*-bis(dimethylhexadecyl)-1,3-propane-diammonium dibromide (G16-3) within PAM212 cellular lysate; achieving the lowest lower limit of quantification (LLOQ). Although the LC-LR-MS/MS method achieved a LLOQ suitable for analysis of G16-3 within PAM212 cell lysate, its limitations made it an inefficient method. In comparison, the four alternative mass spectrometry methods were faster, more efficient and less expensive than a conventional LC-LR-MS/MS method for the post transfection quantification of G16-3 within PAM212 cell lysate to be determined; 1.45 ± 0.06 μM. Future application of the universal fragmentation pathway and each MS-based quantification method will be beneficial for the future development of diquaternary ammonium gemini surfactants to further understand their post transfection fate.

ACKNOWLEDGEMENTS

The recognition of my supervisor, Dr Anas El-Aneed, is paramount. The guidance and contribution he provided to my doctoral research were instrumental in the development and production of the final outcome; include herein. In addition, his advice and guidance during my studies at the University of Saskatchewan were influential in expanding the breadth of my knowledge and enhancing my overall academic experience.

I would also like to thank my advisory committee members; Dr. J. Alcorn, Dr. I. Badea, Dr. R.W. Purves and committee chairs Dr. R. Dobson and Dr. E. Krol. Their constructive criticism and advice have improved my research methodology and outcomes as well as enhanced my grammatical proficiency.

Sincere gratitude needs to be extended to Dr. R.E. Verrall, Dr. G. McKay and Dr. A. Rémillard for their constructive criticism, support and advice during my time within the College of Pharmacy and Nutrition (CPN).

I would like to thank the CPN and the College of Graduate Studies and Research (CGSR) for funding me through a University of Saskatchewan Graduate Scholarship. Additional Funding was provided by the National Science and Engineering Research Council (NSERC) post graduate scholarship. Funding for equipment and supplies was provided by CPN, NSERC discovery grant and Canadian Foundation for Innovation. Laboratory and office space was provided by CPN. I would also like to acknowledge the Canadian Society of Mass Spectrometry, Canadian Society of Pharmaceutical Sciences, CPN and CGSR for travel awards to present my research.

My sincere gratitude is extended to Ms. D. Michel for the training she provided in the techniques of tissue culture as well as advice and support she provided during my studies. My gratitude is extended to Mr. S. Ambrose, Mr. J. Bailey, Dr. J.V. Headley, Mr. L Hodge, Dr. C.C. Mulligan, Ms. J. Nizzia, Mr. K. Peru Mr. K. Thoms, Mr. A. Ton, Mr. K. Vircks and Dr. H. Zhang for training and assisting me in the use of the various mass spectrometry instrumentation. I also acknowledge the training and assistance provided Dr. J. Chitanda in the synthesis of analytes utilized during my research. My gratitude is further extended to my colleagues at the CPN who provided assistance and encouragement throughout my studies; Mr. I. Asiamah, Mr. M. Bagonluri, Dr. J. Bilinski, Mr. M. Donkuru, Ms. H. Elsayed, Dr. B. Fahlman, Ms. R. Kaur,

Dr. B. Ling, Ms. S. Maini, Mr. W. Mohammed-Saeid, Ms. M. Poorghorban, Mr. J. Singh. In addition, I would like to thank the staff within CPN for their aid; Mrs. A. Bergerman, Mrs. J. Huck, Ms. S. Knowles, Ms. B. McCullough, Mrs. C. Ruys, and Dr. E. Smith-Windsor.

Finally, I would like to thank my parents (Arthur and Joanne), brothers (Stephen, Nicolas & Matthew) and my extended family for their persistent emotional, financial and spiritual support during my academic pursuits. Such contributions I sincerely cherish, for without such contributions I would not have been able to realize my academic achievements.

TABLE OF CONTENTS

LIST OF FIGURES

LIST OF TABLES

LIST OF ABBREVIATIONS

ADME	Adsorption, distribution, metabolism, and excretion (pg. 20)
BCG	bacillus Calmette-Guerin (pg. 1)
CAZ	Carbamazepine (pg. 14)
CE	Collision energy (pg. 62)
CID	Collision-induced dissociation (pg. 11)
CMC	Critical micelle concentration (pg. 6)
DART	Direct analysis in real time (pg. 10)
DESI	Desorption electrospray ionization (pg. 10)
DI	Desorption ionization (pg. 11)
DNA	Deoxyribonucleic acid (pg. 1)
DOPE	1,2-dioleoyl-sn-glycero-3-phosphoethanolamine (pg. 8)
ESI	Electrospray ionization (pg. 10)
FAIMS	High-field asymmetric waveform ion mobility spectrometry (pg. 10)
FC	Fast liquid chromatography (pg. 14)
FIA	Flow injection analysis (pg. 14)
G*t-s*	Composition of diquaternary ammonium gemini surfactant represented by carbon tail length – carbon spacer length/composition (pg. 59)
G16-3	*N*,*N*-bis(dimethylhexadecyl)-1,3-propane-diammonium dibromide (pg. 8)
HIV	*Human Immunodeficiency Virus* (pg. 20)
HPLC	High performance liquid chromatography (pg. 121)
HQC	High quantification concentration (pg. 124)
HR-MS	High resolution mass spectrometry (pg. 10)
IFN-γ	Interferon-γ (pg. 8)

LC	Liquid chromatography (pg. 10)
LLOQ	Lowest lower limit of quantification (pg. 34)
LOD	Limit of detection (pg. 16)
LQC	Lower quantification concentration (pg. 124)
MALDI	Matrix assisted laser desorption ionization (pg. 10)
MEM	Minimal essential media (pg. 123)
MQC	Middle quantification concentration (pg. 124)
MRM	Multiple reaction monitoring (pg. 13)
MS	Mass spectrometry (pg. 8)
MS/MS	Tandem mass spectrometry (pg. 10)
MS^n	Multistage mass spectrometry (pg. 10)
m/z	Mass to charge (pg. 10)
PAM212	Murine epidermal keratinocyte cells (pg. 33)
PEG-P[ASP]DET	Poly[N-[N-(2-aminoethyl)-2-aminoethyl]aspartamide] modified with polyethylene glycol (pg. 4)
PEG	Polyethylene Glycol (pg. 4)
PGL	Plasmid/gemini surfactant/DOPE (pg. 124)
PH	Phenyltoin (pg. 14)
PPM	Parts per million (pg. 25)
QHQ-MS	Quadrupole-hexapole-quadrupole mass spectrometer (pg. 64)
QQQ-LR-MS/MS	Triple quadrupole low resolution tandem mass spectrometer (pg. 11)
Q-ToF-MS	Quadrupole time of flight mass spectrometer (pg. 34)
RNA	Ribonucleic Acid (pg. 1)
RSD	Relative standard deviation (pg. 20)

TOF	Time of Flight (pg. 24)
USFDA	United States of America Food and Drug Administration (pg. 16)
UV	Ultraviolet (pg. 13)
VEGF	Vascular endothelial growth factor (pg. 1)

CHAPTER 1
INTRODUCTION

1.1 Biopharmaceutical therapeutics

The combination of technological innovations and a better understanding of biological systems are altering the manner by which diseases are being diagnosed and treated as evident in the steady approval of new biological drugs.[1] The increase in approval rates can be attributed to the success of biopharmaceutical therapeutics that aim to directly mimic the function of the deficient or erroneous biological molecule(s) without inducing toxicity. The first commercially approved biopharmaceutical agent was insulin, which, along with its analogues, is utilized for the treatment of both type I & II diabetes mellitus.[2, 3] These biopharmaceuticals provide medical glycemic control and they remain the prevailing therapeutic agents utilized for the treatment of both type I & II diabetes mellitus after 31 years of marketing biosynthetic human insulin.[2, 3] Insulin's efficacy in the treatment of diabetes was instrumental in the development of future biopharmaceuticals, demonstrating the viability of using replacement proteins, instead of small drug molecules, in the treatment of diseases. For example, interferon-α proteins have replaced corticosteroids for the treatment of Behcet's disease inducing long-lasting remission and significantly improving prognosis.[4] Progress, such as this, has stimulated the use of biological agents, including both proteinaceous and genetic material, for the treatment of a plethora of ailments.[1]

Although proteinaceous biopharmaceuticals are the dominant biological therapeutic, deoxyribonucleic acid (DNA) and ribonucleic acid (RNA) are also being utilized and developed for therapeutic purposes. For example, the RNA sequence Macugen®, an anti-vascular endothelial growth factor (VEGF), is able to block extracellular VEGF, inhibiting its activity and preventing age-related macular degeneration.[5] Intravitreous injection of Macugen® has reduced the risk of visual-acuity loss and induced visual improvement without producing an increased risk of complications associated with intraocular drug injection.[5] Gene therapy's ability to treat a disease state by reducing adverse effects associated with conventional therapies is one of the desired benefits. For example, a mycobacterial cell wall-DNA complex has been effectively employed as an anti-tumor agent for the treatment of bladder cancer in patients, achieving treatment rates comparable to the conventional treatment of bacillus Calmette-Guerin (BCG).[6] However, unlike BCG the adverse reactions were lower and did not limit treatment options.[6] The

development and application of such biopharmaceuticals have demonstrated how they are able to alleviate disease symptoms in a safe and efficacious manner.

1.2 Genetic Biopharmaceuticals

Theoretically, DNA and RNA can treat disease states and/or restore normal cellular function through the correction of a monogenic genetic mutation, insertion of a specific gene, or blockage of gene overexpression. Gene therapy can be utilized to permanently restore normal cellular function if the gene is effectively inserted into the chromosome and subsequently transcribed into the desired messenger RNA producing the desired protein(s). Conversely, transient restoration of normal cellular function can occur if the genetic material is transported into the nucleus, producing the desired biological outcomes without being inserted into the chromosome.[7, 8] In order for the genetic material to be expressed, it should escape cellular degradation and be efficiently delivered into the nucleus. Although this can be achieved using several physical methods, many genetic biopharmaceuticals currently under development utilize a delivery vector; preventing degradation of the genetic material and enabling its cellular uptake/targeting.

Vectors can be classified as either viral, which involves replacing the genetic information within the viral capsid with a therapeutic gene(s),[8] or non-viral, utilizing either physical methods [electroporation, sonoporation, etc.] or chemical methods [lipoplexes, nanoparticles, etc.] to facilitate the transfection of the genetic material into the cells. Although both vector classes have surmounted many hurdles in their application to gene delivery, the task of delivering the genetic material remains a large technical challenge. Viral gene therapy achieves gene delivery, with an efficacy greater than non-viral gene therapy.[8] In addition, some viral vectors are capable of introducing the gene directly into the chromosome.[9, 10] For example, treatment of immune dysfunction through gene therapy resulted in eight of nine patients achieving permanent gene expression following *ex vivo* retrovirus-mediated transfer of γ chain to autologous CD34+ bone marrow cells.[11] Patient follow up demonstrated that the T cells were still producing the transduced gene 10 years after undergoing the *ex vivo* treatment. However, this viral gene therapy has been correlated with a risk of acute leukemia as well as an undesired immune response.[11]

Native defense mechanisms of cytokines and lymphocytes induce an immune response through the recognition of viral peptide antigens, inducing detrimental side effects, including death.[12, 13] The risks associated with viral gene therapy have spurred the exploration of non-viral methods of gene delivery.

1.3 Carriers Utilized for Non-viral Gene Delivery

Although non-viral gene therapy is less effective than viral vectors in the delivery of genetic material, it is a safer and less complex alternative.[14-16] The ability to chemically modify non-viral vectors, preserving their benefits and addressing their deficiencies, is applicable not only to reducing their toxicity, but also for improving their efficiency, biodegradability,[17] handling capacity,[18] and production mechanisms,[19] all of which are properties that play a key role in achieving safe and sustained transgene expression.

A critical feature of many successfully applied non-viral gene delivery vectors is their cationic nature;[20] first introduced by Felgner et al.[21] as well as Wu and Wu[22] in 1987. The cationic nature of the delivery vectors allows them to form ion pair interactions with the polyanionic backbone of genetic material, shielding the genetic material from degradation while allowing for their cellular uptake and release.[20] The ion pair interaction facilitates the compaction and encapsulation of both small and large (>130kDa) DNA or RNA within a simple delivery vector.[23]

Despite being less toxic than viral vector, a result of their reduced propensity for inducing an immunogenic effect,[24] cationic non-viral delivery vectors do impart some toxicity due to their cationic nature.[25-27] For example, polycationic polymers, polyethylenimine,[28] and poly[N-[N-(2-aminoethyl)-2-aminoethyl]aspartamide] modified with polyethylene glycol (PEG-P[ASP]DET), demonstrated excellent gene compaction efficiencies but were found to inflict cellular damage through interactions with anionic molecules(Figure 1.1A).[27] To reduce these interactions, chondroitin sulfate was included in the formulation, neutralizing the cationic region after plasmid release and preventing the interaction of PEG-P[ASP]DET with anionic molecules (Figure 1.1B).[27] The inclusion of chondroitin sulfate within the non-viral gene delivery formulation demonstrates the flexibility of their composition. In fact, modifications to non-viral delivery systems comprised of cationic and neutral lipids have allowed for their application to the treatment of various cancers; including head,[29] neck,[29] kidney,[30] and ovarian cancers.[31] In

addition, non-viral vectors were successfully utilized through the use of targeting ligands, enhancing their efficacy and specificity as well as reducing their overall toxicity.[32, 33]

1.3.1 Lipid-based Non-viral Vectors

Lipid-based non-viral vectors encapsulate the genetic material within lipoplex structures, shielding it from degradation by deoxyribonuclease or ribonuclease[34, 35] and facilitating the interaction of the surface of the lipoplex with cellular surfaces.[36] Such capabilities can lead to the effective delivery of genetic material, with the potential for a 10-fold increase in the stability of the encapsulated genetic material in comparison to unprotected genetic material.[20, 37] The formation of a lipoplex facilitates stabilization, however, the stability is enhanced through an increase in the ratio of the lipid's positive charge to the genetic material's negative charge.[37] Additional innovations are required in order to further improve the encapsulation and efficient delivery of lipoplexes, including altering their size (1-500 nm)[38] and composition (anionic or cationic lipid, protein composite lipid, etc.).[39]

Uptake, a key consideration for the efficacy of a lipoplex formulation, is largely affected by its size and composition. The transfection of C2C12 pluripotent mesenchymal precursor cell lines by cationic lipoplexes with a mean diameter of 130 nm resulted in a 2 fold increase in internalization of the plasmid in comparison to lipoplexes with a mean diameter of 253 nm.[40] Similarly, a decrease in the mean diameter of polyethylene glycol (PEG) phosphatidyl-ethanolamine lipoplexes has led to an increase in delivery efficacy and gene expression.[38] In addition, the circulation time was improved, contributing to the efficient delivery and targeting of lipoplexes containing PEG bearing lipids.[41, 42] The inclusion of PEG increases the surface hydrophilicity of the liposome and reduces the probability of the liposome interacting with opsons, which cause liposomal degradation and removal.[43]

Additional modifications to the lipid structure have the potential to enhance the compaction of genetic material, reduce cellular toxicity, and improve cellular targeting. Gemini surfactants, dimeric surfactant entities, are one class of surfactant molecule that is being developed for lipid-based gene delivery. A variety of structural modifications are employed by gemini surfactants to improve their transfection efficiency and specificity.

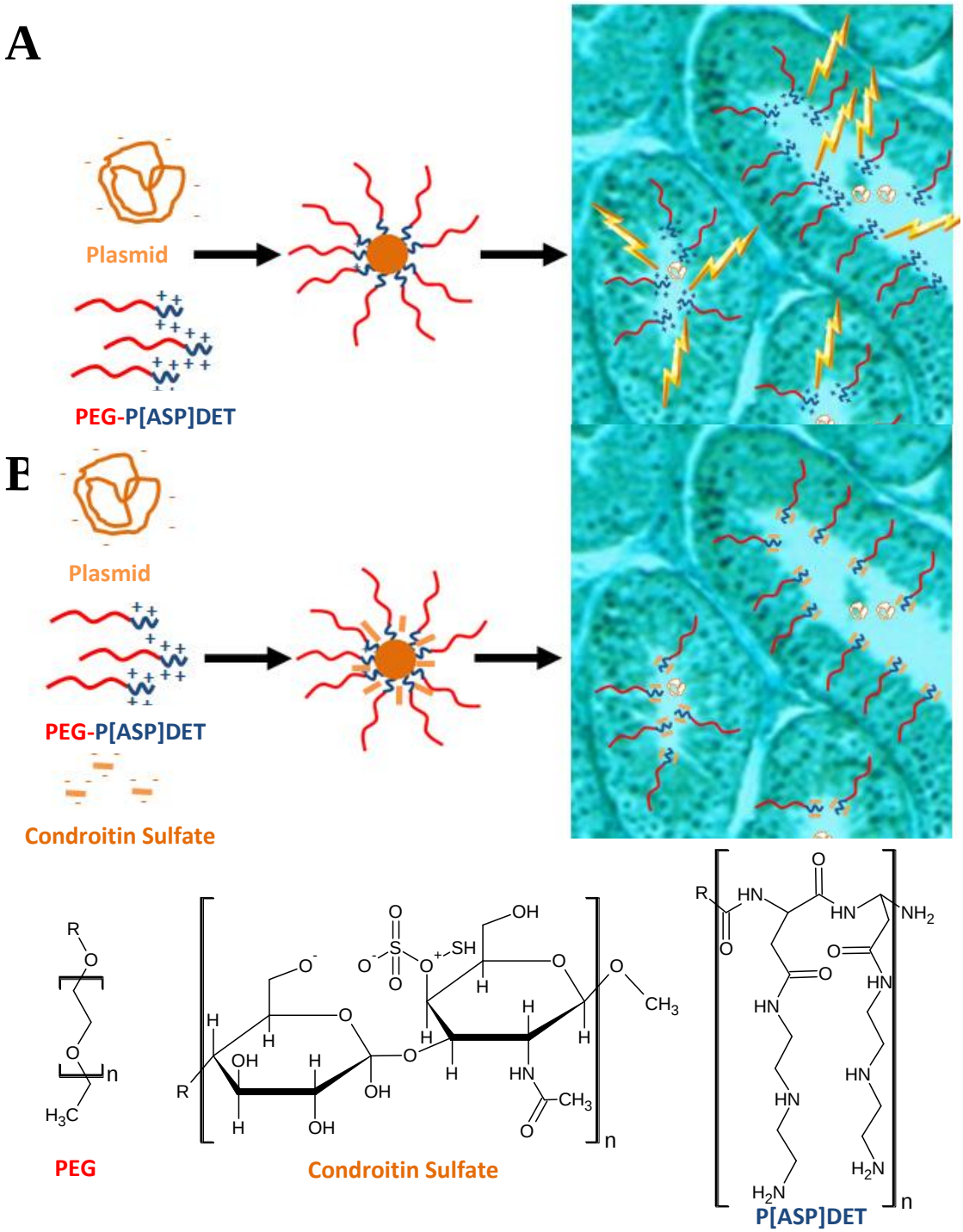

Figure 1.1 Chondroitin sulfate is able to alleviate tissue damage (ϟ) attributed to cationic non-viral gene carriers. The use of cationic non-viral vectors has been associated with cellular and tissue damage due to their non-specific interactions with anionic molecules. For example, the application of PEG-P[ASP]DET as non-viral vectors has been shown to induce damage (bolts) of the membrane due to their polycationic nature (A). The inclusion of chondroitin sulfate, a poly anionic compound, during vector production resulted in a reduction in the observed membrane damage because chondroitin sulfate was found to interact with the cationic region of PEG-P[ASP]DET (B).

1.3.2 Gemini surfactants

The term gemini surfactant was proposed by Fredric Menger in 1991[44] for molecules comprised of two hydrophobic alkyl chains with polar heads separated by a spacer region linking each polar head (Figure 1.2A).[45] Menger solely included bis-surfactants that had a rigid spacer composed of a benzene or stilbene system (Figure 1.2B) in his original definition, however, it has since been extended to include all bis-surfactants joined by a rigid or flexible spacer molecules, including both anionic (Figure 1.2D) and cationic molecules (Figure 1.2D).[45] Conventional surfactants have a single hydrophobic tail connected to polar/ionic head group. The inclusion of two hydrophobic tail regions attached to the polar head groups creates an amphiphilic compound that, when introduced into solution, self-assemble.[45, 46] The self-assembly of the gemini surfactants molecules results from hydrophobic/hydrophilic segregation facilitated by the hydrophobic tail regions as well as the polar headgroups and/or spacer regions.[47] The presence of two hydrophobic tail regions as well as the symmetry of gemini surfactants makes their surface activity stronger than conventional surfactants and more importantly the critical micelle concentration (CMC) is remarkably lower than other surfactants.[45]

Gemini surfactants that are asymmetric,[48] possessing more than two polar groups and/or tails, have also been synthesized.[49, 50] However, the great majority of gemini surfactants are symmetrical, with identical polar head groups and tail regions.[51] The acceptable variations in the structure of the spacer, polar head groups, and hydrophobic tails regions allow for an endless number of possible structures and physicochemical properties. A benefit of the structural variations of gemini surfactants is their numerous applications; including the construction of high porosity materials,[52] antibacterial regimens,[53, 54] analytical processes,[55] and drug delivery systems.[56-59] The cationic nature of diquaternary ammonium gemini surfactants makes them adeptly suited to encapsulate genetic materials and facilitate their transfection. The interaction between the cationic regions of the gemini surfactant and the anionic phosphate backbone of the DNA sequence results in the successful encapsulation of DNA.[60] In addition, the amphiphilic nature of gemini surfactants results in the self-assembly of cationic lipoplexes at concentrations greater than the gemini surfactants CMC.[44] A multitude of gemini compounds are currently assessed for their DNA delivery efficiency, however, those discussed in this dissertation are symmetrical diquaternary ammonium compounds.[61]

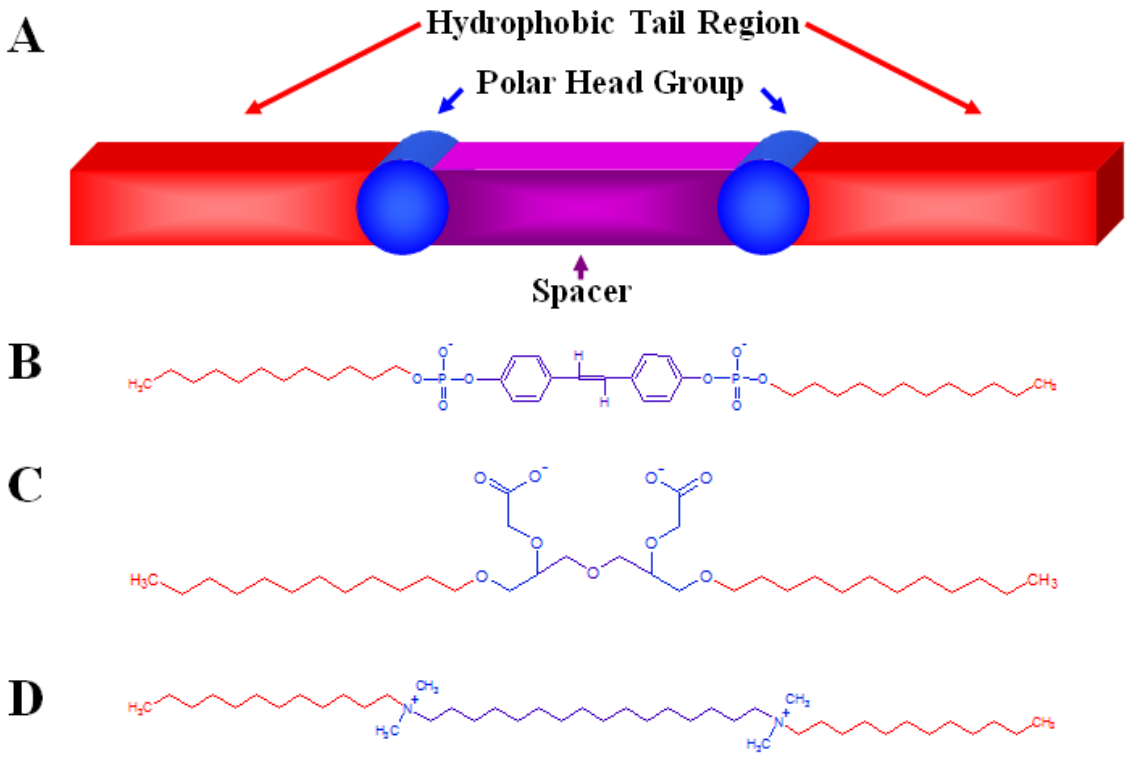

Figure 1.2 Structural characteristics of Gemini surfactants. Gemini Surfactants are comprised of two hydrophobic tail regions, attached to one another through a spacer region that binds to each tail regions terminal polar head group (A). Examples of gemini surfactants include those with a benzene spacer similar to *N*,*N*-bisdodecyl-4,4'-ethene-1,2-phenyldiphosphate (B), an anionic spacer region similar to 2,2'-{oxybis[(3-dodecoxypropane-1,2-diyl)oxy]}diacetic acid (C) or a cationic spacer region similar to *N*,*N*-bis(dimethyldodecyl)-1,16-hexadecanediammonium (D).

1.3.3 Diquaternary ammonium gemini surfactants

The molecular structure of diquaternary ammonium gemini surfactants and their DNA complexes are well-characterized; a result of their usage as gene delivery agents for the past decade and a half.[46, 56, 62, 63] These gemini surfactants can be categorized into one of four individual families based upon the composition of their spacer region; alkyl spacers (Figure 1.3A), secondary and tertiary amines within alkyl spacers (Figure 1.3B), ether linkages between alkyl spacers (Figure 1.3C), or hydroxyl functional groups attached to alkyl spacers (Figure 1.3D). Studies involving diquaternary ammonium gemini surfactants demonstrate that they provide a viable method for non-invasive gene delivery. For example, the transfection of a plasmid, cytomegalovirus immediate early promoter green fluorescent protein, into COS-7 cells utilizing (2S, 3R)-2,3-dimethoxy-1,4-bis(N-hexadecyl-N,N-dimethylammonium)butane

dibromide gemini surfactants was just as efficient as Lipofectin™ and other commercially available cationic lipids.[64-66]

In addition to cellular studies, the topical application of interferon-γ (IFNγ) genes encapsulated within di(dimethyldodecyl)-1,3-propanediammonium:1,2-Dioleoyl-sn-Glycero-3-Phosphoethanolamine (DOPE) and di(dimethylhexadecyl)-1,3-propanediammonium (G16-3):DOPE vectors produced 250% and 450% increase in levels of IFNγ in the epidermis compared to unprotected IFNγ genes within a mouse animal model.[56, 57] The use of neutral helper lipids, including DOPE, as stabilizing agents enhanced gene delivery capability of gemini surfactant nanoparticles[67, 68] while still allowing for the gemini-DNA complexes to be administrated topically or systematically (via oral, mucosal, or injectable forms). [51] These findings demonstrate that the usage of this class of gemini surfactants is a viable method for non-invasive gene delivery.

All of the studies previously reported were exclusively concerned with improving both the transfection efficiency of gemini surfactant nanoparticles while reducing toxicity. Conclusions were based on the correlations between the encapsulation efficiency, transfection efficiency, cell viability, gemini surfactant structure and lipoplex composition. However, no study was conducted to monitor the adsorption, distribution, metabolism, and excretion of the nanoparticles and their contents. An understanding of each of these characteristics is vital to achieving approval for a new drug application. Therefore, qualitative and quantitative analytical methods are needed to further advance the use of diquaternary ammonium gemini surfactants. Mass spectrometry is uniquely suited to quantify gemini surfactants due to the two permanent positive charges on the polar head regions of the gemini surfactants. In addition, innovations in both ionization sources and mass analyzers are stimulating the development and application of specific, selective, and sensitive high-throughput mass spectrometry methods to the quantification of both drug(s) and carrier molecules.

1.4 Mass spectrometry's application to pharmaceutical analysis

Each stage in the drug development process requires qualitative and quantitative analysis, a task commonly achieved using mass spectrometry (MS) because of its ability to identify novel analytes through the determination of their molecular composition.[69, 70] Superior analytical

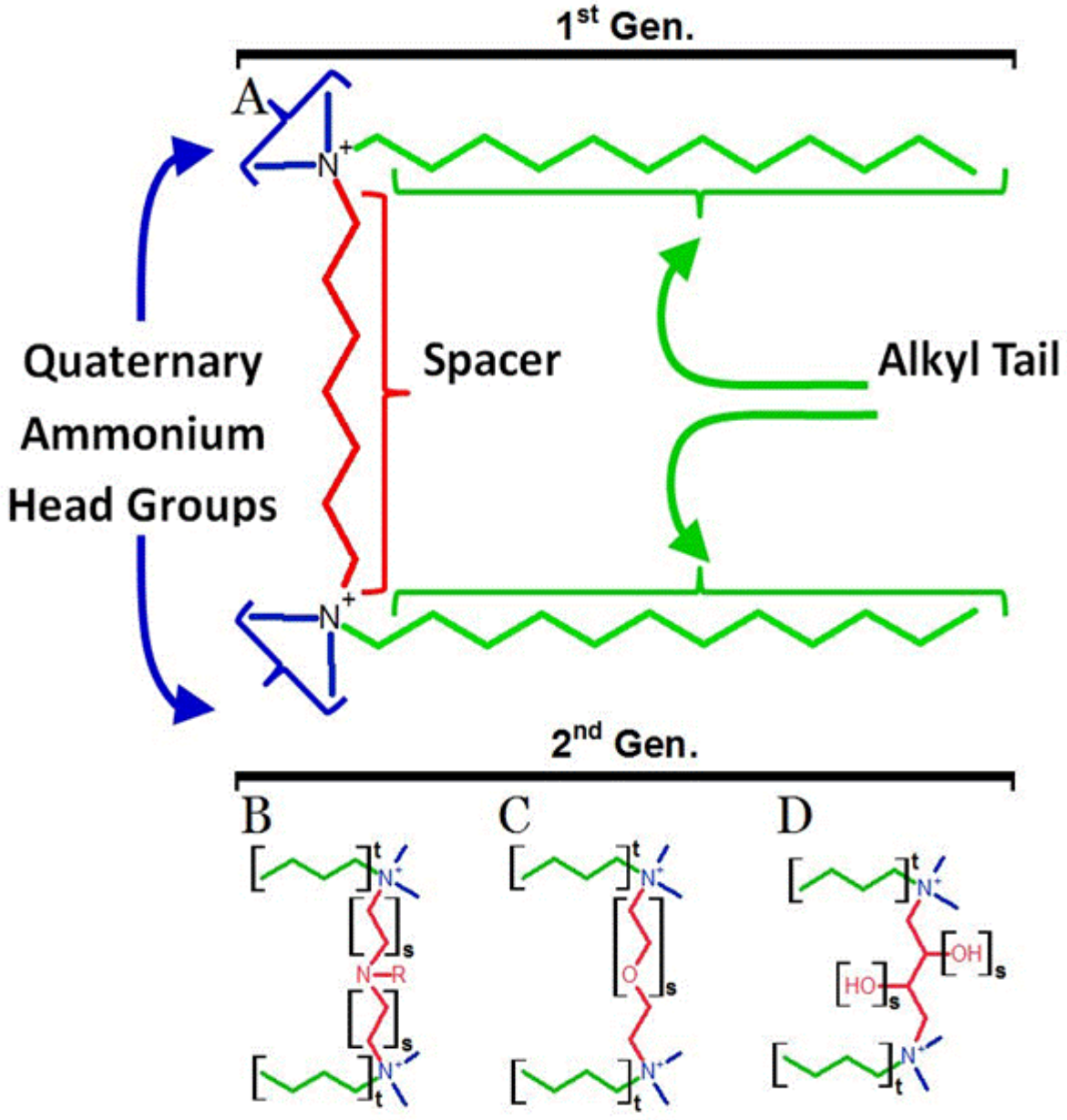

Figure 1.3 The general structure of first and second generation quaternary ammonium gemini surfactants as categorized based upon their spacer composition; Alkyl chain (A), 2° & 3° amine ('R' = hydrogen or methyl) (B), polyethoxylated (C), and hydroxyl (D) substituted alkyl chains. "t" = number of carbons in chain. "s" = fuctional groups in the spacer region

information supplied by MS has been applied to the analysis of the metabolites and degradation products of drug molecules; streamlining the process of drug discovery and development.[71, 72] In addition, recent advances in both ionization sources and mass analyzers have enlarged mass spectrometry's role within the preclinical and clinical assessment of pharmaceuticals.[73]

Revolutionary steps during development of mass analyzers, included the invention of quadrupole mass analyzers[74] and tandem mass spectrometry (MS/MS);[75] allowing for the structural details of analytes to be determined based upon their fragmentation behavior. Recent advances in mass analyzer technology have allowed for a reduction in the total time of analysis while providing more detailed and comprehensive analytical data. For example, analyte quantification can be achieved using high resolution-mass spectrometry (HR-MS) that can differentiate ions based upon minor structural variations.[76-78] The ability to achieve very precise mass to charge ratio (*m/z*) measurements enables analytes to be distinguished from one another based on their unique molecular composition.[78, 79] Similarly, advances in ionization have resulted in improved analytical outcomes. For example, the development of electrospray ionization (ESI) allowed for liquid chromatography (LC) to be easily coupled to MS,[80, 81] while the invention of desorption electrospray ionization (DESI) allowed for analytes to be ionized and introduced into the mass spectrometer under ambient conditions with minimal or no sample preparation.[82]

The continued advancement of MS technology has culminated in commercial products that are better equipped to promptly identify/quantify small drug molecules within complex matrices; including high-field asymmetric waveform ion mobility spectrometry (FAIMS),[83] multistage mass spectrometry (MS^n),[84] direct analysis in real time (DART),[85] and matrix assisted laser desorption ionization (MALDI).[86] Applying these MS technologies to the field of pharmaceutical sciences allows for the rapid acquisition of accurate and precise analytical data that assists in assessing the efficacy and viability of both drugs and formulations. However, the sensitivity, specificity, and selectivity of these modern MS instruments still rely upon the principles of MS proposed by E. Goldstein[87] and J.J. Thomson.[88]

1.5 Historical perspectives on mass spectrometry

The cathode ray tube experiments of both E. Goldstein[87] and J.J. Thomson[88] demonstrated that the path of ions traveling through the cathode ray tube could be deflected using magnetic and electric fields; providing the initial principle of MS.[89] Through an understanding of this principle, ionic atoms and isotopes produced by cathode ray apparatus were separated by magnetic and electric fields based upon differences in their masses and a nominal charge of 1; allowing for the identification of naturally occurring isotopes.[88, 89] The dominant use of MS for the separation of isotopes continued till the 1956 when R. Gohlke and F. McLafferty used MS to

detect and identify analytes separated by gas chromatography.[90] The ability to identify molecular ions led to the subsequent use of MS for the qualitative identification of organic molecules. In addition, it stimulated the development of MS technology, including J.H. Futrell's development of MS/MS,[75] K.R. Jennings application of collision induced dissociation (CID),[91] M. Yasmashita and J.B. Fenn's invention of the ESI[81] as well as the invention of laser desorption ionization by K. Tanaka;[92] amongst a multitude of others.

Prior to the advent of MS/MS, MS analysis had only been able to provide *m/z* information on ions produced during the ionization process, severely limiting the ability to deduce information on their molecular structure. Therefore, the discoveries of MS/MS and CID were critical because they allowed for MS analysis to be applied to the inference of structural information of any ion. CID involves accelerating ions through a potential difference, causing them to collide with neutral gas molecules and one another within the acceleration region. As the ions collided with the neutral species, their ions kinetic energy is transformed into internal energy.[91] The elevated internal energy of the ions causes them to fragment into smaller ions that are detected following *m/z* analysis.[91] Originally deemed a nuisance because they increased the spectrum's background, fragment ions produced through CID became desired with the advent of MS/MS. However, structural information about the precursor ion could only be inferred when CID was observed either in the region prior to the first analyzer or between the analyzers.[74] The principles of CID and MS/MS, however, were not fully embraced until the development of triple quadrupole low resolution tandem mass spectrometers (QQQ-LR-MS/MS).[74]

Another milestone in the history of MS is the invention of ESI, an ionization source that facilitates the evaporation of solvent at atmospheric conditions; revolutionizing how analytes are introduced into the mass spectrometer.[81] Prior to the invention of ESI, many ionization techniques required that sample to be converted into the gas phase or placed under vacuum prior to ionization (a two-step process); limiting the types of samples that could be analyzed. ESI eliminated the need for a two-step process and allowed for the analysis of analytes that could not be ionized by traditional ionization methods because they were either heat sensitive or non-volatile.[93] Conversely, desorption ionization (DI) techniques, produced ions from analytes present on a solid substrate.[92, 94] The novelty of both techniques is the simplicity of how liquid and solid samples are introduced into the gaseous phase and the soft manner by which molecules are ionized. Soft ionization of an analyte prevents its dissociation into fragment ions, thereby

reducing the total number of ions present within the spectrum and allowing for the identification of intact analytes.

The simplification of data provided by both ionization and ion separation/fragmentation techniques advanced the application of MS for quantitative purposes. The most significant outcome of these advancements was the ability to directly couple LC with MS. LC-MS is extensively utilized for the analytical assessment of drug molecules because it provides rich analytical information in a specific, sensitive, selective, and rapid manner.[95, 96]

1.6 Liquid chromatography-mass spectrometric quantification of pharmaceuticals

The development of ESI in the 1980s and the subsequent adoption of LC-MS initiated mass spectrometry's journey to the forefront of analytical chemical analysis.[97, 98] It provided a way to directly convert the liquid effluent of LC to gas phase ions by passing them through a high voltage emitter, positioning LC-MS as the gold standard of analysis for numerous fields.[70, 99] The specificity, selectivity, and sensitivity of MS as well as its ability to differentiate and monitor a large number of analytes has made it the method of choice for qualitative and quantitative analysis of drugs, metabolites, and endogenous molecules within pharmaceutical formulations and biological matrices.[100-102] LC-MS has become the analytical technique of choice within the pharmaceutical industry,[69] surmounting many traditional detection methods (including diode array detection, fluorescence detection, and electron impact detection).[103]

Both high and low resolution MS instruments can be coupled to LC and have been utilized for quantitative purposes. By coupling LC with HR-MS (i.e., LC-HR-MS), the analyte can be specifically identified by its exact mass measurement and isotopic signature.[69] Both the atomic composition and universal isotopic distribution of an ion facilitates the determination of its empirical formula. On the other hand, low resolution mass spectrometers, comprised of two or more mass analyzers, can also provide a high degree of specificity by performing MS/MS analysis by LC-LR-MS/MS.[104] Monitoring an analyte's specific LC retention time as well as its specific *m/z*, isotopic signature, and/or MS/MS signature makes LC-HR-MS and LC-LR-MS/MS more specific than traditional quantitative methods that relied solely upon LC separation and general

Table 1.1 A comparison of the structural and physical characteristics of Amodiaquine and N-desethyl-amodiaquine[106]

Amodiaquine	N-desethyl-amodiaquine
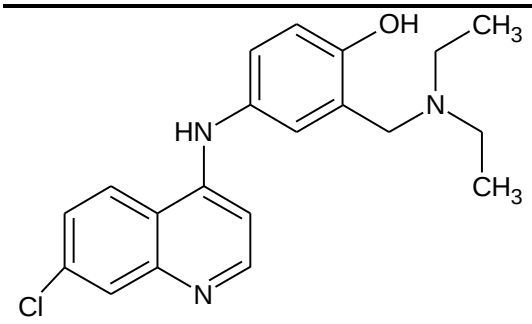	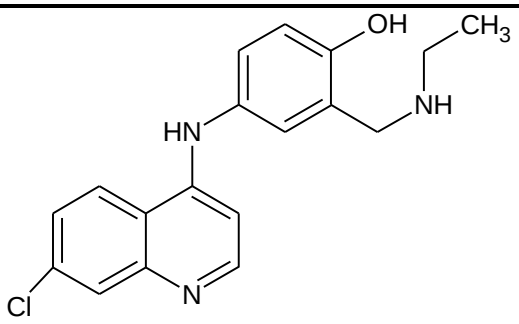
Monoisotopic mass of 355.1451 Da	Monoisotopic mass of 327.1138 Da
Molecular Formula of $C_{20}H_{22}ClN_3O$	Molecular Formula of $C_{18}H_{18}ClN_3O$
UV absorption occurs at 340 nm	UV absorption occurs at 340 nm
MRM transition of 356.3 *m/z* → 283.0 *m/z*	MRM transition of 328.3 *m/z* → 283.0 *m/z*

MRM (Multiple Reaction Monitoring)

absorbance and/or emission properties of an analyte. Due to its capabilities, MS minimizes the interference produced by co-eluting molecules.[105]

An illustrative example of the ability of LC-LR-MS/MS to differentiate between closely related, co-eluting molecules is the identification of 14 structurally-related anti-malarial drugs, including amodiaquine and N-desethyl-amodiaquine. As shown in Table 1.1, these structures differ solely by an ethyl functional group but possess nearly identical physical and ultraviolet (UV) absorbance properties.[106] The specificity provided by MS/MS removes the need for baseline separation of analytes, allowing for the co-elution and quantification of numerous analytes at the same time.[107, 108] By eliminating the need to achieve baseline LC separation of analytes, LC-MS/MS can be utilized to quantitatively analyze hundreds of drugs in a shorter time period. This provides several benefits over LC coupled to conventional detectors, including reducing the total time of analysis, increasing the number of analytes that can be monitored and enhancing the limits of quantification due to an increase in specificity provided by MS.

MS and specifically MS/MS can also minimize matrix interferences and eliminate additional peaks by monitoring the *m/z* values of the precursor ion and/or fragment ions that are

unique for the analyte(s) of interest.[109] For example, the quantitative analysis of phenytoin (PH) and carbamazepine (CAZ) within tablets using LC separation achieved superior accuracy when using mass spectrometry detection in comparison to UV detection (Figure 1.4).[110] Such results are attributed to endogenous molecules interfering with conventional detection methods, a result of the absence of specificity in the absorption properties monitored, potentially compromising quantitative data due to co-eluting molecules. Therefore, concessions must be made when using UV detection for either selectivity or sensitivity in order to improve the other.

Despite superior performance, LC-HR-MS and LC-LR-MS/MS still suffer from the inherent disadvantages of LC and ESI. Firstly, the amount of time required to both develop and run a method can be quite lengthy due to the need to achieve adequate peak shape and minimize ion suppression. Therefore, numerous alterations to a method are needed, resulting in lengthy periods of time for column equilibration/cleaning. Secondly, the developed method can be quite complex, typically requiring different mobile phases and gradients to achieve the desired analyte separation/peak shape. A single flaw in this complex system can cause the peak to drift, broadened, and/or split; potentially inducing a false negative or positive reading for an analyte(s). Such drawbacks of the separation of analytes by LC prompted the development of additional MS-based quantification methods that do not require LC separation; particularly for the analysis of a relatively small number of analytes within the sample.

1.7 Alternative Mass Spectrometry Based Quantification Methods

Traditionally, quantitative mass spectrometric analysis relied heavily upon both chromatography and sample preparation techniques, ensuring optimal results. The advent of new ionization techniques, mass analyzers, and electronics have allowed for enhanced sampling rates and enhanced specificity/accuracy for ion separation, selection, and detection. It has provided ways to circumvent the need for extensive chromatography, method development, and/or sample preparation.[112] For example, the development of flow injection analysis (FIA), fast liquid chromatography (FC), DESI, and MALDI have advanced the application of high-throughput

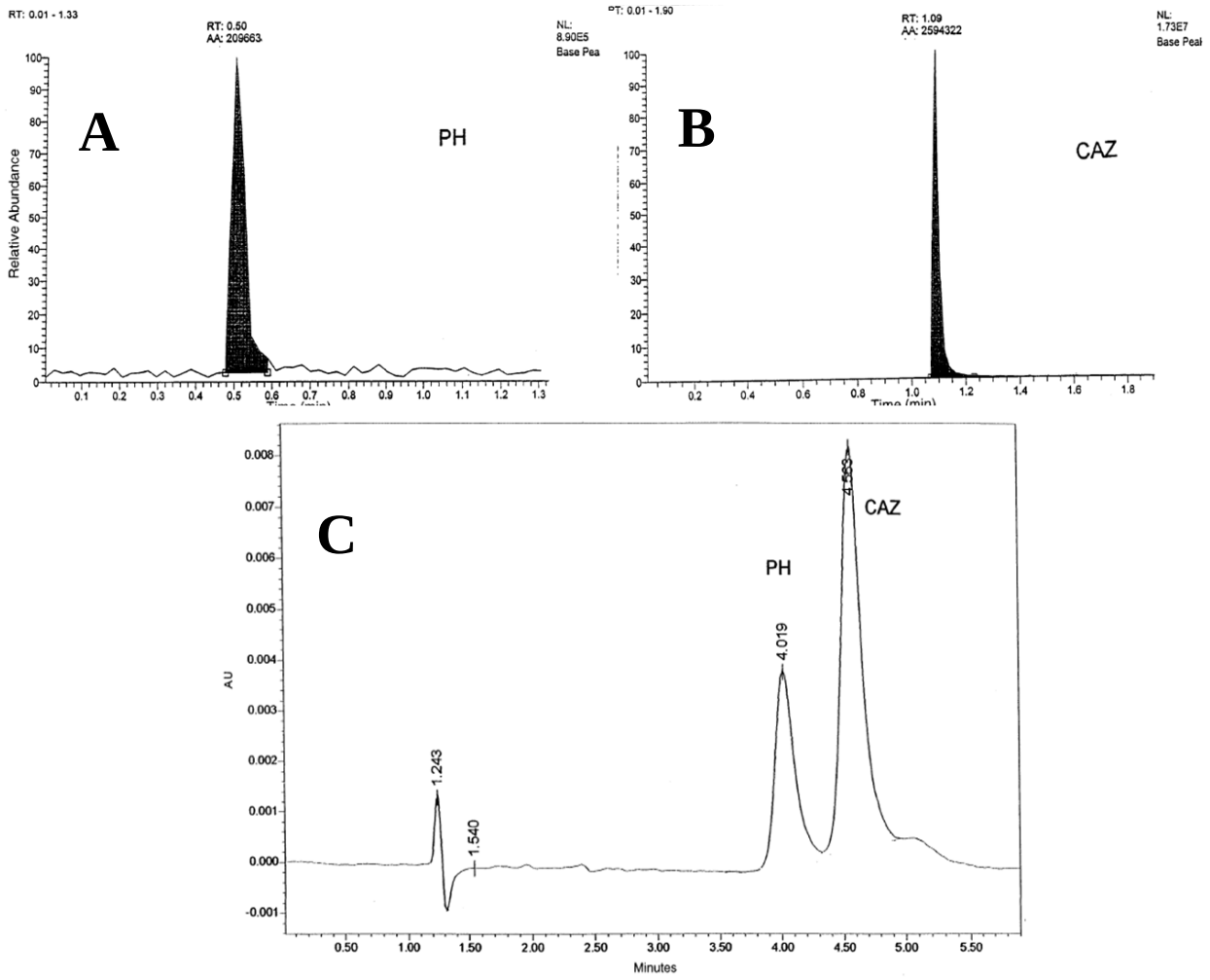

Figure 1.4 A chromatographic comparison of Mass Spectrometric (A & B) and ultraviolet detection (C) detection methods utilized for the quantification of phenyltoin (PH) and carbamazepine (CAZ). Adapted and used with permission from reference 110.

chromatographic methods. These techniques are discussed below as they relate to quantitative workflows.

1.7.1 Fast liquid chromatography and flow injection analysis mass spectrometric analysis

The case for chromatographic separation prior to mass spectrometric detection is typically required for the identification and/or quantification of a large number of analytes and unknowns.[113-115] However, for applications that require the quantification of a single or small number of analytes, high throughput methods such as FIA can achieve results comparable to LC-MS with a reduction in the total time of analysis. An additional benefit is the reduced cost

associated with consumables required for analysis/separation. Two methods that are used to reduce the time of analysis are FIA, which introduces the liquid sample into the instrument as a injected plug (i.e., no analytical column),[116] or FC, which uses a short column to produce chromatographic peaks. The nonspecific and simplistic nature of FIA-MS and FC-MS methods, compared to many LC-MS methods, means they are flexible in their application to a plethora of analytes.[117]

The adoption of FIA and FC-based MS quantification is related to the ability of MS to differentiate between closely related ions, both in composition and/or structure. The presence of structural variations between different molecules, including minute variations such as structural isomers, minimizes the probability of analyte cross-talk and false positives during MS analysis. For example, the quantification of un-related drugs of abuse (bezoylecgonine, amphetamine, and codeine) analyzed by FIA-LR-MS/MS was achieved in the forty-five second period of analysis and provided results that formed the presence of individual drugs.[118] No interference was detected when the drugs were spiked in both serum and urine matrices and provided a limit of detection (LOD) below 2 ng/mL.[118] FIA-LR-MS/MS analysis can also be used when structurally similar analytes are introduced simultaneously with no interference detected for either analyte. For example, the introduction of dihydrocodeine and hydrocodone (analogues of codeine) did not result in any interference for the transitions being monitored for codeine.[118] Identical results were also achieved when ecgonine methylester and methamphetamine were introduced.[118] This demonstrates the ability of FIA-LR-MS/MS to be a sensitive and specific method for quantitative analysis.

The most definitive advantage FIA has over methods that utilize chromatographic separation is speed; allowing up to 100 samples to be analyzed within a one hour period.[118, 119] The rapid analysis of samples is directly beneficial for quality control purposes as it allows for near instantaneous feedback on the composition and uniformity of pharmaceutical formulations. Assessing the uniformity of pharmaceutical formulations containing caffeine and creatine using FIA was shown to be both accurate and precise; achieving results that are within the United States Food and Drug Administration's (USFDA) requirements for bioanalytical validation.[119] Attainment of the required validation parameters demonstrates the applicability of FIA to the rapid assessment of the active ingredient of a formulation. An added benefit of FIA is the

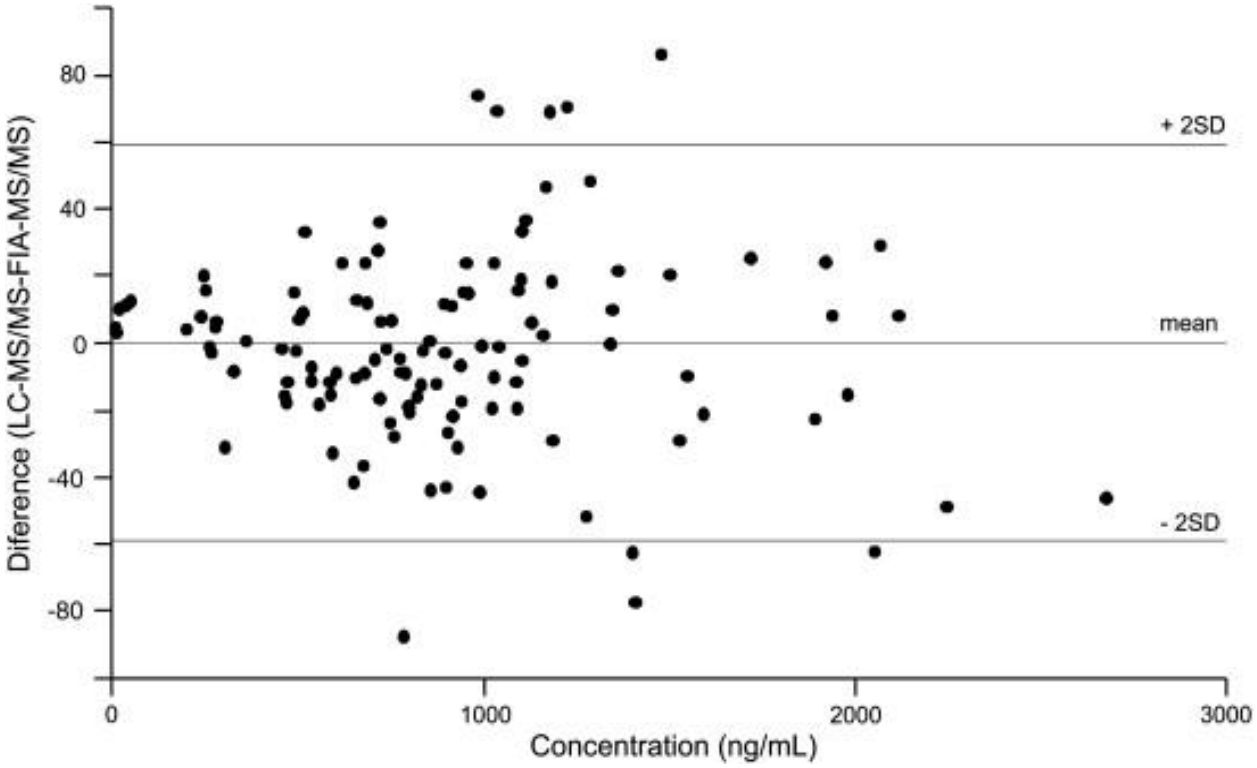

Figure 1.5 A Bland-Altman comparative plot of the LC-LR-MS/MS and FIA-LR-MS/MS results attained for the quantification of imatinib within the plasma of cancer patients. The Bland–Altman plot showed mean difference of -1.46 ng/mL and standard deviation of 28.9 ng/mL. Used with permission from reference 125.

short period of time that analytes interact with the carrier solute, allowing for the assessment of analytes with varying solubility profiles.[119]

Conversely, variations in matrices can have deleterious effects on analyte analysis by interfering with ionization or detection of analytes; diminishing limits of detection/quantification or reducing the linear range of a quantitative method. The use of FC instead of FIA can alleviate these problems by addressing the issue of ion suppression. FC also prevents the co-elution of analytes molecules that may induce ion suppression.[120] It should be noted, however, that variations between matrices and the introduction of molecules that induce ion suppression can occur during all MS assays; including LC, FIA, and FC. Therefore, sample preparation prior to MS analysis is a critical step that can improve the analytical outcome of all methods that utilize mass spectrometry detection.

Application of FIA to pharmaceutical research allows for the realization of real time *in vivo* and *in vitro* monitoring of analytes. Near instantaneous feedback provides information on

synthetic pathways, monitoring of specific chemical changes and the fate of drug candidates.[121] The validation of a FIA-LR-MS/MS method for quantification of topiramate in human plasma provided information on its biological fate and transformation.[122] The FIA-MS method yielded comparable accuracy, precision and reproducibility to that of capillary electrophoresis UV detection, gas chromatography flame ionization detection and LC-LR-MS/MS.[122-124] In addition, the number of samples analyzed within a one hour period was superior to conventional LC-LR-MS/MS methods.[122]

Reducing the time of analysis has a two important benefits as it reduces the demand upon the instrument through a reduction in run time and reduces the overall cost of the analysis. The cost of analysis benefits from a reduction in solvent usage, however, it may also gain an economical advantage through the use of less expensive and/or complex mobile phases. Imatinib, a tyrosine-kinase inhibitor utilized in various cancer treatments, was quantified in human plasma using both ultra-high performance liquid chromatographic-MS/MS and FIA-MS/MS methods.[125] Both methods produced comparable results across concentrations measured within cancer patients, as shown by a bland-altman plot (Figure 1.5), however, the FIA method achieved its results in less than one quarter of the time of ultra-performance liquid chromatography and one quarter of the cost.[125] In addition, additives were simplified as for the analysis of imatinib in human plasma; LC-MS/MS analysis utilized a 4 mM ammonium formate buffer system at pH 3.2, which is time consuming to produce in comparison to the addition of 0.1% formic acid to the methanol mobile phase used in the FIA method.[125]

Finally, the application of FIA techniques to lab on a chip technology has the potential to further simplify pharmaceutical analysis because it integrates several laboratory functions onto a miniaturized chip.[126] The benefits of lab on a chip technology are a reduction in consumables, use of individual ESI tips resulting in no sample carryover and the incorporation of sample preparation techniques into the chip. Application of this technology to the quantification of verapamil and norverapamil in human plasma demonstrated that concentrations lower than 2.5 ng/mL can be detected and quantified; results that are comparable to LC-LR-MS/MS.[127, 128] The elimination of sample carryover has the potential to increase the dynamic range of any bioanalytical assay, especially at the lower limit of quantification, and use relatively inexpensive lab on chip technology and minimal solvent flows.[126, 128] In addition, an enhancement in the limit of quantification following the removal of proteins through precipitation suggests that this

technology can be coupled to a traditional sample clean-up procedure in order to achieve superior limits of detection. The viability of such technology shows the potential for both FIA lab on chip technology MS and FIA-MS to detect and quantify ions without the requirement of chromatographic separation; reduce bioanalysis expenditures while maintaining the sensitivity and linearity of conventional chromatographic techniques.

1.7.2 Matrix assisted laser desorption ionization

MALDI-MS is not commonly associated with the analysis of small molecules or quantification. However, advances in both MALDI-MS technology, sample preparation techniques and matrices has allowed for quantitative data to be rapidly attained for small molecules.[129] The high frequency of the laser pulse utilized during MALDI and the acquisition rate of mass spectrometry allows for rapid sample analysis. In addition to its rapid time of analysis, MALDI-MS is being utilized for the quantification of small molecules due to reduced sample carry over, ability to tolerate salts and propensity to form singly charged molecules.[129-132] In addition, the stability profile of analytes can be extended by some matrices whose deposition provides a protective mechanism that maintains long term analyte stability.[133] Through the minimization of degradation and oxidation, samples may be qualitatively and/or quantitatively re-analyzed in the future.[133] Such MALDI specific characteristics can be beneficial to the pharmaceutical industry, resulting in both improvements in data produced and economical gains. However, the future application of MALDI-MS for the quantification of small molecules will benefit from further improvements in instrumentation and available matrices, leading to enhanced ionization, ion analysis, and reduction in background noise.[129]

1.7.2.1 Small molecule analysis using matrix assisted laser desorption ionization

Analysis of low molecular weight analytes requires better matrices and/or enhanced delayed extraction ion analysis to reduce the background noise associated with MALDI. The introduction of new matrices as well as alterations to existing matrices is an ongoing process with synthetic and purification processes being altered to reduce contaminant levels. In addition, the evaluation of novel matrices strives to not only improve ionization but minimize low molecular weight interference.[134, 135] This can be achieved through the use of matrices that have higher molecular weights and do not contribute to background noise in the low mass region. For example, nanomaterial matrices have been applied to the analysis of small molecules by

MALDI-MS, providing a matrix that ionizes analytes and minimizes background noise by reducing analyte fragmentation.[134] The deposition of silane matrix on the analyzed MALDI surface was achieved through the use of N-(3-trimethoxysilylpropyl)diethylenetriamine and octadecyltricholorosilane, producing homogenous deposition.[134] Laser desorption analysis of analytes deposited on the silane surface resulted in a drastic reduction in non-analyte peaks, simplifying analysis of the small drug molecule acrivastine and angiotensin I.[134] Similarly, exploration of non-traditional small molecule matrices has resulted in a reduction in spectral noise. The combination of 3-hydroxycoumarin and 6-aza-2-thiothymine as a MALDI matrix resulted in the ionization and identification of the drug donepezil in brain tissue with minimal matrix interference.[135] The continued exploration of novel MALDI matrices may result in the expanded use of MALDI for the quantification of low molecular weight drug analytes.

The demand by health professionals to rapidly attain information related to the absorption, distribution, metabolism, and excretion (ADME) properties of a pharmaceutical is one area in which MALDI has a benefit over traditional mass spectrometry methods. MALDI's rapid acquisition of data provides near instantaneous therapeutic drug monitoring that may benefit clinical patient care through an improvement in assessing patients' dosage regimen. The ability to monitor the drugs allows for the creation of a dosage regimen that balances toxicity and efficacy, while MALDI analysis allows for the rapid quantification of multiple analytes, producing near real time feedback. The benefit of instantaneous feedback is particularly important for patients undergoing treatment with toxic drugs, such as those afflicted with *Human immunodeficiency virus* (HIV).[136] Quantification of the HIV drugs lamivudine, lopinavir, and ritonavir by MALDI-HR-MS concur with results provided by LC-MS/MS analysis, though MALDI-HR-MS results were attained significantly faster.[137] The quantitative range of the method was viable for a linear range of at least 100x for each analyte, providing accurate and precise measurements with less than 10% relative standard deviation (RSD).[137] In addition, the LOD attained by a prototype MALDI-LR-MS/MS was 10 fold less than that obtained for LC-LR-MS/MS.[137]

1.7.2.2 MALDI-MS Sample preparation

The ability of MALDI-MS to tolerate salts simplifies sample preparation, further reducing the analysis time, particularly when compared to LC-MS. No sample preparation is

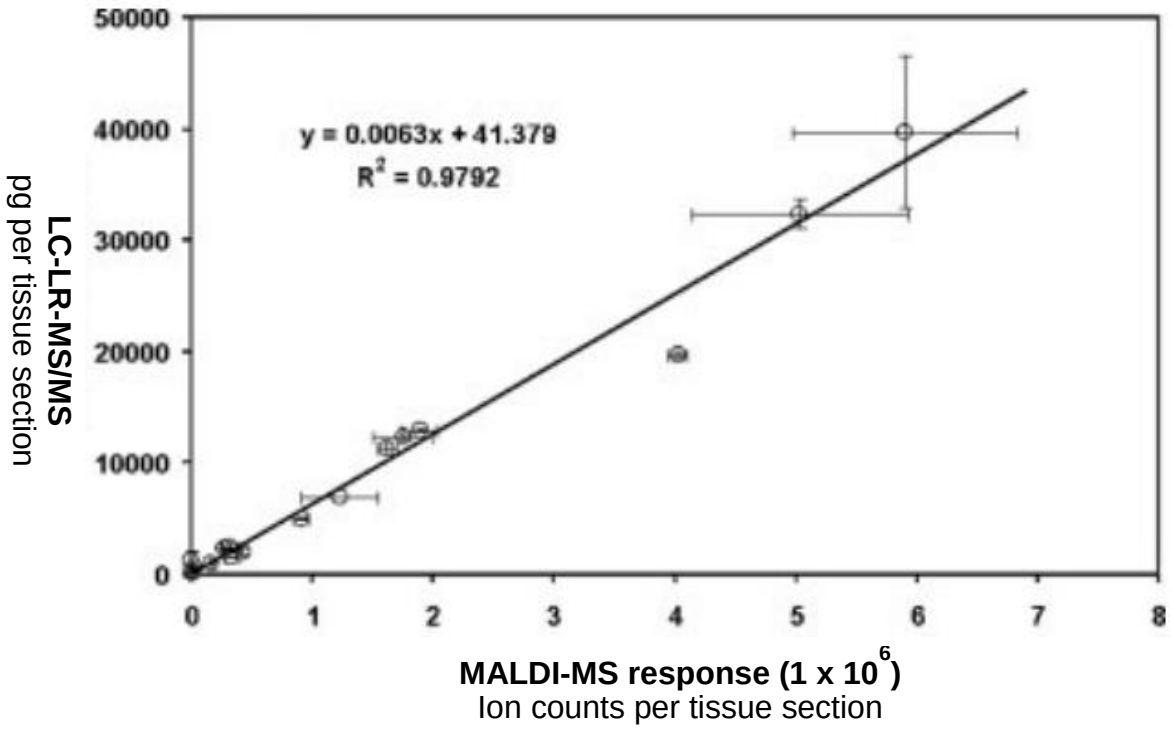

Figure 1.6 A linear relationship is observed between the amount of olanzapine in a single tissue section of rat liver as measured by LC-LR-MS/MS and the integrated MALDI-HR-MS response in an adjacent tissue section. Used with permission from reference 139.

needed to perform drug quantification within tissue samples, as matrix deposition on the tissue surface is the sole procedure performed.[131, 138] For example, the simultaneous imaging and quantification of olanzapine in liver tissue by MALDI-HR-MS achieved quantitative levels comparable to LC-LR-MS/MS, but with 100 µm imaging resolution on the tissue surface.[139] The ability of MALDI-MS to both spatially and rapidly quantify a drug molecule provides a significant advantage over other MS methods and makes MALDI an important tool for assessing drug localization. For example, analysis of olanzapine within liver tissue sections using MALDI-HR-MS provided relative quantification data that correlated with LC-LR-MS/MS of individual tissue segments with an accuracy of 14% (Figure 1.6).[139] Through the addition of an internal standard, MALDI-MS is able to quantify both drug and metabolite analytes within the treated tissue while also enhancing their stability during storage.[133]

The removal of complex sample preparation allows for automated sample processing. The quantification of cyclosporin in whole blood was performed by MALDI-HR-MS following an automated and rapid liquid/liquid extraction.[138] The LOD and accuracy for cyclosporin

achieved by MALDI-HR-MS was superior to immunoassay methods; the conventionally accepted method for monitoring cyclosporin.[138] Selectivity was also enhanced, in comparison to immunoassay, as superior analyte specificity was attained by MALDI-HR-MS, differentiating between the drug molecule and its metabolites to reduce both false positive and false negative results.[138]

1.7.2.3 Quantitative imaging capabilities of matrix assisted laser desorption ionization

MALDI-MS surface analysis provides both quantitative and analyte localization information that is not accessible by chromatographic techniques. Assignment of an analyte to a specific tissue region is beneficial for pharmaceutical discovery and development because it provides better ADME analysis. However, it does require excision of the tissue of interest from the specimen/patient. MALDI-MS imaging is able to achieve micrometer resolution, providing a highly precise representation of analyte distribution.[140, 141] In the study of erlotinib within a rat animal model, MALDI-HR-MS enabled the profiling of erlotinib in liver, spleen, and muscle samples.[141] The quantitative data showed that erlotinib was present at concentration of 5.73 ng per mg of liver tissue, which is beneficial for the treatment of liver cancer.[141] The data correlated with the LC-LR-MS/MS results after taking into account recovery.[141] The close association between LC-MS and MALDI-MS quantitative data highlights the benefits of MALDI-MS analysis, including speed, minimal sample carryover, tolerance for salts and application in imaging.[141] The main drawback of MALDI-MS analysis is the requirement of a matrix, which introduces a required sample preparation step and the potential for interference.[140]

1.7.3 Ambient environment desorption ionization techniques

Analysis of pharmaceuticals by DI mass spectrometry techniques within an ambient environment does not require sample preparation or the addition of matrix, thereby removing limitations associated with other ionization techniques.[142] The techniques of DESI and DART ionization are two of the most widely utilized ambient environment desorption techniques. Although both desorb analytes from a surface, DESI utilizes the principles of ESI to achieve ionization while DART utilizes the principles of atmospheric-pressure chemical ionization.[142-144] The location of the sample and the mechanism of desorption utilized by these ionization techniques minimizes sample carry-over and offers the possibility of using these techniques to determine the localization a molecule on a flat surface; including sectioned tissue samples.[82, 144]

In addition, the elimination or minimization of sample preparation provides considerable benefits over conventional quantitative and imaging techniques. Some DI methods, however, have utilized simple sample preparation methods to improve the limit(s) of detection; achieving limits comparable to chromatographic-MS methods.[142, 144] Although several ambient environment DI techniques exist, this section will focus on the application of DESI, a widely used ambient ionization technique.

DESI's close relation to ESI results in both ionization methods producing identical protonated/deprotonated ionic species.[82] This was demonstrated by the analysis of 21 different pharmaceutical formulations by DESI-MS, where the ions behaved in an identical manner to the ions produced by ESI.[145] The similarities between DESI and ESI ionization mechanisms allows for DESI analysis to take advantage of MS and MS/MS spectra libraries produced by ESI; beneficial for both qualitative and quantitative analysis.[145] Correlating DESI data to previously developed spectral libraries simplifies data analysis, demonstrating that DESI data can be both rapidly acquired and evaluated.

DESI-MS, like MALDI-MS, is rapid in nature due to the absence of chromatographic separation and the high rate of data acquisition provided by mass spectrometry. Data acquisition can be less than ten seconds per sample, confirming the identity of an analyte by both MS and MS/MS analysis.[145] For the quantification of propranolol, a small molecule that acts as a β-blocker, DESI-LR-MS/MS analysis utilized a scan time of less than 10 seconds, per sample, and provided a 10 nM LOD and a dynamic linear range extending to 100 μM.[146] In addition, validation parameters demonstrated that DESI-LR-MS/MS can be successfully employed for high-throughput quantitative analysis.[146] These DI techniques, however, provide time saving benefits over other mass spectrometric ionization techniques because they do not require the sample to be maintained under high vacuum and only require (simple) sample preparation.[147]

The removal of sample preparation has three distinct benefits; reducing analysis time, decreasing sample contamination, and minimizing variables associated with sample introduction. DESI has been applied to the quantification of low-molecular weight analytes within biological fluids, achieving ng/mL LOD, without utilizing any sample preparation. The use of isotope labeled internal standards resulted in USFDA validation parameters being satisfied. The widest application of ambient DI analysis without sample preparation is the analysis of pills and capsules, where they are directly placed on the sample stage and analyzed, providing

instantaneous feedback on the pharmaceuticals composition.[82, 145, 148, 149] The rapid analysis provides the ability to analyze more samples, a feature that is particularly important for the detection of counterfeit drugs.

In a similar manner to MALDI, ambient environment DI techniques can be used for quantitative spatial imaging. The qualitative and quantitative two dimensional spatial distribution of an analyte is valuable information for drug discovery and development process because it correlates information about metabolism and cellular localization.[82] Although the absolute quantification of an analyte requires the addition of an internal standard, the additional sample preparation step, when performed properly, maintains the sample integrity.[150] Clozapine quantification by DESI-HR-MS within rat coronal brain sections showed the localization of clozapine within the lateral ventricles 45 minutes after dosing with concentrations varying between 0.2 to 1.2 ng in individual brain sections.[150] LC-LR-MS/MS analysis confirmed the results obtained by DESI-HR-MS, however, the amount of time required to perform LC-MS/MS analysis of individual sections was longer.[150] The ability of DESI-MS to deliver information on an analytes concentration and spatial distribution makes it a very valuable high-throughput method for MS analysis.[150]

1.7.4 Ion analysis

The quantitative capabilities of mass spectrometry do not rely solely upon analyte ionization, but the complementary nature of ionization and the ion separation methodologies (i.e., mass analyzers). The fast ion analysis required by high-throughput quantitative methods is possible due to the advances in the rate of analysis provided by mass analyzers. Both high and low resolution mass analyzers are able to achieve scan rates that produces the number of scans required for USFDA method validations. The benefit of MS/MS analysis is the specificity it achieves by monitoring the transition of a precursor ion to its product ion(s).[151] HR-MS has the ability to achieve high spectral resolution, allowing for a *m/z* value to be correlated with potential molecular formulae, providing an additional level of specificity and allowing for analyte identification.[151, 152]

1.7.5 Single stage mass spectrometry quantification using high resolution instruments

Advances in the field of mass spectrometry have produced dramatic improvements in the resolution of mass spectrometers.[153] The rapid acquisition of quantitative data with high mass

accuracy is often attained through the use of either an orbitrap or time of flight (TOF) mass analyzers, both are capable of producing quantitative data without comprising resolution. The association of HR-MS peaks to molecular formulae facilitates the identification of precursor molecules and their metabolites.[69] For example, the application of qualitative-quantitative workflows on orbitrap instruments resulted in both the quantification of drug molecules with LLOQ comparable to those achieved on QQQ-MS/MS instruments in addition to providing molecular formula assignment of metabolites.[154]

The use of HR-MS for quantitative analysis requires that the rate of data acquisition be optimized in order to achieve the requirements of the quantification process.[153] For example, on an orbitrap instrument an increase in the monitored *m/z* range results in the acquisition time being lengthened or the resolution and resolving power of the instrument being decreased. A potential result is that an increase in the acquisition time will negatively influence the number of data points collected while a reduction in peak resolution will reduce the accuracy of the measured m/z values, both having a deleterious effect on quantitative data. Therefore, validation of a HR-MS quantification method, like LR-MS(/MS), requires optimal and reproducible chromatographic or chromatographic-like peak shape, and a minimum of 10 data acquisition points across the peaks needed to properly define the eluting components.[155]

The ability of FC to generate optimal peak shape through the use of short columns or guard columns allows HR-MS to achieve a minimum of 10 data points across a chromatographic peak. The reproducible peak shape achieved by FC-HR-MS enhances the accuracy and precision of HR-MS methods, which can provide quantitative data within an 18 second period of analysis.[156] For example, five tricyclic amines, utilized as physiotropic pharmaceuticals, were quantified within fortified human plasma by a FC-HR-MS.[156] The TOF mass analyzer's high resolution capabilities provided mass accuracy values less than 10 parts per million (PPM), using two point internal calibrations, and satisfied all the requirements of USFDA method validation; with an LOD between 1 and 2 ng/mL.[156] Although four of the five tricyclic amines achieved quantitative results comparable to LC-HR-MS, the quantification of desipramine by FC-HR-MS achieved a limit of quantification 5x lower than LC-HR-MS.[156, 157]

The ability of HR mass analyzers to provide quantitative data within a very short elution window is also applicable to FIA-HR-MS, where applications that utilize multiple autosamplers are able to achieve analysis of eight individual samples in the short period of forty-five

seconds.[158] A limitation of high throughput methods, however, is that they are susceptible to ion suppression due to an increase in matrix effects from co-eluting molecules.[78] This can result in a higher limit of quantification and unsatisfactory linear range, precision and accuracy. However, with changes in sample preparation and/or analyte detection, it is possible for the quantitative outcomes of FIA-HR-MS to be similar to LC-HR-MS because of the specificity it provides.[78] To minimize interference produced by the matrix, an optimization of the resolution and resolving power of HR-MS instruments is required, allowing for the separation and identification of isobaric ions. For example, the analysis of a drug mixture of 17 analytes (including isobaric analytes that differed by 8.8 to 23.5 mDa) by a TOF-MS, demonstrated the ability of FIA-HR-MS to resolve and identify isobaric ions (Figure 1.7).[159]

The application of HR-MS to the quantification of pharmaceutical excipients within a formulation, has allowed for an assessment of quality control and assurance. PEG is a widely utilized excipient and as a result numerous methods have been evaluated for its quantification.[160-163] FIA-HR-MS allowed the concurrent resolution and quantification of different PEG oligomer fractions.[164] The limits of quantification are superior to those achieved by conventional quantification methods for PEG without chromatographic separation. [164] PEG can be differentiated from other non-PEG components using HR-MS analysis by selectively monitoring the ions that match the *m/z* of each PEG oligomer.[164] The Specificity of HR-MS allowed for the quantification of PEG oligomer within urine matrices; a matrix that is much more complex than a pharmaceutical formulation.[165]

The HR-MS data acquired across a specific mass range not only allows for the quantitative analysis of analytes but also for mining of the spectra for metabolites, degradation products, and contaminants.[100] For example, triclosan metabolites that had undergone combinations of sulfonation, hydroxylation, and glucuronidation were identified using HR-MS.[166] The inference of each biotransformation relies upon the exact mass measurements provided by HR-MS, allowing for the determination of the analytes' molecular formula; however, it does not provide information on the analytes' molecular structures.

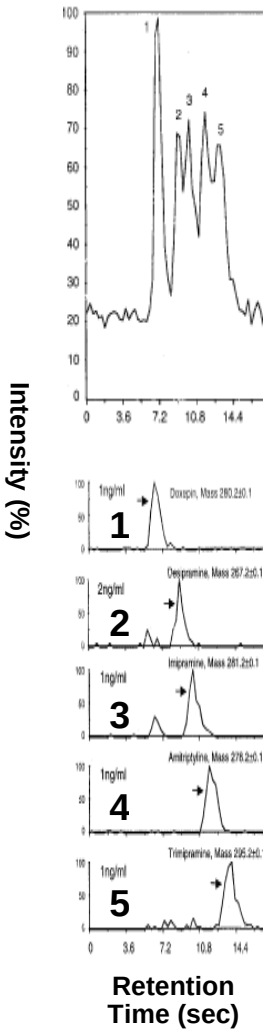

Figure 1.7 Total ion chromatogram and extracted ion chromatograms of the five tricyclic amines, doxepin (1), desipramine (2), imipramine (3), amitriptyline (4) and trimipramine (5) in human plasma extract obtained from their FC-MS elution on a SB-C18 column (15 × 2.1 mm i.d.). Adapted and used with permission from reference 159.

1.7.6 Multistage mass spectrometric quantification using low resolution instruments

MS^n provides structural information by fragmenting precursor ions into their unique product ions, thus resulting in a distinctive spectral fingerprint for quantitative[125, 167, 168] and qualitative analysis.[169-171] The consistent production of unique MS^n spectra provides a means to correlate molecular authenticity to quantitative analysis of active drugs, excipients, and metabolites as well as allowing for structural elucidation.[172] MS/MS, the simplest MS^n experiment, enable the differentiation of closely related analytes by monitoring specific

fragment ions of precursor ions.[173] Analytes that are both structurally related and unrelated can be detected and quantified as well as structurally confirmed via MRM analysis.[173] The ability of MS/MS to minimize interferences from isobaric molecules, molecules that share nominal molecular masses, through MS/MS analysis is a significant benefit over single stage MS.[174] An MS/MS method has been developed to quantify creatine levels within blood to diagnose patients that suffer from primary creatine disorders.[175] The quantification of creatine is difficult because it shares the nominal mass of 131 with leucine and isoleucine, that can also be present in blood samples.[175] The application of MS/MS allowed for creatine to be differentiated from leucine and isoleucine, with no inference being observed within blood samples spiked with μM concentrations of leucine and isoleucine; demonstrating the robust nature of MS/MS detection.[175] Discriminating between each analyte is accomplished using their unique fragment ions.[175] In addition, the butyl ester metabolites of creatine, leucine and isoleucine, which share the nominal mass of 187, were detected and differentiated from one another using MS/MS.[175]

The robust nature of MS/MS produces valid results that display continuity over an extended period of time. An evaluation of MS/MS reproducibility showed that the performance of a single instrument was consistent over a four year period despite contamination, maintenance, and increased usage.[176] In addition, MS/MS spectra were reproducible and consistent between both identical instruments and instruments supplied by different vendors.[176] The consistency is valid for both the analyte's fragment ions and the intensity of those fragment ions when instruments were correctly tuned and standardized.[176] Such results indicate the specificity provided by MS/MS is universal, allowing for the compilation of reference libraries for compound searches.

1.7.7 Quantification using High-field asymmetric waveform ion mobility spectrometry

One disadvantage of MS is that isomeric ions cannot be separated using single stage HR-MS, while MS/MS is not always able to differentiate them.[177] The inability of mass spectrometry to resolve such ions leads to ambiguity in the interpretation of MS or MS/MS data. For example, differentiation of the isomers leucine and isoleucine within full scan MS is not possible and will lead to the uncertain assessment of each diasteroisomer's fragment ions.[177] Chromatographic separation aims to alleviate such issues, however, this may not be possible for closely related molecules, including diastereoisomers. The application of ion mobility techniques, which operate

at atmospheric pressure, allows not only the differentiation of ions but also facilitates their identification based on their respective ion mobilities (a function of size and charge) and *m/z* values when coupled to MS.[177] Ion mobility spectrometry separates ions based on changes in ion mobility between low and high electric fields by applying a high voltage asymmetric waveform between two electrodes. [178] The benefits of FAIMS over traditional separation methods is its ability to rapidly, at atmospheric pressure, separate, focus, and/or trap ions.[179]

The separation of ions within a FAIMS instrument relies upon the application of a high voltage waveform between two metal plates.[179] The applied high voltage waveform causes ion dependent changes in mobility that can be offset by a direct current offset voltage; referred to as the compensation voltage. At a given compensation voltage, some ions will drift toward and impact one of the metal plates, resulting in their neutralization, while other ions are focused between the two plates because the compensation voltage offsets the difference in mobility. This results in those ions not migrating toward either plate.[179] Those ions that are focused between the plates can be transmitted or ejected from the FAIMS device.[179] A FAIMS instrument can also ramp its electric field strength to separate co-eluting analytes prior to their analysis, reducing the spectral interference observed during MS.[180]

Appling FAIMS prior to MS analysis allows for the separation of ions into individual packets of ions, by setting a constant compensation voltage, thereby reducing the spectral interference observed during MS.[180] For example, the quantification of norverapamil in the presence of verapamil within urine samples resulted in mass spectrometry interferences that negatively affected the LLOQ (Figure 1.8).[181] However, the use of FAIMS resulted in spectra and chromatographs that presented less interference, producing chromatographic peaks that were easier to integrate (Figure 1.8).[181] Similarly, over-estimation of the concentration of the amine-drug candidate occurs because the amine drug candidate and its N-oxide metabolite co-eluted during MS-analysis.[182] The use of FAIMS allowed for the efficient separation of the N-oxide metabolite and more accurate quantification of both drug and metabolites (Figure 1.8). [182]
In addition, FAIMS' ability to separate co-eluting analytes has led to its application in FIA-FAIMS-MS as it could reduce interferences that are present during conventional FIA-MS analysis. For example, the quantification of morphine and codeine within human urine by ESI-FAIMS-MS provided a linear dynamic range extending over two orders of magnitude with a LOD of 60 ng/mL and 20 ng/mL, respectively.[183] These results were achieved without the

addition of any internal standard or sample preparation, demonstrating the ability of FAIMS to minimize background interference.[183] Regardless of which mode of analysis is used, FAIMS can assist in the quantification of small molecule analytes by mass spectrometry through a reduction in interfering ions entering the mass spectrometer and by providing the added property of ion mobility for differentiating analytes from one another. [180]

1.8 Perspectives on the application of high-throughput mass spectrometry to the quantitative analysis of small molecules

The recent advancements in high-throughput MS analysis allowed for the procurement of data that is, in many cases, comparable if not better than conventional quantification methods.

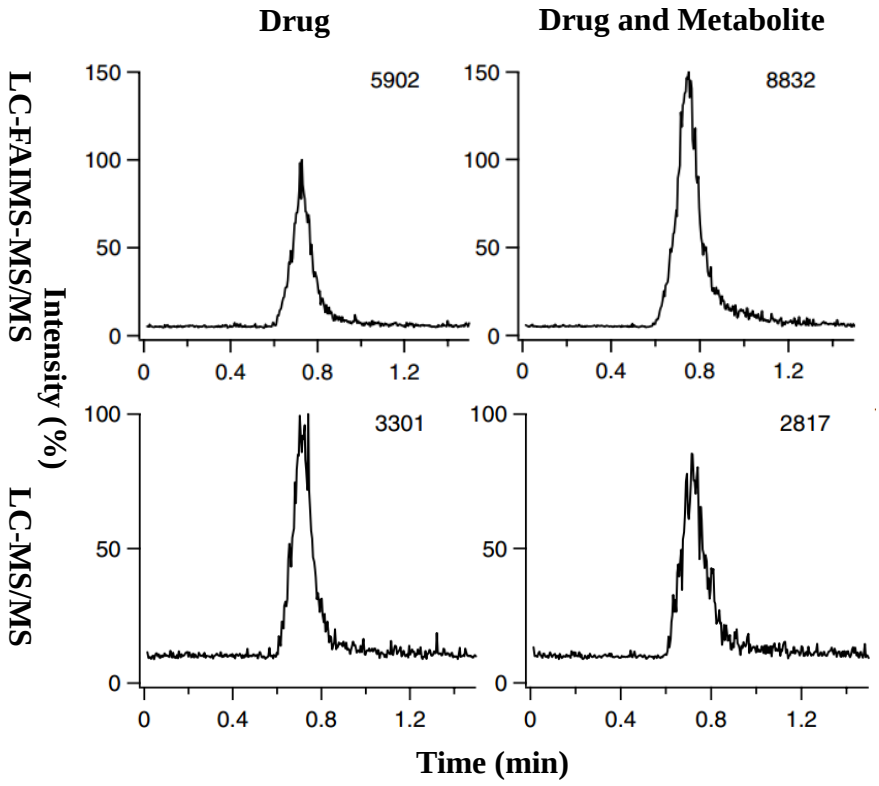

Figure 1.8 Representative chromatographs obtained by LC-LR-MS/MS and LC-FIAMS-MS/MS for an amine compound at 25 ng/mL and a mixture of the amine compound and its metabolite at 25 and 2500 ng/mL, respectively. For LC-LR-MS/MS, the metabolite adds to the peak area of the drug resulting in an erroneously high concentration determination. During LC-FAIMS-MS/MS, however, the presence of the metabolite does not affect the peak area of the drug. Adapted from reference 182 with permission.

Application of these methods to the quantification of small drug molecules within an array of matrices, from solutions to tissue slices, has demonstrated the versatility of MS. Through the implementation of such technology, the pharmaceutical industry has realized the benefit of high-throughput MS, namely a reduction in analysis time, reduction of operating costs, and decrease in sample contamination.

Realizing the advantages of high-throughput methods, the pharmaceutical industry is beginning to transition away from solely utilizing conventional quantification techniques. The ability of high-throughput MS methods to achieve quantitative results in a shorter period of time than LC is their primary advantage. This has a twofold benefit, first allowing for faster decision making based on the results and second it provides important cost savings. The enhanced economy can be attributed to a shorter analysis as well as a reduction and/or simplification in the sample preparation. As a result, the chance of sample contamination and degradation is decreased, thereby improving data quality.

The aptitude of all of high-throughput MS-based methodologies is their ability to rapidly analyze samples; balancing data volume with system performance to achieve the desired level of quantification. Data acquired by high-throughput mass spectrometric analysis provides the advantage of traditional quantification techniques, but some methods have the added benefit of spatial imaging and data mining. Spatial imaging and data mining provide quantitative results that more conclusively explain the fate of molecules though the further understanding of cellular deposition and metabolism. In addition, the data produced by high-throughput MS has the ability to enhance pharmaceutical research by providing additional information on analyte's cellular fate. The incorporation of high throughput MS techniques in the pharmaceutical industry will continue to expand as they provide confirmatory and complementary data in a rapid and sensitive fashion.

1.9 Purpose of research

1.9.1 Perspectives on the need to quantify diquaternary ammonium gemini surfactants

Non-viral gene therapy agents, such as diquaternary ammonium gemini surfactants, ensure cellular delivery of genetic material and its subsequent expression. They facilitate transfection through the formation of a lipoplex around the genetic material that protects it from degradation, assists with cellular uptake, and allows for its subcellular release. There are

numerous studies demonstrating the effective use of diquaternary ammonium gemini surfactants for both *in vivo* and *in vitro* applications.[48, 54] However, to my knowledge, no post transfection quantitative evaluation of diquaternary ammonium gemini surfactants has been undertaken. The need for post transfection evaluation of diquaternary ammonium gemini surfactants' cellular fate stems from their intended use for gene delivery applications, which is heavily regulated. An understanding of the post transfection concentration of gemini surfactants is required because they are new molecular entities governed by the statutes similar to new drug entities; requiring an understanding of their quality, efficacy, and safety.

1.9.2 Perspectives on the need to develop mass spectrometric methods for the quantification of diquaternary ammonium gemini surfactants

MS was chosen for the quantification of diquaternary ammonium gemini surfactants because their structure lacks both a chromophore and fluorophore. Instead, diquaternary ammonium gemini surfactants contain two quaternary ammonium functional groups; each of which possess a permanent positive charge that is ideal for MS analysis. In addition, MS/MS is a very sensitive method that provides a high level of specificity and selectivity by monitoring for specific precursor ion → fragment ion transitions. The selection and detection of the specific *transition* is reliant upon both the method of ionization and the mass analyzer(s).

Validating and comparing several MS-based methods for the quantification of gemini surfactants was undertaken for two reasons. First, the application of quantitative MS or MS/MS methods to the post-transfection evaluation of G16-3 will allow for an assessment of its cellular concentration so that cellular uptake and degradation can be monitored. Second, it is the first comparative study, to my knowledge, of five different MS quantification methods: LC-LR-MS/MS, FC-HR-MS, FC-LR-MS/MS, MALDI-HR-MS, and DESI-LR-MS/MS. These five methods will be compared to one another based upon preparation time, run time, limit of quantification, linearity, accuracy, precision, sample complexity, and cost. Understanding the advantages and disadvantages of each method for the quantification of G16-3 within murine epidermal keratinocyte cells (PAM212) will allow for selection of the optimal method. In addition, this study will provide a valuable comparison of these MS-based methods that can be applied to the development of quantitative methods for other small molecules. The comparison of each validated quantification method to one another provides support for choosing the most advantageous method for quantification within PAM212 cell lysate. Validation of each

quantitative MS-based method complied with the USFDA's criteria for bioanalytical method validation; including recovery, specificity, sensitivity, accuracy, precision and stability. The purpose of performing a method validation is to demonstrate the reliability of using the method for the measurement of analyte concentrations within the biological matrix.

1.9.3 Rationale for research

In order to develop diquaternary ammonium gemini surfactants as carriers for gene delivery, an evaluation of their safety, including an understanding of their post transfection fate, is required. An assessment of diquaternary ammonium gemini surfactants' safety requires analytical methods that specifically, selectively, and sensitively identify and/or quantify these analytes. The choice of MS for this task stems from the nature of the diquaternary ammonium gemini surfactants, containing two permanent cationic entities within their structure. In addition, MS is specific and selective, and allows for the differentiation of molecules based upon their unique MS/MS fragmentation behavior. Each MS-based method will be evaluated based on its own analytical merits to identify and differentiate diquaternary ammonium gemini surfactant, allowing for their quantitative analysis.

The mass spectrometry behavior of these diquaternary ammonium gemini surfactants has not been previously elucidated. Therefore, an understanding of their MS, MS/MS, and quasi MS^3 behavior will confirm their molecular structure and will ensure the selection of the most specific and selective *m/z* signatures during MS(/MS) analysis, allowing for the identification of these analytes within, theoretically, any biological sample. Second, the development of several MS-based quantification methods will ensure that the most efficient, sensitive, and selective method is applied to the evaluation of diquaternary ammonium gemini surfactants. In addition, the ease of method development, efficacy of each method as well as the inherent advantages and disadvantages of each method will be evaluated..

1.9.4 Hypotheses

1.9.4.1 Structural confirmation and identification of diquaternary ammonium gemini surfactants by MS/MS analysis

Hypothesis: The structural similarities between diquaternary ammonium gemini surfactants result in their analogous dissociation, in both fragment structure and pathway

sequence, allowing for the establishment of a universal fragmentation pattern for all 29 evaluated molecules.

The MS/MS dissociation behavior and structural confirmation of each diquaternary ammonium gemini surfactant has been assessed using both a QQQ-MS and quadrupole time of flight mass spectrometer (Q-ToF-MS). High resolution full scan mass spectrometric analysis and MS/MS were applied. HR-MS (i.e., Q-ToF-MS) provided information about the molecular composition of the analyte, while the fragmentation pattern of each surfactant confirmed the proposed structure. Quasi MS^3 analysis, using a QQQ-MS, was employed because of the lack of available trapping instruments that could perform MS^n analysis. Quasi MS^3 analysis confirmed the fragmentation pathways by tracing the origin of each product ion. In addition, the MS analysis will assist in the identification of suitable fragment ions for multiple reaction monitoring (MRM) MS/MS quantitative analysis.

Two specific goals are achieved for each diquaternary ammonium gemini surfactant:

- Confirmation of the molecular structures of the gemini surfactants' using MS, MS/MS, and quasi MS^3 analysis
- Establishment of a universal MS/MS fingerprint

1.9.4.2 Development and validation of five mass spectrometry methods for the quantification of diquaternary ammonium gemini surfactant G16-3 within PAM212 cell lysate

Hypothesis: LC-LR-MS/MS analysis is the most effective quantitative method for the quantification of G16-3 within PAM212 cellular lysate achieving the lowest lower limit of quantification (LLOQ).

LC-LR-MS/MS is highly utilized by the pharmaceutical industry for the quantification of small molecules; including metabolites and degradation products.[69, 70, 99] The prevalence of LC-MS/MS is a result of the ability of mass spectrometry to act as a highly selective and specific method of detection by identifying ionizable analyte(s). Similarly, LC is able to selectively separate an analyte(s) from molecules that may interfere with its detection. The lengthy time of analysis, however, is a prominent disadvantage of LC and led us to compare quantitative LC-MS/MS analysis to other high throughput mass spectrometric methods. Five different MS-based

quantification methods for G16-3 were developed, evaluated, and validated. G16-3 was chosen as a model compound because of the high transfection efficiency as previously demonstrated.[56, 57]

Two specific goals will be achieved during the development/evaluation/validation of each quantitative method:

- The development, evaluation, and/or validation of G16-3 quantification method for the following methods:
    - LC-LR-MS/MS (validated)
    - FC-LR-MS/MS (validated)
    - FC-HR-MS (validated)
    - MALDI-HR-MS (validated)
    - DESI-LR-MS/MS (validated)
    - FC-FAIMS-LR-MS/MS) (evaluated)
- A comparison of the five validated MS methods to determine the competitive advantages and disadvantages of each method.

1.9.4.3 Assessing post-transfection concentration of G16-3 within PAM212 cell lysate

Hypothesis: The concentration of gemini surfactant, G16-3, within PAM212 cellular lysate, displays an increase in concentration during incubation with the transfection solution and will decline in concentration from the maximal value after removal of the transfection solution due to transformation within the PAM212 cells.

Gene transfection into mammalian cells has been demonstrated using gemini surfactants that include alkyl spacers,[56, 57] amino substituted spacers,[184] and amino acid[185] substituted spacers. Previous work, however, did not track the post-transfection cellular concentration of gemini surfactants.[56, 57] Previously reported transfection studies focused on the toxicity and transfection efficacy. [56, 57] The developed mass spectrometry quantification methods, however, allow for insight into the cellular concentrations of gemini surfactants post-transfection. All validated mass spectrometry quantification methods will be used to measure the total amount of intact G16-3 within cellular lysate post-transfection time points, allowing for an assessment of the change in G16-3 concentration over time.

The following specific goal will be achieved for the G16-3 gemini surfactant:

- Application of the mass spectrometry quantification methods to the assessment of the post-transfection concentration of G16-3 within PAM212 cellular lysate

1.10 Literature cited

1. Trusheim M, Aitken ML, Berndt ER 2010. Characterizing Markets for Biopharmaceutical Innovations: Do Biologics Differ from Small Molecules? Forum for Health Economics and Policy 13:1-43.

2. Goeddel DV, Kleid DG, Bolivar F, Heyneker HL, Yansura DG, Crea R, Hirose T, Kraszewski A, Itakura K, Riggs AD 1979. Expression in Escherichia coli of chemically synthesized genes for human insulin. Proceedings of the National Academy of Sciences 76:106-110.

3. Thomas A, Schänzer W, Delahaut P, Thevis M 2009. Sensitive and fast identification of urinary human, synthetic and animal insulin by means of nano-UPLC coupled with high-resolution/high-accuracy mass spectrometry. Drug Testing and Analysis 1:219-227.

4. Deuter CM, Zierhut M, Möhle A, Vonthein R, Stöbiger N, Kötter I 2010. Long-term remission after cessation of interferon-α treatment in patients with severe uveitis due to Behçet's disease. Arthritis & Rheumatism 62:2796-2805.

5. Gragoudas ES, Adamis AP, Cunningham Jr ET, Feinsod M, Guyer DR 2004. Pegaptanib for neovascular age-related macular degeneration. New England Journal of Medicine 351:2805-2816.

6. Morales A, Phadke K, Steinhoff G 2009. Intravesical mycobacterial cell wall-DNA complex in the treatment of carcinoma in situ of the bladder after standard intravesical therapy has failed. The Journal of urology 181:1040-1045.

7. Hacein-Bey-Abina S, Garrigue A, Wang GP, Soulier J, Lim A, Morillon E, Clappier E, Caccavelli L, Delabesse E, Beldjord K 2008. Insertional oncogenesis in 4 patients after retrovirus-mediated gene therapy of SCID-X1. The Journal of clinical investigation 118:3132-3142.

8. Naldini L 2001. Viral vectors for gene therapy: the art of turning infectious agents into vehicles of therapeutics. Nature medicine 7:33-40.

9. Heilbronn R, Weger S 2010. Viral vectors for gene transfer: current status of gene therapeutics. Drug delivery 197:143-170.

10. Kotin RM 1994. Prospects for the use of adeno-associated virus as a vector for human gene therapy. Human Gene Therapy 5:793-801.

11. Hacein-Bey-Abina S, Hauer J, Lim A, Picard C, Wang GP, Berry CC, Martinache C, Rieux-Laucat F, Latour S, Belohradsky BH 2010. Efficacy of gene therapy for X-linked severe combined immunodeficiency. New England Journal of Medicine 363:355-364.

12. McClane SJ, Chirmule N, Burke CV, Raper SE 1997. Characterization of the immune response after local delivery of recombinant adenovirus in murine pancreas and successful strategies for readministration. Human Gene Therapy 8:2207-2216.

13. Chirmule N, Propert K, Magosin S, Qian Y, Qian R, Wilson J 1999. Immune responses to adenovirus and adeno-associated virus in humans. Gene therapy 6:1574-1583.

14. Kay MA, Yant S 2011. Enhanced sleeping beauty transposon system and methods for using the same US Patent 7,985,739.

15. Robbins PD, Ghivizzani SC 1998. Viral vectors for gene therapy. Pharmacology & therapeutics 80:35-47.

16. Beyerle A, Kissel T, Stoeger T. 2011. Toxicity of Polymeric-Based Non-Viral Vector Systems for Pulmonary siRNA Applications. In Yuan X., editor. Non-Viral Gene Therapy, Rijeka, Croatia: InTech. p 481.

17. Uchida S, Itaka K, Chen Q, Osada K, Ishii T, Shibata M, Harada-Shiba M, Kataoka K 2012. PEGylated polyplex with optimized PEG shielding enhances gene introduction in lungs by minimizing inflammatory responses. Molecular Therapy 20:1196-1203.

18. Rettig GR, Rice KG 2007. Non-viral gene delivery: from the needle to the nucleus. Expert Opinion on Biological Therapy 7:799-808.

19. Schmidt-Wolf GD, Schmidt-Wolf IG 2003. Non-viral and hybrid vectors in human gene therapy: an update. Trends in Molecular Medicine 9:67-72.

20. Tros de Ilarduya C, Sun Y, Düzgüneş N 2010. Gene delivery by lipoplexes and polyplexes. European Journal of Pharmaceutical Sciences 40:159-170.

21. Felgner PL, Gadek TR, Holm M, Roman R, Chan HW, Wenz M, Northrop JP, Ringold GM, Danielsen M 1987. Lipofection: a highly efficient, lipid-mediated DNA-transfection procedure. Proceedings of the National Academy of Sciences 84:7413-7417.

22. Wu GY, Wu CH 1987. Receptor-mediated in vitro gene transformation by a soluble DNA carrier system. The Journal of Biological Chemistry 262:4429-4432.

23. Felgner PL, Ringold G 1989. Cationic liposome-mediated transfection. Nature 337:387-388.

24. Stiehler M, Duch M, Mygind T, Li H, Ulrich-Vinther M, Modin C, Baatrup A, Lind M, Pedersen FS, Bünger CE 2007. Optimizing viral and non-viral gene transfer methods for genetic modification of porcine mesenchymal stem cells. Tissue Engineering 585:31-48.

25. Aravindan L, Bicknell KA, Brooks G, Khutoryanskiy VV, Williams AC 2009. Effect of acyl chain length on transfection efficiency and toxicity of polyethylenimine. International Journal of Pharmaceutics 378:201-210.

26. Florea BI, Meaney C, Junginger HE, Borchard G 2002. Transfection efficiency and toxicity of polyethylenimine in differentiated Calu-3 and nondifferentiated COS-1 cell cultures. AAPS PharmSci 4:1-11.

27. Itaka K, Ishii T, Hasegawa Y, Kataoka K 2010. Biodegradable polyamino acid-based polycations as safe and effective gene carrier minimizing cumulative toxicity. Biomaterials 31:3707-3714.

28. Boussif O, Lezoualc'h F, Zanta MA, Mergny MD, Scherman D, Demeneix B, Behr J 1995. A versatile vector for gene and oligonucleotide transfer into cells in culture and in vivo: polyethylenimine. Proceedings of the National Academy of Sciences 92:7297-7301.

29. O'Malley BW, Li D, McQuone SJ, Ralston R 2009. Combination Nonviral Interleukin-2 Gene Immunotherapy For Head and Neck Cancer: From Bench Top to Bedside. Laryngoscope 115:391-404.

30. Hoffman DM, Figlin RA 2000. Intratumoral interleukin 2 for renal-cell carcinoma by direct gene transfer of a plasmid DNA/DMRIE/DOPE lipid complex. World Journal of Urology 18:152-156.

31. Horton HM, Dorigo O, Hernandez P, Anderson D, Berek JS, Parker SE 1999. IL-2 plasmid therapy of murine ovarian carcinoma inhibits the growth of tumor ascites and alters its cytokine profile. The Journal of Immunology 163:6378-6385.

32. Moghimi S, Szebeni J 2003. Stealth liposomes and long circulating nanoparticles: critical issues in pharmacokinetics, opsonization and protein-binding properties. Progress in Lipid Research 42:463-478.

33. Roy I, Mitra S, Maitra A, Mozumdar S 2003. Calcium phosphate nanoparticles as novel non-viral vectors for targeted gene delivery. International Journal of Pharmaceutics 250:25-33.

34. Zhang S, Zhao B, Jiang H, Wang B, Ma B 2007. Cationic lipids and polymers mediated vectors for delivery of siRNA. Journal of Controlled Release 123:1-10.

35. Buñuales M, Düzgüneş N, Zalba S, Garrido MJ, de ILarduya CT 2011. Efficient gene delivery by EGF-lipoplexes in vitro and in vivo. Nanomedicine 6:89-98.

36. Lasic DD. 1993. Liposomes: From Physics to Application, New York, New York, USA: Elsevier.

37. Chan C, Majzoub RN, Shirazi RS, Ewert KK, Chen Y, Liang KS, Safinya CR 2012. Endosomal escape and transfection efficiency of PEGylated cationic liposome–DNA complexes prepared with an acid-labile PEG-lipid. Biomaterials 33:4928-4935.

38. Meerovich GA, Meerovich IG, Pevgov VG, Lukyanets EA, Oborotova NA, Gurevich DG, Zorin AA, Derkacheva VM, Smirnova ZS, Loschenov VB 2008. Influence of liposome size on

accumulation in tumor and therapeutic efficiency of liposomal near-IR photosensitizer for PDT based on aluminum hydroxide tetra-3-phenylthiophthalocyanine. Nanotech 2:41-44.

39. Oliveira AC, Ferraz MP, Monteiro FJ, Simões S 2009. Cationic liposome–DNA complexes as gene delivery vectors: Development and behaviour towards bone-like cells. Acta Biomaterialia 5:2142-2151.

40. Billiet L, Gomez J, Berchel M, Jaffrès P, Le Gall T, Montier T, Bertrand E, Cheradame H, Guégan P, Mével M 2012. Gene transfer by chemical vectors, and endocytosis routes of polyplexes, lipoplexes and lipopolyplexes in a myoblast cell line. Biomaterials 33:2980-2990.

41. Immordino ML, Dosio F, Cattel L 2006. Stealth liposomes: review of the basic science, rationale, and clinical applications, existing and potential. International Journal of Nanomedicine 1:297-315.

42. Maruyama K, Kennel SJ, Huang L 1990. Lipid composition is important for highly efficient target binding and retention of immunoliposomes. Proceedings of the National Academy of Sciences 87:5744-5748.

43. Gabizon A, Catane R, Uziely B, Kaufman B, Safra T, Cohen R, Martin F, Huang A, Barenholz Y 1994. Prolonged circulation time and enhanced accumulation in malignant exudates of doxorubicin encapsulated in polyethylene-glycol coated liposomes. Cancer Research 54:987-992.

44. Menger FM, Littau CA 1991. Gemini-surfactants: synthesis and properties. Journal of the American Chemical Society 113:1451-1452.

45. Menger FM, Keiper JS 2000. Gemini surfactants. Angewandte Chemie International Edition 39:1906-1920.

46. Wang C, Li X, Wettig SD, Badea I, Foldvari M, Verrall RE 2007. Investigation of complexes formed by interaction of cationic gemini surfactants with deoxyribonucleic acid. Physical Chemistry Chemical Physics 9:1616-1628.

47. Fielden ML, Perrin C, Kremer A, Bergsma M, Stuart MC, Camilleri P, Engberts JBFN 2001. Sugar-based tertiary amino gemini surfactants with a vesicle-to-micelle transition in the endosomal pH range mediate efficient transfection in vitro. European Journal of Biochemistry 268:1269-1279.

48. Renouf P, Mioskowski C, Lebeau L, Hebrault D, Desmurs JR 1998. Dimeric surfactants: first synthesis of an asymmetrical Gemini compound. Tetrahedron Letters 39:1357-1360.

49. Gao T, Rosen MJ 1994. Dynamic surface tension of aqueous surfactant solutions. 6. Compounds containing two hydrophilic head groups and two or three hydrophobic groups and their mixtures with other surfactants. Journal of the American Oil Chemists' Society 71:771-776.

50. Esumi K, Goino M, Koide Y 1996. Adsorption and adsolubilization by monomeric, dimeric, or trimeric quaternary ammonium surfactant at silica/water interface. Journal of Colloid and Interface Science 183:539-545.

51. Wettig SD, Verrall RE, Foldvari M 2008. Gemini Surfactants: A New Family of Building Blocks for Non-Viral Gene Delivery Systems. Current Gene Therapy 8:9-23.

52. Garcia-Bennett AE, Williamson S, Wright PA, Shannon IJ 2002. Control of structure, pore size and morphology of three-dimensionally ordered mesoporous silicas prepared using the dicationic surfactant [CH 3 (CH 2) 15 N (CH 3) 2 (CH 2) 3 N (CH 3) 3] Br 2. Journal of Materials Chemistry 12:3533-3540.

53. Murguía MC, Vaillard VA, Sánchez VG, Conza JD, Grau RJ 2008. Synthesis, Surface-Active Properties, and Antimicrobial Activities of New Double-Chain Gemini Surfactants. Journal of Oleo Science 57:301-308.

54. David S, Pérez L, Infante MR 2002. Sequestration of bacterial lipopolysaccharide by bis (args) gemini compounds. Bioorganic & Medicinal Chemistry Letters 12:357-360.

55. Pino V, Baltazar QQ, Anderson JL 2007. Examination of analyte partitioning to monocationic and dicationic imidazolium-based ionic liquid aggregates using solid-phase microextraction–gas chromatography. Journal of Chromatography A 1148:92-99.

56. Badea I, Wettig S, Verrall R, Foldvari M 2007. Topical non-invasive gene delivery using gemini nanoparticles in interferon-γ-deficient mice. European Journal of Pharmaceutics and Biopharmaceutics 65:414-422.

57. Badea I, Verrall R, Baca-Estrada M, Tikoo S, Rosenberg A, Kumar P, Foldvari M 2005. In vivo cutaneous interferon-γ gene delivery using novel dicationic (gemini) surfactant–plasmid complexes. The Journal of Gene Medicine 7:1200-1214.

58. Bell PC, Bergsma M, Dolbnya IP, Bras W, Stuart MCA, Rowan AE, Feiters MC, Engberts J 2003. Transfection Mediated by Gemini Surfactants: Engineered Escape from the Endosomal Compartment. Journal of the American Chemical Society 125:1551-1558.

59. Kirby AJ, Camilleri P, Engberts J, Feiters MC, Nolte RJM, Soderman O, Bergsma M, Bell PC, Fielden ML, Rodriguez CLG 2003. Gemini Surfactants: New Synthetic Vectors for Gene Transfection. Angewandte Chemie International Edition 42:1448-1457.

60. Rosenzweig HS, Rakhmanova VA, MacDonald RC 2001. Diquaternary ammonium compounds as transfection agents. Bioconjugate Chemistry 12:258-263.

61. Wettig SD, Verrall RE 2001. Thermodynamic studies of aqueous m–s–m gemini surfactant systems. Journal of Colloid and Interface Science 235:310-316.

62. Matulis D, Rouzina I, Bloomfield VA 1999. Thermodynamics of cationic lipid binding to DNA and DNA condensation: roles of electrostatics and hydrophobicity. Colloid Polymer Science 112:71-75.

63. Camilleri P, Kremer A, Edwards AJ, Jennings KH, Jenkins O, Marshall I, Neville W, Rice SQ, Smith RJ, Wilkinson MJ 2000. A novel class of cationic gemini surfactants showing efficient in vitro gene transfection properties. Chemical Communications 2000:1253-1254.

64. Ryhanen SJ, Saily VMJ, Parry MJ, Luciani P, Mancini G, Alakoskela JMI, Kinnunen PKJ 2006. Counterion-controlled transition of a cationic gemini from submicroscopic to giant vesicles. Journal of the American Chemical Society 128:8659-8663.

65. Matti V, Säily J, Ryhänen SJ, Holopainen JM, Borocci S, Mancini G, Kinnunen PK 2001. Characterization of mixed monolayers of phosphatidylcholine and a dicationic gemini surfactant SS-1 with a langmuir balance: effects of DNA. Biophysical Journal 81:2135-2143.

66. Ryhänen SJ, Säily MJ, Paukku T, Borocci S, Mancini G, Holopainen JM, Kinnunen PK 2003. Surface charge density determines the efficiency of cationic gemini surfactant based lipofection. Biophysical journal 84:578-587.

67. Foldvari M, Badea I, Wettig S, Verrall R, Bagonluri M 2006. Structural characterization of novel gemini non-viral DNA delivery systems for cutaneous gene therapy. Journal of Experimental Nanoscience 1:165-176.

68. McGregor C, Perrin C, Monck M, Camilleri P, Kirby AJ 2001. Rational approaches to the design of cationic gemini surfactants for gene delivery. Journal of the American Chemical Society 123:6215-6220.

69. Ramanathan R, Jemal M, Ramagiri S, Xia YQ, Humpreys WG, Olah T, Korfmacher WA 2011. It is time for a paradigm shift in drug discovery bioanalysis: from SRM to HRMS. Journal of Mass Spectrometry 46:595-601.

70. Lindegardh N, Tarning J, Toi P, Hien T, Farrar J, Singhasivanon P, White N, Ashton M, Day N 2009. Quantification of artemisinin in human plasma using liquid chromatography coupled to tandem mass spectrometry. Journal of Pharmaceutical and Biomedical Analysis 49:768-773.

71. Shah VP, Midha KK, Findlay JWA, Hill HM, Hulse JD, McGilveray IJ, McKay G, Miller KJ, Patnaik RN, Powell ML 2000. Bioanalytical method validation—a revisit with a decade of progress. Pharmaceutical Research 17:1551-1557.

72. Kostiainen R, Kotiaho T, Kuuranne T, Auriola S 2003. Liquid chromatography/atmospheric pressure ionization–mass spectrometry in drug metabolism studies. Journal of Mass Spectrometry 38:357-372.

73. Lipsky MS, Sharp LK 2001. From idea to market: the drug approval process. The Journal of the American Board of Family Practice 14:362-367.

74. Yost RA, Enke CG 1977. Selected Ion Fragmentation with a Tandem Quadrupole Mass Spectrometer. Journal of the American Chemical Society 100:2274-2275.

75. Futrell JH, Miller C 1966. Tandem Mass Spectrometer for Study of Ion-Molecule Reactions. Review of Scientific Instruments 37:1521-1526.

76. Russell DH, Edmondson RD 1998. High-resolution mass spectrometry and accurate mass measurements with emphasis on the characterization of peptides and proteins by matrix-assisted laser desorption/ionization time-of-flight mass spectrometry. Journal of Mass Spectrometry 32:263-276.

77. Zhang NR, Yu S, Tiller P, Yeh S, Mahan E, Emary WB 2009. Quantitation of small molecules using high-resolution accurate mass spectrometers–a different approach for analysis of biological samples. Rapid Communications in Mass Spectrometry 23:1085-1094.

78. Hopfgartner G, Bourgogne E 2003. Quantitative high-throughput analysis of drugs in biological matrices by mass spectrometry. Mass Spectrometry Reviews 22:195-214.

79. Zhang NR, Yu S, Tiller P, Yeh S, Mahan E, Emary WB 2009. Quantitation of small molecules using high-resolution accurate mass spectrometers–a different approach for analysis of biological samples. Rapid Communications in Mass Spectrometry 23:1085-1094.

80. Dole M, Mack L, Hines R, Mobley R, Ferguson L, Alice M 1968. Molecular beams of macroions. The Journal of Chemical Physics 49:2240-2249.

81. Yamashita M, Fenn JB 1984. Electrospray ion source. Another variation on the free-jet theme. The Journal of Physical Chemistry 88:4451-4459.

82. Takats Z, Wiseman JM, Gologan B, Cooks RG 2004. Mass spectrometry sampling under ambient conditions with desorption electrospray ionization. Science 306:471-473.

83. Purves RW, Guevremont R 1999. Electrospray ionization high-field asymmetric waveform ion mobility spectrometry-mass spectrometry. Analytical Chemistry 71:2346-2357.

84. Cooks RG, Glish G, Mc Luckey SA, Kaiser RE 1991. Ion trap mass spectrometry. Chemical and Engineering News 69:26-37.

85. Petucci C, Diffendal J, Kaufman D, Mekonnen B, Terefenko G, Musselman B 2007. Direct analysis in real time for reaction monitoring in drug discovery. Analytical Chemistry 79:5064-5070.

86. Reyzer ML, Hsieh Y, Ng K, Korfmacher WA, Caprioli RM 2003. Direct analysis of drug candidates in tissue by matrix-assisted laser desorption/ionization mass spectrometry. Journal of Mass Spectrometry 38:1081-1092.

87. Hedenus M 2002. Eugen Goldstein and his laboratory work at Berlin Observatory. Astronomische Nachrichten 323:567-569.

88. Thomson J. 1913. Rays of Positive Electricity and Their Application to Chemical Analyses, London, UK: Longmans, Green.

89. Thomson SJJ. 1921. Rays of positive electricity and their application to chemical analyses: Longmans, Green and Co.

90. Gohlke R 1959. Time-of-flight mass spectrometry and gas-liquid partition chromatography. Analytical Chemistry 31:535-541.

91. Jennings K 1968. Collision-induced decompositions of aromatic molecular ions. International Journal of Mass Spectrometry and Ion Physics 1:227-235.

92. Tanaka K, Waki H, Ido Y, Akita S, Yoshida Y, Yoshida T, Matsuo T 2005. Protein and polymer analyses up to m/z 100 000 by laser ionization time-of-flight mass spectrometry. Rapid Communications in Mass Spectrometry 2:151-153.

93. Whitehouse CM, Dreyer RN, Yamashita M, Fenn JB 1985. Electrospray interface for liquid chromatographs and mass spectrometers. Analytical Chemistry 57:675-679.

94. Venter A, Nefliu M, Graham Cooks R 2008. Ambient desorption ionization mass spectrometry. TrAC Trends in Analytical Chemistry 27:284-290.

95. Ackermann BL, Berna MJ, Murphy AT 2002. Recent advances in use of LC/MS/MS for quantitative high-throughput bioanalytical support of drug discovery. Current Topics in Medicinal Chemistry 2:53-66.

96. Korfmacher WA 2005. Foundation review: Principles and applications of LC-MS in new drug discovery. Drug Discovery Today 10:1357-1367.

97. Whitehouse CM, Dreyer RN, Yamashita M, Fenn JB 1985. Electrospray interface for liquid chromatographs and mass spectrometers. Analalytical Chemistry 57:675-679.

98. Covey TR, Lee ED, Henion JD 1986. High-speed liquid chromatography/tandem mass spectrometry for the determination of drugs in biological samples. Analytical Chemistry 58:2453-2460.

99. Brewer E, Henion J 1998. Atmospheric pressure ionization LC/MS/MS techniques for drug disposition studies. Journal of Pharmaceutical Sciences 87:395-402.

100. Zhu M, Zhang H, Humphreys WG 2011. Drug metabolite profiling and identification by high-resolution mass spectrometry. Journal of Biological Chemistry 286:25419-25425.

101. Van Dongen WD, Niessen WMA 2012. LC-MS systems for quantitative bioanalysis. Bioanalysis 4:2391-2399.

102. Sharma A, Rathore S 2012. Bioanalytical Method development and Validation of Drugs in Biological fluid. International Journal of Pharmaceutical & Research Sciences 1:216-226.

103. Cai Y, Monsalud S, Jaffé R, Jones RD 2000. Gas chromatographic determination of organomercury following aqueous derivatization with sodium tetraethylborate and sodium tetraphenylborate: comparative study of gas chromatography coupled with atomic fluorescence spectrometry, atomic emission spectrometry and mass spectrometry. Journal of Chromatography A 876:147-155.

104. Gentili A, Perret D, Marchese S 2005. Liquid chromatography-tandem mass spectrometry for performing confirmatory analysis of veterinary drugs in animal-food products. TrAC Trends in Analytical Chemistry 24:704-733.

105. Vogeser M, Seger C 2010. Pitfalls associated with the use of liquid chromatography–tandem mass spectrometry in the clinical laboratory. Clinical Chemistry 56:1234-1244.

106. Hodel E, Zanolari B, Mercier T, Biollaz J, Keiser J, Olliaro P, Genton B, Decosterd L 2009. A single LC–tandem mass spectrometry method for the simultaneous determination of 14 antimalarial drugs and their metabolites in human plasma. Journal of Chromatography B 877:867-886.

107. Mueller C, Weinmann W, Dresen S, Schreiber A, Gergov M 2005. Development of a multi-target screening analysis for 301 drugs using a QTrap liquid chromatography/tandem mass spectrometry system and automated library searching. Rapid Communications in Mass Spectrometry 19:1332-1338.

108. Qu J, Chen W, Luo G, Wang Y, Xiao S, Ling Z, Chen G 2001. Rapid determination of underivatized pyroglutamic acid, glutamic acid, glutamine and other relevant amino acids in fermentation media by LC-MS-MS. Analyst 127:66-69.

109. Justesen U, Knuthsen P, Leth T 1998. Quantitative analysis of flavonols, flavones, and flavanones in fruits, vegetables and beverages by high-performance liquid chromatography with photo-diode array and mass spectrometric detection. Journal of Chromatography A 799:101-110.

110. Abdel-Hamid ME 2000. Comparative LC–MS and HPLC analyses of selected antiepileptics and beta-blocking drugs. Il Farmaco 55:136-145.

111. Annesley TM 2003. Ion suppression in mass spectrometry. Clin Chem 49:1041-1044.

112. Kassel D 2001. Combinatorial chemistry and mass spectrometry in the 21st century drug discovery laboratory. Chemical Reviews 101:255-268.

113. Theodoridis GA, Gika HG, Want EJ, Wilson ID 2011. Liquid chromatography mass spectrometry based global metabolite profiling: a review. Analytica Chimica Acta 711:7-16.

114. Bantscheff M, Schirle M, Sweetman G, Rick J, Kuster B 2007. Quantitative mass spectrometry in proteomics: a critical review. Analytical and Bioanalytical Chemistry 389:1017-1031.

115. Rainville PD, Stumpf CL, Shockcor JP, Plumb RS, Nicholson JK 2007. Novel application of reversed-phase UPLC-oaTOF-MS for lipid analysis in complex biological mixtures: A new tool for lipidomics. Journal of Proteome Research 6:552-558.

116. Betteridge D 1978. Flow injection analysis. Analytical Chemistry 50:832A-846A.

117. Lua IA, Lin SL, Lin HR, Lua AC 2012. Replacing Immunoassays for Mephedrone, Ketamines and Six Amphetamine-Type Stimulants with Flow Injection Analysis Tandem Mass Spectrometry. Journal of Analytical Toxicology 36:575-581.

118. Weinmann W, Svoboda M 1998. Fast screening for drugs of abuse by solid-phase extraction combined with flow-injection ionspray-tandem mass spectrometry. Journal of Analytical Toxicology 22:319-328.

119. Wade N, Miller K 2005. Determination of active ingredient within pharmaceutical preparations using flow injection mass spectrometry. Journal of Pharmaceutical and Biomedical Analysis 37:669-678.

120. Romanyshyn L, Tiller PR, Alvaro R, Pereira A, Hop CE 2001. Ultra-fast gradient vs. fast isocratic chromatography in bioanalytical quantification by liquid chromatography/tandem mass spectrometry. Rapid Communications in Mass Spectrometry 15:313-319.

121. Jonas M, LaMarr WA, Ozbal C 2009. Mass spectrometry in high throughput screening: A case study on acetyl-coenzyme a carboxylase using rapidfire-mass spectrometry (RF-MS). Combinatorial Chemistry & High Throughput Screening 12:752-759.

122. Chen S, Carvey PM 2000. Validation of liquid-liquid extraction followed by flow-injection negative ion electrospray mass spectrometry assay to Topiramate in human plasma. Rapid Communications in Mass Spectrometry 15:159-163.

123. Klockow-Beck A, Nick A, Geisshuesler S, Schaufelberger D 1998. Determination of the inorganic degradation products sulfate and sulfamate in the antiepileptic drug topiramate by capillary electrophoresis. Journal of Chromatography B: Biomedical Sciences and Applications 720:141-151.

124. Holland ML, Uetz JA, Ng KT 1988. Automated capillary gas chromatographic assay using flame ionization detection for the determination of topiramate in plasma. Journal of Chromatography B: Biomedical Sciences and Applications 433:276-281.

125. Mičová K, Friedecký D, Faber E, Polýnková A, Adam T 2010. Flow injection analysis vs. ultra high performance liquid chromatography coupled with tandem mass spectrometry for determination of imatinib in human plasma. Clinica Chimica Acta 411:1957-1962.

126. Brönstrup M 2003. High-throughput mass spectrometry for compound characterization in drug discovery. Modern Mass Spectrometry 225:283-302.

127. do C Borges, Ney C, Mendes GD, Barrientos-Astigarraga RE, Galvinas P, Oliveira CH, De Nucci G 2005. Verapamil quantification in human plasma by liquid chromatography coupled to tandem mass spectrometry An application for bioequivalence study. Journal of Chromatography B 827:165-172.

128. Dethy JM, Ackermann BL, Delatour C, Henion JD, Schultz GA 2003. Demonstration of direct bioanalysis of drugs in plasma using nanoelectrospray infusion from a silicon chip coupled with tandem mass spectrometry. Analytical Chemistry 75:805-811.

129. Cohen LH, Gusev AI 2002. Small molecule analysis by MALDI mass spectrometry. Analytical and Bioanalytical Chemistry 373:571-586.

130. LeRiche T, Osterodt J, Volmer DA 2001. An experimental comparison of electrospray ion-trap and matrix-assisted laser desorption/ionization post-source decay mass spectra for the

characterization of small drug molecules. Rapid Communications in Mass Spectrometry 15:608-614.

131. Porta T, Grivet C, Knochenmuss R, Varesio E, Hopfgartner G 2011. Alternative CHCA-based matrices for the analysis of low molecular weight compounds by UV-MALDI-tandem mass spectrometry. Journal of Mass Spectrometry 46:144-152.

132. Wan D, Gao M, Wang Y, Zhang P, Zhang X 2012. A rapid and simple separation and direct detection of glutathione by gold nanoparticles and graphene-based MALDI–TOF-MS. Journal of Separation Science 36:629-635.

133. Bonnel D, Franck J, Mériaux C, Salzet M, Fournier I 2012. Ionic matrices pre-spotted MALDI plates for patients markers following, drugs titration and MALDI MSI. Analytical Biochemistry 434:189-198.

134. Çelikbıçak Ö, Pişkin E, Salih B 2012. Small Molecule Analysis Using Laser Desorption Ionization Mass Spectrometry On Nano-Coated Silicon With Self-Assembled Monolayers. Analytica Chimica Acta 729:54-61.

135. Kim KP, Shanta SR, Kim TY, Hong JH, Lee JH, Shin CY, Kim K, Kim SK 2012. A new combination MALDI matrix for small molecule analysis: application to imaging mass spectrometry for drugs and metabolites. Analyst 137:5757-5762.

136. De Clercq E 2009. Anti-HIV drugs: 25 compounds approved within 25 years after the discovery of HIV. International Journal of Antimicrobial Agents 33:307-320.

137. Notari S, Mancone C, Tripodi M, Narciso P, Fasano M, Ascenzi P 2006. Determination of anti-HIV drug concentration in human plasma by MALDI-TOF/TOF. Journal of Chromatography B 833:109-116.

138. Wu J, Chatman K, Harris K, Siuzdak G 1997. An automated MALDI mass spectrometry approach for optimizing cyclosporin extraction and quantitation. Analytical Chemistry 69:3767-3771.

139. Koeniger SL, Talaty N, Luo Y, Ready D, Voorbach M, Seifert T, Cepa S, Fagerland JA, Bouska J, Buck W 2011. A quantitation method for mass spectrometry imaging. Rapid Communications in Mass Spectrometry 25:503-510.

140. Castellino S, Groseclose MR, Wagner D 2011. MALDI imaging mass spectrometry: bridging biology and chemistry in drug development. Bioanalysis 3:2427-2441.

141. Signor L, Varesio E, Staack RF, Starke V, Richter WF, Hopfgartner G 2007. Analysis of erlotinib and its metabolites in rat tissue sections by MALDI quadrupole time-of-flight mass spectrometry. Journal of Mass Spectrometry 42:900-909.

142. Chen H, Talaty NN, Takáts Z, Cooks RG 2005. Desorption electrospray ionization mass spectrometry for high-throughput analysis of pharmaceutical samples in the ambient environment. Analytical Chemistry 77:6915-6927.

143. Takáts Z, Wiseman JM, Cooks RG 2005. Ambient mass spectrometry using desorption electrospray ionization (DESI): instrumentation, mechanisms and applications in forensics, chemistry, and biology. Journal of Mass Spectrometry 40:1261-1275.

144. Cody RB, Laramée JA, Durst HD 2005. Versatile new ion source for the analysis of materials in open air under ambient conditions. Analytical Chemistry 77:2297-2302.

145. Leuthold LA, Mandscheff JF, Fathi M, Giroud C, Augsburger M, Varesio E, Hopfgartner G 2005. Desorption electrospray ionization mass spectrometry: direct toxicological screening and analysis of illicit Ecstasy tablets. Rapid Communications in Mass Spectrometry 20:103-110.

146. Ifa DR, Manicke NE, Rusine AL, Cooks RG 2008. Quantitative analysis of small molecules by desorption electrospray ionization mass spectrometry from polytetrafluoroethylene surfaces. Rapid Communications in Mass Spectrometry 22:503-510.

147. Wiseman JM, Laughlin BC 2007. Desorption electrospray ionization (DESI) mass spectrometry: a brief introduction and overview. Current Separations and Drug Development 22:11-14.

148. Weston DJ, Bateman R, Wilson ID, Wood TR, Creaser CS 2005. Direct analysis of pharmaceutical drug formulations using ion mobility spectrometry/quadrupole-time-of-flight mass spectrometry combined with desorption electrospray ionization. Analytical Chemistry 77:7572-7580.

149. Williams JP, Scrivens JH 2005. Rapid accurate mass desorption electrospray ionisation tandem mass spectrometry of pharmaceutical samples. Rapid Communications in Mass Spectrometry 19:3643-3650.

150. Vismeh R, Waldon DJ, Teffera Y, Zhao Z 2012. Localization and quantification of drugs in animal tissues by use of desorption electrospray ionization mass spectrometry imaging. Analytical Chemistry 84:5439-5445.

151. Henry H, Sobhi HR, Scheibner O, Bromirski M, Nimkar SB, Rochat B 2012. Comparison between a high-resolution single-stage Orbitrap and a triple quadrupole mass spectrometer for quantitative analyses of drugs. Rapid Communications in Mass Spectrometry 26:499-509.

152. Barbara JE, Kazmi F, Muranjan S, Toren PC, Parkinson A 2012. High-Resolution Mass Spectrometry Elucidates Metabonate (False Metabolite) Formation from Alkylamine Drugs during In Vitro Metabolite Profiling. Drug Metabolism and Disposition 40:1966-1975.

153. Marshall AG, Hendrickson CL 2008. High-resolution mass spectrometers. Annual Review of Analytical Chemistry 1:579-599.

154. Bateman KP, Kellmann M, Muenster H, Papp R, Taylor L 2009. Quantitative–qualitative data acquisition using a benchtop Orbitrap mass spectrometer. Journal of the American Society for Mass Spectrometry 20:1441-1450.

155. Swartz ME, Krull IS. 1997. Analytical method development and validation, Boca Raton, FL, USA: CRC Press.

156. Zhang H, Heinig K, Henion J 2000. Atmospheric pressure ionization time-of-flight mass spectrometry coupled with fast liquid chromatography for quantitation and accurate mass

measurement of five pharmaceutical drugs in human plasma. Journal of Mass Spectrometry 35:423-431.

157. Zhang N, Fountain ST, Bi H, Rossi DT 2000. Quantification and rapid metabolite identification in drug discovery using API time-of-flight LC/MS. Analytical Chemistry 72:800-806.

158. Wang T, Zeng L, Strader T, Burton L, Kassel DB 1998. A new ultra-high throughput method for characterizing combinatorial libraries incorporating a multiple probe autosampler coupled with flow injection mass spectrometry analysis. Rapid Communications in Mass Spectrometry 12:1123-1129.

159. Pelander A, Decker P, Baessmann C, Ojanperä I 2011. Evaluation of a high resolving power time-of-flight mass spectrometer for drug analysis in terms of resolving power and acquisition rate. Journal of the American Society for Mass Spectrometry 22:379-385.

160. Leister WH, Weaner LE, Walker DG 1995. Analysis and purification of modified methoxy(polyethylene glycol) compounds of similar molecular mass by high-performance liquid chromatography. Journal of Chromatography A 704:369-376.

161. Rissler K, Künzi HP, Grether HJ 1993. Chromatographic investigations of oligomeric α, ω-dihydroxy polyethers by reversed-phase high-performance liquid chromatography and evaporative light scattering and UV detection. Journal of Chromatography A 635:89-101.

162. Sefisko B, Delgado C, Fisher D, Ehwald R 1993. Analysis and purification of monomethoxy-polyethylene glycol by vesicle and gel permeation chromatography. Journal of Chromatography A 641:71-79.

163. Vernooij E, Gentry C, Herron J, Crommelin D, Kettenes-Van den Bosch J 1999. 1H NMR quantification of poly (ethylene glycol)-phosphatidylethanolamine in phospholipid mixtures. Pharmaceutical Research 16:1658-1661.

164. Zhang J, Lin J, Anderson TA 2004. A flow injection analysis/mass spectrometry method for the quantification of polyethylene glycol 300 in drug formulations. International Journal of Pharmaceutics 282:183-187.

165. Ashiru DAI, Karu K, Zloh M, Patel R, Basit AW 2011. Relative quantification of polyethylene glycol 400 excreted in the urine of male and female volunteers by direct injection electrospray-selected ion monitoring mass spectrometry. International Journal of Pharmaceutics 414:35-41.

166. Wu J, Leung KF, Tong SF, Lam CW 2012. Organochlorine isotopic pattern-enhanced detection and quantification of triclosan and its metabolites in human serum by ultra-high-performance liquid chromatography/quadrupole time-of-flight/mass spectrometry. Rapid Communications in Mass Spectrometry 26:123-132.

167. Buse J, Badea I, Verrall RE, El-Aneed A 2013. A general liquid chromatography tandem mass spectrometry method for the quantitative determination of diquaternary ammonium gemini surfactant drug delivery agents in mouse keratinocytes' cellular lysate. Journal of Chromatography A 1297:98-105.

168. Salomone A, Gerace E, Brizio P, Gennaro MC, Vincenti M 2011. A fast liquid chromatography–tandem mass spectrometry method for determining benzodiazepines and analogues in urine. Validation and application to real cases of forensic interest. Journal of Pharmaceutical and Biomedical Analysis 56:582-591.

169. Ma S, Zhu M 2009. Recent advances in applications of liquid chromatography-tandem mass spectrometry to the analysis of reactive drug metabolites. Chemico-Biological Interactions 179:25-37.

170. Berberich DW, Jiang T, McClurg J, Moser F, Wilhelm RR. 2011. Impurity Identification for Drug Substances. In Pramanik BN, Lee MS, Chen G, editors. Characterization of Impurities and Degradants Using Mass Spectrometry, Hoboken, NJ, USA: John Wiley & Sons, Inc. p 231-250.

171. Lee MS, Yost RA 1988. Rapid identification of drug metabolites with tandem mass spectrometry. Biological Mass Spectrometry 15:193-204.

172. Gergov M, Ojanperä I, Vuori E 2003. Simultaneous screening for 238 drugs in blood by liquid chromatography–ionspray tandem mass spectrometry with multiple-reaction monitoring. Journal of Chromatography B 795:41-53.

173. Romanyshyn L, Tiller PR, Hop CECA 2000. Bioanalytical applications of 'fast chromatography'to high-throughput liquid chromatography/tandem mass spectrometric quantitation. Rapid Communications in Mass Spectrometry 14:1662-1668.

174. Satulovsky JE, Bynum MA, Staples G 2011. Method For Isomer Discrimination By Tandem Mass Spectrometry US 0295521 A1.

175. Carducci C, Santagata S, Leuzzi V, Carducci C, Artiola C, Giovanniello T, Battini R, Antonozzi I 2006. Quantitative determination of guanidinoacetate and creatine in dried blood spot by flow injection analysis-electrospray tandem mass spectrometry. Clinica Chimica Acta 364:180-187.

176. Gergov M, Weinmann W, Meriluoto J, Uusitalo J, Ojanperä I 2004. Comparison of product ion spectra obtained by liquid chromatography/triple-quadrupole mass spectrometry for library search. Rapid Communications in Mass Spectrometry 18:1039-1046.

177. Barnett DA, Ells B, Guevremont R, Purves RW 1999. Separation of leucine and isoleucine by electrospray ionization–high field asymmetric waveform ion mobility spectrometry–mass spectrometry. Journal of the American Society for Mass Spectrometry 10:1279-1284.

178. Guevremont R 2004. High-field asymmetric waveform ion mobility spectrometry: A new tool for mass spectrometry. Journal of Chromatography A 1058:3-19.

179. Guevremont R, Purves RW 1999. Atmospheric pressure ion focusing in a high-field asymmetric waveform ion mobility spectrometer. Review of Scientific Instruments 70:1370-1383.

180. Gabryelski W, Froese KL 2003. Rapid and sensitive differentiation of anomers, linkage, and position isomers of disaccharides using high-field asymmetric waveform ion mobility spectrometry (FAIMS). Journal of the American Society for Mass Spectrometry 14:265-277.

181. Kapron J 2006. Assay Robustness Improvement for Drug Urinalysis Using FAIMS and H-SRM on a Triple-Quadrupole Mass Spectometer. LC GC Magazine-North America-Solutions for Separation Scientists 34:38-42.

182. Kapron JT, Jemal M, Duncan G, Kolakowski B, Purves R 2005. Removal of metabolite interference during liquid chromatography/tandem mass spectrometry using high-field asymmetric waveform ion mobility spectrometry. Rapid Communications in Mass Spectrometry 19:1979-1983.

183. McCooeye MA, Ells B, Barnett DA, Purves RW, Guevremont R 2001. Quantitation of morphine and codeine in human urine using high-field asymmetric waveform ion mobility spectrometry (FAIMS) with mass spectrometric detection. Journal of Analytical Toxicology 25:81-87.

184. Yang P, Singh J, Wettig S, Foldvari M, Verrall RE, Badea I 2010. Enhanced gene expression in epithelial cells transfected with amino acid-substituted gemini nanoparticles. European Journal of Pharmaceutics and Biopharmaceutics 75:311-320.

185. Singh J, Michel D, Chitanda JM, Verrall RE, Badea I 2012. Evaluation of cellular uptake and intracellular trafficking as determining factors of gene expression for amino acid-substituted gemini surfactant-based DNA nanoparticles. Journal of Nanobiotechnology 10:7.

CHAPTER 2
TANDEM MASS SPECTROMETRY ANALYSIS OF THE NOVEL GEMINI SURFACTANT NANOPARTICLE FAMILIES G12-S AND G18:1-S

Joshua Buse, Ildiko Badea, Ronald E. Verrall, Anas El-Aneed

Published in Spectroscopy Letters 43 (2010), p 447-457

The application of mass spectrometry to answering qualitative and quantitative research questions is a result of its specificity, selectivity, and sensitivity. Mass spectrometry is a powerful analytical tool that can be utilized for assessing the molecular composition of an analyte using high resolution single stage MS as well as MS/MS analysis. The development of MS/MS fingerprints will allow for the rapid screening of biological and environmental samples to determine the presence or absence of particular compounds within the tested samples.

Using ESI quadrupole time-of-flight (Qq-ToF) hybrid MS/MS, the molecular composition and structure of 10 novel diquaternary ammonium gemini surfactants was elucidated, including the establishment of their MS/MS fingerprints. The gemini surfactants tested belong to two different structural families, namely, G12-s and G18:1-s where 's' corresponds to the spacer length. High resolution, single stage MS analysis showed that mass accuracy was less than 5 PPM for all compounds, confirming their molecular composition. In addition, similarities and differences in the fragmentation patterns within and between each gemini surfactant family were identified, allowing for the identification of individual gemini surfactant moieties. A comparison of each gemini surfactant's MS/MS fragmentation pattern demonstrated the presence of fragment ions shared by all gemini surfactants as well as ions which are unique to specific gemini surfactants and/or gemini surfactant families.

Tandem Mass Spectrometry Analysis of the Novel Gemini Surfactant Nanoparticle Families G12-s and G18:1-s

Joshua Buse[1] Ildiko Badea[1] Ronald E. Verrall[2] Anas El-Aneed[1*]

[1.] Drug Discovery and Development Research Group, College of Pharmacy and Nutrition, University of Saskatchewan, 110 Science Place, Saskatoon, SK S7N 5C9, Canada

[2.] Department of Chemistry, University of Saskatchewan, 110 Science Place, Saskatoon, SK S7N 5C9, Canada

*Corresponding Author:

Telephone: +1-306-966-2013

Fax: +1-306-966-6377

E-mail Address: anas.el-aneed@usask.ca

Keywords: Time of Flight Mass spectrometry, Tandem Mass Spectrometry, Gemini Surfactants, Fragmentation Pattern

Introduction

Nanoparticles have garnered attention for their possible use in non-viral gene delivery systems to treat both genetically based and infectious diseases.[1-7] This is due to their relatively low cost of preparation,[8] ability to target specific tissues, capability to encapsulate and carry large amounts of genetic material,[9] and increased safety when compared to viral vectors.[10] One particular group of nanoparticles that have gained attention for their ability to deliver genetic material into cells are gemini surfactants.

Gemini surfactants are constructed by covalently binding the hydrophobic tail regions, (*t*), directly to or near the polar head group of both termini of a spacer molecule, (*s*), to produce a tail-spacer-tail structure, (*t*-*s*-*t*); these structures are given identifier names comprised of G, for gemini surfactant, carbon tail length – carbon spacer length, (G*t*-*s*) (Figure 2.1).[11] The chemical variation in both the spacer and tail regions allows for the production of a wide variety of gemini surfactants. The efficiency of each compound to form a compact and stabilized morphology around unprotected DNA[12] depends upon its ability to self-assemble which in turn depends upon its CMC values,[13] how closely its hydrophobic groups can pack together,[14, 15] and the efficiency with which the positively charged nitrogen interacts with the DNA phosphate groups.[15, 16] Stabilization and compaction of DNA-gemini surfactant complexes is driven by entropy and results from the electrostatic interactions between the polyanionic DNA backbone and the dicationic gemini surfactants as well as the hydrophobic interactions between the gemini surfactants' two apolar hydrocarbon tails.[17]

The two G*t*-*s* gemini surfactant nanoparticle families used in this study are comprised of *N*,*N*-bis(dimethyl'alkyl')-α,ω-'alkane'diammonium dibromide ($[C_{12}H_{[(2\bullet12)+1]}]\ N^{+}(CH_3)_2\ (CH_2)_s\ N^{+}(CH_3)_2\ [C_{12}H_{[(2\bullet12)+1]}] \bullet 2Br^{-}$) (Figure 2.2A) and *N*,*N*-bis(dimethyl'alk-σ-ene')-α,ω-'alkane'diammonium dibromide ($[C_{18}H_{[(2\bullet18)-1]}]\ N^{+}(CH_3)_2\ (CH_2)_s\ N^{+}(CH_3)_2\ [C_{18}H_{[(2\bullet18)-1]}] \bullet 2Br^{-}$) (Figure 2.2B) salts. Gemini surfactants belong to the self-assembling, lipid-based nanoparticle drug delivery systems.[18, 19] They have been used as nanomaterials for nearly two decades[20] and are well-characterized.[21, 22] For example, analysis of the size distribution of many diquaternary ammonium gemini surfactants was performed by either non negative least squares algorithmic (NNLS) analysis (measurement of the light scattered by particles in solution illuminated by a laser beam (γ= 1731)), zeta potential, or atomic force microscopy with size distribution being assessed to be between 100 and 200 ±10 nm.[23, 24] In addition, these polycationic molecules have

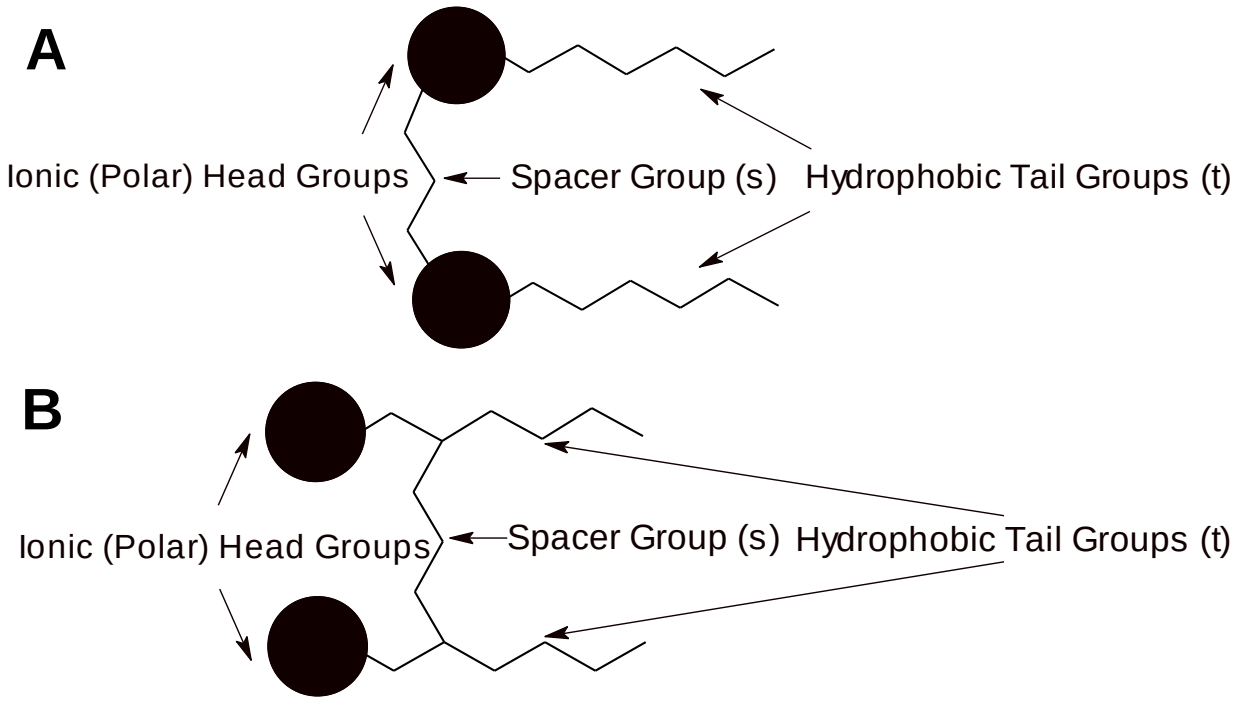

Figure 2.1 The general structure of a gemini surfactant A) that contains a spacer group that is linked directly to the ionic (polar) head groups and B) that contains a spacer group that is linked to the hydrophobic tail group near the ionic (polar) head groups.

been successfully employed for both *in vitro* and *in vivo* gene delivery applications.[13, 22- 25] For example, topical transfection of the IFNγ gene into mouse epidermis using the G12-3 and G16-3 gemini surfactants produced a 250% to 450% increase in levels of IFNγ in the epidermis compared to unprotected IFNγ genes.[9, 23, 24]

Mass spectrometry (MS) is a powerful analytical tool that has been used for both qualitative and quantitative applications.[26- 29] Single stage MS and MS/MS can be utilized for structural determination and MS/MS fingerprint identification.[30] For example, using ESI, the MS/MS analysis of 18 novel cholesteryl neoglycolipids, used in liposomes-based gene delivery, resulted in the formation of specific common fingerprint fragments regardless of the nature of the sugar moiety or the spacer group that link the carbohydrate portion to the lipid cholesteryl moiety.[31] In addition, the unknown molecular structure of lipid A, isolated from the *A. salmonicida* lipopolysaccharide, was established by single stage MS and MS/MS analysis using ESI ionization and Qq-ToF-MS/MS techniques.[32, 33] Similarly, the fragmentation routes of morphine antagonists were precisely determined using ESI-Qq-ToF MS/MS.[32]

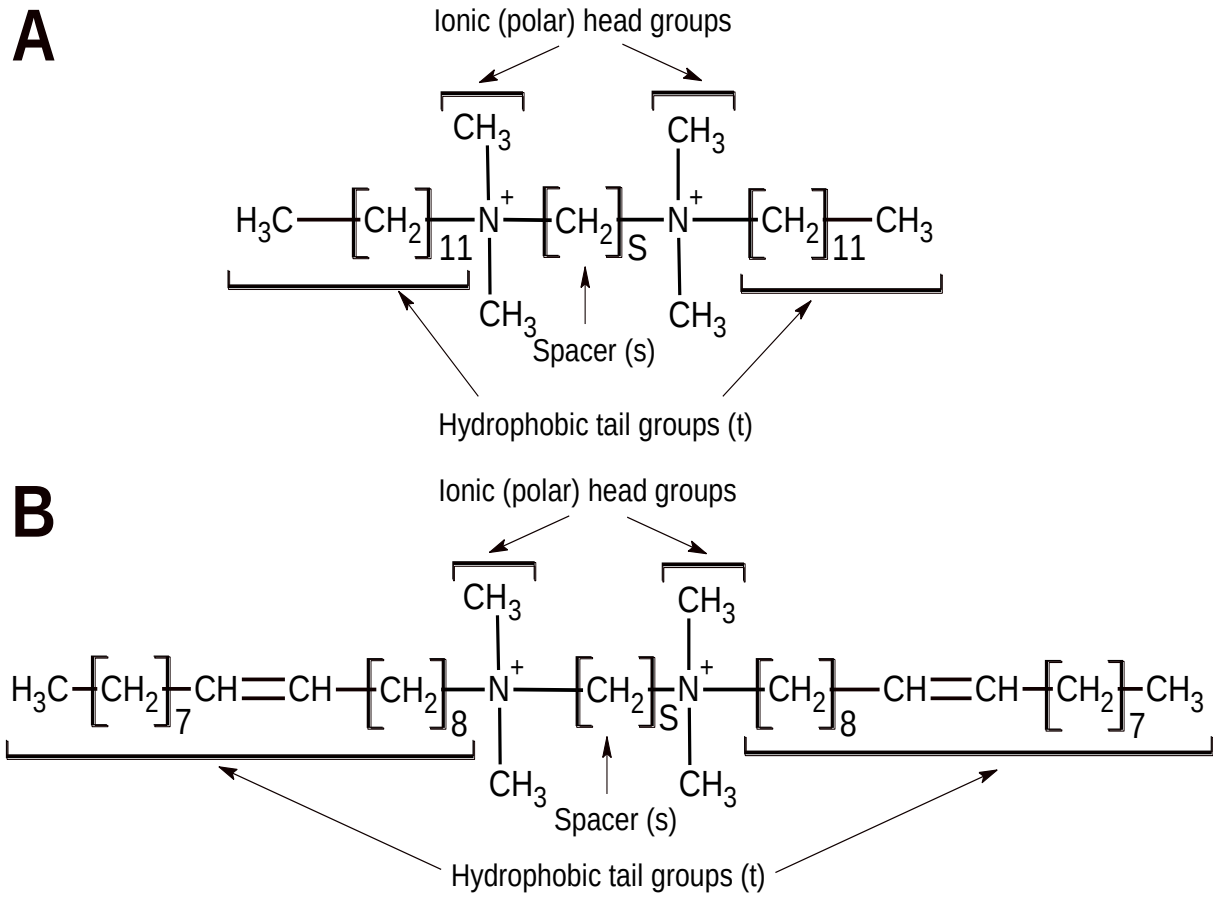

Figure 2.2 The general structure of the gemini surfactants A) G12-s *N*,*N*-bis(dimethyldodecyl)-1,'s'-"alkan"diammonium with the "alkan" and 's' referring to the carbon composition of the spacer region, s, and B) G18:1-s *N*,*N* –bis(dimethylheptadec-9-ene)-1,'s'-"alkan"diammonium with the "alkan" and 's' referring to the carbon composition of the spacer region

MS/MS fingerprints and will allow for the rapid screening of biological materials and environmental samples to determine the absence or presence of particular compounds within the tested samples. In addition, MS/MS data can be used to develop MS-based quantification methods.

This paper describes the findings regarding the elucidation of the exact molecular structure for the G12-*s* and G18:1-*s* families of gemini surfactants as well as the identification of the fingerprint product ions for all 10 gemini surfactants analyzed and their fragmentation pattern using MS/MS. The analysis of an additional 25 gemini surfactants belonging to 3 different structural gemini families are currently being investigated.

Experimental

The G*t-s* gemini surfactant nanoparticles analyzed were obtained from Dr. Ronald E. Verrall's research group in the Department of Chemistry at the University of Saskatchewan.[26] The compounds are from the G12-*s* and G18:1-*s* families (Figure 2.2) and include:

- G12-2 or *N,N*-bis(dimethyldodecyl)-1,2-ethanediammonium dibromide
- G12-4 or *N,N*-bis(dimethyldodecyl)-1,4-butanediammonium dibromide
- G12-6 or *N,N*-bis(dimethyldodecyl)-1,6-hexanediammonium dibromide
- G12-8 or *N,N*-bis(dimethyldodecyl)-1,8-octanediammonium dibromide
- G12-10 or *N,N*-bis(dimethyldodecyl)-1,10-decanediammonium dibromide
- G12-12 or *N,N*-bis(dimethyldodecyl)-1,12-dodecanediammonium dibromide
- G12-16 or *N,N*-bis(dimethyldodecyl)-1,16-hexadecanediammonium dibromide
- G18:1-2 or N,N-bis(dimethyloctadec-9-ene)-1,2-ethanediammonium dibromide
- G18:1-3 or N,N-bis(dimethyloctadec-9-ene)-1,3-propanediammonium dibromide
- G18:1-6 or N,N-bis(dimethyloctadec-9-ene)-1,6-hexanediammonium dibromide

Gemini surfactant solutions were prepared to a concentration of 3 mM in methanol and water (50:50 v:v) containing 0.1 % Trifluoroacetic acid (99% purity) and stored at -20º C. Each sample was further diluted 4000x and 5000x at the time of analysis using the same mixed solvent.

To minimize associated errors in mass measurements, internal calibration was employed during analysis using an Applied Biosystems, API QSTAR XL QqToF-MS/MS. We opted for using doubly charged calibrants since the tested gemini surfactants are doubly charged species. Therefore, we used both [Glu^1]-Fibrinopeptide B, Human (amino acid sequence EGVNDNEEGFFSAR, $[M+2H]^{2+}$ *m/z* 785.8421, $C_{66}H_{95}N_{19}O_{26}$, BaChem Bioscience Inc., King of Prussia, PA, USA) and *N,N*-bis(dimethyldodecyl)-1,2-ethanediammonium dibromide ($[M]^{2+}$ *m/z* 234.2685). The later compound was chosen because its *m/z* value fell within the *m/z* range of the tested compounds. Its molecular structure was previously confirmed by elemental analysis, NMR, and purity evaluation.[34, 35]

The instrument was operated in the positive ion mode with the following parameters: declustering potential of 100.0 V and focusing potential of 290.0 V. The collision gas used

during MS/MS experiments was argon and many MS/MS experiments were performed for each compound with the collision energy (CE) values varying between 15-100 eV. CE was optimized in order to generate product ions while ensuring that the molecular ion remained abundant. Sample aliquots, between 100 μL and 500 μL, were infused into the mass spectrometer with an integrated Harvard Syringe Pump at a rate of 10 μL/min using the Turbo Ionspray source; 5.5 kV at a temperature between 80º and 100º C.

A Micromass Quattro II quadrupole-hexapole-quadrupole mass spectrometer (QHQ-MS) was used to confirm the fragmentation pattern. The instrument was operated in the positive ion mode with the following parameters: infusion rate of 10 uL/min, source temperature of 140º C, HV lens voltate of 0.71 kV and capillary voltage of 3.50 V. The cone voltage was set at 70 V to induce in source fragmentation of the compounds. The collision gas used during MS/MS experiments was argon and the CE was set between 15 and 50 eV in order to generate product ions while ensuring that the precursor ion remained abundant.

Results and Discussion

Single Stage QqToF MS and QqToF MS/MS Analysis:

The results from the single stage QqToF MS analysis are assessed by comparing the observed *m/z* values with the calculated *m/z* values, producing mass accuracies[36] less than 5 PPM for all gemini surfactants using internal calibration (Table 2.1). This confirms the projected molecular composition of each gemini surfactant, which includes the presence of two nitrogen atoms in all compounds.[9, 12, 23, 37, 38]

The variation in spacer lengths within both the G12-*s* and G18:1-*s* gemini surfactant families produces distinctive product ions within each MS/MS spectra (Figure 2.3A and 2.4A). These product ions, although specific for each gemini surfactant, follow a similar fragmentation pattern for each family which is seen by the incremental increases in the gemini surfactant's MS/MS product ion's *m/z* values that are equal to the increase in its molecular ion $[M]^{2+}$ *m/z* values (Table 2.2 and 2.3). The unique spectra and patterns produced by both G12-16 (Figure 2.3A & 2.3B), representative of the G12-*s* family, and G18:1-6 (Figure 2.4A & 2.4B), representative of the G18:1-*s* family, are discussed below. These two compounds produced the most complex spectra for their respective families.

QqToF MS/MS Analysis of G12-15 and the G12-s Gemini Surfactant Nanoparticle Family

In all G12-*s* gemini surfactant nanoparticles, the unique fragmentation pattern starts with the formation of a singly and/or doubly charged product ion(s) that results from the loss of the twelve carbon tail moiety. In G12-16, this creates the singly charged species $[M - C_{12}H_{25}]^+$ of *m/z* 481.55 (**2**) and/or the doubly charged product ion $[M - C_{12}H_{24}]^{2+}$ of *m/z* 241.28 (**2'**) (Table 2.2 and Figure 2.3A & 2.3B). The loss of the hydrocarbon tail in G12-16 occurs by two mechanism and is dependent upon the product ion(s) formed; singly or doubly charged. The elimination of a neutral CH_2=CH $(CH_2)_9$-CH_3 (dodec-1-ene), due to a proton transfer to the nitrogen atom, produces the doubly charged ion observed at *m/z* 241.28 while the heterolytic cleavage of the N-C bond forms the singly charged ion, *m/z* 481.55. The second elimination product (*m/z* 481.55) should, in theory, produce a complementary ion of the tail the region with a theoretical *m/z* 169.19. However, this ion was not observed during MS/MS of the precursor ions using either QqToF-MS or QHQ-MS analysis under various experimental conditions, regardless of the

Table 2.1 Mass accuracies of compounds using the calculated and observed mass to charge ratio (*m/z*) values

Compound Name (Gt-s)	Molecular Formula (M)	Calculated (*m/z*)	Observed (*m/z*)	Mass Accuracy (PPM)
G12-2	$C_{30}H_{66}N_2$	227.2607	227.2604	1.32
G12-4	$C_{32}H_{70}N_2$	241.2769	241.2764	2.07
G12-6	$C_{34}H_{74}N_2$	255.2910	255.2920	3.92
G12-8	$C_{36}H_{78}N_2$	269.3084	269.3077	2.60
G12-10	$C_{38}H_{82}N_2$	283.3230	283.3233	1.06
G12-12	$C_{40}H_{86}N_2$	297.3393	297.3390	1.01
G12-16	$C_{44}H_{94}N_2$	326.3691	326.3703	3.68
G18:1-2	$C_{42}H_{86}N_2$	309.3393	309.3390	0.97
G18:1-3	$C_{43}H_{88}N_2$	316.3458	316.3468	3.16
G18:1-6	$C_{46}H_{94}N_2$	337.3704	337.3703	0.30

Table 2.2A Fragment identification and corresponding m/z value for each gemini surfactant compound in the G12-s family

Compound	G12-2	G12-4	G12-6	G12-8	
Molecular Formula (M)	($C_{30}H_{66}N_2$)	($C_{32}H_{70}N_2$)	($C_{34}H_{74}N_2$)	($C_{36}H_{78}N_2$)	
Spacer Region (s)	(C_2H_4)	(C_4H_8)	(C_6H_{12})	(C_8H_{16})	
Collision Energy (eV)	16	25	25	30	
Product Ions	**(*m/z*)**	**(*m/z*)**	**(*m/z*)**	**(*m/z*)**	**#**
[M]$^{2+}$	227.26	241.28	255.30	269.31	**1**
[M - $C_{12}H_{25}$]$^{+}$	285.32	313.39	341.41	369.42	**2**
[M - $C_{12}H_{25}$ - $C_{12}H_{24}$]$^{+}$				201.12	**3**
[M - $C_{12}H_{25}$ - $C_{12}H_{24}$ - H_2]$^{+}$				199.22	**4**
[M - $C_{12}H_{25}$ - $C_{12}H_{24}$ - H_2 - C_2H_5N]$^{+}$	72.08	100.11	128.15	156.17	**5**
M - $C_{12}H_{25}$ - $C_{12}H_{24}$ - H_2 - C_2H_5N - CH_2]$^{+}$					**6**
[M - $C_{12}H_{24}$]$^{2+}$	143.17	157.19	171.20	185.22	**2'**
[M - $C_{12}H_{24}$ - $C_{12}H_{24}$]$^{+}$			87.11	101.12	**3'**
[M - $C_{12}H_{24}$ - $C_{12}H_{24}$ - C_2H_8N]$^{+}$	72.08	100.11	128.15	156.17	**4'**
[M - $C_{12}H_{24}$ - $C_{12}H_{24}$ - ('s'+C_2H_6N)]$^{+}$	46.06	46.06	46.06	46.06	**5'**
[M - $C_{14}H_{32}N$]$^{+}$					**2''**
[M - $C_{14}H_{32}N$ - $(CH_2)_{S-2}CH=CH_2$]$^{+}$	214.09	214.09	214.10	214.24	**3''**
[M - $C_{14}H_{32}N$ - $(CH_2)_{S-2}CH=CH_2$ - H_2]$^{+}$			212.24	212.24	**4''**
[M - $C_{22}H_{48}N_2$ - 's']$^{+}$	85.10	85.10	85.10	85.10	**2'''**
[M - $C_{23}H_{50}N_2$ - 's']$^{+}$	71.09	71.09	71.09	71.09	**3'''**
[M - $C_{24}H_{52}N_2$ - 's']$^{+}$	57.07	57.07	57.07	57.07	**4'''**

Table 2.2B Fragment identification and corresponding m/z value for each gemini surfactant compound in the G12-s family

Compound	G12-10	G12-12	G12-16	
Molecular Formula (M)	($C_{38}H_{82}N_2$)	($C_{40}H_{86}N_2$)	($C_{44}H_{94}N_2$)	
Spacer Region (s)	($C_{10}H_{20}$)	($C_{12}H_{24}$)	($C_{16}H_{32}$)	
Collision Energy (eV)	30	30	35	
Product Ions	**(*m/z*)**	**(*m/z*)**	**(*m/z*)**	**#**
[M]$^{2+}$	283.32	297.35	325.37	**1**
[M - $C_{12}H_{25}$]$^{+}$	397.45	425.49	481.55	**2**
[M - $C_{12}H_{25}$ - $C_{12}H_{24}$]$^{+}$	229.26	257.30	313.36	**3**
[M - $C_{12}H_{25}$ - $C_{12}H_{24}$ - H_2]$^{+}$	227.25	255.29	311.34	**4**
[M - $C_{12}H_{25}$ - $C_{12}H_{24}$ - H_2 - C_2H_5N]$^{+}$	184.20	212.32	268.30	**5**
M - $C_{12}H_{25}$ - $C_{12}H_{24}$ - H_2 - C_2H_5N - CH_2]$^{+}$			254.29	**6**
[M - $C_{12}H_{24}$]$^{2+}$	199.23	213.25	241.28	**2'**
[M - $C_{12}H_{24}$ - $C_{12}H_{24}$]$^{+}$	115.14	129.16	157.19	**3'**
[M - $C_{12}H_{24}$ - $C_{12}H_{24}$ - C_2H_8N]$^{+}$	184.20	212.32	268.30	**4'**
[M - $C_{12}H_{24}$ - $C_{12}H_{24}$ - ('s'+C_2H_6N)]$^{+}$	46.06	46.06	46.06	**5'**
[M - $C_{14}H_{32}N$]$^{+}$		380.44	436.49	**2''**
[M - $C_{14}H_{32}N$ - $(CH_2)_{S-2}CH=CH_2$]$^{+}$	214.26	214.25	214.26	**3''**
[M - $C_{14}H_{32}N$ - $(CH_2)_{S-2}CH=CH_2$ - H_2]$^{+}$	212.24	212.24	212.24	**4''**
[M - $C_{22}H_{48}N_2$ - 's']$^{+}$	85.10	85.10	85.10	**2'''**
[M - $C_{23}H_{50}N_2$ - 's']$^{+}$	71.09	71.09	71.09	**3'''**
[M - $C_{24}H_{52}N_2$ - 's']$^{+}$	57.07	57.07	57.07	**4'''**

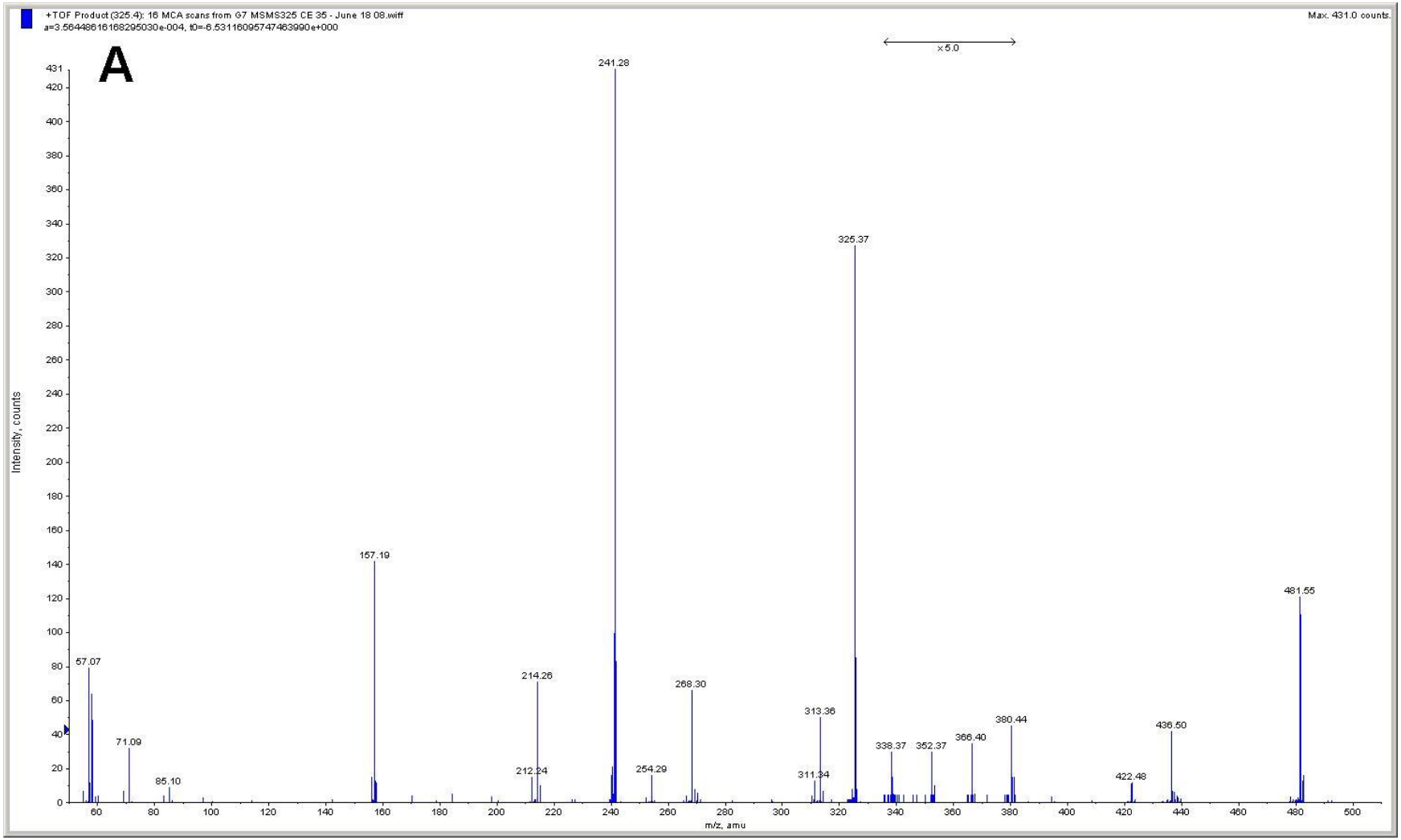

Figure 2.3A The MS/MS spectra or G12-16 which is representative of the G12-s family of gemini surfactants.

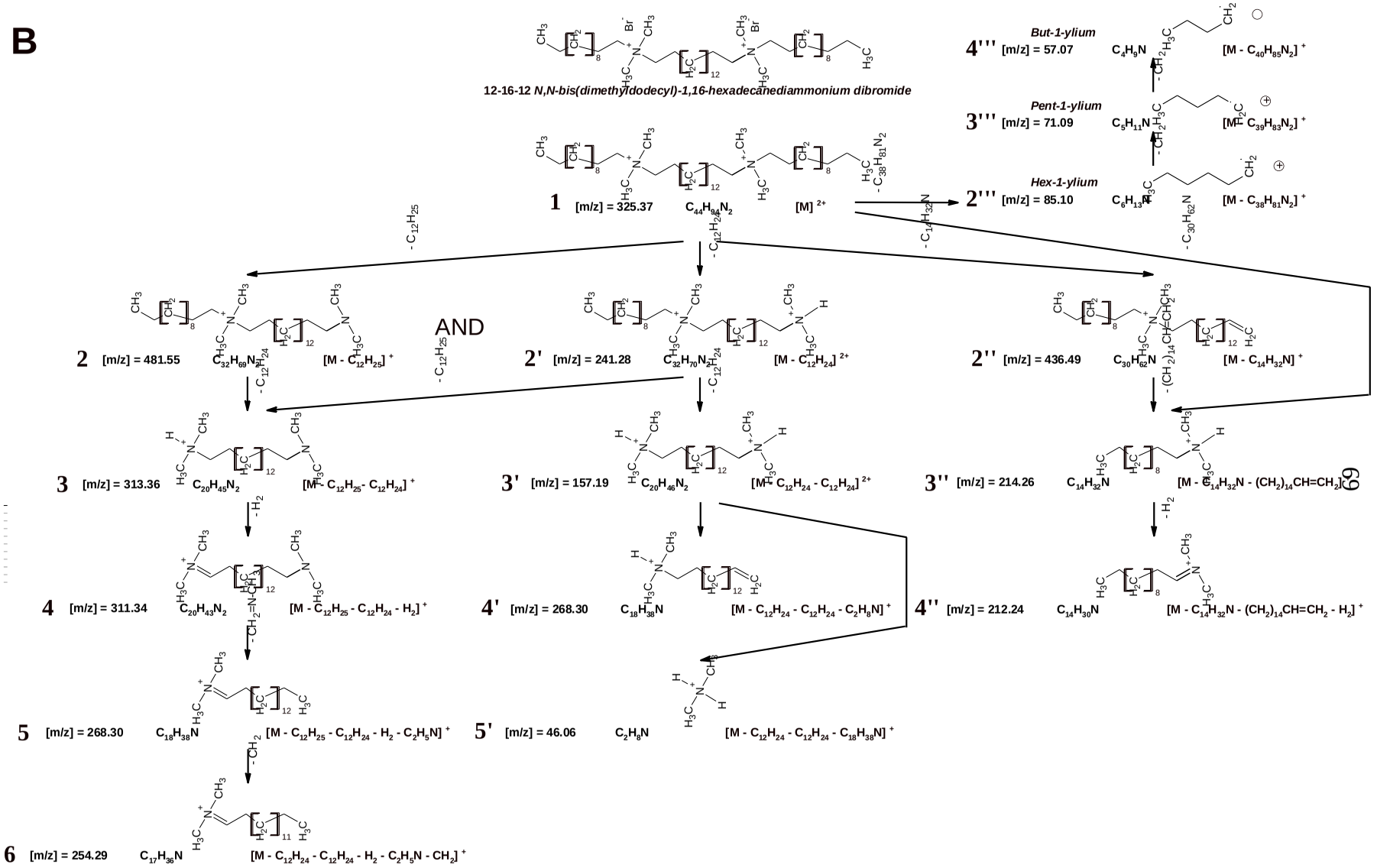

Figure 2.3B The fragmentation pattern of G12-16 which is representative of the G12-s family of gemini surfactants.

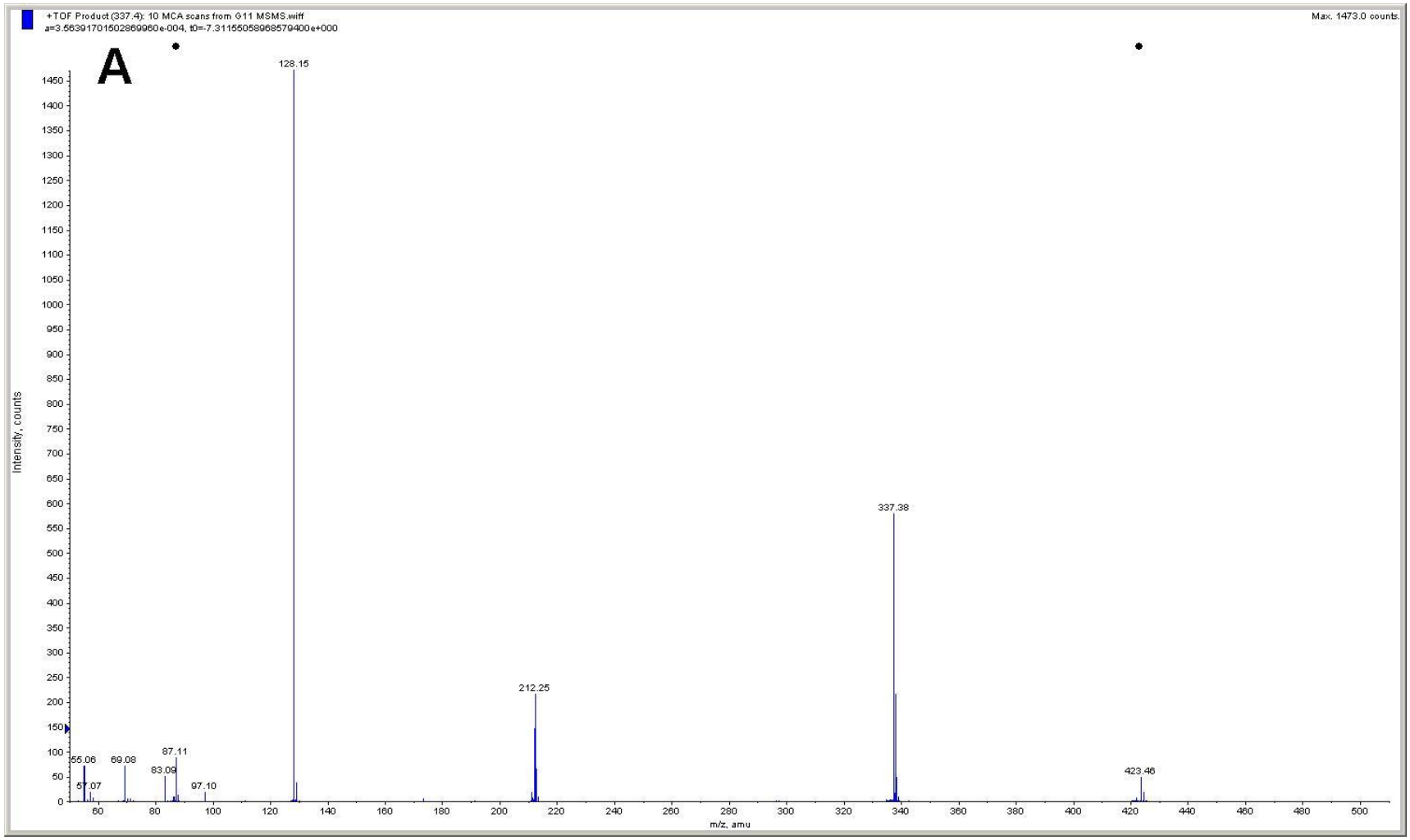

Figure 2.4A The MS/MS spectra or G18:1-6 which is representative of the G18:1-s family of gemini surfactants.

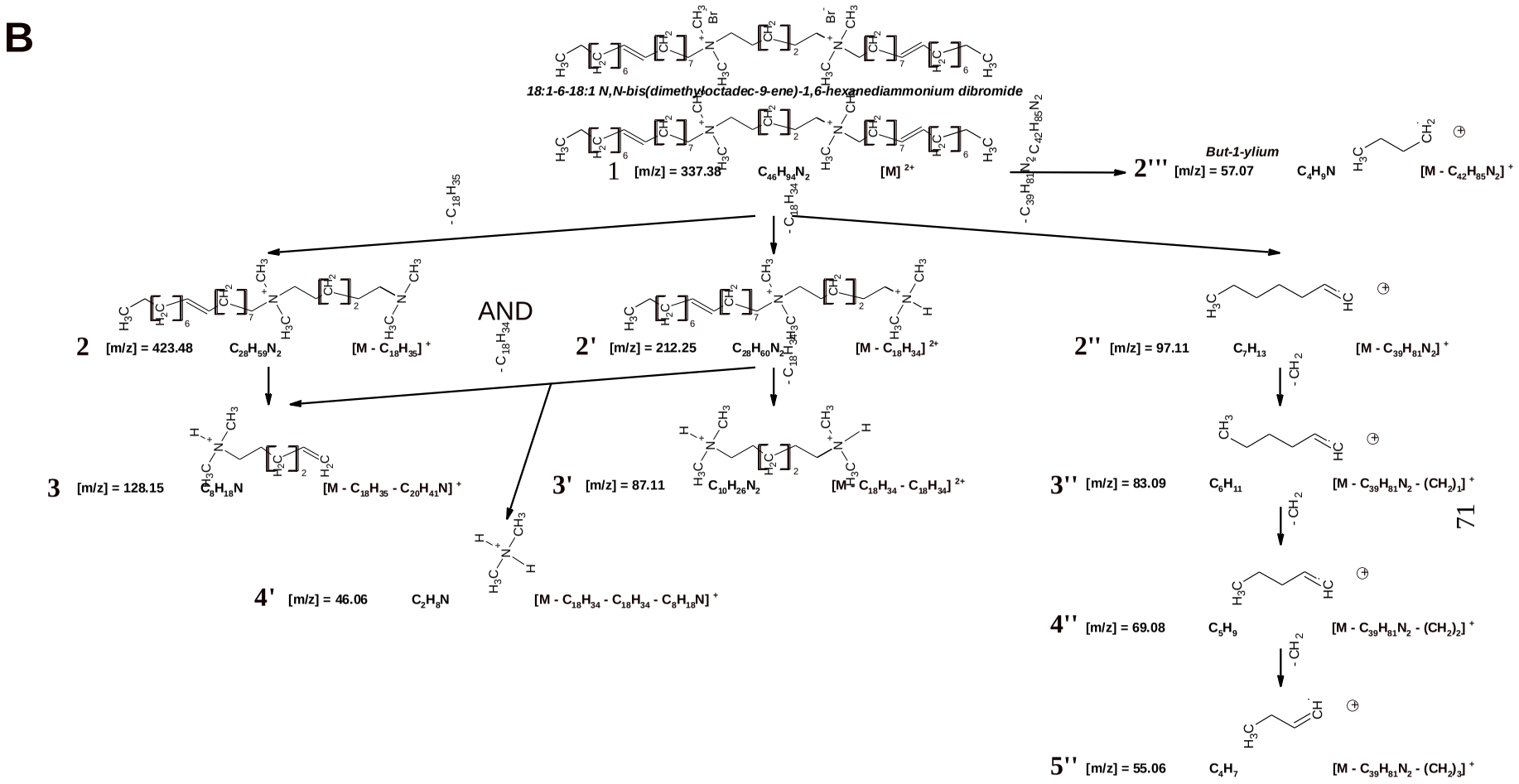

Figure 2.4A The fragmentation pattern of G18:1-6 which is representative of the G18:1-s family of gemini surfactants.

Table 2.3 Fragment identification and corresponding m/z value for each gemini surfactant compound in the G18:1-s family

Compound	G18:1-2	G18:1-3	G18:1-6	
Molecular Formula (M)	$(C_{42}H_{86}N_2)$	$(C_{43}H_{88}N_2)$	$(C_{46}H_{94}N_2)$	
Spacer Region (s)	(C_2H_4)	(C_3H_6)	(C_6H_{12})	
Collision Energy (eV)	20	25	31	
Product Ions	**(*m/z*)**	**(*m/z*)**	**(*m/z*)**	**#**
[M] $^{2+}$	309.34	316.35	337.38	**1**
[M - $C_{18}H_{35}$] $^{+}$	367.41	381.43	423.48	**2**
[M - $C_{18}H_{35}$ - $C_{18}H_{34}$ - $(CH_3)_2NH$] $^{+}$	72.08	86.10	128.15	**3**
[M - $C_{18}H_{34}$] $^{2+}$		191.35	212.25	**2'**
[M - $C_{18}H_{34}$ - $C_{18}H_{34}$] $^{2+}$			87.11	**3'**
M - $C_{18}H_{34}$ - $C_{18}H_{34}$ - ('s'+$(CH_3)_2N$]	46.06	46.06	46.06	**4'**
[M - $C_{30}H_{63}N_2$ - S] $^{+}$	97.10	97.10	97.11	**2''**
[M - $C_{31}H_{65}N_2$ - S] $^{+}$	83.09	83.09	83.09	**3''**
[M - $C_{32}H_{67}N_2$ - S] $^{+}$	69.08	69.08	69.08	**4''**
[M - $C_{33}H_{69}N_2$ - S] $^{+}$	55.06	55.06	55.06	**5''**
[M - $C_{33}H_{67}N_2$ - S] $^{+}$	57.07	57.07	57.07	**2'''**

collision energy. It is possible that the ion expected at *m/z* 169.19 was instantly formed and neutralized via proton transfer from other species within the collision cell. As discussed below and shown in Table 2.2, only short aliphatic radical ions were observed at m/z 85.10 (**2’’’**), 71.09 (**3’’’**), and 57.07 (**4’’’**) (Figure 2.3A & 2.3B), which supports the notion that longer singly charged alkyl chains were neutralized.

Following the same mechanism described in the previous section, the loss of the second twelve carbon tail produces a doubly charged product ion $[M - C_{12}H_{24} - C_{12}H_{24}]^{2+}$, at *m/z* 157.19 (**3'**), and the singly charged ion $[M - C_{12}H_{25} - C_{12}H_{24}]^{2+}$,at *m/z* 313.36 (**3**), from *m/z* 481.55 and 241.28 (Table 2.2 and Figure 2.3A & 2.3B). The origin of the fragment ions was confirmed via MS/MS analysis using QHQ instrument. QHQ, contrary to QqToF, is able to generate strong "in source" fragmentation and hence this allowed us to authenticate the proposed fragmentation pathways and the order in which ions are formed (Table 2.4). An additional aminium ion that is produced by the loss of two hydrogen atoms from the singly charged ion, $[M - C_{12}H_{25} - C_{12}H_{24}]^{2+}$ (**3**), results in the formation of a double bond between the terminal carbon of the spacer and the nitrogen; $[M - C_{12}H_{24} - C_{12}H_{25} - H_2]^{2+}$at *m/z* 311.34 (**4**) (Table 2.2 and Figure 2.3A & 2.3B). The loss of a neutral CH_2=N-CH_3 (*N*-methylidenemethanamine) from the singly charged, *m/z* 311.34 (**4**) produces the product ion of $[M - C_{12}H_{25} - C_{12}H_{24} - H_2 - C_2H_5N]^+$ at *m/z* 268.3 **(5) and** subsequent elimination of a CH_2 yields the ion, $[M - C_{12}H_{25} - C_{12}H_{24} - H_2 - C_2H_5N - CH_2]^+$, at *m/z* 254.29 (**6**) (Table 2.2 & 2.4 and Figure 2.3A & 2.3B). The product ions represented by $[M - C_{12}H_{25} - C_{12}H_{24} - H_2 - C_2H_5N]^+$ (**5**) (Figure 2.3B) are observed in all G12-*s* gemini surfactants nanoparticles presented in table 2.2.

On the other hand, the product ion observed at *m/z* 157.19 (**3'**) is also cleaved at the terminal N-C bond releasing two complementary ions observed at *m/z* 268.3, $[M – C_{12}H_{24} – C_{12}H_{24} – C_2H_8N]^+$, (**4'**) and *m/z* 46.19, *N*-methylmethanaminium, (**5'**). Based upon the diagnostic fragments produced by the ions at *m/z* 311.34 (**4**) and 157.19 (**3'**) (Table 2.4), it can be concluded that two structural isomers exist for the ion observed at m/z 268.3 (Figure 2.3A & 2.3B). In a similar mechanism, another pair of complementary diagnostic product ions were produced from the cleavage of the N-C bond within the molecular ion and observed at *m/z* 436.49 (**2''**) and 214.26 (**3''**) (Table 2.2 and Figure 2.3A & 2.3B). Additional non-diagnostic product ions were observed at *m/*z 422.47, *m/*z 380.43, *m/*z 366.41, *m/*z 352.37, and *m/*z 338.34 in G12-16 (Figure 2.3A & .3B). These minor non-diagnostic ions results from the loss of $(CH_2)_n$ and originated from different sources (m/z 481.55, 241.28, 436.49) as confirmed by QHQ analysis.

Additional non-diagnostic ions are expected and result from the tail region of the G12-s gemini surfactants as a result of their identical nature. Identical fragments seen in all analyzed G12-*s* gemini surfactants are singly charged small product ions, namely, *N*,*N*-dimethyldodecan-

1-aminium (**3’’**), hex-1-ylium (**2’’’**) pent-1-ylium (**3’’’**), and but-1-ylium (**4’’’**) (Table 2.2 and Figure 2.3A & 2.3B). It should be noted that these small fragment ions can be generated from all ions which contain the gemini surfactant tail region; for illustrative purposes, we opted to present these ions being generated from the molecular ion (Figure 2.3B)

Table 2.4 Tandem mass spectrometric analysis using an HQH instrument. The formation of diagnostic ions during MS/MS analysis confirmed the fragmentation pathway for each gemini surfactant structural family.

MS/MS Ions of G12-16	**Diagnostic MS/MS Ions Produced**
241.28	366, 352, 338, 313, 311, 268, 254, 214, 212, 157, 46
481.55	422, 380, 366, 338, 313, 311, 268, 254, 214, 212,
157.19	268, 46
313.36	311, 268, 254
311.00	268
268.30	254
436.49	422, 352, 338, 214, 212
MS/MS Ions of G18:1-6	**Diagnostic MS/MS Ions Produced**
212.25	128, 87, 46
423.48	128

B) **QqToF MS/MS Analysis of G18:1-s Gemini Surfactant Nanoparticle Family**

The fragmentation pattern of the G18:1-*s* family of gemini surfactant nanoparticles follows a similar fragmentation pattern to the G12-*s* family and produces singly and/or doubly charged product ion(s) due to the loss of a tail moiety. In G18:1-6, these product ions are observed as $[M\text{-}C_{18}H_{35}]^{2+}$ at *m/z* 423.48 (**2**) and $[M\text{-}C_{18}H_{34}]^{2+}$ at *m/z* 212.25 (**2'**) (Table 2.3 and Figure 2.4A & 2.4B). The subsequent loss of the second tail moiety from *m/z* 212.25, $[M\text{-}C_{18}H_{34}]^{2+}$, results in the formation of a doubly charged ion $[M\text{-}C_{18}H_{34}\text{-}\ C_{18}H_{34}]^{+}$ at *m/z* 87.11 (**3'**) (Table 2.3 and Figure 2.4A & 2.4B). This doubly charged ion is only observed in G18:1-6. On the other hand, the loss of both tail regions, one bound to a single dimethyl-amino, is observed in all G18:1-*s* gemini surfactant. In G18:1-6, this is observed as,$[M\text{-}C_{18}H_{35}\ \text{-}\ C_{20}H_{41}N]^{+}$ at *m/z* 128.15 (**3**) and is concluded to have been formed from $[M\text{-}C_{18}H_{35}]^{+}$ (**2**) due to the loss of a neutral $CH_3(CH_2)_7CH{=}CH(CH_2)_8N(CH_3)_2$ and from $[M\text{-}C_{18}H_{34}]^{+}$ (**2'**) from the loss of a neutral $CH_3(CH_2)_7CH{=}CH(CH_2)_6CH{=}CH_2$ and the corresponding singly charged ion *m/z* 46.06, *N*-methylmethanaminium (Table 2.3 & 2.4 and Figure 2.4A & 2.4B). In fact, the doubly charged ion observed at *m/z* 87.11 (**3'**) is a very minor product ion (Figure 2.4A) and therefore it is very likely that its formation is transient and it is relatively unstable due to the close proximity of the positive charges in both G18:1-2 and G18:1-3.

Since all G18:1-*s* gemini surfactants contain identical tail regions it is expect that there will be shared fragments within this gemini surfactant family. The presence of a double bond in the tail regions of the G18:1-*s* gemini surfactants results in a double bond also being present in their product ions, producing alk-1-en-1-ylium fragments: hept-1-en-1-ylium (**2''**), *m/z* 97.11, hex-1-en-1-ylium (**3''**), *m/z* 83.09, pent-1-en-1-ylium (**4''**), *m/z* 69.08, and but-1-en-1-ylium (**5''**), *m/z* 55.06 (Table 2.3 and Figure 2.4A & 2.4B). Similar to the G12-*s* family, an additional identical fragment seen in all analyzed G18:1-s gemini surfactants: a singly charged but-1-ylium at *m/z* 57.07 (**2'''**) (Table 2.3 and Figure 2.4A & 2.4B).

Increased fragmentation complexity is observed, in Tables 2.2 and 2.3, as the spacer region length is increased from two to sixteen or two to six carbons in length; with G12-16 and G18:1-6 generating the most complex fragmentation patterns of their respective families (Figure 2.3A, 2.3B, 2.4A & 2.4B). However, these spectra possess the fragments that are present in the spectra of other gemini surfactants and therefore they are representative of the G12-*s* and G18:1-*s* gemini surfactant families of nanoparticles, respectively. Within these distinct spectra there is,

however, one identical product ion shared by all ten compounds, but-1-ylium at *m/z* 57.07 (Tables 2.2 & 2.3), and several ions among the ten compounds which are structurally conserved; for example, the loss of a single tail fragment, **2** and **2'** (Tables 2.2 & 2.3 and Figure 2.3A, 2.3B, 2.4A & 2.4B)

Conclusion

The molecular composition of each G12-*s* and G18:1-*s* gemini surfactant was supported by QqToF-MS analysis. The assessment of the fragmentation pattern for each gemini surfactant was done by QqToF-MS/MS and demonstrated that the gemini surfactants share fragmentation patterns that are specific to their respective gemini surfactant families. Currently, a study of other gemini surfactant families is taking place with the intent of identifying two to three product ions for each gemini surfactant that have unique *m/z* values and will be utilized in multiple reaction monitoring. MRM utilizes both the precursor ion and select diagnostic product ions produced for the quantification of the compound. In addition both the precursor-to-product ion transition and retention times of each compound will allow for their exact identification. By identifying both the similarities and differences between each gemini surfactant product ions, the differing product ions are candidates for use during LC-MS/MS quantification of them and their metabolites in biological samples. By quantifying both the gemini surfactants and their metabolites an evaluation of their toxicity, bioavailability and half-life during the course of transfection can be undertaken. Currently, the LC method required to separate the gemini surfactants is being designed in order to quantify individual gemini surfactants in media mixture.

Literature Cited

1. Bozkir A, Saka OM 2004. Chitosan-DNA nanoparticles: effect on DNA integrity, bacterial transformation and transfection efficiency. Journal of Drug Targeting 12:281-288.

2. Choi SH, Jin SE, Lee MK, Lim SJ, Park JS, Kim BG, Ahn WS, Kim CK 2008. Novel cationic solid lipid nanoparticles enhanced p53 gene transfer to lung cancer cells. European Journal of Pharmaceutics and Biopharmaceutics 68:545-554.

3. de la Fuente M, Seijo B, Alonso MJ 2008. Novel hyaluronic acid-chitosan nanoparticles for ocular gene therapy. Investigative Ophthalmology and Visual Science 49:2016-2024.

4. Kaul G, Amiji M 2005. Tumor-targeted gene delivery using poly(ethylene glycol)-modified gelatin nanoparticles: In Vitro and In Vivo studies. Pharmaceutical Research 22:951-961.

5. Martien R, Loretz B, Schnurch AB 2006. Oral gene delivery: design of polymeric carrier systems shielding toward intestinal enzymatic attack. Biopolymers 83:327-336.

6. Moreira JN, Santos A, Moura V, Pedroso de Lima MC, Simoes S 2008. Non-viral lipid-based nanoparticles for targeted cancer systemic gene silencing. Journal of Nanoscience and Nanotechnology 8:2187-2204.

7. Prabha S, Labhasetwar V 2004. Nanoparticle-mediated wild-type p53 gene delivery results in sustained antiproliferative activity in breast cancer cells. Molecular Pharmaceutics1:211-219.

8. Patil SD, Rhodes DG, Burgess DJ 2005. DNA-based therapeutics and DNA delivery systems: a comprehensive review. The AAPS Journal 7:E61-77.

9. Badea I, Verrall R, Baca-Estrada M, Tikoo S, Rosenberg A, Kumar P, Foldvari M 2005. *In Vivo* cutaneous interferon-γ gene delivery using novel dicationic (gemini) surfactant-plasmid complexes. The Journal of Gene Medicine 7:1200-1214.

10. Dubey PK, Mishra V, Jain S, Mahor S, Vyas SP 2004. Liposomes modified with cyclic RGD peptide for tumor targeting. Journal of Drug Targeting 12:257-264.

11. Zhang N, Chittasupho C, Duangrat C, Siahaan TJ, Berkland C 2008. PLGA nanoparticle-peptide conjugate effectively targets intercellular cell-adhesion molecule-1. Bioconjugate Chemistry 19:145-152.

12. Wettig SD, Verrall RE, Foldvari M 2008. Gemini surfactants: a new family of building blocks for non-viral gene delivery systems. Current Gene Therapy 8:9-23.

13. Thomas M, Klibanov AM 2003. Non-viral gene therapy: polycation-mediated DNA delivery. Applied Microbiology Biotechnology 62:27-34.

14. Menger FM, Littau CA 1991. Gemini-surfactants: synthesis and properties. Journal of the American Chemical Society 113:1451-1452.

15. Karlsson L, van Eijk MCP, Soderman O 2002. Compaction of DNA by gemini surfactants: effects of surfactant architecture. Journal of Colloid and Interface Science 252:290-296.

16. Li J, Dahanayake M, Reierson RL, Tracy DJ 1997. Topical compositions and methods for treatment of skin damage and aging using catecholamines and related compounds. U.S. Patent 5,643,586.

17. Zhu YP, Masuyama A, Kirito YI, Okahara M, Rosen MJ 1992. Preparation and properties of glycerol-based double or triple-chain surfactants with two hydrophilic ionic groups. Journal of the American Oil Chemists' Society 69:626-632.

18. Pinazo A, Diz M, Solans C, Pés MA, Erra P, Infante MR 1993. Synthesis and properties of cationic surfactants containing a disulfide bond. Journal of the American Oil Chemists' Society 70:37-42.

19. Liu L, Rosen MJ 1996. The interaction of some novel diquaternary gemini surfactants with anionic surfactants. Journal of Colloid and Interface Science 179:454-459.

20. Menger FM, Littau CA 1993. Gemini surfactants: a new class of self-assembling molecules. Journal of the American Chemical Society 115:10083-10090.

21. Matulis D, Rouzina I, Bloomfield VA 2002. Thermodynamics of cationic lipid binding to DNA and DNA condensation: roles of electrostatics and hydrophobicity. Journal of the American Chemical Society 124:7331-7342.

22. Kirby AJ, Camilleri P, Engberts JBFN, Feiters MC, Nolte RJM, Soderman O, Bergsma M, Bell PC, Fielden ML, Garcia Rodriguez CL, Guedat P, Kremer A, McGregor C, Perrin C, Ronsin G, van Eijk MCP 2003. Gemini surfactants: new synthetic vectors for gene transfection. Angewandte Chemie International Edition 42:1448-1457.

23. Wang C, Xingfu L, Wettig SD, Badea I, Foldvari M, Verrall RE 2007. Investigation of complexes formed by interaction of cationic gemini surfactants with deoxyribonucleic acid. Physical Chemistry Chemical Physics 9:1616-1628.

24. Badea I, Wettig S, Verrall R, Foldvari M 2007. Topical non-invasive gene delivery using gemini nanoparticles in interferon-γ-deficient mice. European Journal of Pharmaceutics and Biopharmaceutics 65:414-422.

25. Dauty E, Remy JS, Blessing T, Behr JP 2001. Dimerizable cationic detergents with a low CMC condense plasmid DNA into nanometric particles and transfect cells in culture. Journal of the American Chemical Society 123:9227-9234.

26. Wettig SD, Badea I, Donkuru M, Verrall RE, Foldvari M 2007. Structural and transfection properties of amine-substituted gemini surfactant-based nanoparticles. The Journal of Gene Medicine 9:649-658.

27. Fielden ML, Perrin C, Kelmer A, Bergsma M, Stuart MC, Camilleri P, Engberts, JBFN 2001. Sugar-based tertiary amino gemini surfactants with a vesicle-to-micelle transition in the endosomal ph range mediate efficient transfection in vitro. European Journal of Biochemistry 268:1269-1279.

28. Wettig SD, Badea I, Donkuru M 2008. Substitution effects in gemini surfactants: application to DNA transfection. Manuscript in Preparation 2008.

29. Calvo P, Gouritin B, Villarroyo H, Eclancher F, Giannavola C, Klein C, Andreux JP, Couvreur P 2002. Quantification and localization PEGylated polycyanoacrylate nanoparticles in brain and spinal cord during experimental allergic encephalomyelitis in the rat. European Journal of Neuroscience 15:1317-1326.

30. Kim MS, Jin SJ, Kim JS, Park HJ, Song HS, Neubert RHH, Hwang SJ 2008. Preparation, characterization and in vivo evaluation of amorphous atorvastatin calcium nanoparticles using supercritical antisolvent process. European Journal of Pharmaceutics and Biopharmaceutics 69:454-465.

31. Wood M, De Boeck G, Samyn N, Morris M, Cooper DP, Maes RAA, De Bruijn EA 2003. Development of a rapid and sensitive method for the quantification of amphetamines in human plasma and oral fluid by LC-MS/MS. Journal of Analytical Toxicology 27:78-87.

32. Joly N, El Aneed A, Martin P, Cecchelli R, Banoub J 2005. Structural determination of the novel fragmentation routes of morphine opiate receptor antagonists using electrospray ionization quadrupole time-of-flight tandem mass spectrometry. Rapid Communications in Mass Spectrometry 19:3119-3130.

33. Nagele E, Moritz R 2005. Structure elucidation of degradation products of the antibiotic amoxicillin with ion trap MSn and accurate mass determination by ESI TOF. Journal of the American Society for Mass Spectrometry 16:1670-1676.

34. El-Aneed A, Banoub J, Koen-Alonso M, Boullanger P, Lafont D 2007. Establishment of mass spectrometric fingerprints of novel synthetic cholesteryl neoglycolipids: the prescence of a unique c-glycoside species during electrospray ionization and during collision-induced dissociation tandem mass spectrometry. Journal of the American Society for Mass Spectrometry 18:294-310.

35. Wang Z, Li J, Altman E 2006. Structural characterization of the lipid a region of aeromonas salmonicida subspecies salmonicida lipopolysaccharide. Carbohydrate Research 341:2816-2825.

36. El-Aneed A, Banoub J 2005. Elucidation of the molecular structure of lipid an isolated from both a rough mutant and a wild strain of aeromonas salmonicida lipopolysaccharides using

electrospray ionization quadrupole time-of-flight tandem mass spectrometry. Rapid Communications in Mass Spectrometry 19:1683-1695.

37. Wettig SD 2000. Studies of the interaction of gemini surfactants with polymers and triblock copolymers. Ph. D. Thesis University of Saskatchewan, Saskatoon, Canada.

38. Jenkins KM 2000. Thermodynamic studies of bis(quaternary ammonium) and (n-alkyl-) ionic surfactants. M. Sc. Thesis University of Saskatchewan, Saskatoon, Canada.

39. Domon B, Aebersold R 2006. Mass spectrometry and protein analysis. Science 312:212-217.

CHAPTER 3
TANDEM MASS SPECTROMETRY ANALYSIS OF NOVEL DIQUATERNARY AMMONIUM GEMINI SURFACTANTS AND THEIR BROMIDE ADDUCTS IN ELECTROSPRAY-POSITIVE ION MODE IONIZATION

Joshua Buse, Ildiko Badea, Ronald E. Verrall, Anas El-Aneed

Published in Journal of Mass Spectrometry 46 (2011), p 1060-1070

The identification of MS/MS fingerprints for a bioactive molecule is important for the development of qualitative and quantitative analytical methods. Chapter 2 outlined the fragmentation behavior of 10 novel diquaternary ammonium gemini surfactants with alkyl spacer moieties. These gemini surfactants had a conserved fragmentation pattern regardless of the length of the spacer region and provided preliminary data on the fragmentation of simplistic diquaternary ammonium gemini surfactants and their ionization behavior within ESI-MS instruments. In this study, single stage MS and MS/MS analysis of 29 gemini surfactant moieties was undertaken to understand the gas phase and CID behavior of gemini surfactants with various structural features.

Structural elucidation and characterization of 29 novel diquaternary ammonium gemini surfactant molecules was achieved using a QqToF-MS/MS and a QhQ-MS. The tested compounds were categorized into four distinct structural families based upon the composition of the spacer region: alkyl chains, secondary and tertiary amines, hydroxyl functional groups as well as ether linkers. MS, MS/MS, and *quasi* MS^3 analysis of both the gemini surfactants and their bromide adducts allowed for the confirmation of each gemini surfactant's molecular composition and structure through the identification of common and unique product ions as well as their origin.

High resolution, single stage MS analysis showed that mass accuracy was less than 5 PPM for all gemini surfactants and 10 PPM for all gemini surfactant bromide adducts; confirming their molecular composition. Identification of similarities in the gemini surfactants' fragmentation behavior resulted in the production of a universal fragmentation pathway, while differences were identified as unique product ions that are indicative of specific structural elements. Furthermore, evidence for the association of a gemini surfactant with bromine counter ion was confirmed during MS analysis of tested gemini surfactants regardless of their chemical composition. Previously, evidence for bromine and gemini surfactant association was

only observed with compounds bearing short alkyl spacer regions. MS/MS analysis of the bromine adducts was also confirmatory to the molecular structure.

The universal fragmentation pathway has proven beneficial in the qualitative and quantitative analysis of these 29 gemini surfactants by multiple-reaction monitoring methods (CHAPTER 4) because it identifies product ions with unique *m/z* values, ensuring the specificity of the analysis.

Tandem mass spectrometry analysis of novel diquaternary ammonium gemini surfactants and their bromide adducts in electrospray-positive ion mode ionization

Joshua Buse[1] Ildiko Badea[1] Ronald E. Verrall[2] Anas El-Aneed[1*]

[1.] Drug Discovery and Development Research Group, College of Pharmacy and Nutrition, University of Saskatchewan, 110 Science Place, Saskatoon, SK S7N 5C9, Canada

[2.] Department of Chemistry, University of Saskatchewan, 110 Science Place, Saskatoon, SK S7N 5C9, Canada

*Corresponding Author:

Telephone: +1-306-966-2013

Fax: +1-306-966-6377

E-mail Address: anas.el-aneed@usask.ca

Keywords: Fragmentation pattern; diquaternary ammonium gemini surfactant; tandem mass spectrometry; quasi MS^3

Introduction

Drug delivery has been facilitated by various cationic polymers and lipids,[1, 2] such as diquaternary ammonium gemini surfactant lipoplexes.[3] Gemini surfactants are classified as compounds which contain two polar head regions, each covalently bound to a hydrophobic tail region (*t*), separated by a spacer (*s*); producing a tail-spacer-tail configuration (*t*-*s*-*t*) (Figure 3.1).[4] These structures are given identifier names comprised of G, for gemini surfactant, *t* for tail region composition and length as well as *s* for spacer region composition and length: (G*t*-*s*). Numerous functional groups can be incorporated within the spacer region to reduce toxicity and enhance therapeutic outcomes. In this study, four major groups of gemini surfactants were evaluated; the classification of which was dependent on the chemistry of the spacer region: alkyl chains (designated as *s* corresponding to the length of alkyl chain - Figure 3.1A), secondary and tertiary amines (designated as *s*N where s corresponds to length of alkyl chains - Figure 3.1B), hydroxyl functional groups (designated as 4$(OH)_n$ where n corresponds to the number of hydroxyl functional groups - Figure 3.1C) as well as ether linkers ((designated as EO*s* where s is the number of ethoxy moieties - Figure 3.1D).

The formation of cationic liposomal nanostructures occurs spontaneously when a lipid mixture, including cationic diquaternary ammonium gemini surfactants, are introduced into solution with genetic material.[5-7] The electrostatic interactions of the cationic head region with the anionic backbone of the genetic material and the hydrophobic packing of the negative charge results in the internalization of genetic material within the lipoplex.[8] Those gemini surfactants that are symmetrical in nature, specifically the presence of symmetry between the tail regions, were found to have superior interactions with deoxyribonucleic acid, leading to enhanced transfection efficiency, in comparison to asymmetrical gemini surfactants.[9] In addition, the spacer length, valence, head group size, tail length, and molecular architecture of gemini surfactants play a critical role in their interaction with genetic material.[9] An increase in the length of the hydrocarbon tail regions was found to increase the transfection efficacy facilitated by gemini surfactants due to their ability to adopt a variety of polymorphic structures.[11-13] Conversely, modifications in the spacer region were undertaken to ensure optimal spacing of those regions within the molecule involved in interactions with the genetic material.[14] Furthermore, the inclusion of ethylene oxide, hydroxyl, and amine substituent's within the spacer region sought to increase the number of points of interaction between the gemini surfactant and

A^1 [G*t-s*]

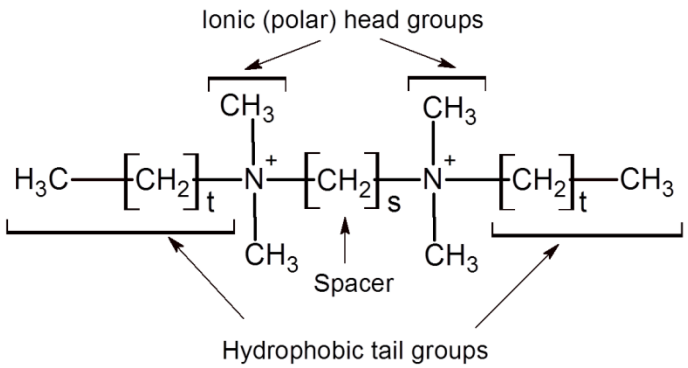

A^2 [G*t:1-s*]

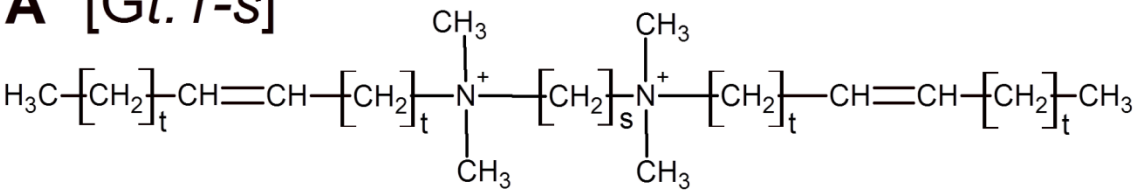

B [G*t-sN*]

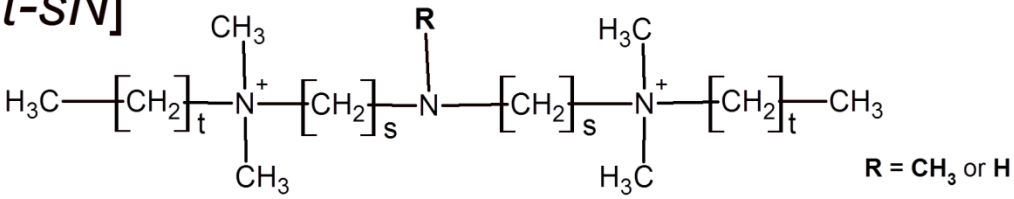

C [G*t-4(OH)$_n$*]

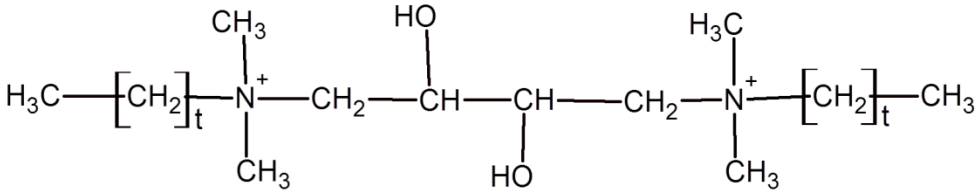

D [G*t-EO$_s$*]

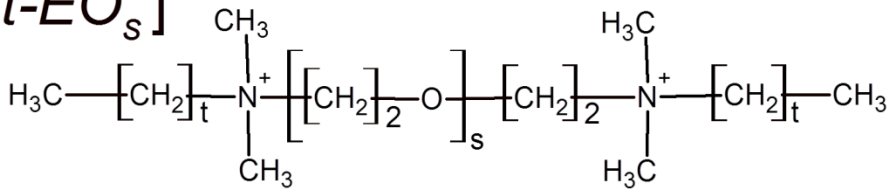

Figure 3.1 Diquaternary ammonium gemini surfactants evaluated in this study are comprised of two tail regions (saturated [A^1] or unsaturated [A^2] alkyl chains) connected to one another through a spacer region. The compounds are categorized based upon the composition of the spacer region: (A^1 & A^2) alkyl chain with no substituent's (B) alkyl chain that include secondary and tertiary amine(s) functional group(s) (C) alkyl chain that includes hydroxyl functional group(s) (D) alkyl chain that contains ether linker(s). The variation in the tail and spacer region can induce difference in the gemini surfactants properties.

the DNA leading to enhanced transfection efficiency through an increase in structure-activity and binding efficiency;[14, 15] the gemini surfactant G12-3NH displayed a 9 fold increase in transfection efficiency in comparison to the compound G12-3.[10]

Gemini surfactants are well-characterized for their use as gene delivery agents.[16-18] The size distribution of many diquaternary ammonium gemini surfactant-based nanoparticles is between 100 and 200 ±10 nm. The nano-scale size distribution of gemini surfactant complexes and their polycationic nature allows for their use for both *in vitro* and *in vivo* gene delivery applications.[3, 17, 19] For example, topical transfection of the IFNγ gene using nanoparticles containing G16-3 into mouse epidermis produced superior results compared to the unprotected IFNγ gene.[17] Similarly, DNA transfection into human fibroblast cells was found to be enhanced by gemini surfactants in comparison to commercially available cationic lipids.[20]

MS is routinely used for qualitative and quantitative applications.[21-25] Single stage MS and MS/MS can be utilized for structural determination and MS/MS fingerprint identification.[26-28] The identification of MS/MS fingerprints for a bioactive molecule is important for identification and quantification purposes within biological or environmental samples.[29, 30] Glycosyl isoflavonoids, for example, can be selectively identified through the fragmentation of the O-glycosidic bond as well as the subsequent loss of methyl functional groups and hydrogen atoms.[31] The spectra produced and corresponding relative *m/z* intensities of each glycosyl isoflavonoids following multi-stage MS analysis are indicative of the their structures and can be utilized in the future for their identification in crude plant extracts.[31] Similarly in our recent communication, 10 novel diquaternary ammonium gemini surfactants with alkyl spacer moieties (Figure 3.1A[1] and 3.1A[2]) were analyzed by ESI-MS/MS.[26] These gemini surfactants had a conserved fragmentation pattern regardless of the length of the spacer region.[26] The information acquired during MS and MS/MS experiments provided preliminary data on the fragmentation of simplistic diquaternary ammonium gemini surfactants and their ionization behavior in ESI-MS instruments.

In this work, the molecular structure of twenty-nine gemini surfactants, with varying spacer complexity, and their MS/MS fingerprint/fragmentation pathways were elucidated using single stage MS, MS/MS, and *quasi* MS^3 experiments. The experimental data provided the basis for the proposed universal fragmentation pathway. The complexity of the fragmentation pattern, however, increased proportionally with the molecular weight as well as the complexity of the

spacer region. In addition, the MS and MS/MS analysis of gemini surfactant bromide adducts demonstrated that ion pair formation can occur within the gas phase between bromide and gemini surfactants of varying composition.

Experimental

Materials

All twenty-nine G*t-s* gemini surfactants, categorized into four families based upon the spacer composition, were synthesized by Dr. Ronald E. Verrall's research group in the Department of Chemistry at the University of Saskatchewan based upon previously reported methods of synthesis.[32-34] Variations in the gemini surfactant's chemical structure included: tail region length and saturation (Figure 3.1A[1] & 3.1A[2]), length of non-substituted alkyl spacers (Figure 3.1A[1] & 3.1A[2]), inclusion in the spacer of secondary and tertiary amines (Figure 3.1B), of hydroxyl functional groups (Figure 5.1C) or of ether linkers (Figure 3.1D). The association of bromide counterions with all gemini surfactants analyzed is due to the action of bromide as a counterion in the starting material utilized during chemical synthesis.[34] Following the synthesis of each gemini surfactant, the purity of each compound was determined from surface tension measurements and the chemical structures of each gemini surfactants was confirmed by ^{1}H NMR in $CDCl_3$.[34]

Sample Preparation

All gemini surfactants solutions were individually prepared to a concentration of 3 mM in methanol-water (50:50 v:v) and stored at -20 °C prior to analysis. For MS, MS/MS, and *quasi* MS^3 analysis, each sample was further diluted 1000 to 5000x at the time of analysis, to achieve optimal ion counts, using methanol-water (50:50 v:v) with 0.1% formic acid. Methanol (LC grade purity, Caledon, Georgetown, ON, Canada), formic acid (98% GR ACS purity, EMD Chemicals Inc., Merck KGaA, Darmstadt, Germany) and Milli-Q organic-free water (Millipore, Bedford, MA, USA) were used as solvents. MS and MS/MS analysis of gemini surfactant bromide adducts, required a 100x to 1000x dilution at time of analysis using methanol.

Single Stage MS Analysis

An Applied Biosystems, API QSTAR XL MS/MS QqToF-MS/MS was used for MS and MS/MS analysis. The instrument was operated in the positive ion mode with the following

parameters: declustering potential between 20.0 and 50.0 V, declustering potential 2 of 100.0 V and focusing potential of 290.0 V. Sample aliquots were infused into the mass spectrometer by an integrated Harvard Syringe pump, through a Turbo Ionspray Source; 5.5 kV at a temperature of 80 °C. Two-point internal calibration was performed for all gemini surfactants. The internal calibrants were chosen because their *m/z* values fall within the *m/z* range of the tested compounds. Internal calibration was performed for the MS analysis of all twenty-nine diquaternary ammonium gemini surfactants using two doubly-charged calibration standards: [Glu1]-Fibrinopeptide B Human (amino acid sequence EGVNDNEEGFFSAR, [M+2H]2+ m/z 785.8421, C66H95N19O26, BaChem Bioscience Inc. [King of Prussia, PA, USA]) and N,N-bis(dimethyldodecyl)-1,2-ethanediammonium dibromide (G12-3 - [M]2+ m/z 234.2685). The molecular structure of G12-3 was previously confirmed by NMR while purity was confirmed by elemental and surface tension measurements.[35]

Analyses of the gemini surfactant's bromide adduct were performed in an identical manner to the above experiment, using an Applied Biosystems, API QSTAR XL QqToF-MS/MS. MS analysis of eight diquaternary ammonium gemini surfactant bromine adducts utilized two external calibrants: the cesium ion (molecular weight = 132.9055) from cesium iodide (CsI) and the iPD1 peptide (amino-acid sequence ALILTLVS ([M]); molecular weight = 828.5315; C39H72N8O11; Bachem Bioscience Inc., King of Prussia, PA, USA).

Low-Energy Collision Induced Dissociation MS/MS Analysis

All parameters applied during MS analysis were maintained for CID-MS/MS analysis of each compound using the API QSTAR XL system. For CID-MS/MS, nitrogen collision gas was infused into the collision cell and the CE was optimized for each compound between 15 and 50 eV to ensure the formation of product ions while maintaining the precursor ion in abundance.

Quasi MS^3 Analysis

A Micromass Quattro II QhQ-MS was utilized during *quasi* MS^3 analysis to establish the gemini surfactants' fragmentation pattern. The instrument was operated in the positive ion mode with an infusion rate of 25 µL/min, source temperature of 140º C, HV lens voltage of 0.71 kV and capillary voltage of 3.50 V. The cone voltage was set at 70 V to induce in source fragmentation of the compounds prior to entering the first quadrupole. The collision gas used during MS/MS experiments was argon and the CE was set between 15 and 50 eV in order to

generate product ions while ensuring that the precursor ion remained abundant. The Micromass Quattro II was superior in terms of inducing insource fragmentation in comparison to the Applied Biosystems, API QSTAR XL QqToF mass spectrometer and was therefore chosen to perform *quasi* MS^3 analysis.

Results and Discussion

Previously structural analysis of the diquaternary ammonium gemini surfactants by ^1H NMR in $CDCl_3$ resulted in the identification of each gemini surfactants structure.[34] The MS, MS/MS, and *quasi* MS^3 outlined here provided data on each gemini surfactant's structure that correlated with previous ^1H NMR results. In addition, the establishment of the universal fragmentation template has resulted in the identification of gemini surfactants within complex matrices and allow for confirmation of the chemical structures of newly synthesized gemini surfactants', including the presence of a bromide counter ion.

Single Stage Mass Spectrometric Analysis of Gemini Surfactants and Corresponding Bromide Adducts

Single stage QqToF MS analysis resulted in the formation of the doubly charged ion of all tested gemini surfactants with mass accuracies of less than 5 PPM (Table 3.1A). As such, the theoretical molecular formula of each gemini surfactant, including the presence of the correct number of nitrogen atoms, was confirmed. The precision and accuracy of these measurements were enhanced through the use of two doubly charged internal calibrants.

The identification of several gemini surfactant bromide adducts confirmed the presence of bromide within the purified samples as well as its action as a counter ion. The detection of the gemini surfactant bromide adduct ions required a greater concentration than the doubly charged gemini surfactants and produced mass accuracy values less than 10 PPM (Table 3.1B). In addition to utilizing mass accuracy data to confirm the presence of a single bromide, the isotopic distribution of bromide was employed to confirm its presence within the singly charged ion (Figure 3.2).

Table 3.1A Mass Accuracy of Gemini surfactants and Gemini Surfactant Bromine Adducts

Gemini Surfactants			
Gemini Surfactant	Theoretical	Observed	Mass Accuracy
Gt-s	m/z	m/z	PPM
G12-2	227.261	227.260	-1.540
G12-3	334.269	334.268	-0.598
G12-4	241.276	241.277	2.072
G12-6	255.292	255.291	-3.917
G12-7	262.300	262.299	-2.669
G12-8	269.308	269.308	2.599
G12-10	283.323	283.323	-1.059
G12-12	297.339	297.339	1.009
G12-16	325.370	325.369	-3.688
G16-3	290.331	290.330	-3.100
G16-6	311.355	311.354	-2.730
G16-7	318.363	318.361	-4.712
G18-3	318.363	318.363	0.314
G18-7	346.394	346.394	0.577
G18:1-2	309.339	309.339	0.970
G18:1-3	316.347	316.345	-4.742
G18:1-6	337.370	337.369	-3.853
G12-EO1	249.274	249.273	-4.613
G12-EO2	271.287	271.286	-2.765
G12-EO3	293.300	293.299	-2.216
G12-4(OH)	249.274	249.274	-1.003
G12-4(OH)2	257.271	257.270	-4.276
G12-2N	255.790	255.789	-2.150
G12-3N	269.805	269.806	3.521
G12-2N_2	284.319	284.318	-1.057
G12-3NH	262.798	262.797	-1.522
G16-3NH	318.860	318.860	-0.627
G18-3NH	346.891	346.893	3.171
G18:1-3NH	344.876	344.875	-3.335

Table 3.1B Mass Accuracy of Gemini surfactants and Gemini Surfactant Bromine Adducts			
Gemini Surfactant Bromine Adducts			
Gemini Surfactant	Theoretical	Observed	Mass Accuracy
Gt-s	m/z	m/z	PPM
G12-16	729.660	729.653	-9.045
G16-3	659.581	659.580	-2.123
G18:1-6	753.660	753.659	-0.133
G12-EO3	665.519	665.520	0.751
G12-4(OH)2	593.462	593.459	-4.718
G12-3N	618.530	618.531	2.587
G16-3NH	730.655	730.649	-7.527
G18-3NH	772.702	772.707	6.600

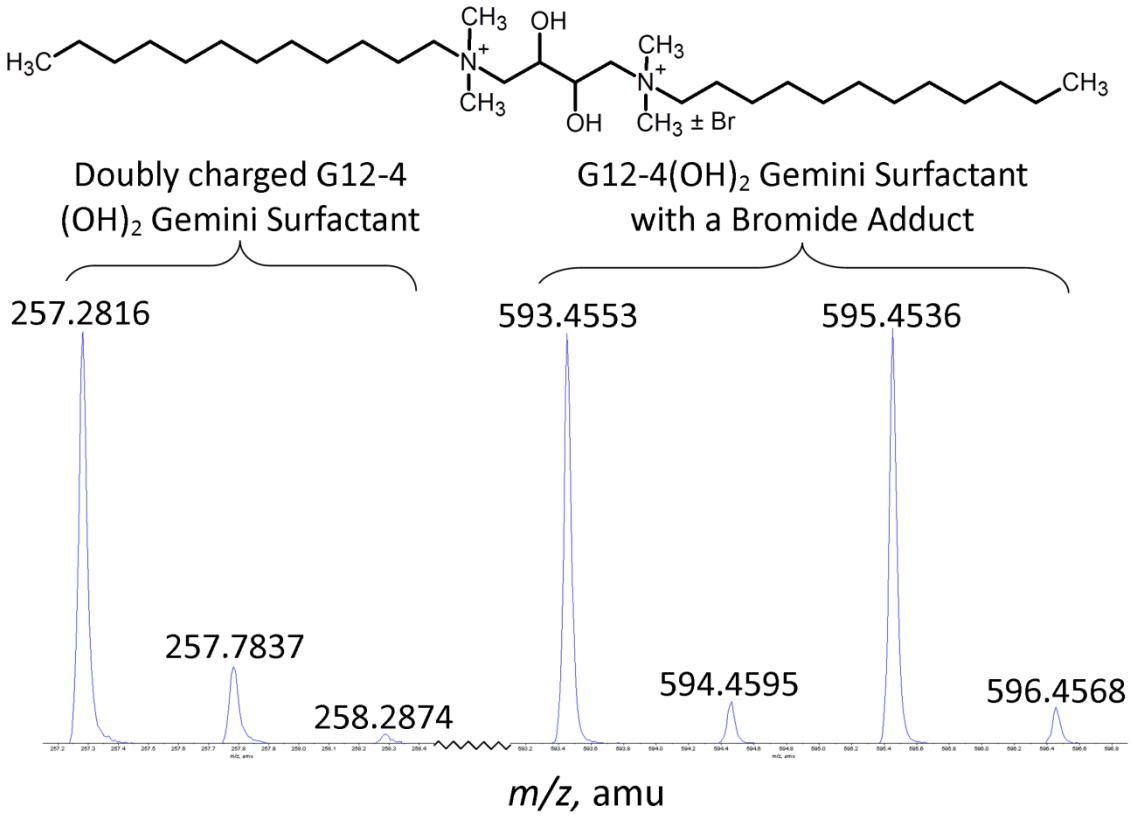

Figure 3.2 The m/z isotopic distribution for both the G12-4$(OH)_2$ gemini surfactant and corresponding bromide adduct clearly depicts the two positive charges found on the gemini surfactant ion and the formation of gemini surfactant bromide adduct ion; respectively.

The degree of ion pair formation between a gemini surfactant and a bromide counter ion in the gas phase was observed in a wide range of gemini surfactants (Table 3.1). This finding contradicts Blomberg *et al.*'s report of gemini surfactants in the liquid phase which indicated that bromide ion pair formation occurred only for gemini surfactants containing short spacer region; verified by surface force measurements.[36] Analysis of the decay length of the repulsive double-layer force at concentration below the CMC showed the gemini surfactants to be mainly dissociated from one another, however, increasing the concentration resulted in an increase in ion pair formation.[36] In addition, such association was observed with gemini surfactants with short alkyl spacer regions.[36] The difference in the degree of ion pair formation between the gas and liquid phases is not unexpected as the dielectric constant is much lower in the gas phase in comparison to the liquid phase.[37, 38] The present results, therefore, confirm the propensity of the gemini surfactant cation to form an ion pair with its counter ion under favorable conditions.

Universal MS/MS Fragmentation

Structural identification of each gemini surfactant was established through both CID-MS/MS and *quasi* MS^3 analysis utilizing a QqToF-MS/MS and QhQ-MS/MS; respectively. *Quasi* MS^3 involves fragmentation of ions within the ionization source, in-source fragmentation, followed by MS/MS of selected product ions.[21, 39] It has been successfully utilized to authenticate the fragmentation pattern of different bioactive compounds and garner further structural information on precursor and product ions.[21, 39, 40] For example, Sioud and coworkers evaluated the fragmentation behaviour of commercial biotin reagents using MS/MS and confirmed the proposed fragmentation pathways using *quasi* MS^3.[40] Therefore, both MS/MS and *quasi* MS^3 data provided structural information about each compound (APPENDIX A) while *quasi* MS^3 analysis rationalized the fragmentation route(s).

Analysis and comparison of the CID-MS/MS and *quasi* MS^3 behavior for all doubly charged gemini surfactant ions, $[M]^{2+}$, resulted in the establishment of a universal MS/MS fragmentation pathway (Figure 3.3A) which was observed during the analysis of all twenty-nine gemini surfactants (Table 3.2). While Figure 3.3A illustrates the universal fragmentation pattern,

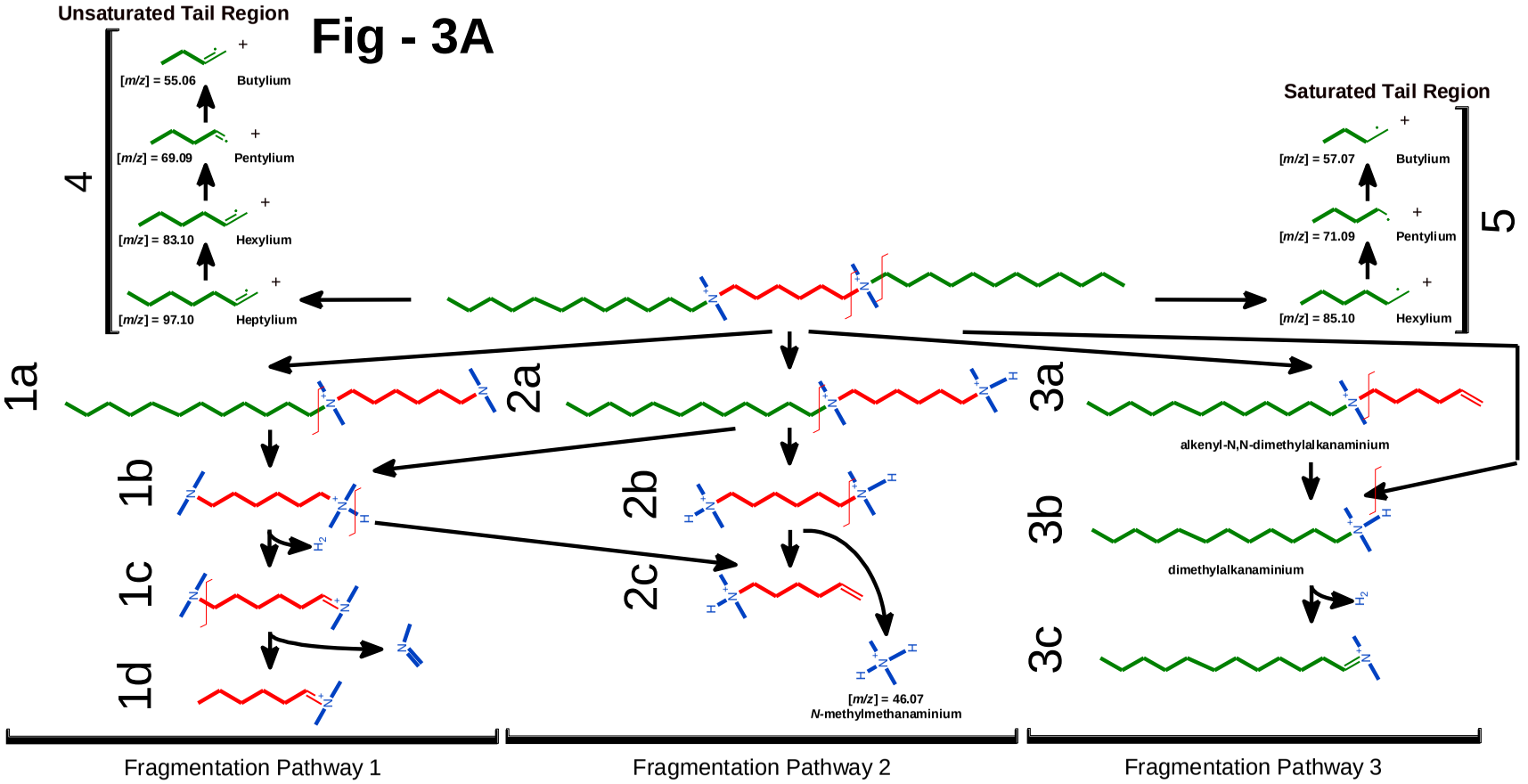

Figure 3.3A MS/MS and Quasi MS^3 analysis of gemini surfactants. The general Fragmentation pathway of native gemini surfactants following MS/MS and quasi MS^3 analysis on a Q-ToF and QQQ mass spectrometers. *Note: The spacer region contained other functional groups such as: hydroxyl groups, secondary and tertiary amines and ether linked alkyls*

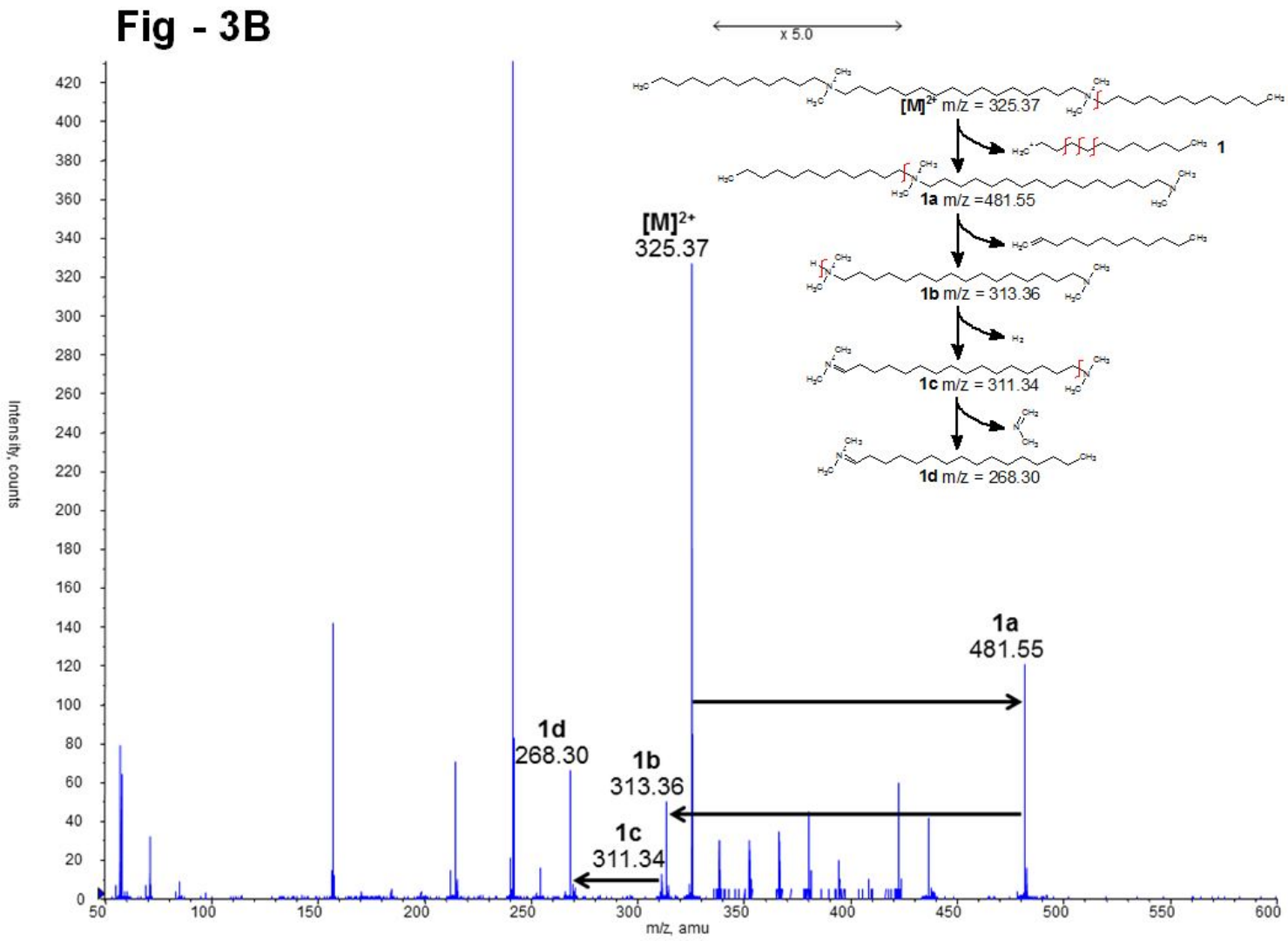

Figure 3.3B The first major fragmentation pathway of the G12-16 gemini surfactant with the associated m/z values and spectra

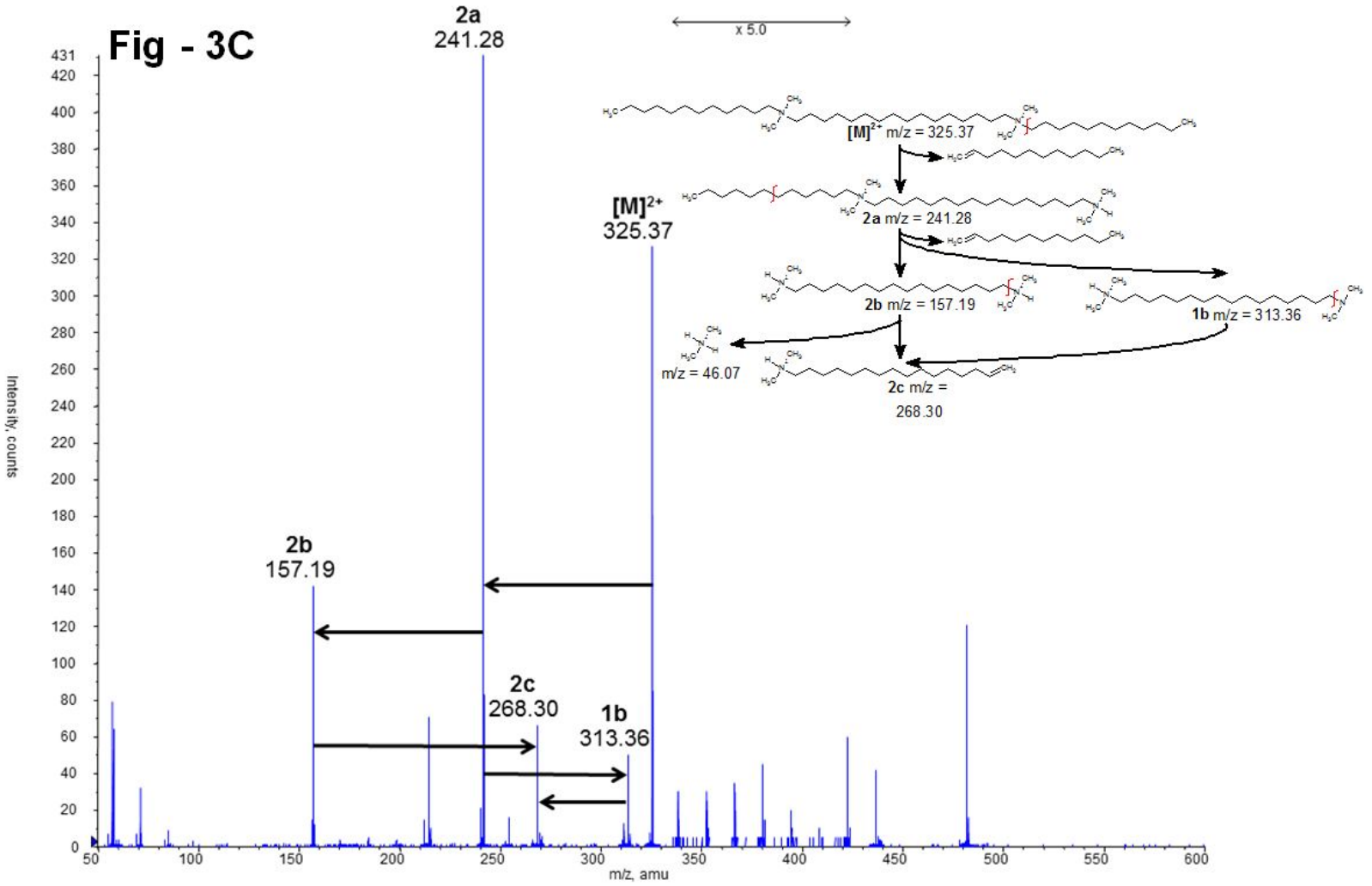

Figure 3.3C The second major fragmentation pathway of the G12-16 gemini surfactant with the associated m/z values and spectra

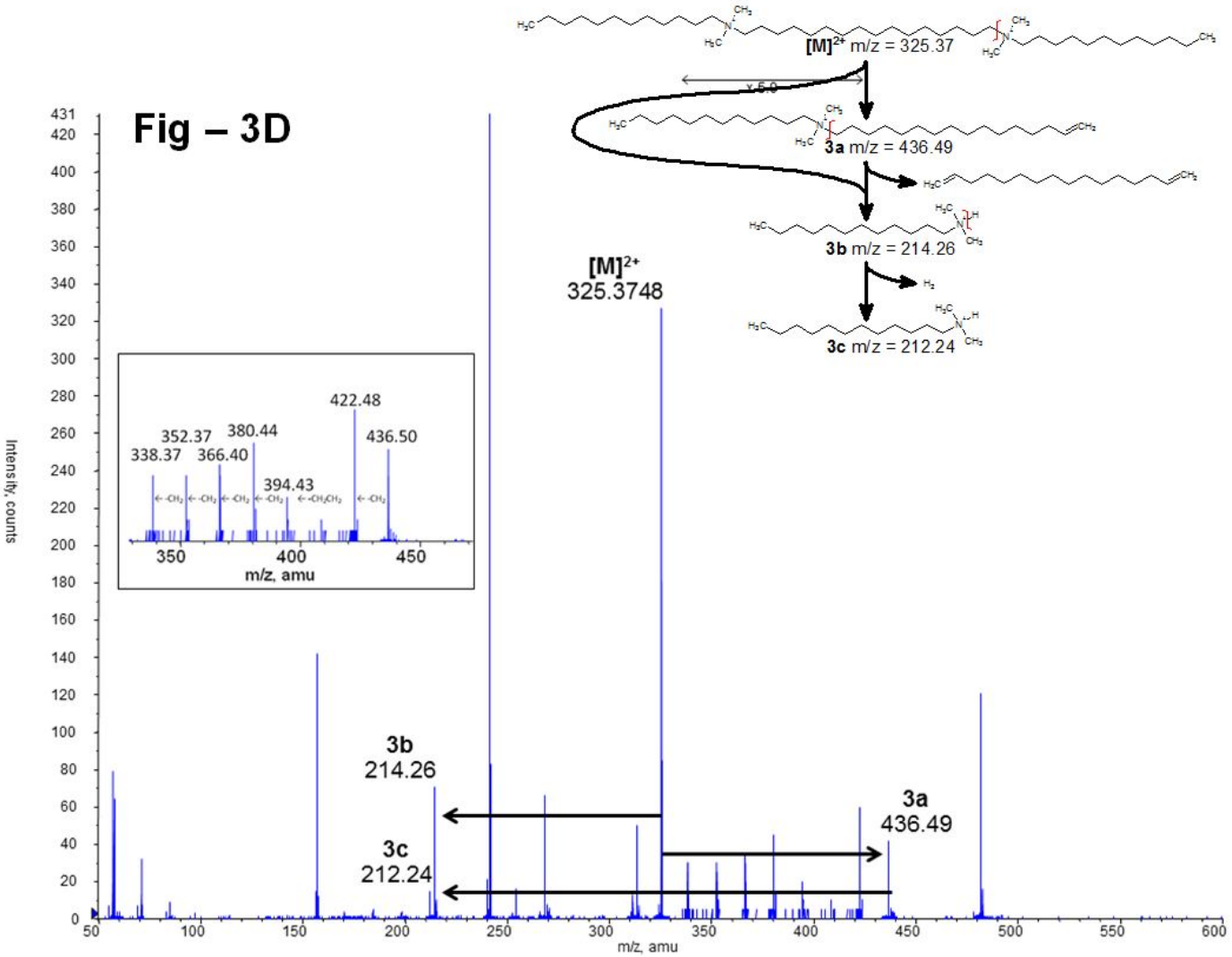

Figure 3.3D The third major fragmentation pathway of the G12-16 gemini surfactant with the associated m/z values and spectra

Table 3.2 Product ions identified following CID-MS/MS analysis of each precursor ion extracted from the Gemini Surfactant Ion. *Unique product ions are 1a, 2a & 3a.*

G12-s Gemini Surfactants (m/z)													
	$[M]^{2+}$	1a	1b	1c	1d	2a	2b	2c	3a	3b	3c	4	5
G12-2	227.26	285.32			72.08	143.17		72.08		214.09			85.1 → 57.07
G12-3	234.28	299.35	131.16		86.1	150.18		86.1					85.1 → 57.07
G12-4	241.28	313.39			100.11	157.19		100.11		214.09			85.1 → 57.07
G12-6	255.3	341.41			128.15	171.2	87.11	128.15		214.1	212.24		85.1 → 57.07
G12-7	262.31	355.42	187.22		142.16	178.21	94.11	142.16	296.34	214.1	212.24		85.1 → 57.07
G12-8	269.31	369.42	201.12	199.22	156.18	185.22	101.12	156.18	310.35	214.25	212.24		85.1 → 57.07
G12-10	283.32	397.45	229.26	227.25	184.2	199.23	115.14	184.2	352.4	214.26	212.24		85.1 → 57.07
G12-12	297.35	425.49	257.3	255.29	212.24	212.24	129.16	212.24	380.44	214.25	212.24		85.1 → 57.07
G12-16	325.37	481.55	313.36	311.34	268.3	241.28	157.19	268.3	436.49	214.26	212.24		85.1 → 57.07
G16-s Gemini Surfactants (m/z)													
	$[M]^{2+}$	1a	1b	1c	1d	2a	2b	2c	3a	3b	3c	4	5
G16-3	290.34	355.41	131.15		86.1	178.21		86.1					85.1 → 57.07
G16-6	311.41	379.34	173.42		128.19	199.21	87.03	128.19		270.33			85.1 → 57.07
G16-7	318.39	411.34	187.36		144.57	206.25	94.03	144.57	352.43				85.1 → 57.07
G18-s Gemini Surfactants (m/z)													
	$[M]^{2+}$	1a	1b	1c	1d	2a	2b	2c	3a	3b	3c	4	5
G18-3	318.38	383.45	131.16		86.1	192.23		86.1					85.1 → 57.07
G18-7	346.41	439.51	187.22		142.17	220.26	94.12	142.17	380.44	297.97			85.1 → 57.07
G18:1-s Gemini Surfactants (m/z)													
	$[M]^{2+}$	1a	1b	1c	1d	2a	2b	2c	3a	3b	3c	4	5
G18:1-2	309.34	367.41			72.08			72.08				97.1→55.06	
G18:1-3	316.35	381.43			86.1	191.35		86.1				97.1→55.06	
G18:1-6	337.38	423.48			128.15	212.25	211.24	128.15				97.1→55.06	

Table 3.2 continued

G12-EOs Gemini Surfactants (m/z)													
	$[M]^{2+}$	1a	1b	1c	1d	2a	2b	2c	3a	3b	3c	4	5
G12-EO1	249.28	329.37	161.21		116.11	165.19		116.11					85.1 → 57.07
G12-EO2	271.3	373.39	205.2		160.14	187.2	103.11	160.14	314.32				85.1 → 57.07
G12-EO3	293.31	417.42	249.23		204.16	209.22	125.12	204.16	346.35				85.1 → 57.07
G12-4(OH)s Gemini Surfactants (m/z)													
	$[M]^{2+}$	1a	1b	1c	1d	2a	2b	2c	3a	3b	3c	4	5
G12-4(OH)	249.29	329.35			116.11	165.19		116.11					85.1 → 57.07
G12-4(OH)2	257.28	345.23			132.11	173.19		132.11					85.1 → 57.07
G12-sN Gemini Surfactants (m/z)													
	$[M]^{2+}$	1a	1b	1c	1d	2a	2b	2c	3a	3b	3c	4	5
G12-2N	255.8				129.14	171.71		129.14	149.17	214.26	212.25		212.25
G12-3N	269.72					185.72			284.32	214.26	212.25		212.25
G12-3NH	262.82		188.23		143.17	178.72		143.17	271.32	214.27	212.25		212.25
G12-sN Gemini Surfactants (m/z)													
	$[M]^{2+}$	1a	1b	1c	1d	2a	2b	2c	3a	3b	3c	4	5
G12-2N2	284.33	423.48			129.15	212.25		129.15					85.1 → 57.07
G16-sN Gemini Surfactants (m/z)													
	$[M]^{2+}$	1a	1b	1c	1d	2a	2b	2c	3a	3b	3c	4	5
G16-3NH	318.87	412.47	188.22		143.17	206.74		143.17	327.38	270.32			85.1 → 57.07
G18-sN Gemini Surfactants (m/z)													
	$[M]^{2+}$	1a	1b	1c	1d	2a	2b	2c	3a	3b	3c	4	5
G18-3NH	346.89		188.21		143.15	220.74		143.15	397.45	297.96			85.1 → 57.07

regardless of the exact molecular structure of the tested compound, the MS/MS spectra of G12-16 will be used in the following sections for illustrative purposes (Figure 3.3B, 3.3C, and 3.3D).

Unique product ions formed from the precursor ion are classified into three distinct fragmentation pathways that involve either heterolytic or homolytic cleavage of the C-N bonds of the quaternary aminium ion. Two fragmentation pathways arise from the removal of the alkyl tail region producing either a singly charged ion containing aminium and amine functional groups through heterolytic cleavage (Figure 3.3A - struc. **1a**) or a doubly charged diaminium ion through homolytic cleavage (Figure 3.3A - struc. **2a**). The third fragmentation pathway results in the production of two complementary ions, a singly charged alkenyl-N,N-dimethylalkanaminium ion (Figure 3.3A - struc. **3a**) and a dimethylalkanaminium ion (Figure 3.3A - struc. **3b**).

Fragmentation pathway 1: As indicated earlier, G16-12 is used as an illustrative example. Doubly charged precursor ion extracted from G16-12 *m/z* 325.37 is cleaved at the C-N bond between the quaternary aminium and the first carbon within the tail region producing a singly charged product ion **1a**, *m/z* 481.55, bearing aminium and amine functional groups (Figures 3.3A & 3.3B). The loss of the second alkyl tail region as a neutral molecule produced the successive singly charged aminium product ion **1b,** *m/z* 313.36 (Figures 3.3A & 3.3B). The subsequent loss of H_2 produced a singly charged product ion **1c**, *m/z* 311.34, containing a double bond within the spacer region (Figures 3.3A & 3.3B). Finally, the dissociation of methylidenemethanamine, yielded the singly charged aminium product ion **1d,** observed at *m/z* 268.30 (Figures 3.3A & 3.3B).

Fragmentation pathway 2: The second fragmentation pathway starts with the homolytic cleavage of the C-N bond between the quaternary aminium and the first carbon within the tail region producing the doubly charged product ion **2a**; observed at *m/z* 241.28 in the case of G16-12 (Figures 3.3A & 3.3C). The loss of the second, uncharged alkyl tail region through homolytic cleavage from the doubly charged product ion **2a** produces the second diaminium product ion **2b**, *m/z* 157.19 (Figures 3.3A & 3.3C). The diaminium product ion **2b** produced a singly charged aminium product ion **2c**, *m/z* 268.30 (Figures 3.3A & 3.3C), through the loss of complementary methylmethanaminium; observed when scanning below 50 Da at *m/z* 46.07.[26]

Quasi MS^3 analysis revealed an interrelation between product ions within pathways 1 and 2. First, the singly charged aminium product ion **1b** (Figure 3.3A) was also generated from the doubly charged product ion **2a** (Figure 3.3A) as a result of cleavage of the alkyl tail region.

Second, the cleavage of methylmethamine from the singly charged species **1b** (Figure 3.3A) resulted in the production of the singly charged aminium species **2c** (Figure 3.3A). In addition, structures **1d** and **2c** (Figure 3.3A) are isobaric structural isomers varying only in the location of the double bond; the formation of which was confirmed via MS^3 analysis of ions **1b, 1c,** and **2b**. Furthermore, ions which precede **2c** within the fragmentation pathway may be either singly (**1b**) or doubly (**2b**) charged in nature (Figure 3.3A).

Fragmentation pathway 3: The third fragmentation pathway occurs as a result of cleavage of the C-N bond between the quaternary aminium and the neighboring carbon within the spacer region, producing two complementary ions confirmed via *quasi* MS^3: alkenyl-N,N-dimethylalkanaminium ion **3a**, *m/z* 436.49, and dimethylalkanaminium ion **3b**, *m/z* 214.26 (Figures 3.3A & 3.3D). Subsequent loss of H_2 from dimethylalkanaminium ion **3b** (Figures 3.3A & 3.3D) produced a dimethylalkenaminium ion **3c**, *m/z* 212.24 (Figures 3.3A & 3.3D). Further fragmentation of the spacer or tail regions in alkenyl-N,N-dimethylalkanaminium ions (Figures 3.3A & 3.3D - Struc. **3a**) resulted from loss of methylium (Figure 3.3D insert). The nature of this fragmentation was confirmed by the sequential loss of CH_2 during *quasi* MS^3 analysis and was solely observed in gemini surfactants that contained ten or more linear carbon atoms within their spacer region (Figure 3.3D - Struc. **3a** & insert). Due to such fragmentation, ion **3a** is not suitable for LC-MS/MS ion identification during multiple reaction monitoring, because of the observed sequential loss of CH_2. For example, the 3a ions of both G12-12 and G12-10 were observed in the MS/MS spectra of G12-16.

In addition to the three major fragmentation pathways, non-diagnostic ions are observed in the low *m/z* range and result from fragmentation of the alkyl tail region of gemini surfactants. The product ions observed differed solely based on the saturation of the tail region. Those gemini surfactants with a single unsaturation produced hept-1-en-1-ylium, hex-1-en-1-ylium, pent-1-en-1-ylium, and but-1-en-1-ylium ions (Figure 3.3A - Struc. **4**) while those with saturated tail regions produced hex-1-ylium, pent-1-ylium, and but-1-ylium ions (Figure 3.3A - Struc. **5**). These ions were observed in the *quasi* MS^3 analysis of any species bearing a tail region, hence it was suitable to illustrate the precursor ion as the source in Figure 3.3A.

In summary, the three ion types found to be unique during gemini surfactant MS/MS analysis were produced from 1) the loss of a singly charged tail region (Figure 3.3A - Struc. **1a**), 2) the loss of a neutral tail region (Figure 3.3A - Struc. **2a**) or 3) the loss of a

dimethylalkanaminium ion (Figure 3.3A - Struc. **3a**). At least one unique product ion is observed in the MS/MS analysis of all tested gemini surfactants, while two or more unique product ions being observed in the MS/MS analysis of 27 of 29 gemini surfactants (Table 3.2). In addition, increased MS/MS data complexity is observed for gemini surfactants with a greater number of atoms within their spacer region (Table 3.2). It is speculated that the increased complexity is a result of decreased repulsion between the quaternary ammonium functional groups resulting in the formation of stabilized product ions.

Unique Fragmentation Observed in the MS/MS Analysis of Gemini Surfactants

Unique fragmentation was observed during the MS/MS analysis of the G*t-EOs* (Figure 3.4) as well as G*t-sN* and G*t-sNH* (Figure 3.5) gemini surfactant families in addition to the universal fragmentation pattern aforementioned. The unique product ions that result from G*t*-EO*s* gemini surfactants were concluded to be formed from the product ion **2a** (Figure 3.3A). For example, the fragmentation of the product ion **2a** of G12-EO_3, *m/z* 209.22, at two different ether bond locations within the spacer region produced two singly charged product ions. Specifically cleavage between the oxygen and neighboring carbon nearest to the quaternary amine produced an ion observed at *m/z* 242.35 (Figure 3.4 – **Frag. 2**), while cleavage between the oxygen and neighboring carbon nearest to the tertiary amine produced an ion observed at *m/z* 346.35 (Figure 3.4 - **Frag. 3**). The later ion at m/z 346.35 yielded the formation of an ion at m/z of 178.37 (Figure 3.4 – **Frag. 4)**, which occurs in an identical manner to that observed for the production of the doubly charged product ion, *m/z* 209.22 through the loss of a neutral tail region (Figure 3.4 – **Frag. 1**).

The origin and structural elucidation of these unique product ions were confirmed by *quasi* MS^3 analysis. The product ion observed at *m/z* 209.22 is produced solely from *m/z* 293.32 following the transfer of a proton to the tertiary nitrogen and the elimination of a neutral dodecene molecule (Figure 3.4 – **Frag 1**). Subsequent fragmentation of the *m/z* 209.22 ion produces the product ions with *m/z* 242.35 (Figure 3.4 – **Frag 2**) and *m/z* 346.35 (Figure 3.4 – **Frag. 3**). However, the manner of the fragmentation is different because of differences in the electronegativity between the nitrogen atoms within the product ion.[41] In the case of product ion at *m/z* 346.35, the tertiary ammonium would have a greater electronegativity and this may influence the formation of a double bond between the two terminal carbons within the

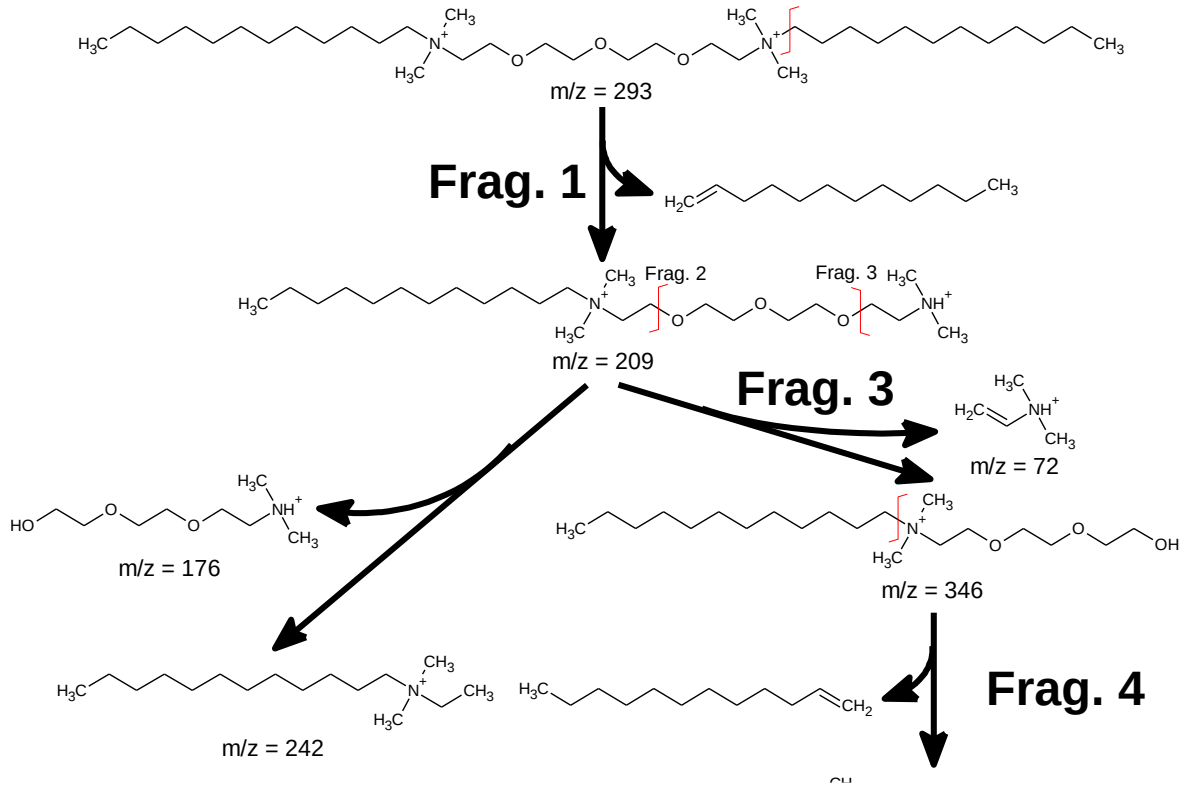

Figure 3.4 Unique fragment ions produced by Gt-EOs gemini surfactants as represented by the G12-EO_3 gemini surfactant

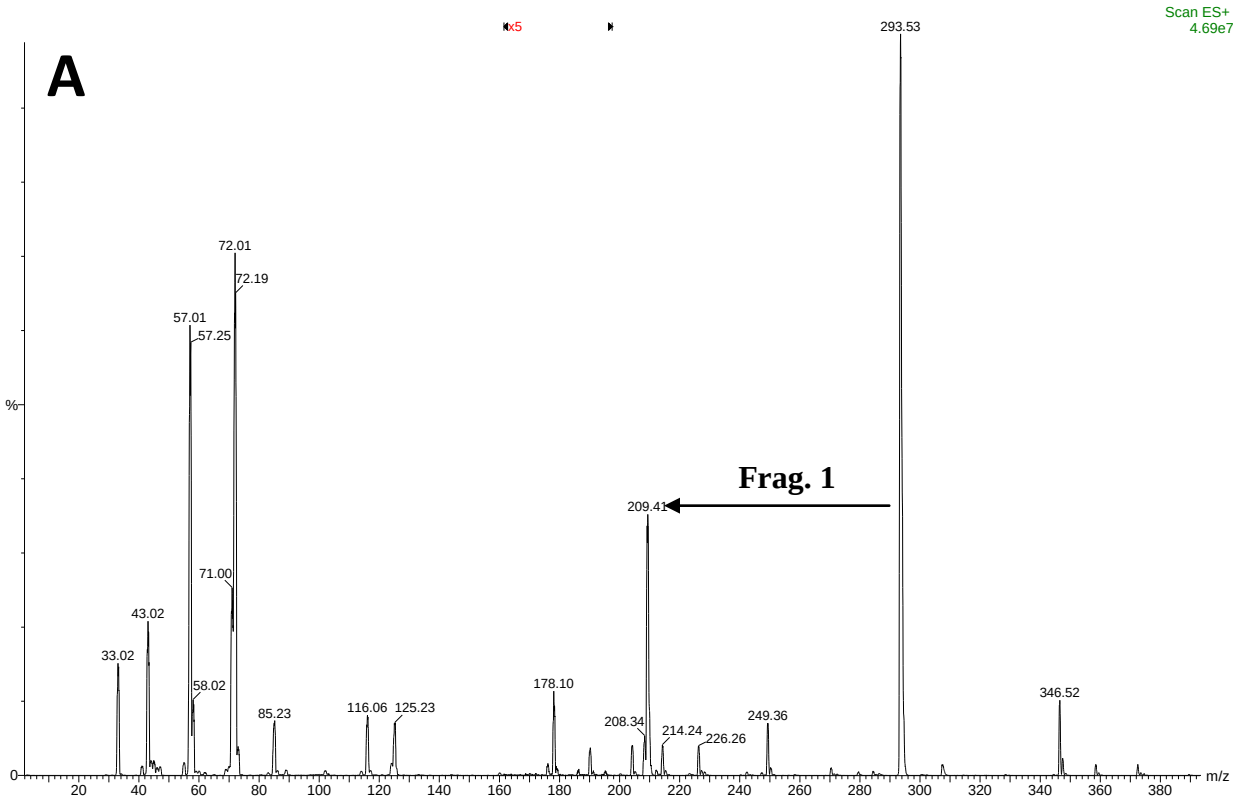

Figure 3.4A Corresponding MS/MS spectra for *m/z* 293 → 209 demonstrating the sequential fragmentation pattern.

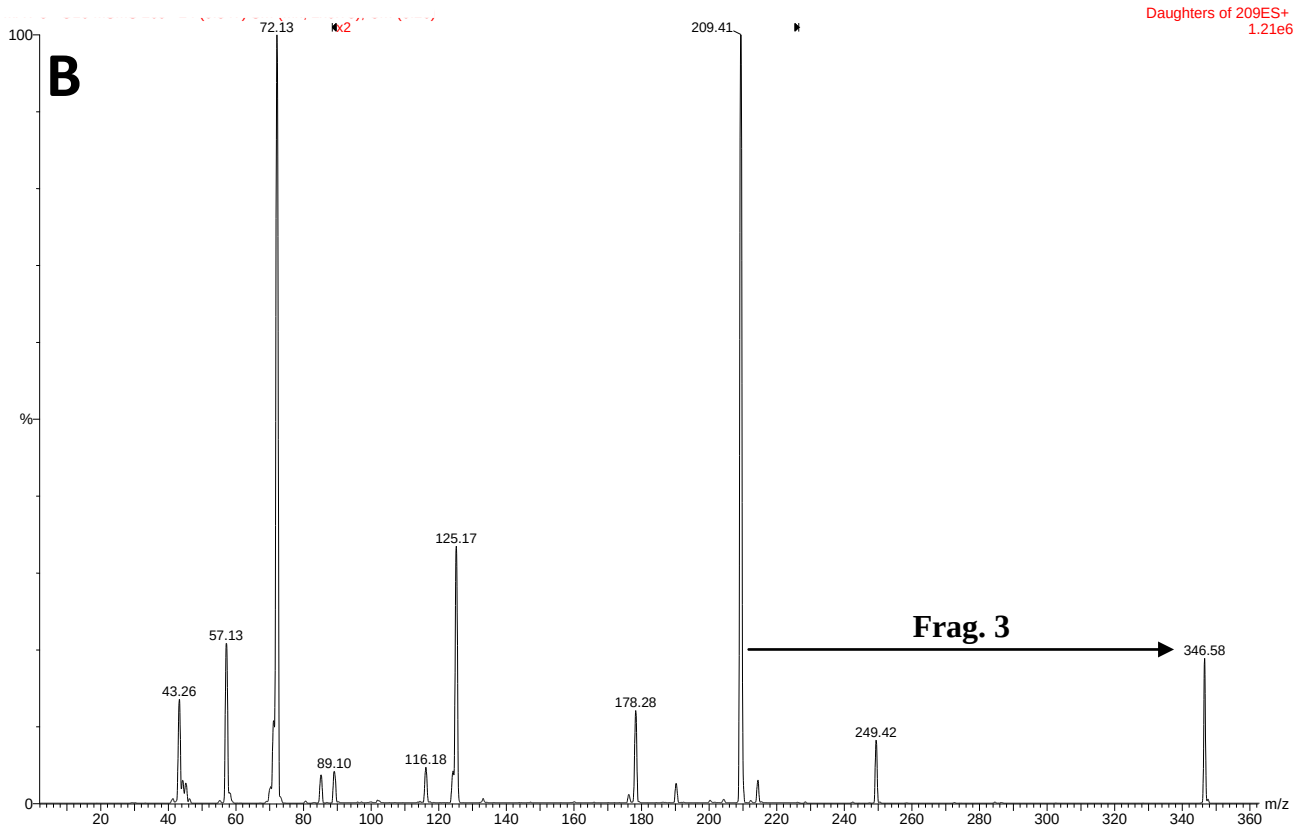

Figure 3.4B Corresponding quasi MS^3 spectra for *m/z* 209 → 346 (C) demonstrating the sequential fragmentation pattern.

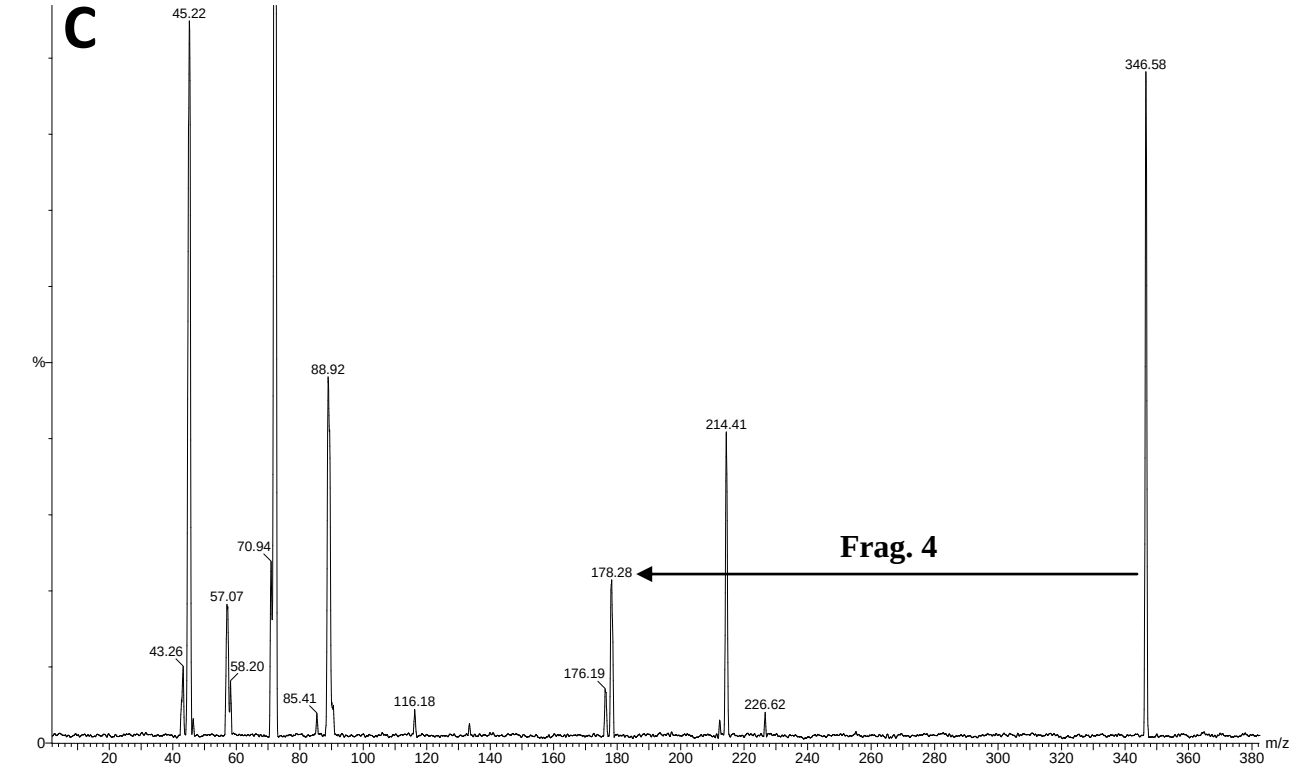

Figure 3.4C Corresponding quasi MS^3 spectra for *m/z* 346 → 178 demonstrating the sequential fragmentation pattern.

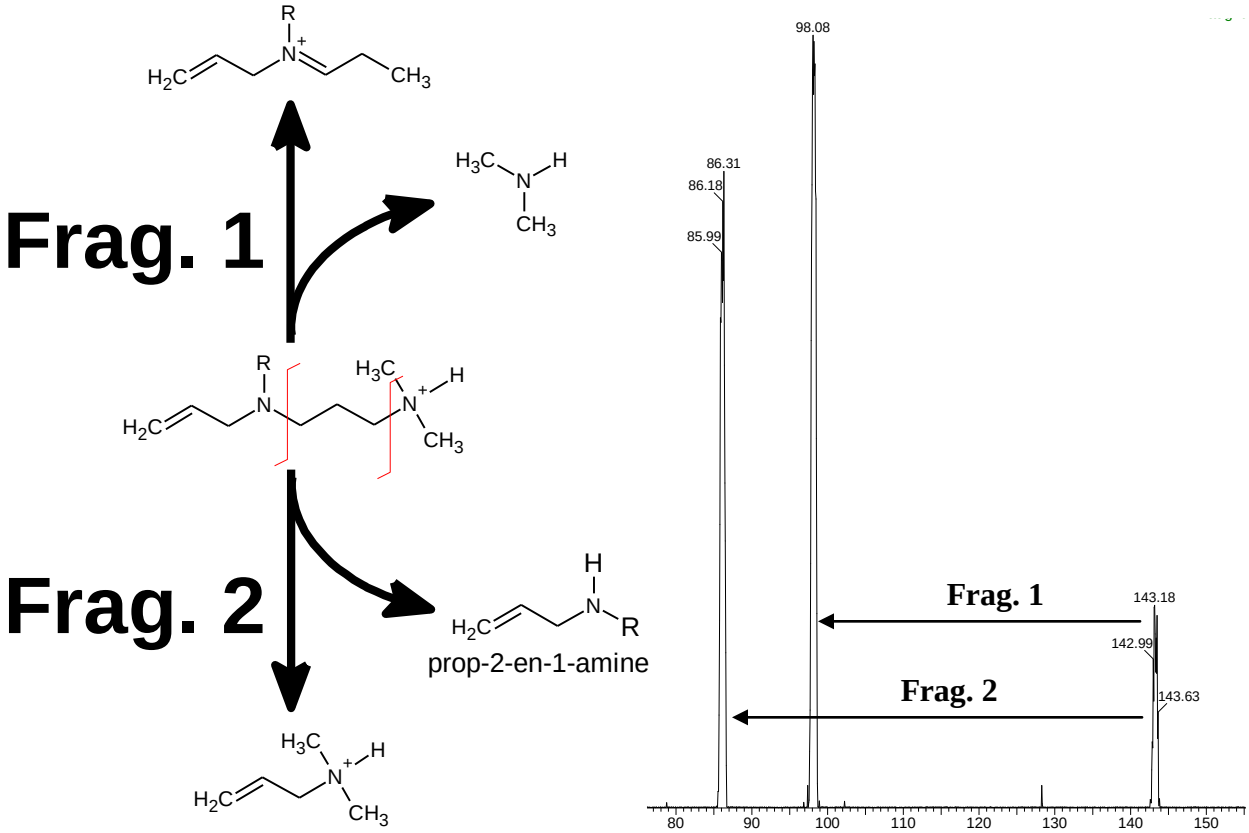

Figure 3.5 Unique fragment ions produced by Gt-sN and Gt-sNH gemini surfactants and the corresponding quasi MS^3 spectrum.

complementary ion observed at *m/z* 72.12 (Figure 3.4 – **Frag. 3**).[41] Conversely, the reduced electronegativity of the quaternary ammonium ion may result in a reduction in attraction which it has for electrons,[41] allowing for the terminal carbon to be saturated within the ion of *m/z* 242.35 (Figure 3.4 – **Frag. 2**) and production of the complementary ion at *m/z* 176.16.

Another structural family that produced unique ions are gemini surfactants bearing a secondary and tertiary amine within their spacer region. These compounds produced product ions which resulted from the loss of any uncharged alkyl amine (Figure 3.5 - **Frag. 1**); and cleavage between the amine of the spacer region and its neighboring carbon atom (Figure 3.5 - **Frag. 2**). G12-3NH, for example, produced both product ions during *quasi* MS^3 analysis of ion *m/z* 143.18, resulting in *m/z* 98.08 (Figure 3.5 - **Frag. 1**), due to loss of the terminal amine, and *m/z* 86.31 (Figure 3.5 - **Frag. 2**), due to cleavage of the spacer amine; such fragmentation was observed solely in product ions that had terminal tertiary ammonium atoms due to the loss of the tail region.

Tandem Mass Spectrometric and *Quasi* MS^3 analysis of Gemini Surfactant Bromide Adducts

Structural confirmation of several gemini surfactants was further supported by the MS and MS/MS analysis of their bromide adducts. The mass accuracy and isotopic data corroborated the projected molecular formula of 8 selected gemini surfactants from each family analyzed (Figure 3.1) and the formation of a bromide ion pair. The 8 gemini surfactants chosen covered all four families of gemini surfactants (Figure 3.1) and included variation in the size and composition of both the spacer and tail regions. The benefit of the MS/MS analysis of the gemini surfactant's bromide adducts is the ability to correlate the product ions to the gemini surfactants structure. Both the $[M + Br^{79}]^+$ and $[M + Br^{81}]^+$ molecular ions were analyzed by MS/MS to identify product ions which contain bromide adducts.

Five dominant product ions were observed following the fragmentation of 8 gemini surfactant bromide adducts with three of five producing distinct *m/z* for each gemini surfactant; G16-3 is used as an illustrative example. The first product observed resulted from the dissociation of the bromide ion from the gemini surfactant producing the doubly charged gemini surfactant observed at *m/z* 290.34 (Figure 3.6 - **Struc. 1**); distinct for all gemini surfactants analyzed. The dissociation of the bromide ion with the a methylium group heterolytically cleaved from a quaternary aminium resulted in a singly charged product ion *m/z* 565.66 (Figure 3.6 - **Struc. 2**). Similarly, dissociation of the bromide ion with an alkyl tail moiety due to heterolytic cleavage produced a singly charged ion bearing aminium and amine functional groups with a single tail region, *m/z* 355.41 (Figure 3.6 - **Struc. 3**). The ion observed at *m/z* 310.35 was produced via heterolytic cleavage of the precursor ion's dimethyl"alkan"aminium tail region, giving rise to a singly charged product ion comprised of a spacer attached to a tail region via a dimethyl aminium group (Figure 3.6 - **Struc. 4**). Finally, cleavage of the tail region as dimethyl"alkan"aminium can produce a doubly charged product ion comprised of a cationic spacer attached to a tail region via a dimethyl aminium group; one cationic charge is offset by a bromide counter ion, *m/z* 390.28 (Figure 3.6 - **Struc. 5**). The presence of each general structure in the MS/MS spectrum of 8 gemini surfactants is visually displayed in Table 3.3.

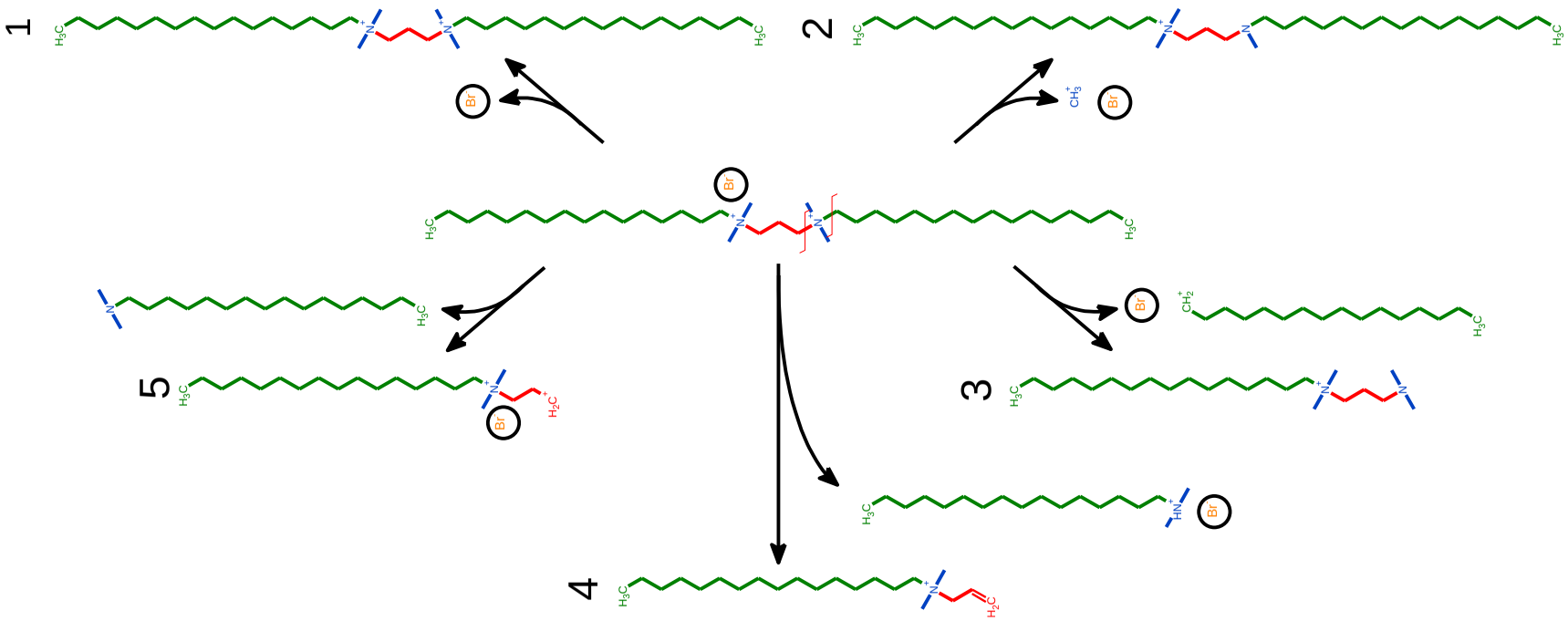

Figure 3.6 General fragmentation products of bromide adduct gemini surfactants following MS/MS analysis on a Q-ToF mass spectrometer.

Table 3.3 - Fragment ions identified in the MS/MS analysis of several bromine adduct gemini surfactant ions.

Gemini Surfactant Bromine Adducts						
	$[M+Br]^+$	1	2	3	4	5
G12-16	729.64	325.37	635.72	481.55	436.48	517.41
G16-3	659.58	290.34	565.66	355.41	310.35	390.28
G18:1-6	753.67	337.38	659.72	423.47	364.39	458.34
G12-EO3	665.52	293.3	571.58	417.41		452.28
G12-$(OH)_2$	593.45	257.27			300.29	
G12-3N	618.53		524.59	370.41	311.35	405.28
G16-3NH	730.65		636.72	426.48	367.4	461.35
G18-3NH	772.69		678.76	440.5	381.45	375.37

Additional fragmentation of the gemini surfactant bromide adducts is observed in both the Gt-sN and Gt-sNH families, including the formation of a tail region attached to an ionized tertiary amine. In addition, cleavage of the carbon-nitrogen bond of the secondary/tertiary amine located within the spacer region also produced unique product ions that could be utilized for MS/MS identification of such gemini surfactants. The uniqueness of each structure will allow for the identification of gemini surfactant bromide adducts within various medium, including formulations and cell cultures.

Conclusion

Confirmation of the projected molecular formula of 29 novel gemini surfactants was achieved by MS analysis of both the doubly charged ions and bromide adducts on a Qq-ToF mass spectrometer using two point internal calibration and external calibration, respectively. The observed *m/z* value for each doubly charged, gemini surfactant differed from the theoretical value by less than 5 PPM, while the singly charged, bromide adduct gemini surfactant ions differed by less than 10 PPM. Confirming the molecular formula and the molecular structure of each gemini surfactant required MS/MS and *quasi* MS^3 analysis on QqToF and QhQ mass spectrometers; respectively. The product ions produced during MS/MS and *quasi* MS^3 analysis of gemini surfactants and their bromide adducts confirmed their proposed molecular structures and fragmentation pathways. This allowed for the development of a universal fragmentation

pathway (Figure 3.3A). The universal fragmentation pathway will be beneficial in future quantitative and qualitative analysis of these 29 gemini surfactants by multiple-reaction monitoring methods because it identifies product ions with unique *m/z* values, ensuring the specificity of the analysis.

Quantitation of G16-3, for example, has been achieved within a tissue culture matrix at concentrations up to 3 μM by LC-MS/MS (data will be reported in a future manuscript) using the MS/MS fingerprint reported within this paper. Similarly, the quantitation of G12-3NH within COS-7 African Green monkey kidney fibroblast cells, has been achieved following gene transfection using a formulation containing a 111 μM of G12-3NH (data will be reported in a future manuscript). In addition, the universal fragmentation pattern was utilized to predict the dissociation behavior of novel amino acid-substituted gemini surfactants (data will be published upon completion of analysis). The overall fragmentation observed followed the universal fragmentation pathway (Figure 3A) with novel fragmentation being associated with the amino acids/dipeptide conjugated to the spacer region. From our experience, the use of the universal fragmentation pathway in the identification of the product ions shortened the time required for MS/MS analysis of novel diquaternary ammonium gemini surfactants.

Acknowledgements

The authors would like to acknowledge the technical support provided by Mr. Ken Thomas and the Saskatchewan Structural Science Center (SSSC) for the use of the QSTAR system. Funding was provided by the Natural Sciences and Engineering Research Council of Canada (NSERC) through an NSERC Discovery Grant.

Literature Cited

1. Kale AA, Torchilin VP 2007. Enhanced transfection of tumor cells in vivo using "smart" pH-sensitive TAT-modified pegylated liposomes. Journal of Drug Targeting 15:538-545.

2. Davis ME 2009. The first targeted delivery of siRNA in humans via a self-assembling, cyclodextrin polymer-based nanoparticle: from concept to clinic. Molecular Pharmaceutics 6:659-668.

3. Badea I, Verrall R, Baca-Estrada M, Tikoo S, Rosenberg A, Kumar P, Foldvari P 2005. In vivo cutaneous interferon-gamma gene delivery using novel dicationic (gemini) surfactant-plasmid complexes. Journal of Gene Medicine 7:1200-1214.

4. Menger FM, Keiper JS 2000. Gemini surfactants. Angewandte Chemie International Edition 39:1906-1920.

5. Kerner M, Meyuhas O, Hirsch-Lerner D, Rosen LJ, Min Z, Barenholz Y 2001. Interplay in lipoplexes between type of pDNA promoter and lipid composition determines transfection efficiency of human growth hormone in NIH3T3 cells in culture. Molecular and Cell Biology of Lipids 1532:128-136.

6. Zuidam NJ, Barenholz Y, Minsky A 1999. Chiral DNA packaging in DNA-cationic liposome assemblies. FEBS Letters 457:419-422.

7. Simberg D, Danino D, Talmon Y, Minsky A, Ferrari ME, Wheeler CJ, Barenholz Y 2001. Phase behavior, DNA ordering, and size instability of cationic lipoplexes. The Journal of Biological Chemistry 276:47453-47459.

8. Matulis D, Rouzina I, Bloomfield VA 2002. Thermodynamics of cationic lipid binding to DNA and DNA condensation: roles of electrostatics and hydrophobicity. Journal of the American Chemical Society. 124:7331-7342.

9. Jiang N, Wang J, Wang Y, Yan H, Thomas RK 2005. Microcalorimetric study on the interaction of dssymmetric gemini surfactants with DNA. Journal of Colloid and Interface Science 284:759-764.

10. Wettig SD, Badea I, Donkuru MD, Verrall RE, Foldvari M 2007. Structural and transfection properties of amine-substituted gemini surfactant-based nanoparticles. Journal of Gene Medicine 9:649-658.

11 Foldvari M, Badea I, Wettig S, Verrall R, Bagonluri M 2006. Structural characterization of novel gemini non-viral DNA delivery systems for cutaneous gene therapy. Journal of Experimental Nanoscience 1:165-176.

12 Badea I 2006. Gemini cationic surfactant-based delivery systems for non-invasive cutaneous gene therapy. Ph.D. Thesis. University of Saskatchewan, Saskatoon, SK.

13 M. Foldvari, S. Wettig, I. Badea, R. Verrall, M. Bagonluri 2006. Structural characterization of novel micro- and nano-scale non-viral DNA delivery systems for cutaneous gene therapy. Technical proceedings of the 2006 NSTI Nanotechnlogy Conference and Trade Show 2:400-403.

14. Vijayanathan V, Thomas T, Shirahata A, Thomas TJ 2001. DNA condensation by polyamines: A laser light scattering study of structural effects. Biochemistry. 40:13644-13651.

15. Ikeda I 2004. Novel surfactants: synthesis of gemini (dimeric) and related surfactants. Surfactant Science Series, (Eds: R. Zana, J. Xia), Marcel Dekker, New York, 9-35.

16. Wang C, Li X, Wettig SD, Badea I, Foldvari M, Verrall RE 2007. Investigation of complexes formed by interaction of cationic gemini surfactants with deoxyribonucleic acid. Physical Chemistry Chemical Physics 9:1616-1628.

17. Badea I, Wettig SD, Verrall RE, Foldvari M 2007. Topical non-invasive gene delivery using gemini nanoparticles in interferon-γ-deficient mice. European Journal of Pharmaceutics and Biopharmaceutics 65:414-422.

18 Wettig SD, Verrall RE, Foldvari M 2008. Gemini surfactants: a new family of building blocks for non-viral gene delivery systems. Current Gene Therapy 8:9-23.

19 Yang P, Singh J, Wettig S, Foldvari M, Verrall RE, Badea I 2010. Enhanced gene expression in epithelial cells transfected with amino acid-substituted gemini nanoparticles. European Journal of Pharmaceutics and Biopharmaceutics 75:311-320.

20 Bombelli C, Faggioli F, Luciani P, Mancini G, Sacco MG 2005. Efficient transfection of DNA by liposomes formulated with cationic gemini amphiphiles. Journal of Medicinal Chemistry 48:5378-5382.

21. Joly N, El-Aneed A, Martin P, Cecchelli R, Banoub J 2005. Structural determination of the novel fragmentation routes of morphine opiate receptor antagonists using electrospray ionization quadrupole time-of-flight tandem mass spectrometry. Rapid Communications in Mass Spectrometry 19:3119-3130.

22. Kim MS, Jin SJ, Kim JS, Park HJ, Song HS, Neubert RHH, Hwang SJ 2008. Preparation, characterization and in vivo evaluation of amorphous atorvastatin calcium nanoparticles using supercritical antisolvent (SAS) process. European Journal of Pharmaceutics and Biopharmaceutics 69:454-465.

23. Teske J, Weller JP, Fieguth A, Rothämel T, Schulz Y, Tröger HD 2010. Sensitive and rapid quantification of the cannabinoid receptor agonist naphthalen-1-yl-(1-pentylindol-3-yl) methanone (JWH-018) in human serum by liquid chromatography-tandem mass spectrometry. Journal of Chromatography B 878:2659-2663.

24. Gallo P, Fabbrocino S, Serpe L, Fiori M, Civitareale C, Stacchini P 2010. Determination of the banned growth promoter moenomycin A in feed stuffs by liquid chromatography coupled to electrospray ion trap mass spectrometry. Rapid Communications in Mass Spectrometry 24:1017-1024.

25. Grant-Klein RJ, Baldwin CD, Turell MJ, Rossi CA, Li F, Lovari R, Crowder CD, Matthews HE, Rounds MA, Eshoo MW 2010. Rapid identification of vector-borne flaviviruses by mass spectrometry. Molecular and Cellular Probes 24:219-228.

26. Buse J, Badea I, Verrall RE, El-Aneed A 2010. Tandem Mass Spectrometric Analysis of the Novel Gemini Surfactant Nanoparticle Families G12-s and G18: 1-s. Spectroscopy Letters 43:447-457.

27. Li M, Wang X, Chen B, Lin M, Buevich AV, Chan TM, Rustum AM 2009. Use of liquid chromatography/tandem mass spectrometric molecular fingerprinting for the rapid structural identification of pharmaceutical impurities. Rapid Communications in Mass Spectrometry 23: 3533-3542.

28. Nägele E, Moritz R 2005. Structure elucidation of degradation products of the antibiotic amoxicillin with ion trap MS^n and accurate mass determination by ESI TOF. Journal of the American Society of Mass Spectrometry 16:1670-1676.

29. Johnson RD, Lewis RJ. Quantitation of atenolol, metoprolol, and propranolol in postmortem human fluid and tissue specimens via LC/APCI-MS. Forensic Science International 156:106-117.

30. Eide I, Zahlsen K, Kummernes H, Neverdal G 2006. Identification and quantification of surfactants in oil using the novel method for chemical fingerprinting based on electrospray mass spectrometry and chemometrics. Energy Fuels 20:1161-1164.

31. Ablajan K. A Study of Characteristic Fragmentation of Isoflavonoids by Using Negative Ion ESI-MS^n. Journal of Mass Spectrometry 46:77-84.

32. Zana R, Benrraou M, Rueff R 1991. Alkanediyl-α,ω-bis(dimethylalkylammonium bromide) Surfactants. 1. Effect of the Spacer Chain Length on the Critical Micelle Concentration and Micelle Ionization Degree. Langmuir 7:1072-1075.

33. Song LD, Rosen MJ 1996. Surface Properties, Micellization, and Premicellar Aggregation of Gemini Surfactants with Rigid and Flexible Spacers. Langmuir 12:1149-1153.

34. Wettig SD, Verrall RE 2001. Thermodynamic Studies of Aqueous m-s-m Gemini Surfactant Systems. Journal of Colloid and Interace Science 235:310-316.

35 Wettig SD 2000. Studies of the Interaction of Gemini Surfactants with Polymers and Triblock Copolymers. Ph.D. Thesis, University of Saskatchewan, Saskatoon, Canada.

36. Blomberg E, Verrall RE, Claesson PM 2008. Interactions between Adsorbed Layers of Cationic Gemini Surfactants. Langmuir 24:1133-1140.

37. Nohmi T, Fenn JB 1992. Electrospray Mass Spectrometry of Poly(ethylene) Glycols with Molecular Weights up to Five Million. Journal of the American Chemical Society 114:3241-3246.

38. Schnier PD, Gross DS, Williams ER 1995. Electrostatic Forces and Dielectric Polarizability of Multiply Protonated Gas-Phase Cytochrome *c* Ions Probed by Ion/Molecule Chemistry. Journal of the American Chemical Society 117:6747-6757.

39. Liao SG, Zhang LJ, Li CB, Lan YY, Wang AM, Huang Y, Zhen L, Fu XZ, Zhou W, Qi XL 2010. Rapid screening and identification of caffeic acid and its esters in Erigeron breviscapus by ultra-performance liquid chromatography/tandem mass spectrometry. Rapid Communications in Mass Spectrometry 24:2533-2541.

40. Sioud S, Genestie B, Jahouh F, Martin P, Banoub J 2009. Gas-phase fragmentation study of biotin reagents using electrospray ionization tandem mass spectrometry on a quadrupole orthogonal time-of-flight hybrid instrument. Rapid Communications in Mass Spectrometry 23:1941-1956.

41. Kertes AS, Grauer F 1973. Effect of chain length on heats of mixing in tri-n-alkylamine-benzenes systems. The Journal of Physcial Chemistry 77:3107-3110.

CHAPTER 4
A GENERAL LC-MS/MS METHOD FOR THE QUANTITATIVE DETERMINATION OF DIQUATERNARY AMMONIUM GEMINI SURFACTANT DRUG DELIVERY AGENTS IN PAM212 CELLULAR LYSATE

Joshua Buse, Ildiko Badea, Ronald E. Verrall, Anas El-Aneed

Published in the Journal of Chromatography A 1294 (2013), p 98-105

The continued development of efficient and safe gene delivery agents will benefit directly from an understanding of their cellular fate upon transfection. The development of a simple and rapid LC-LR-MS/MS method for their quantification is, therefore, required. Previous work (CHAPTER 2 & 3) on the low-energy CID-MS/MS behavior of twenty-nine gemini surfactant analytes was instrumental in the selection of diagnostic MRM transitions used during LC-MS/MS analysis.

A LC-MS/MS method is reported that is specific for the quantification of twenty-nine individual diquaternary ammonium gemini surfactant molecules and was validated for G16-3 within PAM212 cell lysate according to USFDA bioanalytical method validation guidelines. The ten minute chromatographic separation procedure utilized an Agilent Zorbax CN column (100 x 2.1 mm with 3 micron particles) with LC-MS grade water and acetonitrile, both containing 0.3% (vol:vol) formic acid and 1 mM triethylamine. Extraction of the gemini surfactant from PAM212 keratinocyte cell lysate was performed using octanol and 10 μL aliquots were injected onto the column.

The standard curve was linear from 0.30 μg/mL to 220 μg/mL ($r^2 \geq 0.999$) for G16-3 and precision and accuracy were within USFDA specified limits. G16-3 analyte was assessed as stable during storage in the auto-injector, bench-top, freeze-thaw cycling, and long-term (60 days) storage at -20 °C. Cellular uptake and fate of G16-3, during both the incubation and post incubation periods was monitored for 55 hours. The absence of a change in concentration after the removal of the transfection solution at the 5 hour mark indicates the absence of metabolic activity that would degrade G16-3 within PAM212 cells.

A general LC-MS/MS method for the quantitative determination of diquaternary ammonium gemini surfactant drug delivery agents in PAM212 Cellular Lysate

Joshua Buse[1] Ildiko Badea[1] Ronald E. Verrall[2] Anas El-Aneed[1*]

[1.] Drug Discovery and Development Research Group, College of Pharmacy and Nutrition, University of Saskatchewan, 110 Science Place, Saskatoon, SK S7N 5C9, Canada

[2.] Department of Chemistry, University of Saskatchewan, 110 Science Place, Saskatoon, SK S7N 5C9, Canada

*Corresponding Author:

Telephone: +1-306-966-2013

Fax: +1-306-966-6377

E-mail Address: anas.el-aneed@usask.ca

Keywords: Tandem Mass Spectrometry, Liquid Chromatography, Diquaternary Ammonium Gemini Surfactant, Gene Transfection

Introduction

Gemini surfactants (G*t*-*s*) are compounds comprised of two hydrophobic tail regions (*t*) covalently bound to individual polar head groups that are linked chemically to one another by a spacer region (*s*).[1] The potential for numerous structural modifications, e.g., variations in the chemical nature and structure of the hydrophobic tails, head groups, and spacer, has resulted in the synthesis of an array of structurally unique gemini surfactants which fulfill specific roles in soil remediation,[2] agrichemical spreading,[3] anti-foaming agents,[4] as well as pharmaceutical formulations.[5] The benefits of the gemini surfactants in comparison to monovalent surfactants include enhanced surface active properties and a lower CMC.[6, 7] These characteristics permit the use of a lower molar concentration of gemini surfactant(s) to achieve the desired outcome(s) in comparison to conventional surfactants. For example, the remediation of 2-napthanol contaminated soil by diquaternary ammonium gemini surfactants was superior to conventional quaternary ammonium surfactants.[2]

Prominent use of gemini surfactants has also occurred in pharmaceutical formulations, particularly gene delivery. For example, modification of the gemini surfactants' structures, including variations in the spacer and tail substituent's, were found to achieve the desired compaction and protection of DNA.[8, 9] The benefit of using a diquaternary ammonium gemini surfactant is that the electrostatic interaction between the cationic ammonium head groups and the genetic material's anionic backbone compacts the DNA to form a lipoplex.[10] The formulations utilized for gene delivery are typically heterogeneous mixtures of a single diquaternary ammonium gemini surfactant, helper lipid, most commonly DOPE, and genetic material.[5, 11] At present, diquaternary ammonium gemini surfactants can achieve a rate of transfection, as assessed by expression of the transfected gene, which is comparable or superior to commercial transfection systems. In cellular models, gene expression was comparable to that achieved with, commercially available, Lipofectamine plus™.[9] Similarly, gene delivery in animal models using gemini surfactants was found to be more effective in comparison to unprotected DNA as well as a cationic lipid: cholesteryl 3β-(N-[dimethylaminoethyl]carbamate) delivery system; respectively.[5] Additional research has further supported the efficacy of gemini surfactants for the intracellular delivery of genetic material.[12-15] However, the gene delivery efficacy of the diquaternary ammonium gemini surfactants is offset by an absence of detailed information about their fate; e.g., biological stability, action following transfection. The benefits

of determining their post-transfection fate include an enhanced understanding of the rate of gemini nanoparticle uptake, the occurrence of cellular interactions, the formation of toxic metabolites. This can be attributed to the absence of suitable analytical methods to detect, differentiate, and quantify diquaternary ammonium gemini surfactants within biological matrices.

Therefore, prior to an investigation of the fate of gemini surfactants in mammalian cells, a validated quantification method is required. Mass spectrometry (MS) detection was chosen for the quantification of gemini surfactants because of the absence of a chromophore or fluorophore on the diquaternary ammonium gemini surfactants and the presence of two permanently charged diquaternary ammonium groups, making it specifically detectable by MS. Previous work on the low-energy CID-MS/MS behavior of twenty-nine gemini surfactant analytes was instrumental in the selection of diagnostic MRM transitions used during LC-MS/MS analysis.[16, 17] An understanding of the fragmentation behavior of each gemini surfactant was needed to confirm the molecular structure and understand the behavior of the tested compounds after undergoing ESI and CID-MS/MS analysis within a mass spectrometer. Such MS/MS knowledge lays the foundation for developing a MRM quantification method. Analyte separation by liquid chromatography, prior to MRM analysis, has been demonstrated to be critical, in many situations, to minimize the influence of co-eluting analytes within the matrix;[18] hence, allowing for the identification and quantification of the gemini surfactants.

Although high performance liquid chromatographic quantification methods are available for some ionic[19] and nonionic[20] gemini surfactants, the existence of significant structural differences prevent such methods from being directly applied to the gemini surfactants utilized for gene delivery. Our development of an LC-MS/MS method allows for confirmation of the specific diquaternary ammonium gemini surfactants through the monitoring of their specific retention times and precursor/product ion transitions.[21, 22] The validated method presented in this manuscript can be utilized for the quantification of 29 diquaternary ammonium gemini surfactants (Table 4.1), including those which contain an alkyl spacer region (Figure 4.1A), secondary and tertiary amine(s) (Figure 4.1B), polyethyoxylated (Figure 6.1C) or hydroxyl (Figure 4.1D) substituted alkyl chains. MRM transitions were specifically chosen to take

Table 4.1 LC-MS/MS analysis of 29 diquaternary ammonium gemini surfactants

Reference ID	**Spacer Region**		**Tail Region**		**Retention Time**	**MRM Transitions Monitored**
Gt-s	*Name*	*Molecular Formula*	*Name*	*Molecular Formula*	*Minutes*	*m/z → m/z*
G12-2	Ethyl	C_2H_4	Dodecyl	$C_{12}H_{25}$	4.77	227 → 285
G12-3	Propyl	C_3H_6	Dodecyl	$C_{12}H_{25}$	4.81	234 → 299
G12-4	Butyl	C_4H_8	Dodecyl	$C_{12}H_{25}$	4.83	241 → 313
G12-6	Hexyl	C_6H_{12}	Dodecyl	$C_{12}H_{25}$	4.94	255 → 341
G12-7	Heptyl	C_7H_{16}	Dodecyl	$C_{12}H_{25}$	5.02	262 → 355
G12-8	Octyl	C_8H_{16}	Dodecyl	$C_{12}H_{25}$	5.19	269 →369
G12-10	Decyl	$C_{10}H_{20}$	Dodecyl	$C_{12}H_{25}$	5.34	283 → 397
G12-12	Dodecyl	$C_{12}H_{24}$	Dodecyl	$C_{12}H_{25}$	5.55	297 → 425
G12-16	Hexadecyl	$C_{16}H_{32}$	Dodecyl	$C_{12}H_{25}$	5.8	325 → 481
G16-3	Propyl	C_3H_6	Hexadecyl	$C_{16}H_{33}$	5.03	290 → 355
G16-6	Hexyl	C_6H_{12}	Hexadecyl	$C_{16}H_{33}$	5.76	311 → 379
G16-7	Heptyl	C_7H_{16}	Hexadecyl	$C_{16}H_{33}$	5.82	318 → 411
G18-3	Propyl	C_3H_6	Octadecyl	$C_{18}H_{37}$	6.02	318 → 383
G18-7	Heptyl	C_7H_{16}	Octadecyl	$C_{18}H_{37}$	6.43	346 → 439
G18:1-2	Ethyl	C_2H_4	Octadec-9-ene	$C_{18}H_{35}$	5.65	309 → 367
G18:1-3	Propyl	C_3H_6	Octadec-9-ene	$C_{18}H_{35}$	5.87	316 → 381
G18:1-6	Hexyl	C_6H_{12}	Octadec-9-ene	$C_{18}H_{35}$	6.14	337 → 423
G12-2N	*N*-ethyl-*N*-methylethanamine	$C_5H_{11}N$	Dodecyl	$C_{12}H_{25}$	4.37	256 → 172
G12-3N	*N*-propyl-*N*-methylpropanamine	$C_7H_{15}N$	Dodecyl	$C_{12}H_{25}$	4.7	270 → 186
G12-3NH	*N*-propylpropanamine	$C_6H_{13}N$	Dodecyl	$C_{12}H_{25}$	4.57	263 → 179
G12-2N2	*N*,*N'*-diethyl-*n*,*N'*-dimethyleethane-1,2-diamine	$C_8H_{18}N_2$	Dodecyl	$C_{12}H_{25}$	4.78	284 → 423

Table 6.1 Continued

Reference ID	Spacer Region		Tail Region		Retention Time	MRM Transitions Monitored
Gt-s	*Name*	*Molecular Formula*	*Name*	*Molecular Formula*	*Minutes*	*m/z → m/z*
G16-3NH	N-propylpropanamine	$C_6H_{13}N$	Hexadecyl	$C_{16}H_{33}$	5.52	319 → 412
G18-3NH	*N*-propylpropanamine	$C_6H_{13}N$	Octadecyl	$C_{18}H_{37}$	5.99	347 → 221
G18:1-3NH	*N*-propylpropanamine	$C_6H_{13}N$	Octadecyl	$C_{18}H_{35}$	5.65	345 → 220
G12-4OH	Butane-2-diol	C_4H_6O	Dodecyl	$C_{12}H_{25}$	3.99	249 → 165
G12-4OH2	Butane-2,3-diol	$C_4H_6O_2$	Dodecyl	$C_{12}H_{25}$	4.28	257 → 345
G12-EO1	1,1'-oxydiethane	C_4H_8O	Dodecyl	$C_{12}H_{25}$	4.88	249 → 165
G12-EO2	1,2-diethyoxylethane	$C_6H_{12}O_2$	Dodecyl	$C_{12}H_{25}$	4.96	271 → 187
G12-EO3	1-ethoxy-2-(2-ethoxyethoxy) ethane	$C_8H_{16}O_3$	Dodecyl	$C_{12}H_{25}$	4.88	293 →209

advantage of the doubly charged nature of the gemini surfactants, which gave product ions with a m/z value greater than the precursor ion. The validated MRM analytical method for gemini surfactant G16-3 utilized two product ions, the first was chosen for its unique nature, whereas the other for its superior ionization intensity. We applied the quantification method to effectively measure the cellular uptake of the G16-3 gemini surfactants in PAM212 keratinocyte cell lysate, contributing to an understanding of the post transfection fate of the gemini surfactants.

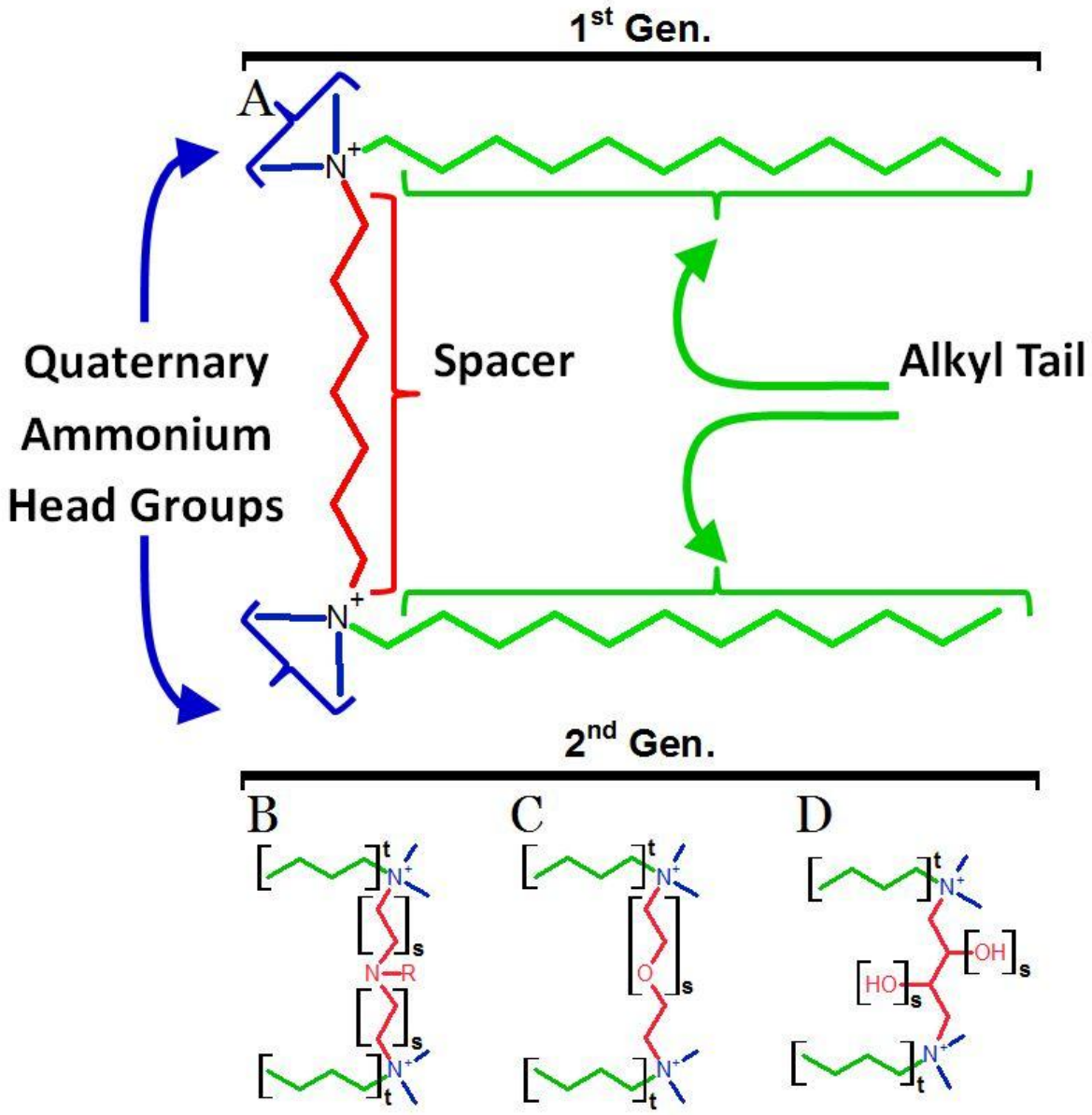

Figure 4.1 The general structure of first and second generation quaternary ammonium gemini surfactants as categorized based upon their spacer composition; Alkyl chain (A), 2 & 3 amine ('R' can be a hydrogen or methyl substituent) (B), polyethoxylated (C), and hydroxyl (D) substituted alkyl chains.

Experiments

Chemicals

The diquaternary ammonium gemini surfactants used in this study were synthesized by Dr. Ronald E. Verrall's research group in the Department of Chemistry, University of Saskatchewan, using previously reported procedures.[9, 23] 1-Octanol (99%) was purchased from

Acros Organics (Geel, Belgium). Mass spectrometry-grade water and acetonitrile were purchased from Fisher Scientific (Ottawa, ON, Canada). Formic acid and triethylamine (TEA) were purchased from EMD (Gibbstown, NJ, USA). PAM212 cells were grown in MEM modified medium obtained from ATCC (Manassa, VA, USA). Media supplements of Fetal Bovine Serum Albumin and Antibiotic were obtained from Sigma Aldrich (St. Louis, MO, USA). DOPE was purchased from Avanti Polar Lipids Inc. (Alabaster, AL, USA).

Instrumentation

The high performance liquid chromatography (HPLC) MS/MS system consisted of an Agilent series 1100 quaternary pump with an online degasser and auto sampler (Agilent Technologies, Mississauga, ON, Canada) coupled to an AB Sciex API 4000 QTRAP mass spectrometer (AB Sciex, Concord, ON, Canada). HPLC separation of the analytes was achieved by using an Agilent Eclipse CN column (100 x 2.1 mm with 3 micron particles) with an Agilent Eclipse CN column guard (12.5 x 2.1 mm with 5 micron particles) (Agilent Technologies, Mississauga, ON, Canada). The mass spectrometry grade water and acetonitrile mobile phases both contained 0.3% (% vol) formic acid and 1 mM triethylamine (Figure 4.2). Sample aliquots of 10 μL were injected onto the column and eluted using a gradient flow of 400 μL/min (Figure 4.2). Sample carryover in the autosampler was negated by the injection of double blank following injection of the highest standard curve concentration. No carryover was detected. The column was maintained at room temperature during the run and subsequently washed with water followed by acetonitrile after every use.

The ABSciex QTRAP 4000 mass spectrometry utilized a curtain gas pressure of 30 psi as well as GS1 and GS2 parameters set at 40 psi. The ionspray voltage was set at 5500 V and the temperature of the ESI source interface was maintained at 600 °C. The mass spectrometer utilized MRM to identify and/or quantify each gemini surfactant analyte. Assessing the chromatographic retention time of each gemini surfactant required that 10 μL of a homogenous 50 μg/mL solution be injected onto the column with specific transitions being monitored for each analyte (Table 4.2).

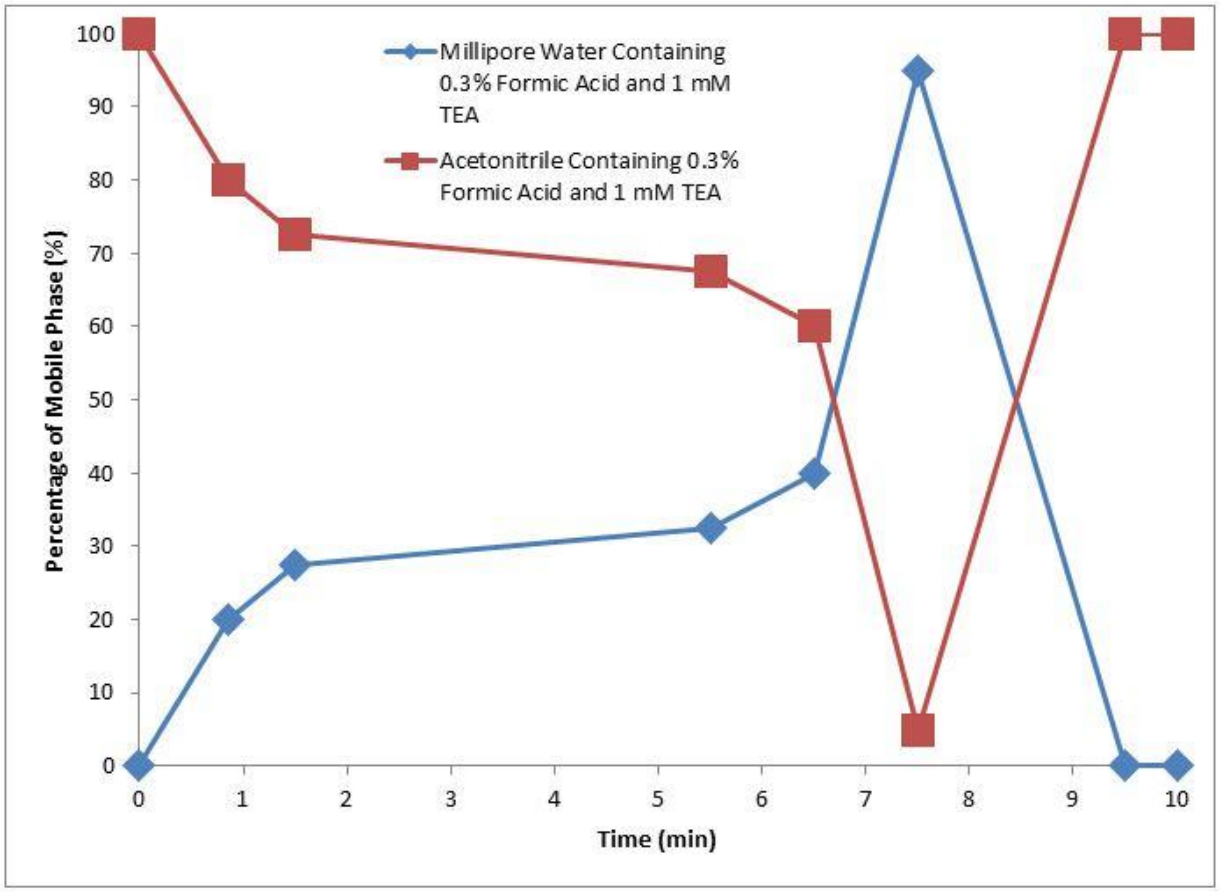

Figure 4.2 Gradient chromatographic conditions utilized for the elution of diquaternary ammonium gemini surfactants for MS/MS detection and quantification

Table 4.2 ABSCIEX QTRAP 4000 MRM instrument parameters

Transition		**Declustering Potential**	**Collision Energy**	**Collision Cell Exit Potential**
$[M]^{2+} \rightarrow [M\text{-}X]^{+}$	*m/z* → *m/z*	*eV*	*eV*	*eV*
$[M]^{2+} \rightarrow [M\text{-}C_{16}H_{33}]^{+}$	*m/z* 290 → 355	40	21	10
$[M]^{2+} \rightarrow [M\text{-}C_{33}H_{70}N_2]^{+}$	m/z 290 → 86	40	35	6
$[M]^{2+} \rightarrow [M\text{-}C_{16}D_{33}]^{+}$	m/z 323 → 388	35	25	10

Quantification of G16-3 was achieved through use of the transitions $[M]^{2+}$ to $[M\text{-}C_{16}H_{33}]^{+}$ (*m/z* 290 → 355) and $[M]^{2+}$ to $[M\text{-}C_{33}H_{70}N_2]^{+}$ (*m/z* 290 → 86) (Figure 4.3) at the instrument conditions defined in Table 4.2; peak areas were summed through use of Analyst

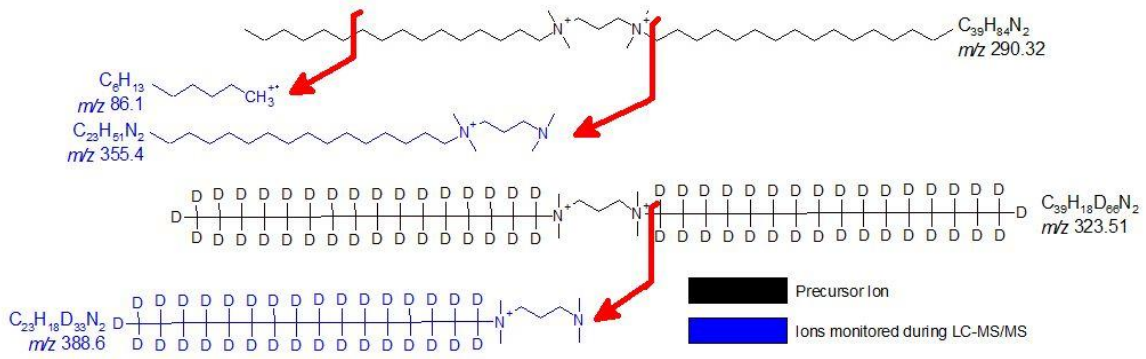

Figure 4.3 The product ions of the analyte (G16-3) and internal standard ($G16D_{66}$-3) that were monitored during LC-MS/MS analysis

Software. The internal standard utilized a transition from $[M]^{2+}$ to $[M\text{-}C_{16}D_{33}]^{+}$ (*m/z* 323 → 388) (Figure 4.3) at the instrument conditions defined in Table 4.2.

Preparation of Standard Solutions

Accurately weighed gemini surfactant analyte were dissolved in minimal essential media (MEM) modified media to prepare 10 mM stock solutions. Stock solutions of the internal standard $G16D_{66}$-3 were produced by dissolving an accurately weighed amount of analyte in octanol to produce a 200 µM concentration. Stock solutions were prepared weekly and were serially diluted with MEM modified media immediately before use. All analyte solutions were stored under darkness at -20 °C.

Sample preparation

PAM212 murine keratinocytes (kindly provided by Dr. S. Yuspa, National Cancer Institute, Bethesda, MD, USA), which did not undergo transfection, were seeded on Falcon 75 cm^2 tissue culture flasks (BD, Mississauga, ON) with MEM media at a density of 1×10^4 cells/mL.[5] To ensure complete lysis of the PAM212 cells, they were directly transferred immediately after harvesting to -80 °C, followed by six freeze/thaw cycles and sonication at 25 kHz for one hour prior to analysis. The analyzed solutions were comprised of 200 µL of the cell lysate of 1.0 $x10^6$ PAM212 cells, to which 200 µL of a 40mM $G16D_{66}$-3 in octanol were added. Prior to injection, the samples were vortexed for 30 seconds to ensure partitioning of the diquaternary ammonium gemini surfactant into the organic phase. Separation of the aqueous and

organic phases was allowed to occur at room temperature using pulse centrifugation and the organic phase, containing G16-3, was extracted for analysis.

Method validation

Full method validation for G16-3 was performed in accordance with USFDA guidance. Specificity was evaluated by analysis of six different passages of PAM 212 cells to detect any potential interference with co-eluting endogenous substances. Linearity was determined across the linear range of 0.30 to 220 μg/mL by plotting the ratio of the summed peak areas associated with G16-3 and the peak area associated with $G16D_{66}$-3. A linear least square analysis was conducted with $1/\chi$ as weighting factor, and the slope, intercept and coefficient of determination (r^2) were determined to establish linearity. The LOD was defined as the lowest detectable concentration with a signal to noise ratio of 3. The lowest limit of quantification was defined at the lowest concentration that gives precision and accuracy within ±20% of the nominal value.

The intra- and inter-day precision and accuracy of the method was established through the analysis of six replicates of samples at four different concentrations (LLOQ, lower quantification concentration [LQC], middle quantification concentration [MQC], and high quantification concentration [HQC]) on three different days. Single assay runs were accepted only when the relative standard deviation (RSD) was found to be less than ±15% at concentrations other than the LLOQ, which allowed ±20%. The criterion for accuracy was set at ±15% of the nominal concentration of the QC samples and ±20% for LLOQ. In no case did more than one third of the QC samples violate these criteria. Studies involving freeze–thaw stability, bench-top stability, and long-term stability were undertaken at LQC, MQC, and HQC. Freeze–thaw stability was tested after three freeze–thaw cycles spaced at least twenty-four hours apart with sample storage at −20 ± 5 °C between sample thawing. Twenty-four hour stability of G16-3 in PAM212 cell lysate under bench-top conditions was established. Predicted concentrations were calculated using newly prepared calibration standards. Samples were stored at −20 ± 5 °C for 30 and 60 days prior to analysis of long-term stability. Samples were considered stable when the criteria for precision and accuracy were met.

Preparation of the G16-3 Gemini Surfactant/DOPE Gene Delivery system

Transfection experiments utilized a pGT·IFN-GFP plasmid.[24] Transfection formulations of plasmid/gemini surfactant/DOPE (PGL) particles were prepared as previously described.[24] A

1:10 charge ratio of plasmid:gemini surfactant facilitated transfection and DOPE was utilized as a colipid at a 1:100 (wt:wt) ratio of plasmid:DOPE.

Transfection of PAM212 cells using Gemini Surfactant G16-3 and DOPE

PAM212 murine keratinocytes were seeded on Falcon 6-well tissue culture plates (BD, Mississauga, ON) with MEM media at a density of 3×10^5 cells/well 24 hours prior to transfection. Transfection experiments were carried out using 100 ng plasmid DNA/well. Cells were harvested at prescribed periods of time using trypsin to lift the cells and stored in 200 μL of unsupplemented MEM media prior to analysis by LC-MS/MS. The reported results are the average of two individual transfection assays of triplicate wells.

Results

The simplicity of the sample preparation methodology as well as the selectivity and sensitivity of the LC-MS/MS technique indicates that this approach is suitable for the measurement of the cellular concentration of gemini surfactants. The benefits of LC separation, included the mitigation of analyte carryover and assignment of a retention time to each analyte, resulted in its choice over flow injection analysis-tandem mass spectrometry for quantitative analysis of gemini surfactants. Analysis of the gemini surfactants by FIA-MS/MS, involving the direct injection of samples into the mass spectrometer, resulted in sample carryover and therefore, was not suitable for quantitative analysis of gemini surfactants. In addition, chromatographic separation provided analyte selectivity based upon each analytes specific retention time (Table 4.1), while MRM analysis provided structural specificity for each gemini surfactants based upon the precursor/product ion transitions monitored. By combining LC and MS/MS, highly specific and selective quantification of gemini surfactants can be achieved as demonstrated by G16-3. In addition, the LC-MS/MS method allowed for an evaluation of the rate of cellular uptake of the nanoparticles and the level of metabolism/excretion of the analyte(s).

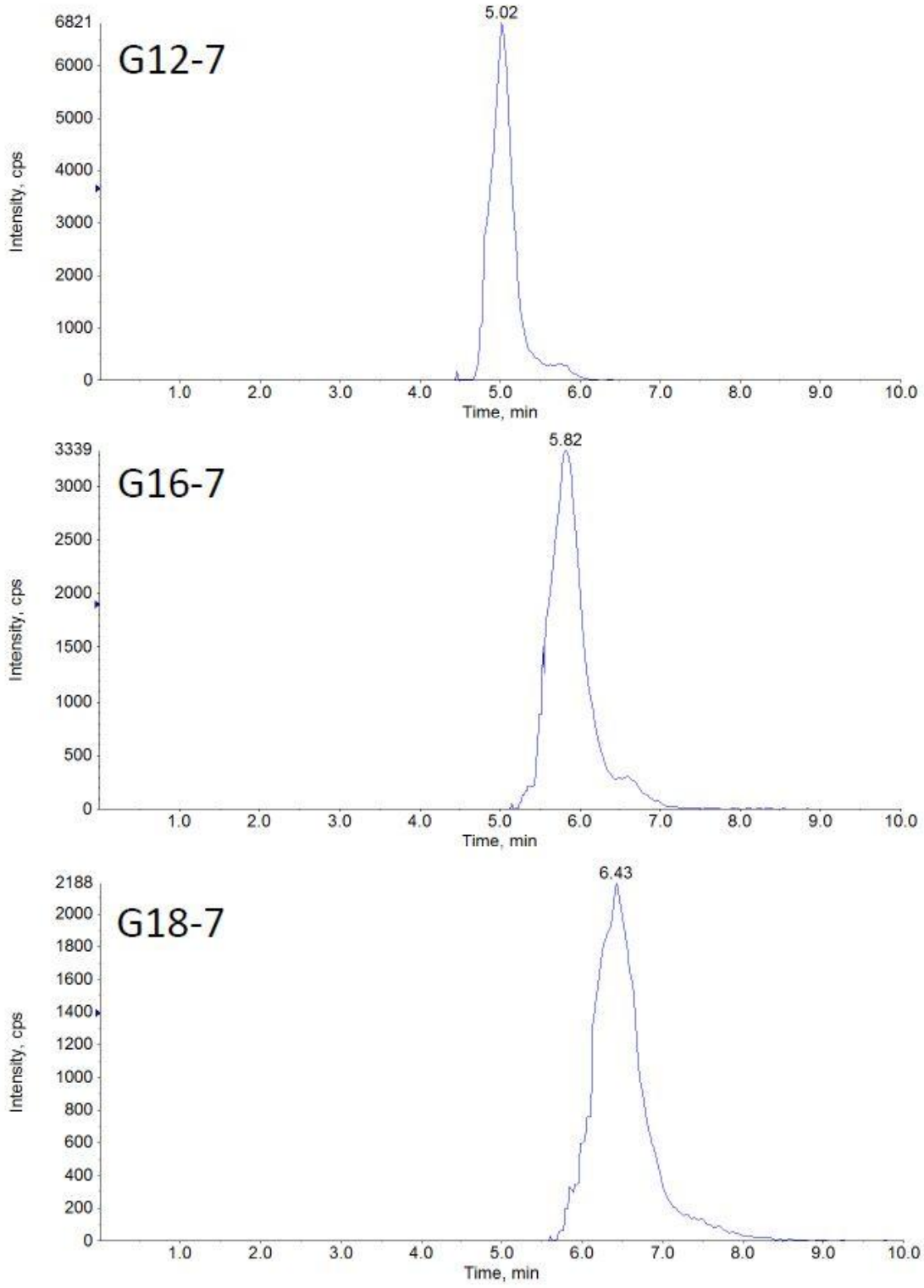

Figure 4.4 An increase of gemini surfactants' tail length results in an increase in the corresponding retention time (RT). This is demonstrated by G12-7 (RT = 5.02), G16-7 (RT = 5.81) and G18-7 (RT = 6.43)

Although, the current method validation was completed for a single gemini surfactant, G16-3, it may be applied to other diquaternary ammonium gemini surfactants. The retention times of each of the twenty-nine bisquaternary ammonium gemini surfactants analyzed by LC-MS/MS were within 3.99 and 6.42 minutes of the ten minute chromatographic run (Table 4.1). In addition, the elution behavior of the gemini surfactants was predictable: longer spacer and tail regions took a greater length of time to elute in comparison to their shorter counterparts. For example, as the alkyl tail region of gemini surfactants, containing a hexadecyl spacer region, increase from an dodecyl to octadecyl the elution time increased from 5.01 minutes to 6.43minutes (Figure 4.4). The MS/MS provided a high level of specificity for all gemini surfactants based upon the specific MRM transitions monitored (Table 4.1), producing no observable carry-over from one run to the next.

Based upon the previous success of G16-3 for the transfection of genetic material,[5] it was chosen as a model compound for which a LC-MS/MS method would need to be validated in order to monitor its post transfection fate. For example, topical application of the IFNγ gene into mouse epidermis using the gemini surfactant G16-3 produced a 450% increase in levels of IFNγ in the epidermis compared to unprotected IFNγ genes.[5, 11, 13] Diquaternary ammonium gemini surfactants possessing a shorter spacer also showed a lower toxicity than those gemini surfactants with longer spacer or those containing secondary amines.[25]

LC-MS/MS Method Validation for the Analysis of G16-3 in PAM212 Cells

Specificity for G16-3 and $G16D_{66}$-3 was established using mass spectrometry analysis, by monitoring the transitions of $[M]^{2+}$ (*m/z* 290) to both $[M\text{-}C_{16}H_{33}]^{+}$ (*m/z* 355) and $[M\text{-}C_{33}H_{70}N_2]^{+}$ (*m/z* 86) and the transitions of $[M]^{2+}$ (*m/z* 323) to $[M\text{-}C_{16}D_{33}]^{+}$ (*m/z* 388); respectively (Figure 4.3). No interference was observed for the analyte's and internal standard's transitions within the PAM212 cell lysate (Figure 4.5A). The transitions specificity was observed while monitoring blank PAM212 cell lysate within MEM media for both $G16D_{66}$-3 (Figure 4.5B) and G16-3 (Figure 4.5C & D).

Recovery

The concentration of analyte recovery was consistent within the lower, middle, and upper limit of quantification. The mean±SD recoveries of G16-3 in PAM212 cells were 71.3±4.7,

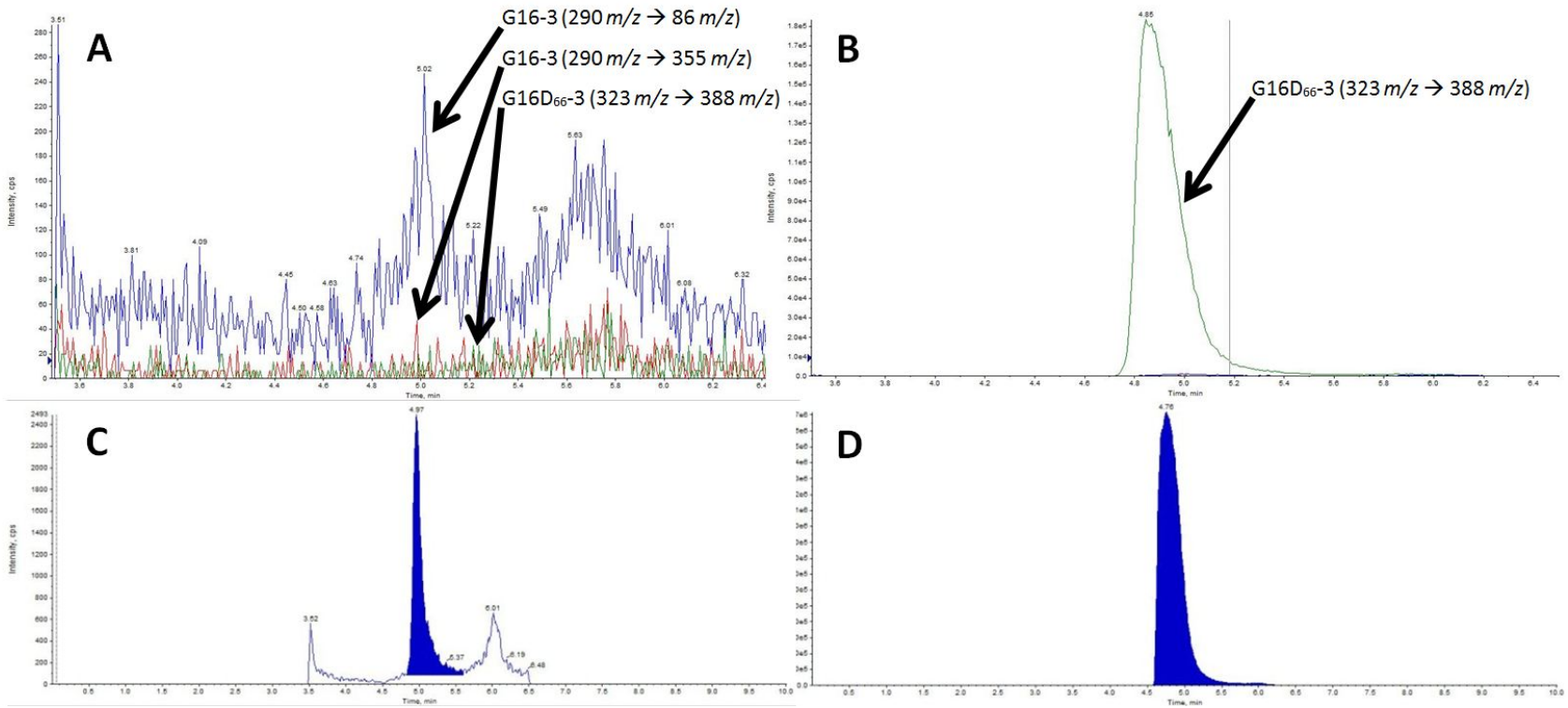

Figure 4.5 Chromatographs of G16-3 and G16D_{66}-3 within PAM212 cell lysate. No interference within the PAM212 cell lysate was found for either G16-3 (transitions 290 *m/z* → 355 *m/z* nor 290 *m/z* → 86 *m/z*) and G16D_{66}-3 (transition 323 *m/z* → 388 *m/z*) (A).The internal standard G16D_{66}-3 did not interfere with the analysis of G16-3 because its injection did not produce any interference with the G16-3 transitions (B). Representative chromatographs of the LLOQ (C) and HLOQ (D) peaks which exhibited smooth peak shape.

Table 4.3 Intra-day assay of precision and accuracy for G16-3 using LC-MSMS in PAM212 cell lysate

Quality Control	Analysis Day (#)	Observed Concentration (mean±SD, μg/mL)			Accuracy %	Precision %RSD
LLQC	1	0.273	±	0.023	90.6	7.9
0.300 μg/mL	2	0.295	±	0.051	98	7.1
	3	0.278	±	0.024	92.6	9.1
LQC	1	3.37	±	0.13	90.9	3.4
3.71 μg/mL	2	3.38	±	0.19	91.2	5.1
	3	3.34	±	0.22	88.4	6.3
MQC	1	39.87	±	1.64	107.7	4.6
37.1 μg/mL	2	40.75	±	0.99	110	2.89
	3	38.4	±	2.41	103.6	6.4
HQC	1	161.17	±	3.71	87.1	1.9
185 μg/mL	2	168	±	8.7	90.7	4.7
	3	175.16	±	5.5	94.5	3

70.1±5.9, and 68.2±3.3% at lower, middle, and upper limit of quantitation: respectively. Similarly, recovery of the internal standard $G16D_{66}$-3 was assessed to be 69.7±5.3%.

Method Validation

The validation results for diquaternary ammonium gemini surfactant G16-3 within PAM212 cell lysate satisfied the requirements specified by the USFDA for analytical method validations. Additional method validations on the remaining twenty-eight diquaternary ammonium gemini surfactants were not carried out at this time.

The LOD was based upon a signal to noise ratio of 3:1, leading to an assessment of 0.180 μg/mL for LOD. The LLOQ was based upon a reproducibility of 20% accuracy, leading to an assessment of 0.300 μg/mL for LLOQ (Figure 4.5C). The linearity of the method had an r^2 value of ≥0.999 for the range of 0.30-220.00 μg/mL. The reproducibility of the calibration curve was consistent on all occasions.

The accuracy of the validated method varied between 89.3 and 109.5 for all evaluated calibration curve concentrations (data not shown). The intra- and inter-day accuracy of the method was established in replicates of six at the LLOQ, LQC, MQC, and HQC concentrations (Tables 4.3 & 4. 4). The

Table 4.4 Inter-day assay of precision and accuracy for G16-3 using LC-MSMS in PAM212 cell lysate

Quality Control	Concentration (µg/mL)	Observed Concentration (mean±SD, µg/mL)			Accuracy %	Precision %RSD
LLQC	0.3	0.282	±	0.032	93.7	8
LQC	3.71	3.36	±	0.18	90.2	4.9
MQC	37.1	39.67	±	1.68	107.1	4.6
HQC	185	168.11	±	5.97	90.8	3.2

Table 4.5 Stability assays of precision and accuracy for G16-3 using LC-MSMS in PAM212 cell lysate

Quality Control	Analysis Type	Observed Concentration (mean±SD, µg/mL)			Accuracy %	Precision %RSD
LQC	0 hour	3.55	±	0.62	95.8	2.2
3.71 µg/mL	24 hours RT	3.62	±	0.5	97	14.5
	F/T - 3rd Cycle	3.81	±	0.46	102.7	12.5
	LT - 60 day	4	±	0.19	108.3	4.72
MQC	0 hour	35.9	±	1.9	96.9	5.2
37.1 µg/mL	24 hours RT	38.8	±	1.21	104.7	3.5
	F/T - 3rd Cycle	35.67	±	2.65	96.2	7.2
	LT - 60 day	37.5	±	2.8	97.6	5.6
HQC	0 hour	181.33	±	2.5	98.9	1.4
185 µg/mL	24 hours RT	190.33	±	4.16	102.96	10.4
	F/T - 3rd Cycle	190.33	±	3.24	103	1.73
	LT - 60 day	184	±	1.84	99.4	10.3

intra-day accuracy was assessed between 87.1 and 107.7% while inter-day accuracy was between 90.2 and 107.1%. Intra-day precision was assessed between 1.9 and 9.1 % relative standard deviation while inter-day precision was between 3.2 and 8.0 % relative standard deviation.

Gemini surfactants were stable when stored at room temperature for short periods of time and at -20°C for extended lengths of time. Both twenty-four hour bench top (~22 °C) stability studies and freeze/thaw (-80 °C <> 22 °C) stability studies, spaced twenty-four hours apart, produced suitable accuracy and precision at the LQC, MQC, and HQC concentrations. The calculated accuracy and precision values for LQC, MQC, and HQC were between 108.3 and

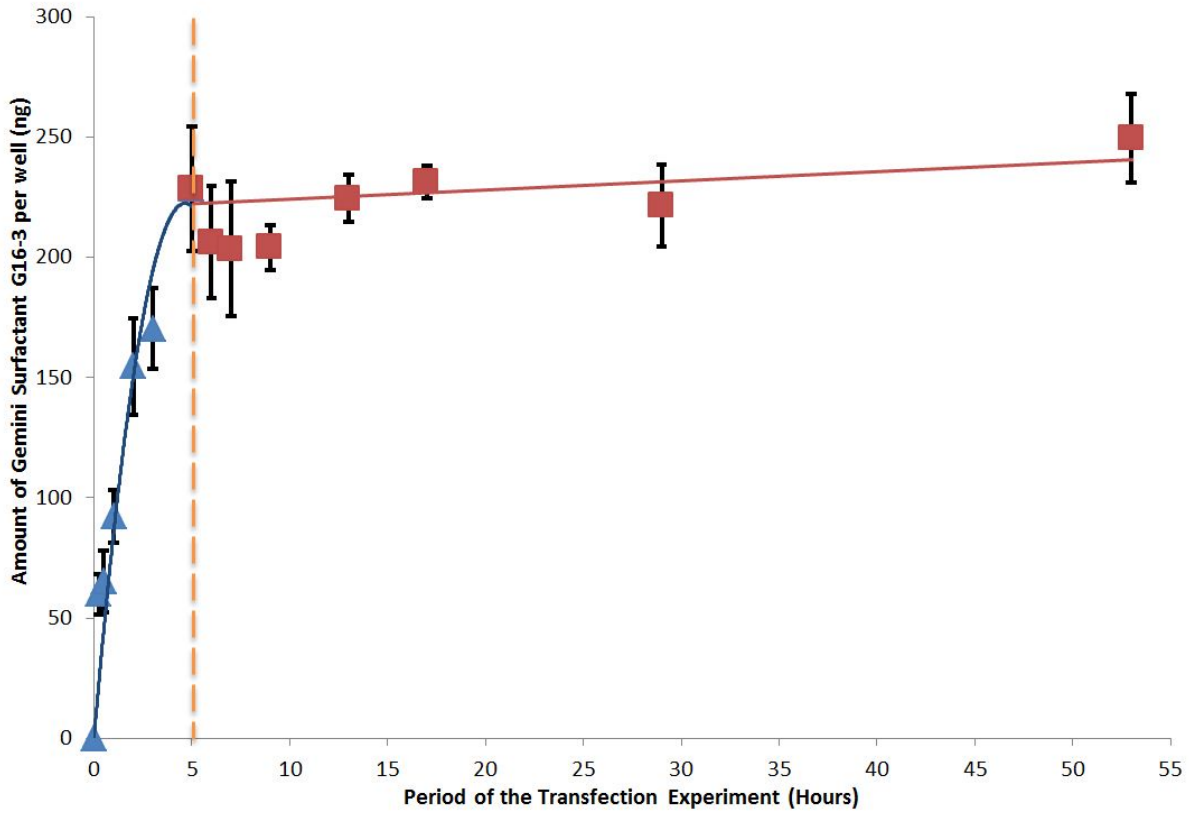

Figure 4.6 Mean G16-3 concentration ± SD post transfection within the PAM212 cell lysate. An increase in G16-3 concentration was observed during incubation with the transfection solution (Δ), while the cellular concentration of G16-3 was maintained after the transfection solution was removed (□); solution was removed at 5 hours (orange dotted line)

95.8% as with 1.4 and 14.5% relative standard deviation, respectively (Table 4.5). Such values were within the acceptable parameters when performed in triplicate (Table 4.5).

Quantification of Diquaternary Ammonium Gemini Surfactant G16-3 in PAM212 Cell Lysate Transfected with a G16-3 Gemini Surfactant/DOPE Gene Delivery System

The validated quantification method was applied to diquaternary ammonium gemini surfactant G16-3 extracted from PAM212 cells transfected with a G16-3 gemini surfactant/DOPE gene delivery system. All quality control tests met the set criteria during the analysis. The sensitivity and specificity of the assay were found to be adequate for accurately assessment of the uptake of G16-3 and monitor its post-transfection cellular concentration. Linear uptake of the G16-3 gemini surfactant following addition of the transfection solution was observed during the zero to five hour period (Figure 4.6).

No significant change in the concentration of G16-3 gemini surfactant within PAM212 cells was observed (220.1±16.0 ng/well) over the five to fifty-three hour period following removal of the transfection solution. This suggests the absence of any metabolism/excretion mechanisms within PAM212 cells that would diminish the cellular concentration of the G16-3 gemini surfactant.

Discussion

LC-MS/MS has been deemed the gold standard for the quantification of small molecules by the pharmaceutical industry because of the selectivity and specificity that it provides.[26, 27] LC provided analyte selectivity based upon the measured retention time while mitigating analyte carryover through use of gradient elution conditions,[28] results which could not be achieve through use of FIA-MS/MS alone. Use of MRM analysis allows for all 29 gemini surfactants to be distinguished from one another, achieving analyte selectivity without the need for baseline separation. In addition, the use of liquid:liquid extraction and liquid chromatography[29] prior to MRM detection allowed for a LOD to be achieved through removal of interfering molecules.

Use of a cyano column, instead of other columns tested during method development (i.e., C18, C4, and phenyl stationary phases), for liquid chromatographic separation was based upon its ability to achieve selective and reproducible separation of structurally-related gemini surfactants. The selectivity and reproducibility achieved by the cyano stationary phase was superior to a C18 stationary phases which was unable to elute the gemini surfactants as well as a C4 or a phenyl stationary phase which exhibited poor elution behavior and sporadic selectivity (APPENDIX B). In addition, the reproducibility of peak shape was achieved through the inclusion of 1 mM TEA within both mobile phases which resulted in a large reduction in the observation of peak tailing.[30] The inclusion of TEA and 0.3 % formic acid as mobile phase organic modifiers resulted in each gemini surfactant displaying a specific retention time based upon its structural properties. Increases in the retention time of gemini surfactants as the size of the tail and/or spacer region increases incrementally demonstrate that the cyano column is selective in its separation (Table 4.1). In addition, the ability to easily couple LC and mass spectrometry through an ESI interface allows for the analysis of every surfactant molecule. The need to minimize matrix effects attributed to the PAM212 cell lysate samples and sample carryover resulted in the choice of liquid:liquid extraction and LC for sample preparation and analyte separation. Use of octanol, toluene, and hexane for liquid: liquid extraction resulted in

the gemini surfactants

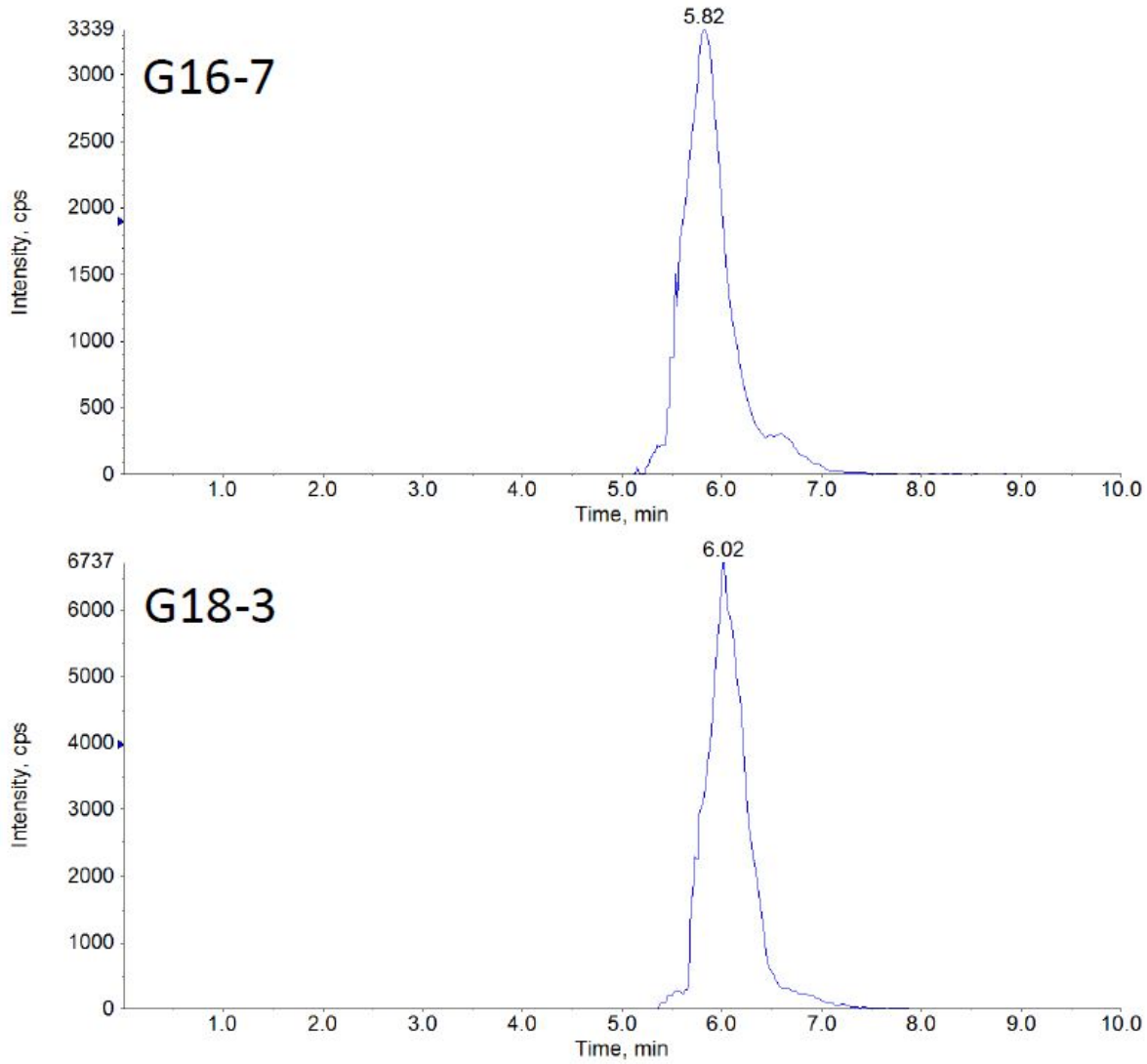

Figure 4.7 Gemini surfactants G16-7 and G18-3 have identical molecular formulae and m/z values. Differentiation between both analytes can be achieved based upon the unique MRM transitions for both analytes (G16-7 = 318 *m/z* → 411 *m/z* and G18-3 = 318 *m/z* → 383 *m/z*) as well as the different retention times (G16-7 = 5.81 and G18-3 = 6.02)

partitioning out of the PAM212 cell lysate into the octanol phase (APPENDIX C). The structural complementarities between the hydrophobic tail regions and polar head regions of octanol and the gemini surfactants facilitated their interaction.

Quantification of surfactants by UV absorption or fluorescence detection has previously been reported.[31] However, due to the absence of a chromophore and flourophore on the 29 tested gemini surfactants, analysis by these detection methods was not amenable to our analytes of

interest.[17, 18] The presence of two quaternary ammonium moieties, both of which possess a permanent positive charge, makes bisquaternary ammonium gemini surfactants ideal for mass spectrometric detection. The use of MS/MS allowed for the differentiation of all 29 gemini surfactants, including those with identical m/z values. For example, G16-7 and G18-3, both with a molecular formula $C_{43}H_{92}N_2$ and *m/z* of 318, are differentiated by both liquid chromatography, with retention times of 5.81 and 6.02 (Figure 4.7), and mass spectrometry, based upon the fragment ions of m/z 411 and 383 (Table 4.1); respectively.[16, 17] The use of both retention time and MRM analysis provides analyte specificity which can be correlated to individual gemini surfactant structures.[21] In addition, the selectivity of MRM analysis provides the ability to distinguish and quantify structurally similar analytes without it the need to achieve their baseline separation, an inherent advantage of MS/MS.[32, 33] Analysis of the fragmentation pathways was confirmed the unique identities of each gemini surfactant through MRM analysis; monitored MRM transitions were unique for each gemini surfactants (Table 6.1).[16, 17]

Validation of the quantitative method was performed for a single gemini surfactant, G16-3, within PAM212 cell lysate based upon FDA guidelines. The cell culture media and PAM212 cell lysate presented no interference with the selected MRM transitions and minimal carryover was detected (Figure 4.5A). The limit of quantification was suitable for monitoring the post transfection cellular uptake of the nanoparticles. We believe that in addition to monitoring cellular uptake, our method can serve as a starting point to quantify gemini surfactants for other applications, including pharmacokinetic studies and quality control purposes.

Quantification of Gemini surfactant G16-3 post transfection demonstrates the cellular uptake of the G16-3 gemini surfactant/DOPE gene delivery systems. This post-transfection uptake over the five hour incubation period results in a G16-3 concentration of 220.1±16.0 ng/well being observed. The absence of a change in concentration after the removal of the transfection solution at the 5 hour mark indicates the absence of metabolic activity that would degrade G16-3. Future studies include testing other gemini surfactants and monitoring their subcellular localization. The goal is to link cellular fate to the observed variations in toxicity.[5, 9] Completion of this work will assist in producing a gemini surfactant which have a higher efficacy and lower toxicity.

Conclusion

The expanding interest in utilizing non-viral gene delivery agents as treatment options requires their continued evaluation for delivery efficacy and cellular fate. Gemini surfactants have been previously assessed for delivery efficacy and cellular toxicity, however, no previous study has been performed to track the cellular concentration of gemini surfactants, including cellular uptake and post-transfection fate. The LC-MS/MS technique provides a highly suitable method of cellular quantification of gemini surfactants that lack a chromophore or fluorophore within the structure In addition, the specificity provided by MS/MS detection allows for the quantification of multiple analytes during each acquisition and took advantage of previous studies that discussed the fragmentation behavior of the gemini surfactants.[16, 17] Therefore this method is suitable for an evaluation of the cellular uptake and excretion of gemini as well as analysis of both simple and complex nano-sized gene delivery systems. Currently, the developed method is being evaluated for the quantification of gemini surfactants and drugs which they can encapsulate, as well as being applied to the sub-cellular quantification of the gemini surfactant, G16-3, within PAM212 cells.

Acknowledgements

The authors thank the tissue culture and transfection expertise of Ms. Deborah Michel and Mr. Jagbir Singh from the College of Pharmacy and Nutrition. The authors also acknowledge the editing suggestions provided by Ms. Hanan Awad (College of Pharmacy and Nutrition, University of Saskatchewan). This project is funded through a National Science and Engineering Research Council of Canada (NSERC) Research Discovery Grant. Mr. Buse acknowledged NSERC and the University of Saskatchewan for providing Postgraduate Scholarships. Funding for the purchase of the ABSciex QTRAP 4000 instrument was obtained through a Canada Foundation for Innovation grant- Leaders Opportunity Fund.

Literature Cited

1. Menger FM, Keiper JS 2000. Gemini surfactants. Angewandte Chemie International Edition 39:1906-1920.

2. Rosen M, Li F 2001. The adsorption of gemini and conventional surfactants onto some soil solids and the removal of 2-naphthol by the soil surfaces. Journal of Colloid and Interface Science 234:418-424.

3. Sanchez-Martin M, Rodriguez-Cruz M, Andrades M, Sanchez-Camazano M 2006. Efficiency of different clay minerals modified with a cationic surfactant in the adsorption of pesticides: Influence of clay type and pesticide hydrophobicity. Applied Clay Science 31:216-228.

4. Cheon HY, Kim MS, Jeong NH 2005. Experimental and Theoretical Studies of Cationic Gemini Surfactant and Anionic Sodium Lauryl Ether Sulfate. Journal of Industrial and Engineering Chemistry 11:10-19.

5. Badea I, Verrall R, Baca-Estrada M, Tikoo S, Rosenberg A, Kumar P, Foldvari M 2005. In vivo cutaneous interferon-gamma gene delivery using novel dicationic (gemini) surfactant-plasmid complexes. The Journal of Gene Medicine 7:1200-1214.

6. Menger FM, Littau CA 1991. Gemini-surfactants: synthesis and properties. Journal of the American Chemical Society 113:1451-1452.

7. Fielden ML, Perrin C, Kremer A, Bergsma M, Stuart MC, Camilleri P, Engberts JBFN 2001. Sugar-based tertiary amino gemini surfactants with a vesicle-to-micelle transition in the endosomal pH range mediate efficient transfection in vitro. European Journal of Biochemistry 268:1269-1279.

8. Donkuru MD, Badea I, Wettig S, Verrall R, Elsabahy M, Foldvari M 2010. Advancing nonviral gene delivery: lipid-and surfactant-based nanoparticle design strategies. Nanomedicine 5:1103-1127.

9. Wettig SD, Badea I, Donkuru MD, Verrall RE, Foldvari M 2007. Structural and transfection properties of amine-substituted gemini surfactant-based nanoparticles. The Journal of Gene Medicine 9:649-658.

10. Rosenzweig HS, Rakhmanova VA, MacDonald RC 2001. Diquaternary ammonium compounds as transfection agents. Bioconjugate Chemistry 12:258-263.

11. Badea I, Wettig S, Verrall R, Foldvari M 2007. Topical non-invasive gene delivery using gemini nanoparticles in interferon-γ-deficient mice. European Journal of Pharmaceutics and Biopharmaceutics 65:414-422.

12. Wang C, Wettig SD, Foldvari M, Verrall RE 2007. Synthesis, characterization, and use of asymmetric pyrenyl-gemini surfactants as emissive components in DNA-lipoplex systems. Langmuir 23:8995-9001.

13. Singh J, Michel D, Chitanda JM, Verrall RE, Badea I 2012. Evaluation of cellular uptake and intracellular trafficking as determining factors of gene expression for amino acid-substituted gemini surfactant-based DNA nanoparticles. Journal of Nanobiotechnology 10:7-11.

14. Wang H, Wettig SD 2010. Synthesis and aggregation properties of dissymmetric phytanyl-gemini surfactants for use as improved DNA transfection vectors. Physical Chemistry Chemical Physics 13:637-642.

15. Kirby AJ, Camilleri P, Engberts J, Feiters MC, Nolte RJM, Soderman O, Bergsma M, Bell PC, Fielden ML, Rodriguez CLG 2003. Gemini Surfactants: New Synthetic Vectors for Gene Transfection. Angewandte Chemie International Edition 42:1448-1457.

16. Buse J, Badea I, Verrall RE, El-Aneed A 2011. Tandem mass spectrometric analysis of novel diquaternary ammonium gemini surfactants and their bromide adducts in electrospray-positive ion mode ionization. Journal of Mass Spectrometry 46:1060-1070.

17. Buse J, Badea I, Verrall RE, El-Aneed A 2010. Tandem Mass Spectrometric Analysis of the Novel Gemini Surfactant Nanoparticle Families G12-s and G18:1-s. Spectroscopy Letters 43:447-457.

18. Taylor PJ 2005. Matrix effects: the Achilles heel of quantitative high-performance liquid chromatography–electrospray–tandem mass spectrometry. Clinical Biochemistry 38:328-334.

19. Piera E, Infante MR, Clapés P 2000. Chemo-enzymatic synthesis of arginine-based gemini surfactants. Biotechnology and Bioengineering 70:323-331.

20. Seguer J, Selve C, MaR. Infante 1994. New non-ionic surfactants from lysine and their performance. Journal of Dispersion Science and Technology 15:591-610.

21. Causon R 1997. Validation of chromatographic methods in biomedical analysis viewpoint and discussion. Journal of Chromatography B: Biomedical Sciences and Applications 689:175-180.

22. Shabir GA 2003. Validation of high-performance liquid chromatography methods for pharmaceutical analysis: Understanding the differences and similarities between validation requirements of the US Food and Drug Administration, the US Pharmacopeia and the International Conference on Harmonization. Journal of Chromatography A 987:57-66.

23. Wettig SD, Verrall RE 2001. Thermodynamic Studies of Aqueous m–s–m Gemini Surfactant Systems. Journal of Colloid and Interface Science 235:310-316.

24. Yang P, Singh J, Wettig S, Foldvari M, Verrall RE, Badea I 2010. Enhanced gene expression in epithelial cells transfected with amino acid-substituted gemini nanoparticles. European Journal of Pharmaceutics and Biopharmaceutics 75:311-320.

25. Donkuru MD, Wettig SD, Verrall RE, Badea I, Foldvari M 2012. Designing pH-sensitive gemini nanoparticles for non-viral gene delivery into keratinocytes. Journal of Materials Chemistry 22:6232-6244.

26. Saint-Marcoux F, Sauvage FL, Marquet P 2007. Current role of LC-MS in therapeutic drug monitoring. Analytical and Bioanalytical Chemistry 388:1327-1349.

27. Déglon J, Thomas A, Daali Y, Lauer E, Samer C, Desmeules J, Dayer P, Mangin P, Staub C 2011. Automated system for on-line desorption of dried blood spots applied to LC/MS/MS pharmacokinetic study of flurbiprofen and its metabolite. Journal of Pharmaceutical and Biomedical Analysis 54:359-367.

28. Hughes NC, Wong EY, Fan J, Bajaj N 2007. Determination of carryover and contamination for mass spectrometry-based chromatographic assays. The AAPS journal 9:353-360.

29. Chambers E, Wagrowski-Diehl DM, Lu Z, Mazzeo JR 2007. Systematic and comprehensive strategy for reducing matrix effects in LC/MS/MS analyses. Journal of chromatography.B, Analytical technologies in the biomedical and life sciences 852:22-34.

30. Gill R, Alexander S, Moffat A 1982. Comparison of amine modifiers used to reduce peak tailing of 2-phenylethylamine drugs in reversed-phase high-performance liquid chromatography. Journal of Chromatography A 247:39-45.

31. Schoester M, Kloster G 1993. HPLC separation and quantification of anionic surfactants using an automated on-line ion pair extraction system. Fresenius Journal of Analytical Chemistry 345:767-772.

32. Prinsen E, Redig P, Van Onckelen HA, Van Dongen W, Esmans EL 2005. Quantitative analysis of cytokinins by electrospray tandem mass spectrometry. Rapid Communications in Mass Spectrometry 9:948-953.

33. Raith K, Neubert RH 2000. Liquid chromatography–electrospray mass spectrometry and tandem mass spectrometry of ceramides. Analytica Chimica Acta 403:295-303.

CHAPTER 5
COMPARATIVE ASSESSMENT OF FIVE QUANTITATIVE HIGH-THROUGHPUT MASS SPECTROMETRY-BASED METHODS

Joshua Buse, Randy W. Purves, Ronald E. Verrall, Ildiko Badea, Haixia Zhang, Christopher C. Mulligan, Kerry M. Peru, Jonathan Bailey, John V. Headley, Anas El-Aneed

Liquid chromatography-high resolution-tandem mass spectrometry (LC-LR-MS/MS) is considered the gold standard for the quantification of small molecules due to its specificity and sensitivity. However, the length of time required for sample analysis and method development as well as the amount of solvent required for sample analysis makes LC-LR-MS/MS inefficient for the quantification of a low number of analytes. We compared four alternative, high-throughput mass spectrometry (MS) quantitative methods, namely fast liquid chromatography-low resolution-tandem mass spectrometry (FC-LR-MS/MS), fast liquid chromatography-high resolution-mass spectrometry, desorption electrospray ionization-low resolution-tandem mass spectrometry and matrix assisted laser desorption ionization-high resolution-mass spectrometry (MALDI-HR-MS), to a previously developed LC-LR-MS/MS for the quantification of a drug delivery agent (G16-3) within PAM212 cellular lysate. In comparison to LC-LR-MS/MS, each high-throughput MS method utilized less consumables to provide quantitative data in a shorter period of time. In addition, FC-LR-MS/MS achieved a superior lower limit of quantification in comparison to LC-LR-MS/MS, while MALDI-HR-MS and LC-LR-MS/MS provided increased linear dynamic ranges. Comparing all five quantitative MS methods demonstrated that: (i) the time of analysis for high-throughput MS methods is at least one quarter of that required for LC-LR-MS/MS; (ii) the time required for the method development of high-throughput MS methods is reduced; and (iii) the results of the validated methods are comparable to those of LC-LR-MS/MS. These results demonstrate that the four high-throughput MS methods are faster, more efficient, and less expensive than a conventional LC-LR-MS/MS method for the quantification of a single analyte within a biological sample.

Comparative assessment of five quantitative high-throughput mass spectrometry-based methods

Joshua Buse[1] Randy W. Purves[2] Ronald E. Verrall[3] Ildiko Badea[1] Haixia Zhang[2] Christopher C. Mulligan[4] Kerry M. Peru[5] Jonathan Bailey[5] John V. Headley[5] Anas El-Aneed[1]

1. Drug Discovery and Development Research Group, College of Pharmacy and Nutrition, University of Saskatchewan, 110 Science Place, Saskatoon, SK S7N 5C9, Canada

2. Mass Spectrometry Lab, National Research Council of Canada, 110 Gymnasium Place, Saskatoon, SK S7N 0W9, Canada

3. Department of Chemistry, University of Saskatchewan, 110 Science Place, Saskatoon, SK S7N 5C9, Canada

4. Department of Chemistry, Illinois State University, Campus Box 4160, Normal, IL 61790-4160, United States of America

5. Aquatic Contaminants Research Division, Water Science and Technology Directorate, Science and Technology Branch, Environment Canada, 11 Innovation Boulevard, Saskatoon, SK S7N 3H5, Canada

*Corresponding Author:

Telephone: +1-306-966-2013

Fax: +1-306-966-6377

E-mail Address: anas.el-aneed@usask.ca

Keywords: Tandem Mass Spectrometry, High resolution Mass Spectrometry, Liquid Chromatography, Fast Chromatography, Matrix Assisted Laser Desorption Ionization, Desorption Electrospray Ionization, Diquaternary Ammonium Gemini Surfactant, Gene Transfection

Introduction

The approval of new biological drugs has been continually growing, with biopharmaceuticals accounting for one third of approved new products since 2004,[1] including eleven products in 2012.[2] The processes associated with the approval of a biopharmaceutical strive to ensure that novel and innovative formulations possess superior properties; including enhance stability and cellular targeting.[3-6] For example, gene-based biopharmaceuticals generally require a delivery vector, which can effectively transport the genetic material into the target cell where it is subsequently transcribed into mRNA, producing the desired protein(s) and restoring normal cellular function.[5, 6] The viability of such therapy relies heavily upon the delivery vector's capacity to protect, target, and/or deliver the gene-based therapeutic. Cationic lipids are one class of delivery vectors that have facilitated the encapsulation and compaction of genetic material into non-immunogenic lipoplexes; protecting the genetic cargo from degradation and ensuring efficient delivery.[7, 8] Delivery of the genetic cargo and its subsequent expression has been achieved by numerous cationic lipoplex systems; however, the cellular and sub-cellular fates of lipoplex components are substantially understudied.

Diquaternary ammonium gemini surfactants are one class of cationic lipid molecules that are being utilized for gene delivery; achieving both *in vitro*[9, 10] and *in vivo* success.[11] The structural organization of two hydrophobic tail regions (*t*) attached to the polar head groups, and separated by a spacer region (*s*), creates an amphiphilic compound (G*t*-*s*) that self-assembles into lipoplex structures when introduced into solution with genetic material.[12] We recently developed a quantitative LC-LR-MS/MS method to monitor the cellular uptake and fate of G16-3 into PAM212 cell lysate using its deuterated analog as an internal standard (Figure 5.1).[12] The selectivity, specificity, and sensitivity of LC-LR-MS/MS[13-16] and its recognition as the gold standard in the pharmaceutical industry[17-19] influenced our decision to utilize it for the quantification of G16-3. The final method achieved a LOD of 405 nM with a linear range approaching 1000-fold.[12] However, this method required a time of analysis of eleven minutes per sample, and its LOD was negatively affected by the addition of triethylamine in the elution buffer, which was required to reduce peak tailing. In an attempt to improve the quantitative results and reduce the total time of analysis, alternative high-throughput mass

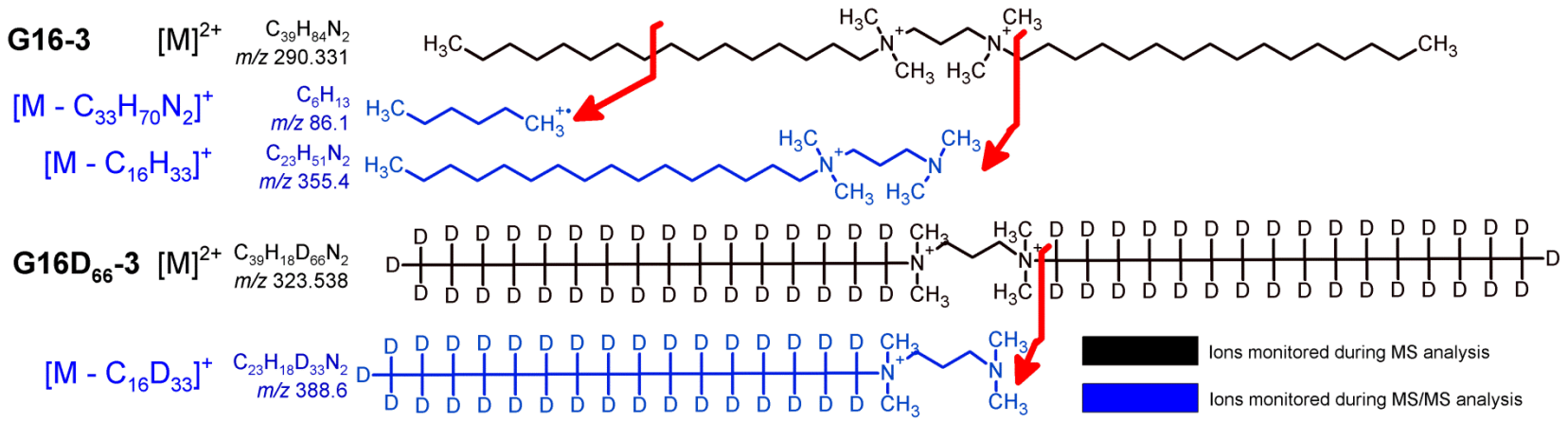

Figure 5.1 The molecular structures, monoisotopic mass and MS/MS product ions of G16-3 and its internal standard, $G16D_{66}$-3 monitored during both HR-MS (black) and LR-MS/MS (blue) analysis

spectrometric methods for the quantification of G16-3 were developed using fast chromatography (FC), desorption electrospray ionization (DESI), and matrix assisted laser desorption ionization (MALDI). These ionization and sample introduction techniques were chosen because of their rapid nature and ability to attain quantitative results comparable with LC-LR-MS/MS.[20-23]

Both LR[24] and high resolution (HR)[19] mass analyzers coupled to alternative ionization/introduction methods have been applied to the quantitative analysis of pharmaceutical formulation components. Attaining quantitative data that satisfies the USFDA guidelines for bioanalytical analysis has been demonstrated for both LR and HR mass analyzers coupled to either LC or FC by ESI; to achieve a minimum of 10 data points across a chromatographic peak required for quantification.[25, 26, 27] For example, five tricyclic amines, utilized as physiotropic pharmaceuticals, were quantified within fortified human plasma by FC-HR-MS.[27] Mass accuracy values that confirmed the molecular composition of each analyte are provided by a high resolution time of flight mass analyzers, utilizing two point internal calibrations.[27] In addition, each analyte satisfied all USFDA requirements for bioanalytical method validation and attained a LOD between 1 and 2 ng/mL.[27]

While ESI is the prevalent ionization method for quantitative analyses because of the ease of coupling LC to MS, surface DI techniques (i.e., MALDI, DESI) can be effectively coupled to either LR or HR MS instruments for the quantitative analysis of analytes.[28-30] Surface DI techniques offer the potential advantage of eliminating or minimizing sample preparation, providing considerable benefits over conventional LC-MS quantitative techniques.[31, 32] Although rarely associated with the analysis of small molecules or quantification, advances in MALDI-MS technology and matrices have extended its use for the quantification of small molecules.[33] The quantification of chlormequat by MALDI-MS achieved a LLOQ of 50 ng/mL by impacting each sample spot with 50 laser shots, requiring less than 1 second of instrument time per sample. In addition to its rapid analysis time, MALDI-MS offers advantages that include the elimination of sample carry over as well as the ability to tolerate salts.[33-36] Similarly, DESI-MS analysis allowed for rapid quantitative analysis. However, unlike MALDI-MS, DESI-MS analysis does not require the addition of matrix to facilitate ionization. DESI-MS takes advantage of the specificity, selectivity, and sensitivity of the mass spectrometer to alleviate limitations associated with other ionization techniques.[37] For example, the inclusion of simple sample preparation

protocol prior to DESI-MS analysis of anisodamine improved the LOD and enabled an LLOQ comparable to that of chromatographic-MS methods. [37]

To our knowledge, there has not been a comprehensive comparison of the technical abilities of various MS-based quantification methods. We have, therefore, assessed the quantitative ability of four high-throughput mass spectrometric methods (FC-HR-MS, FC-LR-MS/MS, DESI-LR-MS/MS, and MALDI-HR-MS) for the quantification of G16-3 within PAM212 cell lysate. Each method's quantitative capabilities are compared with a recently developed LC-LR-MS/MS method.[12] Based upon the comparison of these four quantitative high-throughput methods to the LC-LR-MS/MS[12] method we can conclusively state that: (i) the analysis time for high-throughput mass spectrometric methods is less than LC-LR-MS/MS; (ii) the time required for method development is reduced when employing high-throughput mass spectrometry methods; and (iii) the results of the validated methods are comparable with those of LC-LR-MS/MS. This indicates that the quantification of a single cationic delivery agent by high-throughput mass spectrometry methods are faster, more efficient, and less expensive than a conventional LC-LR-MS/MS method.

Materials and Methods

Chemicals and reagents

Gemini surfactant G16-3 and the internal standard, $G16D_{66}$-3 (Figure 5.1), were synthesized as described previously.[38-40] All methods of analysis utilized mass spectrometry grade water, acetonitrile, and/or methanol, purchased from Fisher Scientific (Ottawa, ON, Canada). Formic acid was purchase from EMD (Gibbstown, NJ, USA). Octanol (99% grade) was acquired from Acros Organics (New Jersey, USA). MALDI grade sinapinic acid was purchased from Sigma Aldrich (St. Louis, MO, USA). Minimal essential media (MEM) for tissue culture was obtained from ATCC (Manassa, VA, USA). Media supplements of Fetal Bovine Serum Albumin and antibiotic were obtained from Sigma Aldrich (St. Louis, MO, USA). 1,2 Dioleyl-s*n*-glycerophosphatidylethanolamine (DOPE; Avanti Polar Lipids, Alabaster, AL, USA) and α-tocopherol (Spectrum, Gardena, CA, USA) were utilized for the preparation of transfection lipoplexes.

Preparation of standard solutions

Stock solutions of G16-3 (10 mM) were prepared by dissolving the gemini compound in MEM modified media. Stock solutions of the internal standard $G16D_{66}$-3, with a concentration of 200 μM, were made by dissolving the analyte in octanol. Stock solutions were prepared weekly (stored at -20 °C). Serial dilutions were performed immediately prior to use.

Preparation of double blank and blank PAM212 cell lysate

Untransfected PAM212 murine keratinocytes (provided with thanks by Dr. S. Yuspa, National Cancer Institute, Bethesda, MD, USA) were seeded on Falcon 75 cm^2 tissue culture flasks (BD, Mississauga, ON) with MEM media at a density of 1×10^5 cells/mL.[41] To ensure complete lysis of the PAM212 cells, they were transferred immediately after harvesting to -80 °C, followed by six freeze/thaw cycles and sonication at 25 kHz for one hour prior to analysis. Double blank PAM212 cell lysate was not supplemented with either G16-3 or $G16D_{66}$-3, while blank PAM212 cell lysate was only supplemented with $G16D_{66}$-3 at the internal standard concentration stipulated for each method.

Sample preparation for FC-MS(/MS)

The analyzed solutions comprised 200 μL of the cell lysate from 1.0×10^6 PAM212 cells, to which 200 μL of a solution of 20μM $G16D_{66}$-3 in octanol or methanol were added. Samples were subsequently vortexed for 30 seconds to ensure partitioning of the diquaternary ammonium gemini surfactant into the octanol phase. Separation of the aqueous and organic phases was allowed to occur at room temperature using pulse centrifugation and the organic phase containing G16-3 and $G16D_{66}$-3 was extracted for analysis. Methanol protein precipitation required that the samples experience a force of 2000 times gravity for five minutes with the supernatant being analyzed by FC-MS(/MS).

Instrumentation methodology for FC-LR-MS/MS quantification

The LC-LR-MS/MS system was comprised of an Agilent series 1200 quaternary pump with an online degasser and auto sampler (Agilent Technologies, Mississauga, ON, Canada) coupled to an AB Sciex API 4000 QTRAP mass spectrometer (AB Sciex, Concord, ON, Canada). Aliquots of 7.5 μL were injected onto an Agilent Eclipse CN guard column (12.5 x 2.1 mm with 5 micron particles) (Agilent Technologies, Mississauga, ON, Canada) and analytes

Table 5.1 ABSCIEX QTRAP 4000 MRM instrument parameters

Transition		**Declustering Potential**	**Collision Energy**	**Collision Cell Exit Potential**
$[M]^{2+}$ to $[M\text{-}X]^{+}$	*m/z to m/z*	*eV*	*eV*	*eV*
$[M]^{2+}$ to $[M\text{-}C_{16}H_{33}]^{+}$	290 to 355	40	21	10
$[M]^{2+}$ to $[M\text{-}C_{33}H_{70}N_2]^{+}$	290 to 86	40	35	6
$[M]^{2+}$ to $[M\text{-}C_{16}D_{33}]^{+}$	323 to 388	35	25	10

were eluted using a gradient with mobile phases consisting of MS grade A) water and B) methanol; both containing 0.1% (v:v) formic acid (Appendix D Figure 1). The LC system (samples and guard column) was maintained at room temperature during the run and methanol was utilized for washing and storage of the guard column after each batch. The carry over into the autosampler was negated by the injection of a double blank following injection of the highest standard curve concentration; detected carryover was not greater than the initial double blank. Three MRM scan events were optimized on the AB Sciex API 4000 QTRAP instrument and used for quantitative analysis (Table 5.1); two for the analyte (290 *m/z* → 355 *m/z* and 290 *m/z* → 86 *m/z*) and one for the internal standard (323 *m/z* → 388 *m/z*) (Figure 5.1).

Instrumentation methodology for FC-HR-MS quantification

A high resolution LTQ Orbitrap Velos mass spectrometer (Thermo Scientific, Mississauga, ON, Canada) was utilized for the FC-HR-MS quantification of G16-3 from PAM212 cell lysate. The LC system was comprised of a Thermo Scientific Accela 1250 series quaternary pump with an online degasser and auto sampler (Thermo Scientific, Mississauga, ON, Canada). The LC system was utilized in an identical manner to FC-LR-MS/MS analysis (*Section - Instrumentation methodology for FC-LR-MS/MS quantification*) with the exception of the sample storage unit that was maintained at 10°C during analysis. Therefore, autosampler stability was assessed in addition to room temperature stability. The LTQ Orbitrap Velos mass spectrometer was operated in the positive ion mode, covering a range from *m/z* 150 to 500 using a resolving power of 30,000. The optimization procedure resulted in a sheath gas flow of 0.6

L/min, an auxiliary gas flow of 0.9 L/min, a spray voltage of 4.5 kV and a capillary temperature of 320 °C being utilized. Individual *m/z* values for G16-3 (290.331 *m/z*) and $G16D_{66}$-3 (323.538 *m/z*) were extracted from the full spectrum scan and utilized for quantification (Appendix D Figure 2).

Sample preparation for MALDI-HR-MS

The analyzed solutions comprised 200 μL of the cell lysate from 1.0 $x10^6$ PAM212 cells, to which 200 μL of a 40 μM $G16D_{66}$-3 methanol solution were added. Prior to the addition of the matrix, the samples were vortexed for 30 seconds and centrifuged at 1500 *x g* for 5 minutes to ensure removal of the precipitated proteins from the cellular lysate solution. Aliquots of the solution were mixed with an acetonitrile solution containing 10 μg/μL sinapinic acid (5:1) and subsequently vortexed for 10 seconds. Aliquots of the final solution (1 μL) were spotted on the stainless steel Opti-TOF MALDI sample plate and allowed to air dry.

Instrumentation methodology for MALDI-HR-MS quantification

An Applied Biosystems 4800 MALDI-TOF/TOF MS analyzer (AB Sciex, Concord, ON, Canada), operating in reflector positive ion mode, was utilized to analyze a mass range between *m/z* 150 and 500; the focusing mass was set at *m/z* 300. The neodymium-doped yttrium aluminum garnet 200 Hz laser was operated at a fixed laser intensity of 4200 and 500 laser shots were acquired for each sample. Internal calibration for MALDI-HR-MS was obtained using signals from the sinapinic acid matrix; including monomers and dimers as well as their potassium and sodium adducts. MALDI-HR-MS analysis caused instability of both the analyte and internal standard ions, resulting in complete fragmentation between the quaternary ammonium moiety and the α-carbon in the spacer region; this fragmentation was consistent and reproducible. Both the G16-3 (290.331 *m/z* → 310.346 *m/z* and 268.299 *m/z* [Figure 5.2]) and $G16D_{66}$-3 (323.538 *m/z* → 343.554 *m/z* and 301.507 *m/z* [Appendix D Figure 3]) ions fragmented in an identical fashion into two fragment ions that were utilized for quantification. The individual G16-30 fragment ion at 310.346 *m/z* and the corresponding $G16D_{66}$-3 ion at 343.554 *m/z* were utilized for quantification, with the other complementary fragment ions used for confirmation of the data. The absence of sample to sample interference was verified by analyzing double blanks on a sample spot adjacent to the highest standard curve concentration, with no interference being detected.

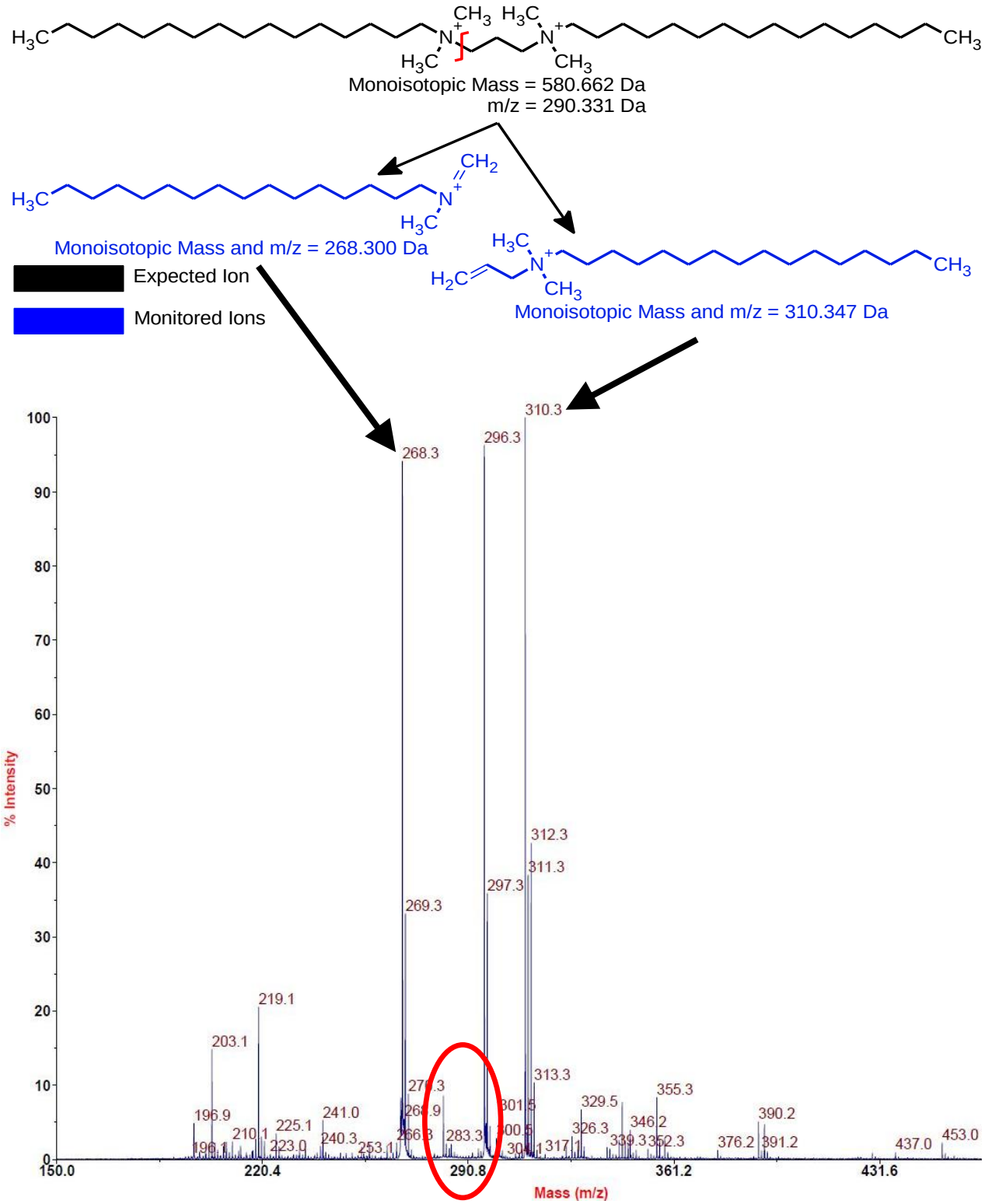

Figure 5.2 Fragmentation of G16-3 (*m/z* 290.331), in sinapinic acid matrix, into two ions of *m/z* 310.346 and *m/z* 268.299 during MALDI-HR-MS analysis. No precursor ion was observed at the expected *m/z* value for G16-3 ($[M]^{2+}$ = *m/z* 290.33)

Sample preparation for DESI-LR-MS/MS

G16-3 was extracted from 200 µL of the cell lysate from 1.0 x10^6 PAM212 cells by adding 200 µL of an octanol solution containing 50µM G16D_{66}-3 and vortexing each sample for 30 seconds to ensure partitioning of the diquaternary ammonium gemini surfactant into the organic phase. Separation of the aqueous and organic phases was allowed to occur at room temperature using pulse centrifugation and 1 µL of the organic phase was spotted on a Prosolia's 66 teflon well hydrophobic array (Omni Slides™, 26x76 mm, Indianapolis, IN, USA) and dried for one hour in an oven set at 60 °C.

Instrumentation methodology for DESI-LR-MS/MS quantification

The DESI-LR-MS/MS system was comprised of a Prosolia OmniSpray™ one dimensional automated sample stage coupled to a Thermo Scientific LCQ Fleet Ion Trap MS (Thermo Scientific, San Jose, CA, USA). Analysis of G16-3 utilized the 66 well Omni Slides™ mentioned above, with a total of 18 hydrophobic spotting regions being used per slide; 9 were located on both leading edges of the slide. Spotting of 1.5 µL of the extracted octanol sample solution utilized less than 50% of the total surface area of each hydrophobic spotting region (i.e., individual teflon well) and enhanced ionization was observed when the spot was positioned on the hydrophobic spotting region located adjacent to the leading edge of the slide. The slide was maintained at atmospheric conditions during the run. Each spotting region was analyzed by oscillating ±0.5 mm over the centre of the spot 14 times during the 0.73 minutes time of analysis. Carry over was negated by monitoring the blank glass region between each spot for 0.10 minutes by oscillating ±0.05 mm from the centre of these regions 6 times following analysis of each sample. No carry over was detected. Three MRM scan events were optimized on the LCQ Fleet Ion Trap MS^n instrument and utilized for quantitative analysis (Table 5.2); two for the analyte (*m/z* 290 → *m/z* 355 and *m/z* 290 → *m/z* 86) and one for the internal standard (*m/z* 323 → *m/z* 388) (Figure 5.1).

Method validation

The quantitative assay for G16-3 underwent full method validation in accordance with USFDA guidelines. Six different passages of PAM 212 cells were evaluated to detect any potential interference with co-eluting endogenous substances. The linearity of each method was

Table 5.2 Thermo Scientific LCQ Fleet Ion Trap MRM instrument parameters

Transition		**Ion Spray Voltage**	**Capillary Voltage**	**Collision Energy**
$[M]^{2+}$ to $[M\text{-}X]^{+}$	*m/z to m/z*	*kV*	*V*	*eV*
$[M]^{2+}$ to $[M\text{-}C_{16}H_{33}]^{+}$	290 to 355	4.46	24.29	35
$[M]^{2+}$ to $[M\text{-}C_{33}H_{70}N_2]^{+}$	290 to 86	4.46	24.29	35
$[M]^{2+} \rightarrow [M\text{-}C_{16}D_{33}]^{+}$	323 to 388	4.46	24.29	35

determined by plotting the peak area ratio of analyte to internal standard versus the analyte concentration of seven or eight calibration standards. A linear least square analysis was conducted without use of a weighting factor, and the slope, intercept and coefficient of determination (r^2) were used to establish linearity. The lowest limit of quantification was defined at the lowest concentration that gives precision and accuracy within ±20% of the nominal value.

The intra- and inter-day precision as well as accuracy of the method was established by analysis of six replicates of samples at four different concentrations (LLOQ, LQC, MQC, and HQC) on three different days. Single assay runs were accepted only when the relative standard deviation (RSD) was found to be less than ±15% at all other concentrations, except at LLOQ which allowed ±20%. The criteria for accuracy was set at ±15% of the nominal concentration of the QC samples, except at LLOQ where it was set at ±20%. In no case did more than one third of the QC samples violate these criteria.

Stability studies involving freeze–thaw stability, bench-top stability, autosampler stability, and long-term stability were undertaken at LQC, MQC, and HQC as per USFDA guidelines. Samples were considered stable when the criteria for precision and accuracy were met.

Preparation of the G16-3 gemini surfactant/DOPE gene delivery system

A pGT·IFN-GFP plasmid was used as a model for DNA transfection experiments.[10] Transfection formulations of PGL particles were prepared as previously described.[10] A 1:10

charge ratio of plasmid:gemini surfactant facilitated transfection and DOPE was utilized as a co-lipid at a 1:100 (w:w) ratio of plasmid:DOPE.[10]

PAM212 transfection by gemini surfactant G16-3/DOPE gene delivery system

PAM212 murine keratinocytes were seeded on Falcon 6-well tissue culture plates (BD, Mississauga, ON) with MEM media at a density of 3×10^5 cells/well 24 hours prior to transfection. Transfection experiments were carried out using 100 ng plasmid DNA/well. Cells were harvested at prescribed periods of time using trypsin to lift the cells and stored in 200 μL of unsupplemented MEM media prior to analysis by LC-LR-MS/MS. Transfection efficiency was visually monitored by green fluoresce protein expression and the reported results are the average of two individual transfection assays of triplicate wells.

Results

The recent development and application of a LC-LR-MS/MS method for the quantification of gemini surfactants within PAM212 cell lysate achieved a LLOQ of 0.406 μM and linear range extending to 298 μM for G16-3.[12] Unfortunately, the LC-LR-MS/MS method suffered from a long analysis time and ion suppression due to the addition of triethylamine used to minimize peak tailing. The exploration of FC-LR-MS/MS, FC-HR-MS, DESI-LR-MS/MS, and MALDI-HR-MS for the quantification of G16-3 was undertaken in order to understand the inherent benefits of each method and to compare them with our recently reported LC-LR-MS/MS method.[12]

Structural Specificity for G16-3 and G16D_{66}-3

Differentiation of G16-3 from its internal standard, G16D_{66}-3, was achieved through the presence of sixty-six deuterium atoms on the internal standard's alkyl chains. The difference in the molecular composition of G16-3 and G16D_{66}-3 imparted a mass shift of 66.4143 Da and allowed for their differentiation by both MS and MS/MS when using FC-LR-MS/MS, FC-HR-MS, and DESI-LR-MS/MS methods. Initial MALDI-HR-MS quantification experiments of G16-3 were set to utilize the ions of G16-3 and G16D_{66}-3 in an identical manner to FC-HR-MS. However we speculate that the propensity of MALDI to ionize analytes through formation of singly charged ions may cause instability of both the analyte and internal standard ions.[36] The resulting fragmentation between the quaternary ammonium and the α-carbon in the spacer region

resulted in the fragmentation of G16-3 (*m/z* 290.331*)* into two ions of *m/z* 310.346 and *m/z* 268.299 (Figure 5.2) where as $G16D_{66}$-3 (*m/z* 323.538) gave rise to fragment ions of *m/z* 343.554 and *m/z* 301.507*;* these ions were utilized for quantification (Appendix D Figure 3).

Signal Interference

An assessment of each method's specificity requires that the *m/z* values and transitions monitored be free of interference from both the internal standard and endogenous molecules during both HR-MS and LR-MS/MS analysis. An interference was observed for both G16-3 and the internal standard during the analysis of a double blank PAM212 cell lysate by FC (Appendix D Figure 4A & 5A), resulting in an increase in the LLOQ. The level of interference for both FC methods was greater than that observed during LC-LR-MS/MS, however, the interference appeared to be more substantial for FC-HR-MS analysis and negatively impacted its LLOQ. Conversely, this interference was not observed for G16-3 and $G16D_{66}$-3 transitions during either DESI-LR-MS/MS or MALDI-HR-MS analyses of double blank PAM212 cell lysate (Appendix D Figure 6A & 7A). During the evaluation of blank samples by each method, $G16D_{66}$-3 was not found to produce interference in the quantification of G16-3 (Appendix D Figure 4-7B).

Lower limit of quantification

Using FC-LR-MS/MS analysis, the LLOQ was assessed to be 0.037 μM for G16-3 (Appendix D Figure 4C), which is 25 times more sensitive than the LLOQ of 1.0000 μM (Appendix D Figure 5C) achieved by FC-HR-MS. The absence of interference for both DESI-LR-MS/MS and MALDI-HR-MS blank spectra enhanced the final LLOQ achieved by both methods. DESI-LR-MS/MS quantification of G16-3 within PAM212 cellular lysate allowed for the LLOQ to be assessed at 1.00 μM (Appendix D Figure 6C), which was attributed to the relatively poor sensitivity of the instrument. Conversely, MALDI-HR-MS achieved a LLOQ of 0.400 μM (Appendix D Figure 7C), which may have been hindered by the inability to employ an octanol liquid:liquid extraction during sample preparation.

Linearity

Intra-day analysis by FC-LR-MS/MS of six replicates at the LLOQ, LQC, MQC, and HQC (Appendix D Figure 4C-F: respectively) allowed the determination of the accuracy between 95.6 and 109.6% with a relative standard deviation (RSD) of 1.5 to 18.0 (Appendix E

Tables 1 & 2). The linearity of the FC-LR-MS/MS method achieved a dynamic range of 1000-fold across concentrations ranging between 0.0375 and 37.5 μM (Appendix D Figure 8) with a r^2 value of ≥0.999; the reproducibility of the calibration curve was consistent in all instances.

Although both the LLOQ and linear range of the FC-HR-MS method were lower than those observed for the FC-LR-MS/MS method, the accuracy and precision results were within the acceptable parameters of USFDA method validation. The reproducibility of the calibration curve was consistent in all cases, achieving an r^2 value of ≥0.999 for the concentration range of 1.00-500. μM (Appendix D Figure 9). In addition, FC-HR-MS achieved an accuracy at the LLOQ, LQC, MQC, and HQC concentrations (Appendix D Figure 5C-F) in the range of 89.7 to 110.7% and RSD values between 2.3 and 13.9% (Appendix E Tables 3 & 4).

The detection of G16-3 by DESI-LR-MS/MS resulted in a linear range of 100-fold between 1.00 and 200 μM, with a r^2 value of ≥0.99 (Appendix D Figure 10). Although both the intra- and interday accuracy and precision values of the DESI-LR-MS/MS method were lower than both FC-LR-MS/MS and FC-HR-MS, they were within acceptable USFDA parameters. The accuracy was determined to vary between 88.5% and 110.3% with RSD values ranging between 3.6% and 18.2% (Appendix E Tables 5 & 6). MALDI-HR-MS/MS, in contrast to the DESI-LR-MS/MS method, presented a large dynamic range from .400 to 440 μM, with an r^2 value of ≥0.99 (Appendix D Figure 11). Six replicates at the LLOQ, LQC, MQC, and HQC concentrations (Appendix D Figure 7) resulted in the intra- and interday accuracy varying between 85.4% and 111.5% with RSD values of 3.5% to 18.5 % (Appendix E Tables 7 & 8).

Short and long term stability of gemini surfactant G16-3 within PAM212 cell lysate

Stability studies of gemini surfactant G16-3 were undertaken during the validation of each quantification method. Short term stability was assessed at both room temperature (Appendix E Table 9) and under autosampler conditions (Appendix E Table 10). Similarly, freeze/thaw (-80 °C ↔ 22 °C) stability studies, using thaw periods spaced twenty-four hours apart, produced suitable accuracy and precision at the LQC, MQC, and HQC concentrations (Appendix E Table 11). All short term stability results were within validation parameters and G16-3 was stable under these conditions. In addition, gemini surfactant G16-3 was stable for extended periods of time when stored at both -20 °C (Appendix E Table 12) and room temperature (Appendix D Table 13).

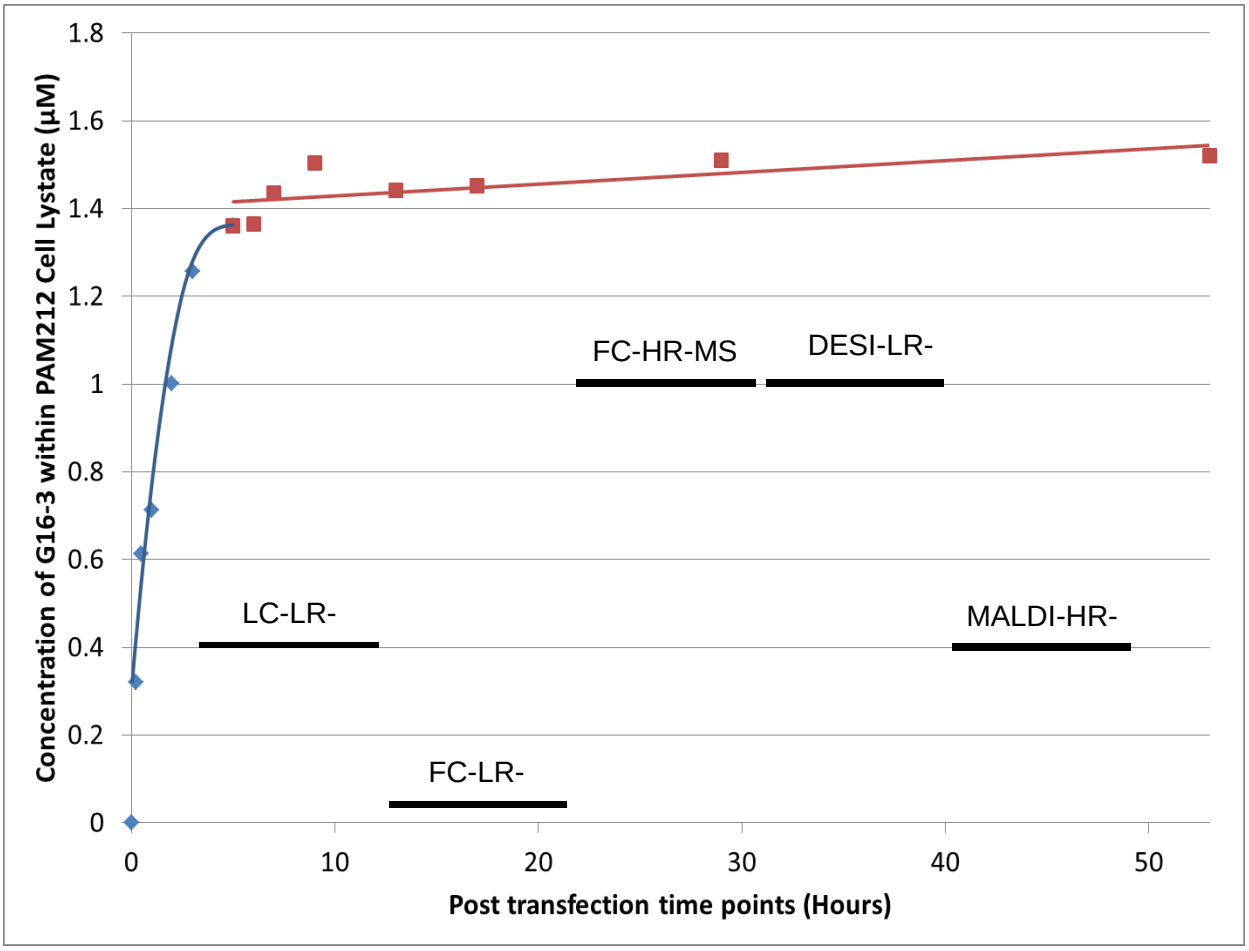

Figure 5.3 Mean G16-3 concentration post transfection within the PAM212 cell lysate for FC-LR-MS/MS, FC-HR-MS, DESI-LR-MS/MS and MALDI-HR-MS. An increase in G16-3 concentration was observed during incubation with the transfection solution (◊), while the cellular concentration of G16-3 was maintained after the transfection solution was removed (■). In addition, the LLOQ of each method is included as a labeled bar on the graph.

Quantification of G16-3 within PAM212 Cell Lysate

Each validated G16-3 quantification method was applied to PAM212 cells transfected with a G16-3 gemini surfactant/DOPE gene delivery system. The sensitivity and specificity of each assay were adequate for accurately assessing the post-transfection cellular concentration of G16-3. However, not all methods could reasonably monitor its cellular uptake due to their respective LLOQ. This resulted in MALDI-HR-MS being unable to quantify the 0.25 hour time point, while FC-HR-MS and DESI-LR-MS/MS were unable to quantify the sample prior to the 2 hour time point. Regardless, linear uptake of the G16-3 gemini surfactant following addition of

the transfection agent was observed during the zero to five hour period (Figure 5.3) and correlated with LC-LR-MS/MS data.[12] No significant change in the concentration of G16-3 gemini surfactant within PAM212 cells was observed (1.45 ± 0.06 μM) between 5 to 53 hours following removal of the transfection mixture (Figure 5.3). This suggests the absence of any metabolism/excretion from PAM212 cells that would diminish the cellular concentration of the G16-3 gemini surfactant.

Assessing the efficacy of each method in determining the concentration of G16-3 within PAM212 cell lysate was demonstrated by the consistency of measurements for each method (Table 5.3).[12] The average concentration determined by each method was within the error measurements observed for all four methods.

Discussion

The ability of MS to monitor analytes in a specific, selective and sensitive nature contributed to its wide acceptance for quantitative and qualitative analysis of drugs, metabolites, and endogenous molecules within pharmaceutical formulations and biological matrices.[42-44] However, unlike LC-MS analysis, FC, DESI, and MALDI do not rely upon chromatographic separation to achieve their LLOQ and dynamic linear range. Application of these technologies to the quantification of the gemini surfactant G16-3 provided quantitative measurements comparable to those obtained using LC-LR-MS/MS. By achieving such results, these methods have proven their ability to minimize or remove the need for extensive method development and chromatographic separation.

Which mass spectrometric method provided the easiest process of method development?

Optimization of each mass spectrometry method ensures that the sample preparation, introduction/ionization, and detection protocols ensure optimum LLOQ, linearity, and reproducibility. Two sample preparation methods were utilized, one involving protein precipitation with methanol and another using octanol in a liquid:liquid extraction. By using an octanol liquid:liquid extraction both the LLOQ and linear range of the FC-LR-MS/MS method were improved by 10-fold compared to the methanol protein precipitation (Figure 4), leading to its use for DESI and FC sample preparation. The 10-fold increase in the LLOQ for

Table 5.3 Post transfection concentration of G16-3 within PAM212 cell lysate measured by each mass spectrometry quantification method

Time (Hour)	Method Utilized for Quantification (Average ± Standard Deviation)				
	FC-LR-MS/MS	FC-HR-MS	MALDI-HR-MS	DESI-LR-MS/MS	LC-LR-MS/MS[12]
0.25	0.320 ± 0.019	Below LLOQ	Below LLOQ	Below LLOQ	0.404 ± 0.057
0.5	0.633 ± 0.003	Below LLOQ	0.594 ± 0.024	Below LLOQ	0.441 ± 0.086
1	0.712 ± 0.034	Below LLOQ	0.715 ± 0.033	Below LLOQ	0.622 ± 0.074
2	1.05 ± 0.08	1.03 ± 0.09	1.01 ± 0.04	0.923 ± 0.134	1.04 ±0.14
3	1.24 ± 0.01	1.27 ± 0.04	1.25 ± 0.05	1.27 ± 0.14	1.15 ± 0.11
5	1.44 ± 0.01	1.11 ± 0.92	1.49 ± 0.03	1.41 ± 0.16	1.54 ± 0.18
6	1.44 ± 0.16	1.06 ± 0.81	1.46 ± 0.17	1.50 ±0.15	1.39 ± 0.16
7	1.45 ± 0.13	1.56 ± 0.10	1.32 ± 0.15	1.36 ± 0.12	1.37 ± 0.19
9	1.50 ± 0.07	1.60 ± 0.04	1.56 ± 0.10	1.35 ± 0.16	1.38 ± 0.06
13	1.52 ± 0.05	1.56 ± 0.08	1.30 ± 0.02	1.38 ± 0.13	1.51 ± 0.07
17	1.50 ± 0.10	1.50 ± 0.07	1.43 ± 0.06	1.37 ± 0.15	1.56 ± 0.05
29	1.48 ± 0.07	1.52 ± 0.001	1.48 ± 0.04	1.57 ± 0.11	1.50 ± 0.12
53	1.56 ± 0.03	1.52 ± 0.08	1.55 ± 0.17	1.45 ± 0.16	1.68 ± 0.12

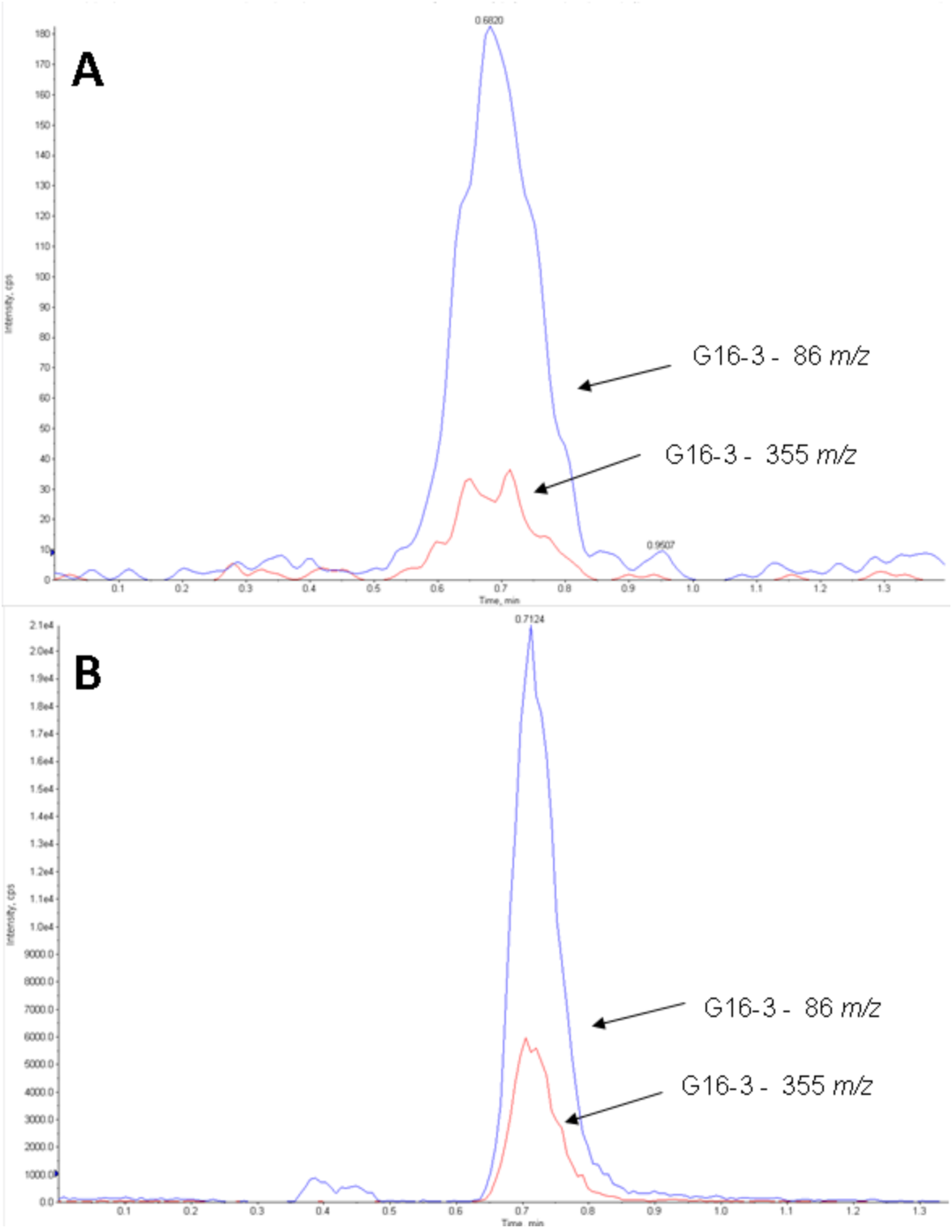

Figure 5.4 FC-LR-MS/MS chromatographs of methanol extraction (A) and octanol extraction (B) of G16-3 (2.7 μM) in PAM212 cell lysate

FC-LR-MS/MS was a result of an increase in sample recovery that provided an increase in the signal to noise (Figure 4) and were within 20% accuracy and precision (Appendix E Tables 1 & 2). The octanol liquid:liquid extraction provided enhanced recovery and/or ionization of G16-3 in comparison with methanol protein precipitation, which may be a result of the reduction of endogenous molecules extracted into the octanol phase.

The octanol extraction was not utilized for MALDI sample preparation because MALDI requires the co-crystallization of the matrix and sample, which is difficult to achieve with octanol due to its low vapor pressure. Although MALDI-HR-MS was able to achieve quantification across a wide linear range, a result of minimal interference and resolving power of the instrument, the need to apply an inferior sample preparation method negatively impacted the LLOQ.

By comparing the four sample introduction/ionization methods it is clear that DESI required the minimal amount of method development, with only three parameters being manipulated: spray solvent composition, flow rate, and ionization parameters. Evaluation of spray solvent composition and its impact on the solubility as well as ionization of the analyte of interest prompted the use of a methanol spray solvent containing 0.1% formic acid instead of unmodified methanol. Ionization parameters for DESI were optimized by using ESI to infuse and ionize G16-3 while flow rate was optimized to prevent the infusion of liquid into the mass spectrometer. Each of the parameters was rapidly optimized in comparison with the selection of the suitable sinapinic acid matrix for MALDI analysis or chromatographic conditions for FC and LC analysis. For example, eight MALDI matrices, including matrix free, were tested prior to the selection of sinapinic acid. This required an additional time commitments to determine if matrix interference would impede detection of the analyte, assess the optimal matrix to sample ratio as well as determine the ideal laser intensity, number of shots, and shot pattern.

All four methods, however, were much easier to develop than the previously developed LC-LR-MS/MS method,[12] because no consideration was required to minimize peak tailing and/or shifting or to ensure the absence of ion suppression from endogenous compounds. The benefits of having a previously developed LC-LR-MS/MS method were readily observed for both FC methods, which used the gradient elution profile similar to those previously developed for LC separation of diquaternary ammonium gemini surfactants. Optimization of the LC

chromatographic method for FC analysis minimized carryover and abnormal peak shape, while the absence of triethylamine within the mobile phases resulted in an enhanced LLOQ.

The complexity of both MALDI and FC resulted in extensive time being devoted to the choice of mobile phases/conditions, matrices, and instrument conditions. Absence of a matrix during DESI-LR-MS/MS analysis resulted in a simplified surface DI method that eliminates the interference from matrix ions. Equally, the use of a spray solvent instead of chromatographic conditions reduces complexity, while the ability to optimize and utilize ESI conditions for G16-3 reduce the time required for method development. The combination of DESI's simple sample introduction/ionization and its ability to utilize an effective sample preparation method ensured that it provided suitable quantitative data. It also confirmed that the development of an assay for the quantification of G16-3 with PAM212 cellular lysate was most efficiently achieved by DESI-LR-MS/MS.

Does one method provide superior quantitative data?

Utilizing mass spectrometry for detection allowed the accuracy, precision, selectivity, and sensitivity of all four quantitative methods to be comparable with a validated LC-LR-MS/MS method.[12] The selectivity achieved by both HR-MS and LR-MS/MS analysis resulted in the specific identification of G16-3 based upon either its molecular composition or structural characteristics. The sole exception was MALDI-HR-MS, which induced fragmentation of both the analyte and internal standard. Application of each method to the quantification of G16-3 demonstrated that the methods are reproducible and highly suitable in assessing the cellular concentration of G16-3.

Quantification of G16-3 within PAM212 cell lysate was influenced by the method of ionization, sensitivity of the instrument as well as the accuracy and precision of each method. A comparison among the methods conclusively demonstrated that FC-LR-MS/MS achieved the lowest LLOQ at a concentration of 0.037 μM (Figure 5.5 & Table 5.4), which is 10-fold lower than the LLOQ achieved by the LC-LR-MS/MS method.[12] Peak tailing associated with the FC elution of G16-3 was minimal and no interference with quantitative analysis was observed (Appendix D Figure 4). Comparing FC-LR-MS/MS to the other four quantification methods demonstrated that it achieved a LLOQ 10 to 25 fold better than the other three methods. However, the inability to couple identical mass spectrometers to each ionization method for the detection of G16-3 prevented a direct comparison between methods. The use of various

instruments and ionization configurations is a common occurrence within multi-use mass spectrometry laboratories, where each instrument is often utilized in a single configuration

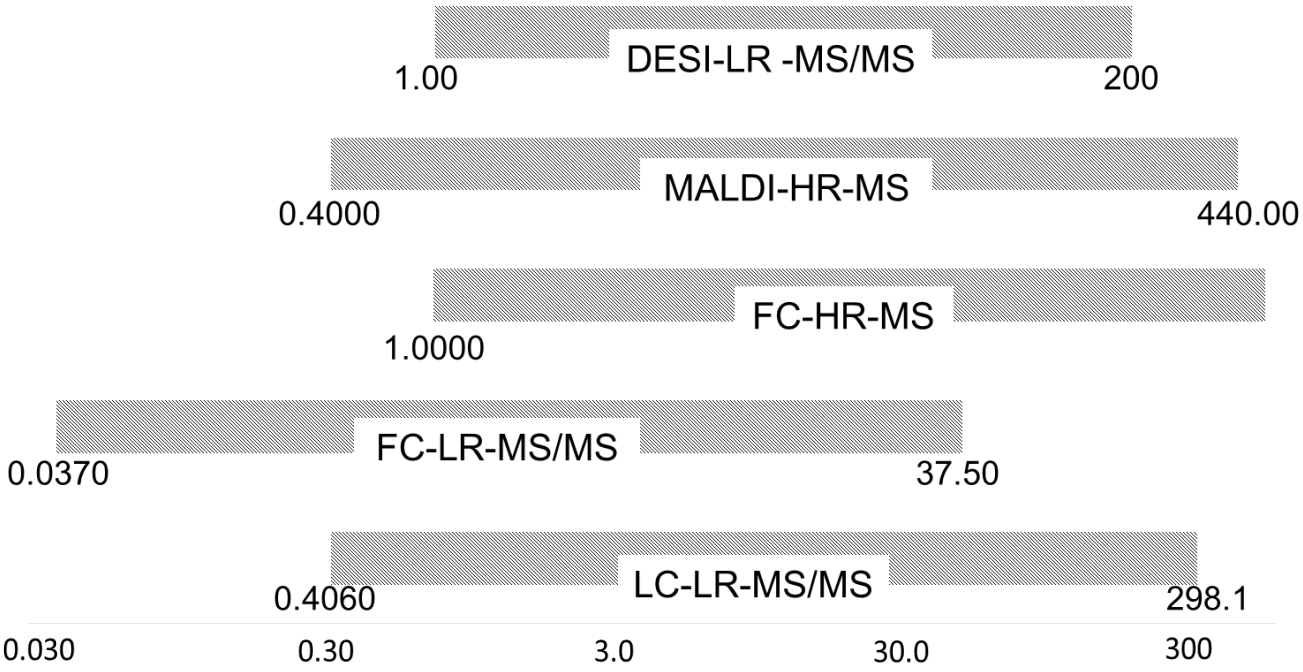

Figure 5.5 The linear range of G16-3 quantification for all five quantitative mass spectrometric methods

Table 5.4 Method validation parameters for each method

	LLOQ	**ULOQ**	**Linear Range**
LC-LR-MS/MS	0.406 μM	298 μM	734x
FC-LR-MS/MS	0.0375 μM	37.5 μM	1000x
FC-HR-MS	1.00 μM	500. μM	500x
DESI-LR-MS/MS	1.00 μM	200 μM	200x
MALDI-HR-MS	0.400 μM	440. μM	1000x

Table 5.5 Sensitivity of Mass Spectrometry Instruments utilized for G16-3 quantification

Method	**Instrument**	**Reserpine Sensitivity**
LC-LR-MS/MS	AB Sciex QTRAP 4000 MS/MS	200 fg on column
FC-LR-MS/MS	AB Sciex QTRAP 4000 MS/MS	200 fg on column
FC-HR-MS	Thermo Scientific Orbitrap LTQ Velos	100 fg on column
DESI-LR-MS/MS	Thermo Scientific LCQ Fleet Ion Trap	2000 fg on column
		Neurotensin Sensitivity
MALDI-HR-MS	AB Sciex 4800 MALDI ToFToF	418 fg per 400 laser pulses

to reduce setup-time, maintenance/repair costs, and instrument instability. Since the same mass spectrometer could not be used for all five methods, Table 5.5 provides the relative sensitivity of each mass spectrometer so that a fair comparison can be made. A comparison of instrument sensitivity between instruments resulted in FC-LR-MS/MS attaining the superior LLOQ. After adjusting for instrument sensitivity, the LLOQ of FC-LR-MS/MS was 2 fold lower than DESI-LR-MS/MS, while MALDI-HR-MS was merely 5 fold larger than FC-LR-MS/MS. Further adjusting the LLOQ of MALDI-HR-MS to account for improved sample preparation may provide an improved LLOQ compared to FC-LR-MS/MS.

In an attempt to further improve the LLOQ for FC-LR-MS/MS, FAIMS was utilized. The aim of using FAIMS was to utilize its selectivity to remove ions which may interfere with the identification of G16-3. Selection of instrument parameters for both ESI, FAIMS, and MS/MS analysis was determined by instrument optimization; dispersion voltage of -5000 V, spray voltage of 4000V, 50% helium gas additive, compensation voltages were assessed as -48 V (*m/z* 290 → *m/z* 355*)* and -48 V (*m/z* 290 → *m/z* 86*)* as well as collision energies of 5 V (*m/z* 290 → *m/z* 355*)* and 16 V (*m/z* 290 → *m/z* 86*)* (Appendix F Figure 1-3). An evaluation of blank PAM212 (Appendix F Figure 4) and PAM212 cell lysate spiked with G16-3 (Appendix F Figure 5-7) demonstrated that an improvement in sensitivity was not achieved through an enhancement of S/N by FC-FAIMS-MS/MS and thus a method validation was not performed.

The linearity of both FC-LR-MS/MS and MALDI-HR-MS methods were both accurate and precise across a range spanning over the 1000 fold linear range (Table 5.4). MALDI-HR-MS achieved linearity of nearly 10,000 fold based upon an r^2 equal to 0.99, however, the LLOQ was negatively influenced by such a large linear range and concentrations beyond 400 μM were not seen as experimentally relevant to the quantification of G16-3 within cell lysate. The large linear range can be beneficial for other quantitative applications, such as quality control of pharmaceutical formulations as no dilution is needed, thereby reducing the possibility of measurement errors due to sample handling. A disadvantage of MALDI-HR-MS was the complementary fragmentation of both G16-3 (Figure 5.2) analyte and $G16D_{66}$-3 (Appendix D Figure 3), as confirmed by their monoisotopic masses. If the fragmentation of G16-3 had been excessive or incomplete it would potentially inhibit the collection of quantitative data. However, the identification of fragment ions, the consistency of fragmentation and the identical manner by which it occurred in both the analyte and internal standard allowed for both fragment ions to be utilized for quantitative analysis.

FC-LR-MS/MS, conversely, did not display linearity beyond the 1000x linear range of the method due to uneven peak tailing which negatively influenced the accuracy and precision of LLOQ and LCQ samples. The linearity of the FC-HR-MS method was only 500 fold due to the inferior LLOQ. The inclusion of concentration values beyond the HLOQ of DESI-LR-MS/MS negatively influencing the precision and accuracy of lower concentration samples.

It was hypothesized that unfavorable effects may be associated with the introduction of an entire sample into the mass spectrometer during FC-MS(/MS) analysis. The continual introduction of a mixture of compounds would lead to an increase in instrument contamination, which would negatively influence accuracy and precision of subsequently injected samples. To test this hypothesis, four hundred injections of an extracted PAM212 sample with a G16-3 concentration at the HCQ were sequentially analyzed by FC-LR-MS/MS on a QTRAP 4000 instrument. Deviations in the response of the MS to G16-3 were compensated by the inclusion of the internal standard, $G16D_{66}$-3, leading to sample accuracy of ±10% for nearly all 400 samples (Figure 5.6). Deterioration in MS stability over time was not observed, confirming the sample-to-sample stability of the FC-LR-MS/MS method.

By maintaining their accuracy and precision values within the accepted limits during both the validation process and application, each method demonstrated its reproducibility. Each

method confirmed the post transfection concentration of G16-3 to be 1.50 ± 0.15 μM (Figure 5.3), a value which concurs with the results obtained by LC-LR-MS/MS.[12] Evaluating the efficacy of each mass spectrometric method in the quantification of G16-3 within PAM212 cell lysate demonstrates that FC-LR-MS/MS is more effective than LC-LR-MS/MS as well as the other three methods evaluated in this work (Table 5.4). Conversely, limitations in the LLOQ prevented FC-HR-MS and DESI-LR-MS/MS from assessing the PAM212 cellular uptake of G16-3. Its achievement of the lowest LLOQ and 1000x linear range, surpassing even LC-LR-MS/MS, provides evidence for the future application of FC-LR-MS/MS in the quantification of a low number of analytes for, theoretically, any bioanalytical applications (Table 5.4).

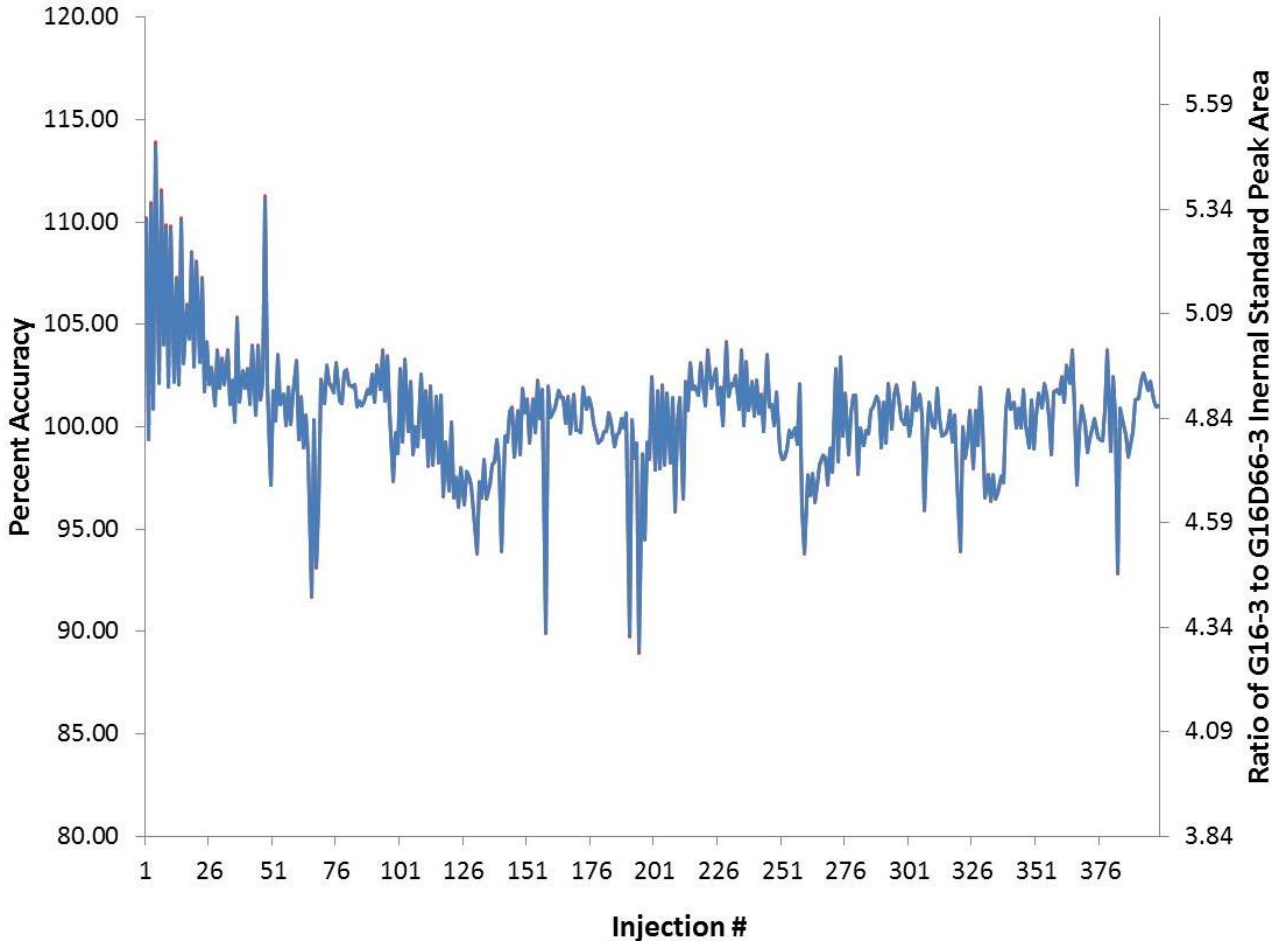

Figure 5.6 Repeat injections of the HCQ using FC-LR-MS/MS on a QTRAP 4000 instrument

Table 5.6 Time and consumable expenditure related to MS analysis (100 samples)

	Sample Analysis	Solvent/Solid Amount
LC-LR-MS/MS	18 Hours 17 Minutes	332.6 mL Acetonitrile 116 mL Water
FC-LR-MS/MS	3 Hours 57 Minutes	78.9 mL Methanol 15.7 mL Water
FC-HR-MS	4 Hours 16 Minutes	86.9 mL Methanol 15.7 mL Water
DESI-LR-MS/MS	1 Hours 49 Minutes	2.9 mL Methanol
MALDI-HR-MS	8 Minutes 11 Seconds	N/A

Is one method more conservative in time and consumable usage?

Time and consumable expenditures associated with instrument analysis are often interrelated. This is apparent for each method evaluated with the exception of MALDI-HR-MS, where no solvent or gas is utilized for the ionization and introduction of ions into the instrument (Table 5.6). Conversely, there is no correlation between time and consumable expenditure during sample preparation because each is dependent upon the requirements of sample volume, solvents, materials, and procedures (Table 5.7). Relating the consumption of each method to their quantitative capabilities highlights the advantages and disadvantages of each method.

The basis of each sample preparation method utilized by the five quantitative methods was indistinguishable in total consumable consumption and time expenditure (Table 5.6). The ability of FC to analyze the octanol phase of the liquid:liquid extraction without further sample preparation results in time saving of 1 hour or greater for the preparation of 100 samples. Using a sample size of 100 to compare time and consumable requirements of each method allows for the data to be normalize in order to better illustrate the advantages of each method. The additional time required for DESI and MALDI analysis is a result of the final step in their sample preparation procedure. For example, DESI analysis of G16-3 requires sample deposition and 1

Table 5.7 Time and consumable expenditure related to sample preparation for each MS method (100 samples)

	Sample Preparation	Solvent/Solid Amount	Final Sample Volume
LC-LR-MS/MS	3 Hours 45 Minutes	20 mL Octanol	10 μL
FC-LR-MS/MS	3 Hours 45 Minutes	20 mL Octanol	7.5 μL
FC-HR-MS	3 Hours 45 Minutes	20 mL Octanol	7.5 μL
DESI-LR-MS/MS	4 Hours 45 Minutes	20 mL Octanol	1 μL
MALDI-HR-MS	5 Hours 10 Minutes	20 mL Methanol 2 mg Sinapinic Acid	1 μL

hour of drying time at 60 °C to ensure the octanol is evaporated from the sample deposited. Similarly, MALDI requires a dry sample for analysis; however, the addition of sinapinic acid to the sample adds a step to sample preparation, thus increasing the total sample preparation time. The additional time and consumables required for DESI and MALDI sample preparation are compensated by their rapid MS analysis time as well as minimal use or absence of solvent for sample introduction (Table 5.7), respectively. FC, conversely, utilizes a relatively large volume of solvent to introduce a sample into the instrument. In addition, FC is a slow method of analysis, requiring twice as much time as DESI and 30 times more time than MALDI to analyze 100 samples, which led to at least a 5 fold greater use of solvent (Table 5.7). However, FC-LR-MS/MS remained superior to LC-LR-MS/MS as it required less than one fifth the total time to produce analytically superior data. In fact, a comparison of each method to the previously developed LC-LR-MS/MS method demonstrated that all four methods were at least four times faster and utilized less than a quarter of the total solvent consumption (Table 5.7).

Conclusion

The comparison of the efficacy of several different MS quantification methods, including FC-LR-MS/MS, FC-HR-MS, MALDI-HR-MS, and DESI-LR-MS/MS, demonstrates their

potential benefits in the quantification of G16-3 compared to LC-LR-MS/MS. Expedited method development is achieved by every method in comparison with LC-LR-MS/MS. DESI-LR-MS/MS was the simplest method to develop and required only the optimization of transitions and spray solvent. The rapid nature of each method is directly tied to the short time of analysis and minimal use of consumables. These savings in both time and consumable expenditure were evident for all methods in comparison with LC-LR-MS/MS with minimal effect on validation parameters. In fact, FC-LR-MS/MS provided a LLOQ of 36.9 ng/mL, 8x lower than LC-LR-MS/MS, while MALDI-HR-MS and FC-LR-MS/MS methods were valid across a 1000x linear range. Each MS methods were successfully applied to the quantification of G16-3 within PAM212 cell lysate. The ability of all methods to quantify G16-3 within PAM212 cellular lysate demonstrates that the extensive time and consumable usage associated with LC-LR-MS/MS is not required to achieve sensitive quantitative results. This will be beneficial in the future development of other diquaternary ammonium gemini surfactants as well as small molecule drugs and excipients.

Acknowledgements

The authors thank the tissue culture and transfection expertise of Ms. Deborah Michel and Mr. Jagbir Singh from the College of Pharmacy and Nutrition. This project is funded through a National Science and Engineering Research Council of Canada (NSERC) Research Discovery Grant. Mr. Buse acknowledged NSERC and the University of Saskatchewan for providing Postgraduate Scholarships. Funding for the purchase of the ABSciex QTRAP 4000 instrument was obtained through a Canada Foundation for Innovation grant- Leaders Opportunity Fund.

Literature Cited

1. Mullard A 2012. 2011 FDA drug approvals. Nature Reviews Drug Discovery 11:91-94.

2. Mullard A 2013. 2012 FDA drug approvals. Nature Reviews Drug Discovery 12:87-90.

3. Schäfer-Korting M, Mehnert W, Korting H 2007. Lipid nanoparticles for improved topical application of drugs for skin diseases. Advanced Drug Delivery Review 59:427-443.

4. Chen M 2008. Lipid excipients and delivery systems for pharmaceutical development: a regulatory perspective. Advanced Drug Delivery Review 60:768-777.

5. Unciti-Broceta A, Moggio L, Dhaliwal K, Pidgeon L, Finlayson K, Haslett C, Bradley M 2011. Safe and efficient in vitro and in vivo gene delivery: tripodal cationic lipids with programmed biodegradability. Journal of Materials Chemistry 21:2154-2158.

6. Scholz C, Wagner E 2012. Therapeutic plasmid DNA versus siRNA delivery: Common and different tasks for synthetic carriers. Journal of Controlled Release 161:554-565.

7. Zuhorn IS, Hoekstra D 2012. How Cationic Lipids transfer Nucleic Acids into Cells and across Cellular Membranes: Recent Advances. Journal of Controlled Release 166:46-56.

8. Fattal E 2013. Lipid-Based Nanovectors for Targeting of CD44-Overexpressing Tumor Cells. Journal of Drug Delivery Article ID 860780.

9. Yang P, Singh J, Wettig S, Foldvari M, Verrall RE, Badea I 2010. Enhanced gene expression in epithelial cells transfected with amino acid-substituted gemini nanoparticles. European Journal of Pharmaceutics and Biopharmaceutics 75:311-320.

10. Badea I, Verrall R, Baca‐Estrada M, Tikoo S, Rosenberg A, Kumar P, Foldvari M 2005. In vivo cutaneous interferon‐γ gene delivery using novel dicationic (gemini) surfactant–plasmid complexes. The Journal of Gene Medicine 7:1200-1214.

11. Badea I, Wettig S, Verrall R, Foldvari M 2007. Topical non-invasive gene delivery using gemini nanoparticles in interferon-γ-deficient mice. European Journal of Pharmaceutics and Biopharmaceutics 65:414-422.

12. Buse J, Badea I, Verrall RE, El-Aneed A 2013. A general liquid chromatography tandem mass spectrometry method for the quantitative determination of diquaternary ammonium gemini surfactant drug delivery agents in mouse keratinocytes' cellular lysate. Journal of Chromatography A 1297:98-105.

13. Barton C, Kay RG, Gentzer W, Vitzthum F, Pleasance S 2009. Development of high-throughput chemical extraction techniques and quantitative HPLC-MS/MS (SRM) assays for clinically relevant plasma proteins. Journal of Proteome Research 9:333-340.

14. Becker S, Kortz L, Helmschrodt C, Thiery J, Ceglarek U 2011. LC-MS-based metabolomics in the clinical laboratory. Journal of Chromatography B 883:68-75.

15. Geenen S, Michopoulos F, Kenna JG, Kolaja KL, Westerhoff HV, Wilson I 2011. HPLC–MS/MS methods for the quantitative analysis of ophthalmic acid in rodent plasma and hepatic cell line culture medium. Journal of Pharmaceutical and Biomedical Analysis 54:1128-1135.

16. Shushan B 2010. A review of clinical diagnostic applications of liquid chromatography–tandem mass spectrometry. Mass Spectrometry Reviews 29:930-944.

17. Lindegardh N, Tarning J, Toi P, Hien T, Farrar J, Singhasivanon P, White N, Ashton M, Day N 2009. Quantification of artemisinin in human plasma using liquid chromatography coupled to tandem mass spectrometry. Journal of Pharmaceutical and Biomedical Analysis 49:768-774.

18. Grebe SK, Singh RJ 2011. LC-MS/MS in the Clinical Laboratory–Where to From Here? The Clinical Biochemist Reviews 32:5-31.

19. Ramanathan R, Jemal M, Ramagiri S, Xia YQ, Humpreys WG, Olah T, Korfmacher WA 2011. It is time for a paradigm shift in drug discovery bioanalysis: from SRM to HRMS. Journal of Mass Spectrometry 46:595-601.

20. Signor L, Varesio E, Staack RF, Starke V, Richter WF, Hopfgartner G 2007. Analysis of erlotinib and its metabolites in rat tissue sections by MALDI quadrupole time-of-flight mass spectrometry. Journal of Mass Spectrometry 42:900-909.

21. Chen S, Carvey PM 2000. Validation of liquid‐liquid extraction followed by flow‐injection negative ion electrospray mass spectrometry assay to Topiramate in human plasma. Rapid Communications in Mass Spectrometry 15:159-163.

22. Mičová K, Friedecký D, Faber E, Polýnková A, Adam T 2010. Flow injection analysis vs. ultra high performance liquid chromatography coupled with tandem mass spectrometry for determination of imatinib in human plasma. Clinica Chimica Acta 411:1957-1962.

23. Vismeh R, Waldon DJ, Teffera Y, Zhao Z 2012. Localization and quantification of drugs in animal tissues by use of desorption electrospray ionization mass spectrometry imaging. Analytical Chemistry 84:5439-5445.

24. Gergov M, Ojanperä I, Vuori E 2003. Simultaneous screening for 238 drugs in blood by liquid chromatography–ionspray tandem mass spectrometry with multiple-reaction monitoring. Journal of Chromatography B 795:41-53.

25. Plumb R, Castro‐Perez J, Granger J, Beattie I, Joncour K, Wright A 2004. Ultra‐performance liquid chromatography coupled to quadrupole‐orthogonal

time‐of‐flight mass spectrometry. Rapid Communications in Mass Spectrometry 18:2331-2337.

26. Zhang H, Heinig K, Henion J 2000. Atmospheric pressure ionization time‐of‐flight mass spectrometry coupled with fast liquid chromatography for quantitation and accurate mass measurement of five pharmaceutical drugs in human plasma. Journal of mass spectrometry 35:423-431.

27. Henry H, Sobhi HR, Scheibner O, Bromirski M, Nimkar SB, Rochat B 2012. Comparison between a high‐resolution single‐stage Orbitrap and a triple quadrupole mass spectrometer for quantitative analyses of drugs. Rapid Communications in Mass Spectrometry 26:499-509.

28. Romanyshyn L, Tiller PR, Hop CECA 2000. Bioanalytical applications of ‘fast chromatography’ to high‐throughput liquid chromatography/tandem mass spectrometric quantitation. Rapid Communications in Mass Spectrometry 14:1662-1668.

29. Kennedy JH, Wiseman JM 2010. Evaluation and performance of desorption electrospray ionization using a triple quadrupole mass spectrometer for quantitation of pharmaceuticals in plasma. Rapid Communications in Mass Spectrometry 24:309-314.

30. Takats Z, Wiseman JM, Gologan B, Cooks RG 2004. Mass spectrometry sampling under ambient conditions with desorption electrospray ionization. Science 306:471-473.

31. Cody RB, Laramée JA, Durst HD 2005. Versatile new ion source for the analysis of materials in open air under ambient conditions. Analytical Chemistry 77:2297-2302.

32. Cohen LH, Gusev AI 2002. Small molecule analysis by MALDI mass spectrometry. Analytical and Bioanalytical Chemistry 373:571-586.

33. LeRiche T, Osterodt J, Volmer DA 2001. An experimental comparison of electrospray ion‐trap and matrix assisted laser desorption/ionization post-source decay mass spectra for the characterization of small drug molecules. Rapid Communications in Mass Spectrometry 15:608-614.

34. Porta T, Grivet C, Knochenmuss R, Varesio E, Hopfgartner G 2011. Alternative CHCA based matrices for the analysis of low molecular weight compounds by UV MALDI tandem mass spectrometry. Journal of Mass Spectrometry 46:144-152.

35. Wan D, Gao M, Wang Y, Zhang P, Zhang X 2012. A rapid and simple separation and direct detection of glutathione by gold nanoparticles and grapheme based MALDI-TOF-MS. Journal of Separation Science 36:629-635.

36. Chen H, Talaty NN, Takáts Z, Cooks RG 2005. Desorption electrospray ionization mass spectrometry for high-throughput analysis of pharmaceutical samples in the ambient environment. Analytical Chemistry 77:6915-6927.

37. Zana R, Benrraou M, Rueff R 1991. Alkanediyl-. alpha.,. omega.-bis (dimethylalkylammonium bromide) surfactants. 1. Effect of the spacer chain length on the critical micelle concentration and micelle ionization degree. Langmuir 7:1072-1075.

38. Rosen MJ, Liu L 1996. Surface activity and premicellar aggregation of some novel diquaternary gemini surfactants. Journal of the American Oil Chemists' Society 73:885-890.

39. Wettig SD, Verrall RE 2001. Thermodynamic Studies of Aqueous m–s–m Gemini Surfactant Systems. Journal of Colloid and Interface Science 235:310-316.

40. Badea I, Verrall R, Baca-Estrada M, Tikoo S, Rosenberg A, Kumar P, Foldvari M 2005. In vivo cutaneous interferon-gamma gene delivery using novel dicationic (gemini) surfactant-plasmid complexes. The Journal of Gene Medicine 7:1200-1214.

41. Zhu M, Zhang H, Humphreys WG 2011. Drug metabolite profiling and identification by high-resolution mass spectrometry. Journal of Biological Chemistry 286:25419-25425.

42. Van Dongen WD, Niessen WMA 2012. LC-MS systems for quantitative bioanalysis. Bioanalysis 4:2391-2399.

43. Sharma A, Rathore S 2012. Bioanalytical Method development and Validation of Drugs in Biological fluid. International Journal of Pharmaceutical & Research Sciences 1:216-226.

44. Kassel D 2001. Combinatorial chemistry and mass spectrometry in the 21st century drug discovery laboratory. Chemical Reviews 101:255-268.

CHAPTER 6
GENERAL DISCUSSION

6.1 General Discussion

Successful utilization of diquaternary ammonium gemini surfactants for the transfection of DNA and RNA has been intensely investigated because of their ability to form lipoplexes with the DNA and RNA to facilitate its protection, delivery, and intracellular release.[1-4] *In vitro* and *in vivo* applications of diquaternary ammonium gemini surfactants have demonstrated their applicability to such endeavors, achieving expression levels that are greater than the unprotected genetic material[4, 5] and comparable to commercially available cationic lipids.[6-8] In fact, a 450% increase in the levels of IFNγ in the epidermis of mice was reported for G16-3:DOPE vectors in comparison to unprotected IFNγ genes within a mouse animal model.[5] All previous studies, however, were exclusively concerned with the enhancement of the diquaternary ammonium gemini surfactants' encapsulation efficiency, transfection capability as well as reducing their toxic effects without assessing the cause of toxicity.

Understanding the post transfection fate, including cellular disposition and tissue accumulation, of diquaternary ammonium gemini surfactants is vital to designing future cationic lipids that are less toxic. There are no studies that provided information on the cause of toxicity due to the lack of analytical methods available to identify/quantify diquaternary ammonium gemini surfactants post transfection. Therefore, qualitative and quantitative methods are needed to improve the current understanding of the post transfection fate of gemini surfactants as well as to advance their use as gene carriers. Mass spectrometry is ideally suited to detect and quantify gemini surfactants due to the permanent positive charges within their molecular structure (Figure 1.2 and 1.3). Therefore, an understanding of their ionization, gas phase and/or CID behavior is needed as it ensures that the developed analytical methods are specific for the analyte(s) of interest.

Specificity and selectivity are provided by mass spectrometry through both ionization and ion separation as each analyte behaves in a unique and reproducible manner during ionization, single-stage MS, MS/MS, and multi-stage MS^n analysis. Most analytes can be differentiated easily from one another using MS, ensuring specificity for the analytical method. Method reproducibility ensures that the data is consistent across analysis of a batch of samples, between batches of samples and between instruments. The ability of mass spectrometry analysis to

achieve both specificity and reproducibility is a result of the ionization method and ion separation.

Each ionization method will provide the analyte with a specific *m/z* value based upon the addition or removal of a hydrogen atom, an electron, or the formation of adducted ion. For ESI, the removal of either a single bromide counter ion or both bromide counterions results in the formation of a singly charged bromide adduct or doubly charge diquaternary ammonium gemini surfactant ion; respectively (Figure 3.2). Conversely, MALDI-HR-MS did not maintain the intact structure of the diquaternary ammonium gemini surfactant analytes, but instead cleaved each molecule into two individual fragment ions (Figure 5.2). Although all the ionization methods did not produce identical ions for each diquaternary ammonium gemini surfactant, each ionization method produced ions that were specific and reproducible, allowing for quantitative analysis.

6.1.1 Mass spectrometric analysis of 29 diquaternary ammonium gemini surfactants

MS (Table 3.1 and Figure 3.2) and MS/MS (Table 3.2 and Figure 3.3A) analysis of each diquaternary ammonium gemini surfactant ion allows for the confirmation of its molecular composition or structural feature(s). Specifically, MS identification of analytes can be performed using either MS/MS analysis or accurate mass measurement during single-stage MS experiments. LR instruments were utilized for quantitative MS/MS, while HR instruments were utilized for quantitative single-stage MS. The use of both MS and MS/MS for quantitative analysis demonstrated their capability to specifically select the precursor and/or product ion(s) of interest, while providing specificity by preventing other ions from reaching the detector. The confirmation of the molecular formula of 29 novel gemini surfactants was achieved by both HR-MS (Table 3.1 and Figure 3.2) and LR-MS/MS, which induces unique CID fragment ions for each of the tested 29 gemini surfactants (Table 3.2 and Figure 3.3A).

An AB Sciex QSTAR XL Q-ToF-HR-MS instrument was used for accurate mass measurements. Doubly charged ion for each of the gemini surfactant was observed as well as gemini surfactant bromide adducts (Table 3.1 and Figure 3.2). Mass accuracies were less than 5 PPM for gemini surfactants while the bromide adducts had mass accuracies less than 10 PPM (Table 3.1). Observation of superior mass accuracies for the doubly charged diquaternary ammonium gemini surfactant ions is a result of internal calibration while only external calibration was utilized for the corresponding bromide adducts. These results confirmed the

molecular formula of each gemini surfactant as well as the propensity of gemini surfactant cations to form an ion pair with its bromide counter ion under favorable conditions.

While the molecular composition of each gemini surfactant was solely assessed by HR-MS, structural identification of each diquaternary ammonium gemini surfactant and bromide adducts were established through both CID-MS/MS and *quasi* MS^3 analysis utilizing a QqToF-HR-MS/MS and QhQ-LR-MS/MS; respectively. The MS/MS and *quasi* MS^3 data provided structural information about each compound (Table 3.2 and Figure 3.3B-D) while *quasi* MS^3 analysis rationalized the fragmentation route(s) (Table 2.4). MS/MS and quasi MS^3 analysis allowed for the identification of a universal fragmentation pathway which pertains to all 29 gemini surfactants. (Figure 3.3A). Three unique CID-MS/MS product ion types were identified, with at least one unique product ion being observed during MS/MS analysis of all 29 gemini surfactants analyzed. After the completion of this work, the universal fragmentation behavior was applied for the analysis of novel amino-acid substituted gemini surfactants.[9]

6.1.2 Quantitative liquid chromatography low resolution tandem mass spectrometric analysis

Development and validation of an analytical method that is suitable for the quantification of gemini surfactants within PAM212 cellular lysate was required to assess their post transfection fate. The ability of mass spectrometry to differentiate drug molecules from their metabolites and endogenous molecules has made mass spectrometric analysis the analytical gold standard for the pharmaceutical industry; specifically LC-MS/MS.[10-12] Therefore, the first method developed and validated was an LC-LR-MS/MS method which utilized an CN stationary phase column a gradient of water and acetonitrile, both containing 0.3% (vol:vol) formic acid and 1 mM triethylamine, (Figure 4.2) to separate and elute all 29 diquaternary ammonium gemini surfactants (Table 4.1). The ability to correlate each gemini surfactant with a LC retention time and a product ion with a unique MRM ensured each analyte was specifically identified (Table 4.1). In addition, the selectivity of MRM analysis provides the ability to distinguish and quantify structurally similar analytes without the need to achieve their baseline separation, an inherent advantage of MS/MS.[13, 14] The LC-LR-MS/MS quantitative method was validated for a single diquaternary ammonium gemini surfactant, G16-3, following USFDA guidelines for bioanalytical method validation. Quantification of G16-3 resulted in an LLOQ of 0.406 µM and the ULOQ assessed at 298.1 µM (Figure 4.5 & 5.5 and Table 5.4); producing a 744 fold linear

range. Unfortunately, this method suffered from ion suppression due to the addition of triethylamine, an LC additive used to minimize peak tailing, and a large time of analysis that results from chromatographic separation.

The observed ion suppression spurred the investigation of other high-throughput mass spectrometric methods; including FC-LR-MS/MS, FC-HR-MS, DESI-LR-MS/MS, and MALDI-HR-MS (Table 5.5). Applying alternative high-throughput mass spectrometric techniques eliminated the time required for chromatographic separation while attaining quantitative results comparable/superior to LC-LR-MS/MS.

6.1.3 Alternative high-throughput mass spectrometric-based methods

Two FC methods were developed utilizing a CN stationary phase that was 8x shorter than the stationary phase utilized by the LC-LR-MS/MS. This allowed for the use of a more rapid gradient, using water and methanol containing 0.1% formic acid, to achieve a time of analysis that is ~4.5 fold faster than the LC-LR-MS/MS method (Appendix D Figure 1). In addition, the FC-LR-MS/MS analysis of G16-3 resulted in an LLOQ of 0.037 μM for G16-3, which is 27 times more sensitive than LLOQ of 1.0000 μM achieved by FC-HR-MS and 11 times more sensitive than the LLOQ of the LC-LR-MS/MS method (Figure 5.5 and Table 5.4).

Although additional time and consumables are required for DESI and MALDI sample preparation, the period of analysis was substantially abbreviated for both surface sampling ionization techniques. DESI-LR-MS/MS utilized a methanol spray solvent containing 0.1% formic acid to achieve desorption of the analyte from the hydrophobic surface in less than 45 seconds (Table 5.6), which is ~14.5 times faster than the LC-LR-MS/MS method (Table 7.4). MALDI-HR-MS was ~146 times faster than LC-LR-MS/MS and utilized a sinapinic acid matrix during its 4.3 second analysis (Table 5.6). Sinapinic acid did not interfere with the analysis allowing for a LLOQ of 0.400 μM to be achieved, which is comparable to the LLOQ achieved by LC-LR-MS/MS (Figure 5.5 and Table 5.4).

Each alternative method provides a more rapid quantitative analysis of G16-3 within PAM212 cell lysate than the developed LC-LR-MS/MS (Table 5.6). In addition, two of the four alternative quantitative mass spectrometric methods achieved a LLOQ that was superior or comparable to that of the LC-LR-MS/MS (Figure 5.5 and Table 5.4).

In addition to the rapid nature of each alternative method several other benefits were realized. Both the FC-LR-MS/MS and MALDI-MS methods achieved a 1000x linear range and

were superior to the LC-LR-MS/MS method (Figure 5.5 and Table 5.4). Extending the linear ranges can be beneficial for other quantitative applications, such as quality control of pharmaceutical formulations, as dilutions may not be needed to ensure the analyte's concentration is within the acceptable linear range. In addition, a comparison of all five quantitative methods demonstrates that DESI-LR-MS/MS requires the least amount of method development. DESI-LR-MS/MS parameters were optimized rapidly in comparison to selection of a suitable MALDI matrix or chromatographic conditions for LC and FC. However, all alternative MS methods were much easier to develop than LC-LR-MS/MS that is limited by peak tailing, shifts in retention time and ion suppression from endogenous compounds. The efficacy of FC-LR-MS/MS, FC-HR-MS, MALDI-HR-MS, and DESI-LR-MS/MS demonstrates their potential benefits for quantitative analysis not realized by the industry's gold standard LC-LR-MS/MS.

6.1.4 Quantification of G16-3 within PAM212 cell lysate

The ability of all methods to quantify G16-3 within PAM212 cellular lysate demonstrates that the extensive time and consumable usage associated with LC-LR-MS/MS is not required in order to achieve sensitive quantitative results. All five methods were able to accurately assess the post-transfection cellular concentration, 5 to 53 hours, of G16-3 within PAM212 cellular lysate; 1.45 ± 0.06 μM. Each method was within the 15% accuracy when compared to the average concentration for each time point with a RSD of 15%. However, not all methods could reasonably monitor the cellular uptake of G16-3 by PAM212 cells at early concentrations because they were below the LLOQ. MALDI-HR-MS was unable to quantify the 0.25 hour time point, while FC-HR-MS and DESI-LR-MS/MS were unable to quantify sample prior to the 2 hour time point. Regardless, linear uptake of the G16-3 gemini surfactant following addition of the transfection solution was observed during the zero to five hour period and correlated with LC-LR-MS/MS data. Finally, the absence of a change in concentration after the removal of the transfection solution at the 5 hour mark indicates the absence of metabolic activity that would degrade G16-3.

6.2 Conclusion

The development of five quantitative mass spectrometric methods to assess the concentration of G16-3 with PAM212 cellular lysate demonstrates the benefits alternative MS

methods have over LC-LR-MS/MS. While the validation of all five methods was performed solely for G16-3, the MS and MS/MS analysis of 29 diquaternary ammonium gemini surfactants ensures that each method can be tailored to other analytes. The specificity of analysis is ensured by the evaluation of the MS behavior and MS/MS fragmentation pattern of each diquaternary ammonium gemini surfactants, to confirm the precursor ion and the unique fragmentation pattern.[9]

6.3 Future Directions

Understanding the MS behavior of diquaternary ammonium gemini surfactants, including the establishment of a universal MS/MS fragmentation pathway, ensures that they can be differentiated from one another within a variety of matrices. Application of this knowledge to the development and validation of several MS quantitative methods would allow for the evaluation of their post transfection fate.

6.3.1 Evaluation of the MS behavior of novel gemini surfactants

The establishment of the universal fragmentation pathway of gemini surfactants has proven to be valuable as it identifies unique fragment ions for structural identification. Currently new diquaternary ammonium gemini surfactant molecules are being designed in order to enhance encapsulation efficiency, delivery, and cell viability. Such modifications include the inclusion of amino acid moieties within the spacer region[9] or more recently the incorporation of cyclodextrin, to expand gemini surfactants's use towards hydrophobic drugs.[15] The use of the universal fragmentation pathway will ensure that the CID behavior of diquaternary ammonium gemini surfactants will be easier to predict and that only unique MRM transitions are utilized for analytical analysis. Application of the universal fragmentation pathway assisted in assessing the CID behavior of amino acid/di-peptide modified diquaternary ammonium gemini surfactants[9] and continues to assist in the elucidation of the CID behavior of novel diquaternary ammonium gemini surfactants.

6.3.2 Quantification of diquaternary ammonium gemini surfactants

Assessing the post transfection fate of diquaternary ammonium gemini surfactants has benefited from the development of MS-based quantitative methods. I have evaluated the fate of gemini surfactants within the whole cellular matrix. Expansion of this work will include the

quantitative analysis at the sub-cellular level. The goal is to understand the effect of chemical modifications on sub-cellular localization or *in vivo* tissue distribution. Finally, extrapolation of the CID-MS/MS behavior of diquaternary ammonium gemini surfactants will provide a basis for the discovery of their metabolites through the use of either precursor ion or neutral loss scans.

6.3.3 Sub-cellular quantitative analysis of diquaternary ammonium gemini surfactants

An evaluation of the sub-cellular localization of the gemini surfactant G16-3 in a PAM212 cell line as well as the identification of any metabolites will provide information on the post-transfection fate of gemini surfactants. An assessment of their *in vitro* behavior (including its cellular uptake, intracellular interactions, and elimination) is important in evaluating their safety and toxicity profile. Previous evaluations of each gemini surfactant's toxicity shows that gemini surfactants induce cytotoxicity, however, the question of how they induce toxicity was never identified. Application of the developed quantitative MS methods to the determination of the subcellular localization of diquaternary ammonium gemini surfactants allows for a more detailed understanding of the post transfection fate. Subcellular fractionation can be achieved following the sequential actions of disrupting the cellular architecture and separating the subcellular components.[16] A basic method allows for the isolation of four main fractions, including the nuclear, mitochondrial, microsomal, and cytosolic fractions.[17] Identification of the sub-cellular localization of the diquaternary ammonium gemini surfactants could address how their structure affects cellular toxicity.

6.3.4 Assessment of the metabolites of diquaternary ammonium gemini surfactants

Mass spectrometry can identify structural modifications through accurate and precise mono-isotopic mass measurement of xenobiotic metabolites during single stage MS analysis as well as through differences in the fragmentation patterns produced by multi stage MS^n analysis following CID.[18] Single stage MS analysis can provide structural information based upon changes in *m/z* values. Metabolites may include methylation[19] (14 Da difference) or conjugation of glutathione,[20] (i.e., 300 Da) with MS analysis providing information on the type of metabolism undergone by the analyte.[21] Similarly, MS^n analysis can provide information on metabolic transformations,[22] by monitoring the CID of analytes.[22] For example, the conjugation of

glutathione to acetaminophen was identified by monitoring for the neutral loss of 129.042 *m/z*, loss of pyroglutamic acid from glutathione, during MS/MS analysis.[23] Application of the developed quantitative MS methods and metabolic knowledge can provide information on both the type and site of metabolism based upon observed differences between their MS and MS/MS spectra. Lightsight software, available from AB Sciex, could be used in the identification of metabolites.

6.4 Literature Cited

1. Matulis D, Rouzina I, Bloomfield VA 1999. Thermodynamics of cationic lipid binding to DNA and DNA condensation: roles of electrostatics and hydrophobicity. Colloid Polymer Science 112:71-75.

2. Camilleri P, Kremer A, Edwards AJ, Jennings KH, Jenkins O, Marshall I, Neville W, Rice SQ, Smith RJ, Wilkinson MJ 2000. A novel class of cationic gemini surfactants showing efficient in vitro gene transfection properties. Chemical Communications 2000:1253-1254.

3. Wang C, Li X, Wettig SD, Badea I, Foldvari M, Verrall RE 2007. Investigation of complexes formed by interaction of cationic gemini surfactants with deoxyribonucleic acid. Physical Chemistry Chemical Physics 9:1616-1628.

4. Badea I, Wettig S, Verrall R, Foldvari M 2007. Topical non-invasive gene delivery using gemini nanoparticles in interferon-γ-deficient mice. European Journal of Pharmaceutics and Biopharmaceutics 65:414-422.

5. Badea I, Verrall R, Baca-Estrada M, Tikoo S, Rosenberg A, Kumar P, Foldvari M 2005. In vivo cutaneous interferon-γ gene delivery using novel dicationic (gemini) surfactant–plasmid complexes. Journal of Gene Medicine 7:1200-1214.

6. Ryhanen SJ, Saily VMJ, Parry MJ, Luciani P, Mancini G, Alakoskela JMI, Kinnunen PKJ 2006. Counterion-controlled transition of a cationic gemini from submicroscopic to giant vesicles. Journal of the American Chemical Society 128:8659-8663.

7. Matti V, Säily J, Ryhänen SJ, Holopainen JM, Borocci S, Mancini G, Kinnunen PK 2001. Characterization of mixed monolayers of phosphatidylcholine and a dicationic gemini surfactant SS-1 with a langmuir balance: effects of DNA. Biophysical Journal 81:2135-2143.

8. Ryhänen SJ, Säily MJ, Paukku T, Borocci S, Mancini G, Holopainen JM, Kinnunen PK 2003. Surface charge density determines the efficiency of cationic gemini surfactant based lipofection. Biophysical journal 84:578-587.

9. Mohammed-Saeid W, Buse J, Badea I, Verrall R, El-Aneed A 2012. Mass spectrometric analysis of amino acid/di-peptide modified gemini surfactants used as gene delivery agents: Establishment of a universal mass spectrometric fingerprint. International Journal of Mass Spectrometry 309:182-191.

10. Lindegardh N, Tarning J, Toi P, Hien T, Farrar J, Singhasivanon P, White N, Ashton M, Day N 2009. Quantification of artemisinin in human plasma using liquid chromatography coupled to tandem mass spectrometry. Journal of Pharmaceutical and Biomedical Analysis 49:768.

11. Ramanathan R, Jemal M, Ramagiri S, Xia YQ, Humpreys WG, Olah T, Korfmacher WA 2011. It is time for a paradigm shift in drug discovery bioanalysis: from SRM to HRMS. Journal of Mass Spectrometry 46:595-601.

12. Rudaz S, Geiser L, Guillarme D, Veuthey J 2005. Development of rapid analytical methods in the Laboratory of Pharmaceutical Analytical Chemistry (LCAP). CHIMIA International Journal for Chemistry 59:303-307.

13. Prinsen E, Redig P, Van Onckelen HA, Van Dongen W, Esmans EL 2005. Quantitative analysis of cytokinins by electrospray tandem mass spectrometry. Rapid Communications in Mass Spectrometry 9:948-953.

14. Raith K, Neubert RH 2000. Liquid chromatography–electrospray mass spectrometry and tandem mass spectrometry of ceramides. Analytica Chimica Acta 403:295-303.

15. Michel D, Chitanda JM, Balogh R, Yang P, Singh J, Das U, El-Aneed A, Dimmock J, Verrall R, Badea I 2012. Design and evaluation of cyclodextrin-based delivery systems to incorporate poorly soluble curcumin analogs for the treatment of melanoma. European Journal of Pharmaceutics and Biopharmaceutics 81:548-556.

16. Kislinger T, Cox B, Kannan A, Chung C, Hu P, Ignatchenko A, Scott MS, Gramolini AO, Morris Q, Hallett MT 2006. Global survey of organ and organelle protein expression in mouse: combined proteomic and transcriptomic profiling. Cell 125:173-186.

17. Cox B, Emili A 2006. Tissue subcellular fractionation and protein extraction for use in mass-spectrometry-based proteomics. Nature protocols 1:1872-1878.

18. Ragu R. 2009. Mass spectrometry in drug metabolism & pharmacokinetics, Hoboken, New Jersey: John Wiley & Sons, Inc.

19. Keski-Hynnilä H, Kurkela M, Elovaara E, Antonio L, Magdalou J, Luukkanen L, Taskinen J, Kostiainen R 2002. Comparison of electrospray, atmospheric pressure chemical ionization, and atmospheric pressure photoionization in the identification of apomorphine, dobutamine, and entacapone phase II metabolites in biological samples. Anal Chem 74:3449-3457.

20. Thatcher NJ, Murray S 2001. Analysis of the glutathione conjugate of paracetamol in human liver microsomal fraction by liquid chromatography mass spectrometry. Biomedical Chromatography 15:374-378.

21. Chernushevich IV, Loboda AV, Thomson BA 2001. An introduction to quadrupole-time-of-flight mass spectrometry. Journal of Mass Spectrometry 36:849-865.

22. Anari MR, Baillie TA 2005. Bridging cheminformatic metabolite prediction and tandem mass spectrometry. Drug Discovery Today 10:711-717.

23. Gottardo R, Fanigliulo A, Sorio D, Liotta E, Bortolotti F, Tagliaro F 2011. Monitoring compliance to therapy during addiction treatments by means of hair analysis for drugs and drug metabolites using capillary zone electrophoresis coupled to time-of-flight mass spectrometry. Forensic Science International 216: 101-107.

CHAPTER 7
APPENDICES

APPENDIX A
Diquaternary ammonium gemini surfactant MS/MS fragmentation analysis

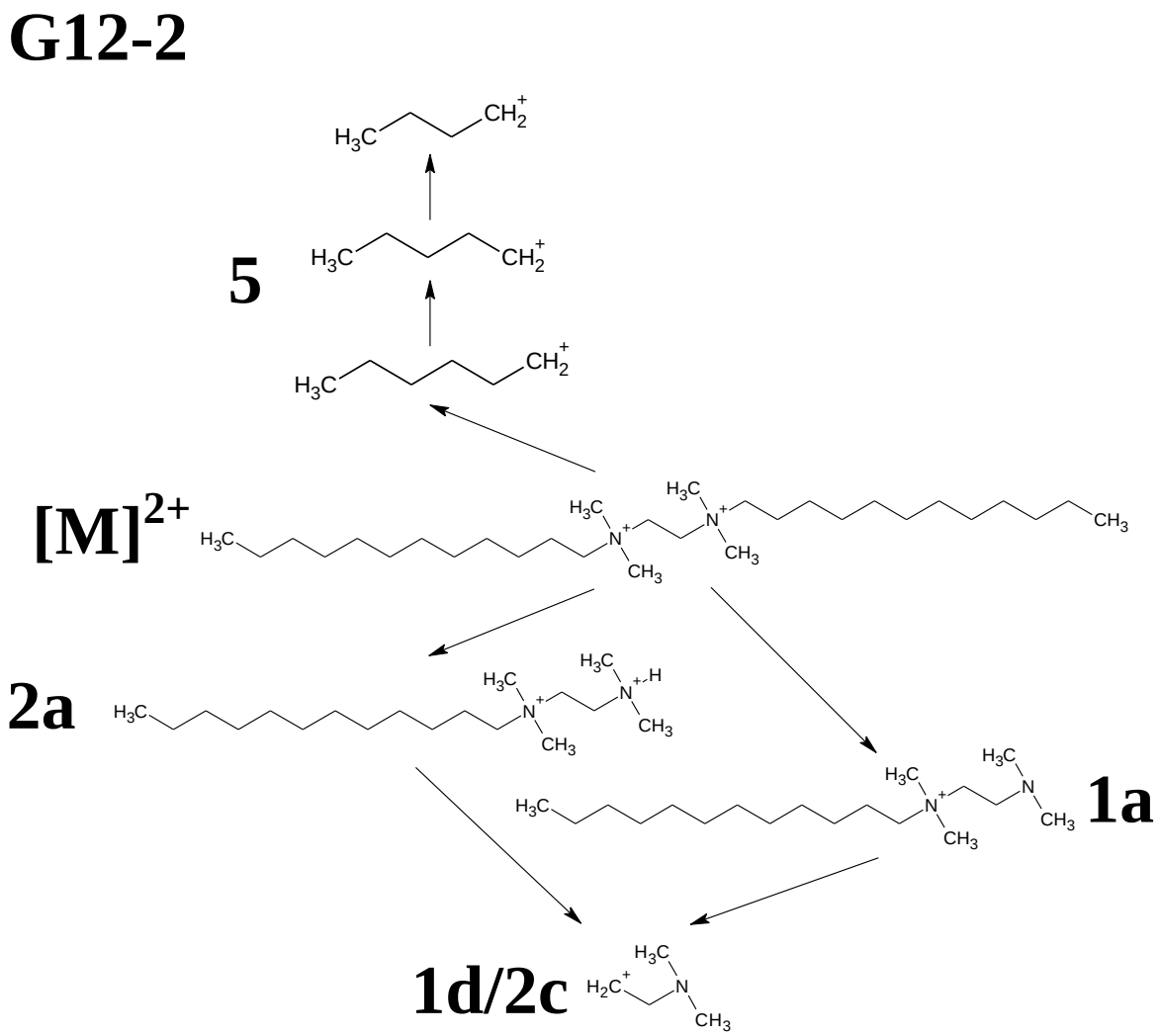

Appendix A Figure 1.1 Fragmentation pattern of G12-2

Appendix A Table 1 G12-2 gemini surfactant fragment ions (m/z)

$[M]^{2+}$	1a	1b	1c	1d	2a	2b	2c	3a	3b	3c	4	5
227.26	285.32			72.08	143.17		72.08					85.1 → 57.07

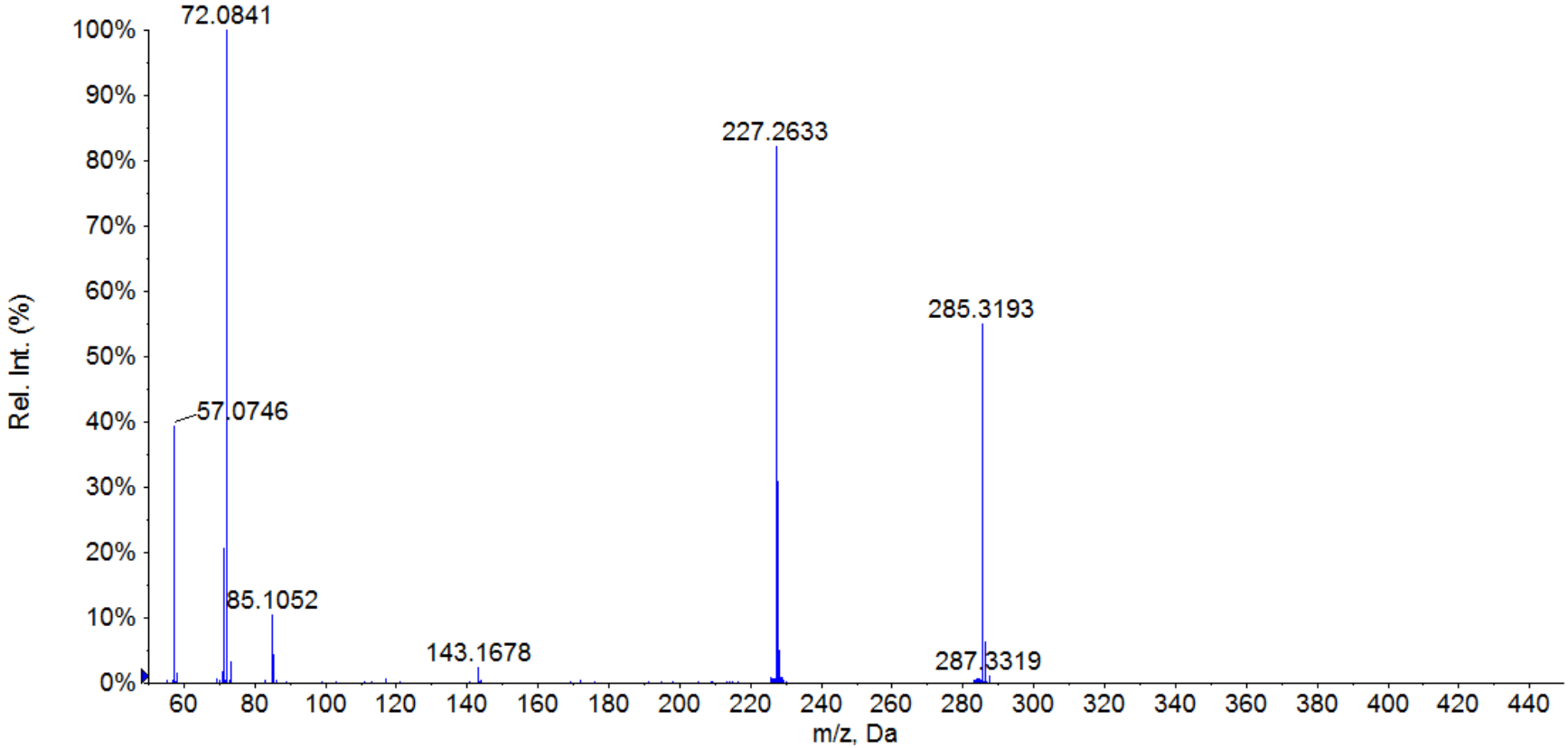

Appendix A Figure 1.2 A MS/MS spectra of G12-2 provided by an AB Sciex QSTAR XL qToF-MS

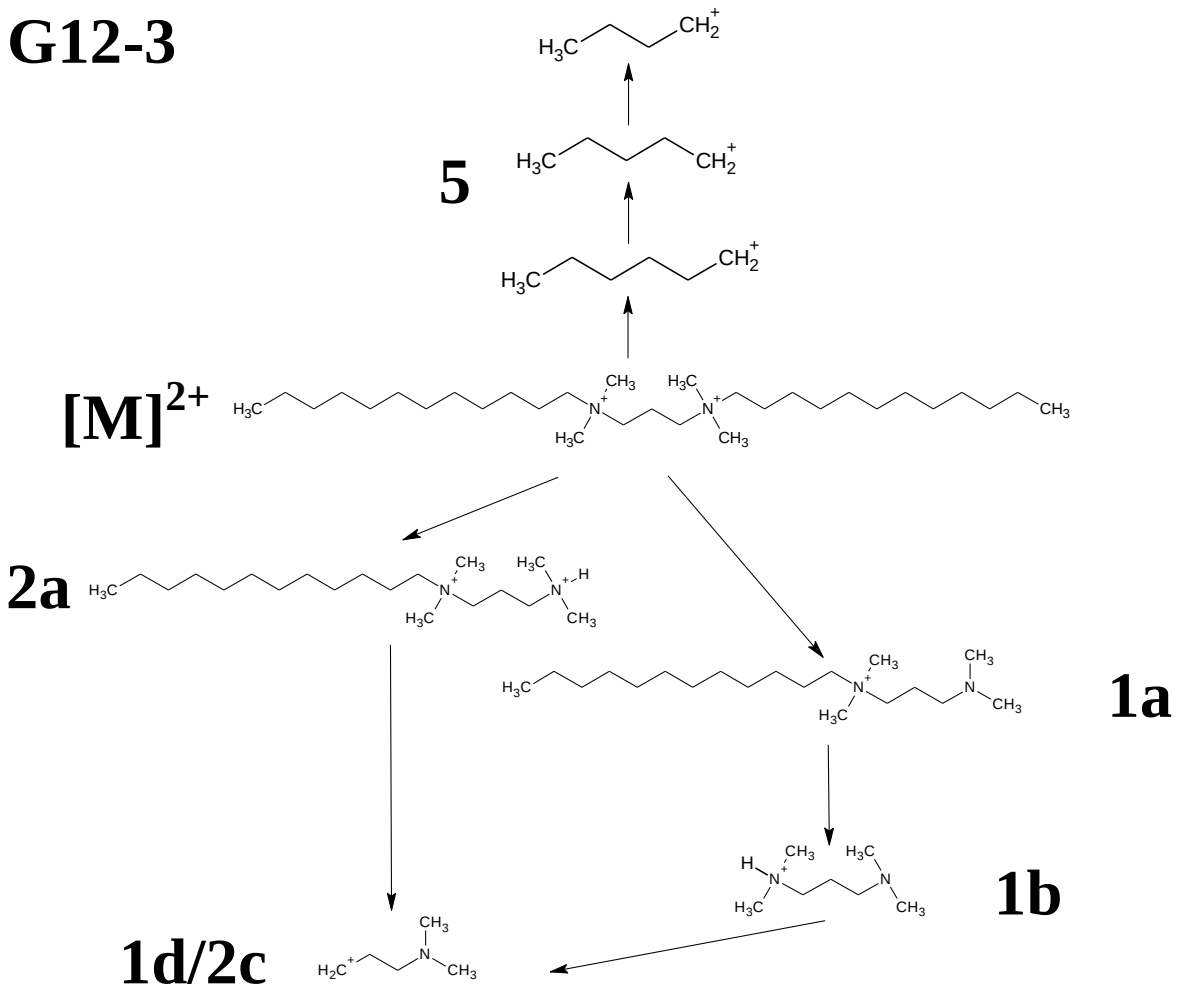

Appendix A Figure 2.1 Fragmentation pattern of G12-3

Appendix A Table 2 G12-3 gemini surfactant fragment ions (m/z)

$[M]^{2+}$	1a	1b	1c	1d	2a	2b	2c	3a	3b	3c	4	5
234.28	299.35	131.16		86.1	150.18		86.1					85.1 → 57.07

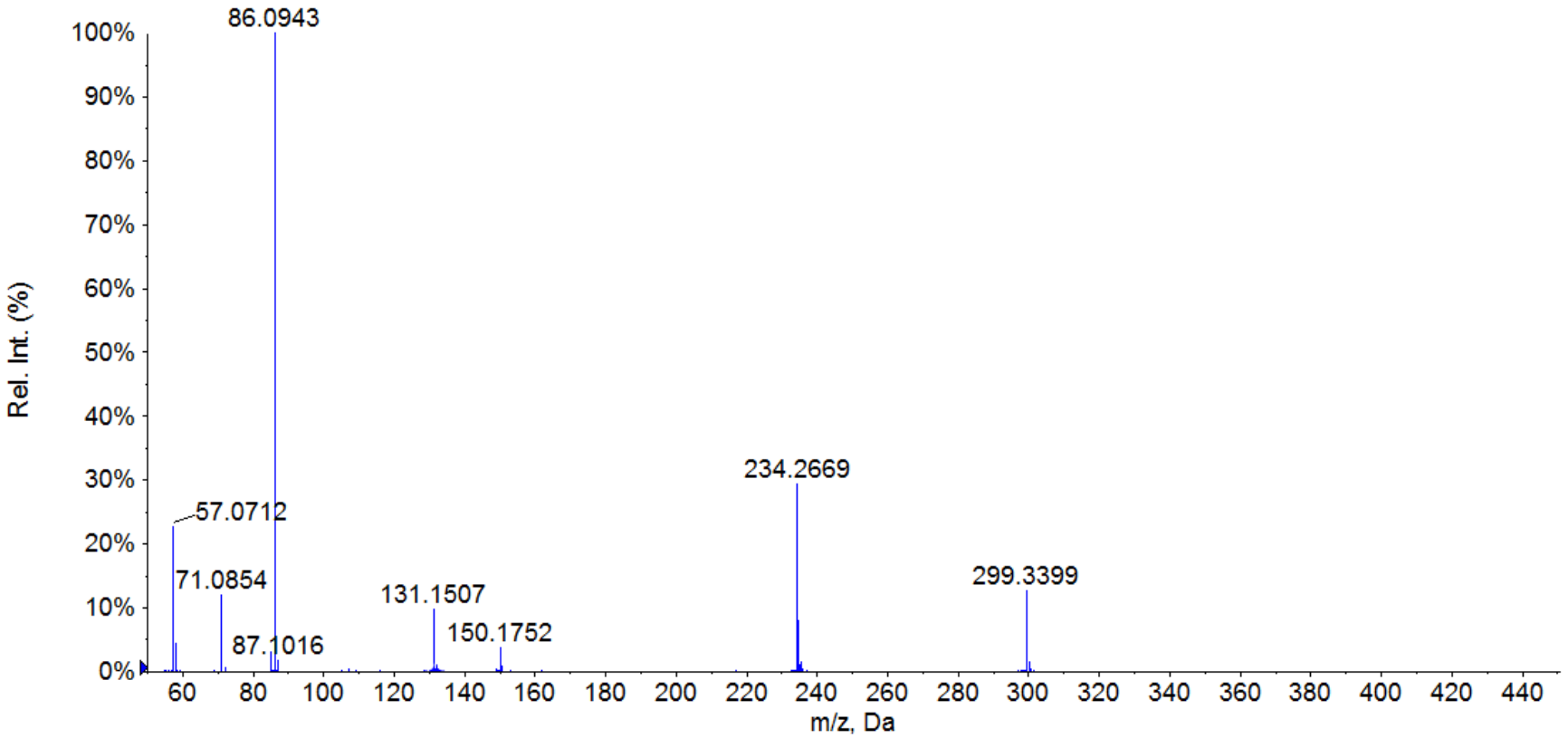

Appendix A Figure 2.2 A MS/MS spectra of G12-3 provided by an AB Sciex QSTAR XL qToF-MS

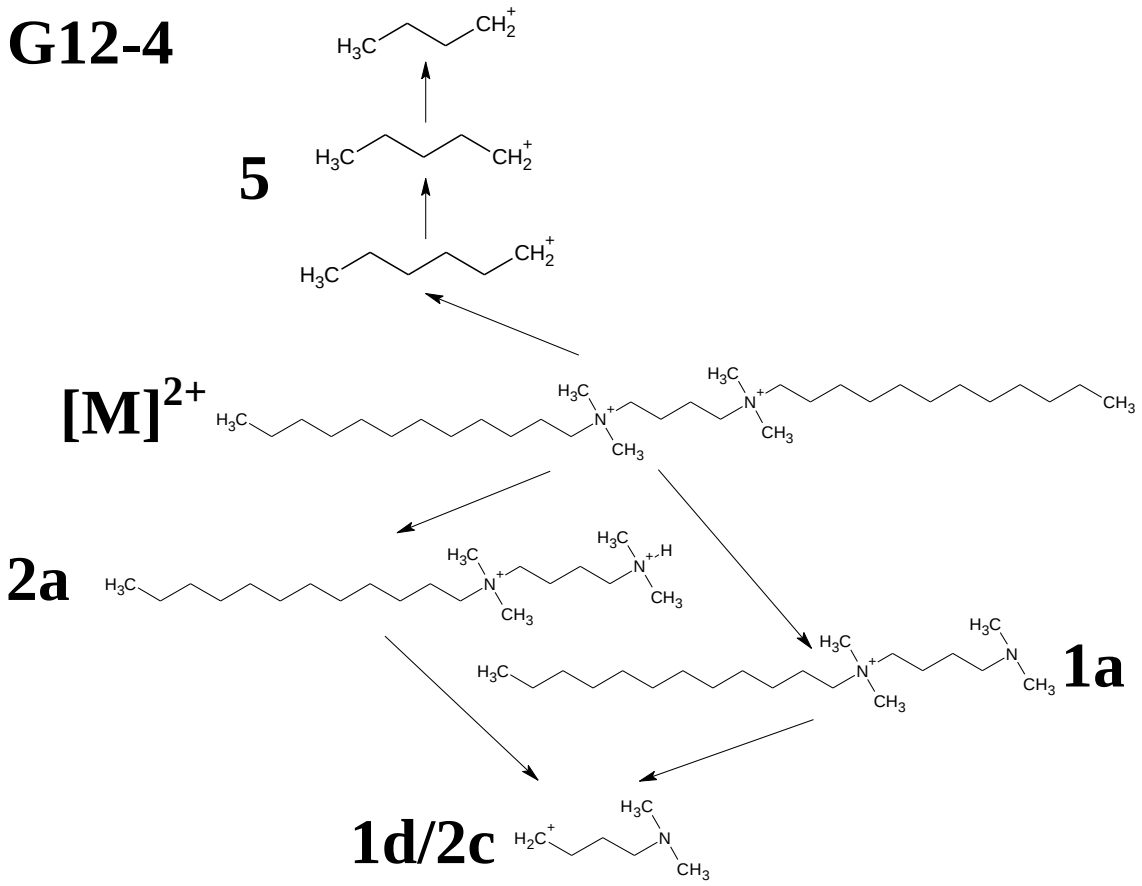

Appendix A Figure 3.1 Fragmentation pattern of G12-4

Appendix A Table 3 G12-4 gemini surfactant fragment ions (m/z)

$[M]^{2+}$	1a	1b	1c	1d	2a	2b	2c	3a	3b	3c	4a	5
241.28	313.39			100.11	157.19		100.11					85.1 → 57.07

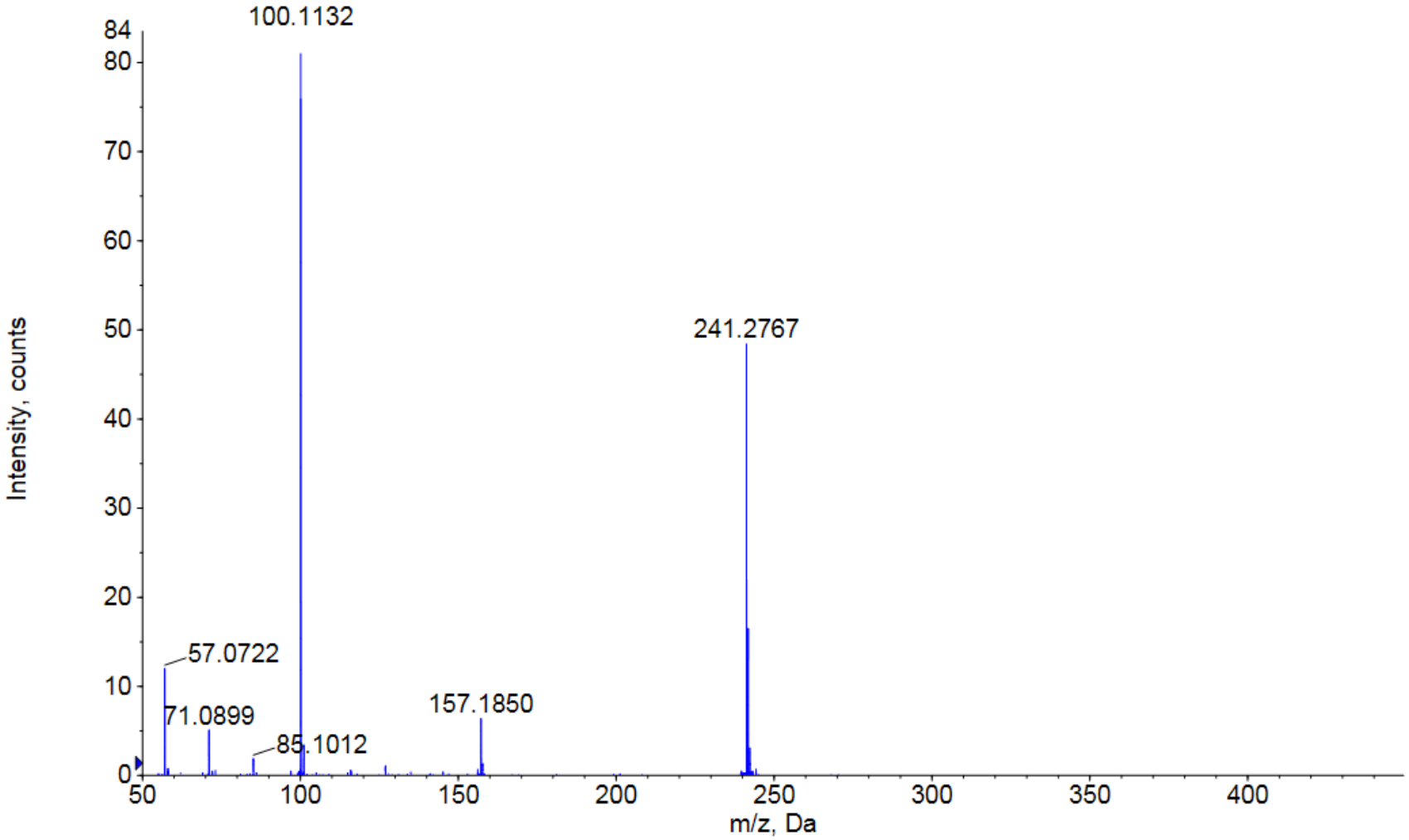

Appendix A Figure 3.2 A MS/MS spectra of G12-4 provided by an AB Sciex QSTAR XL qToF-MS

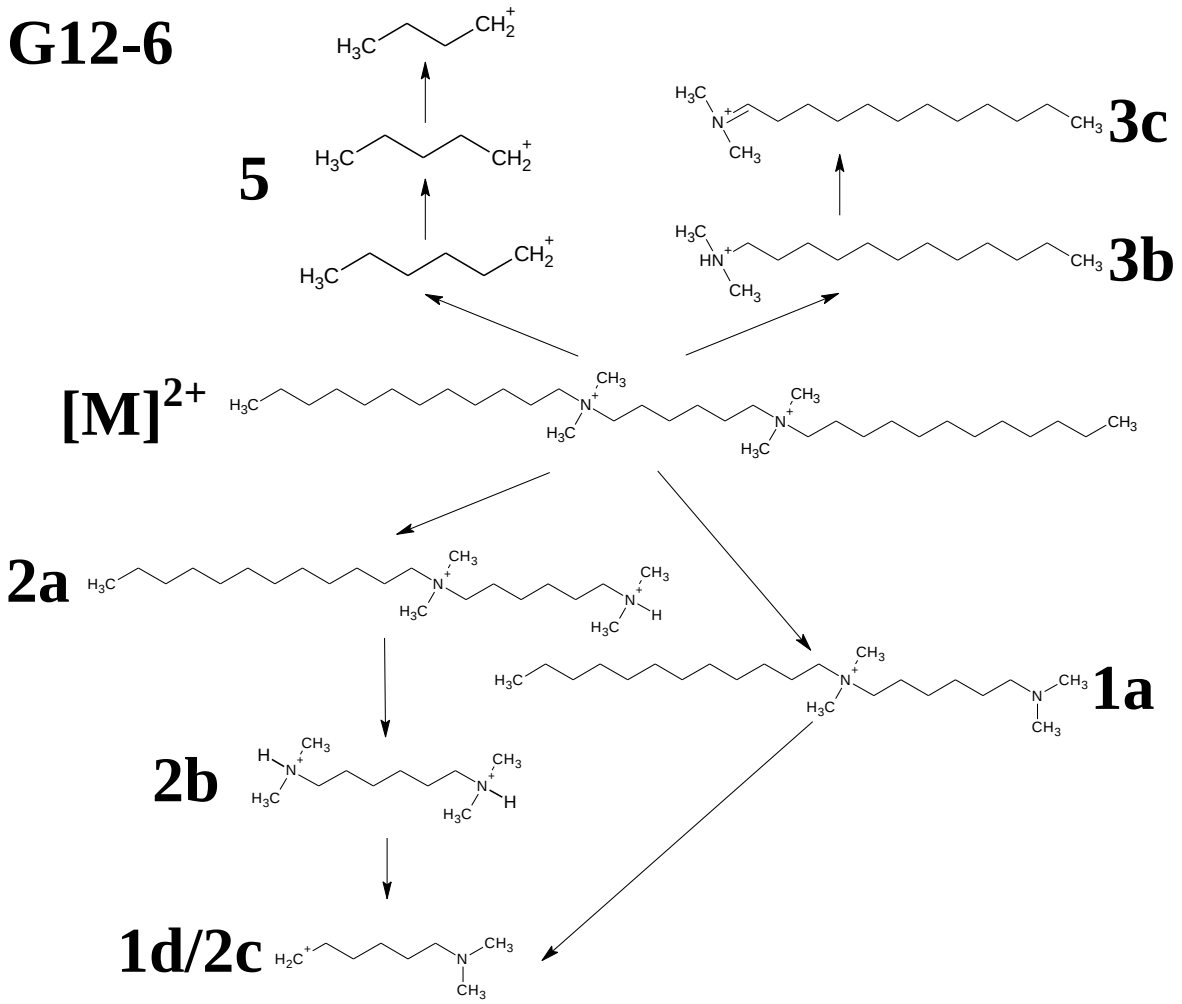

Appendix A Figure 4.1 Fragmentation pattern of G12-6

Appendix A Table 4 G12-6 gemini surfactant fragment ions (m/z)

$[M]^{2+}$	1a	1b	1c	1d	2a	2b	2c	3a	3b	3c	4	5
255.3	341.41			128.15	171.2	87.11	128.15		214.1	212.24		85.1 → 57.07

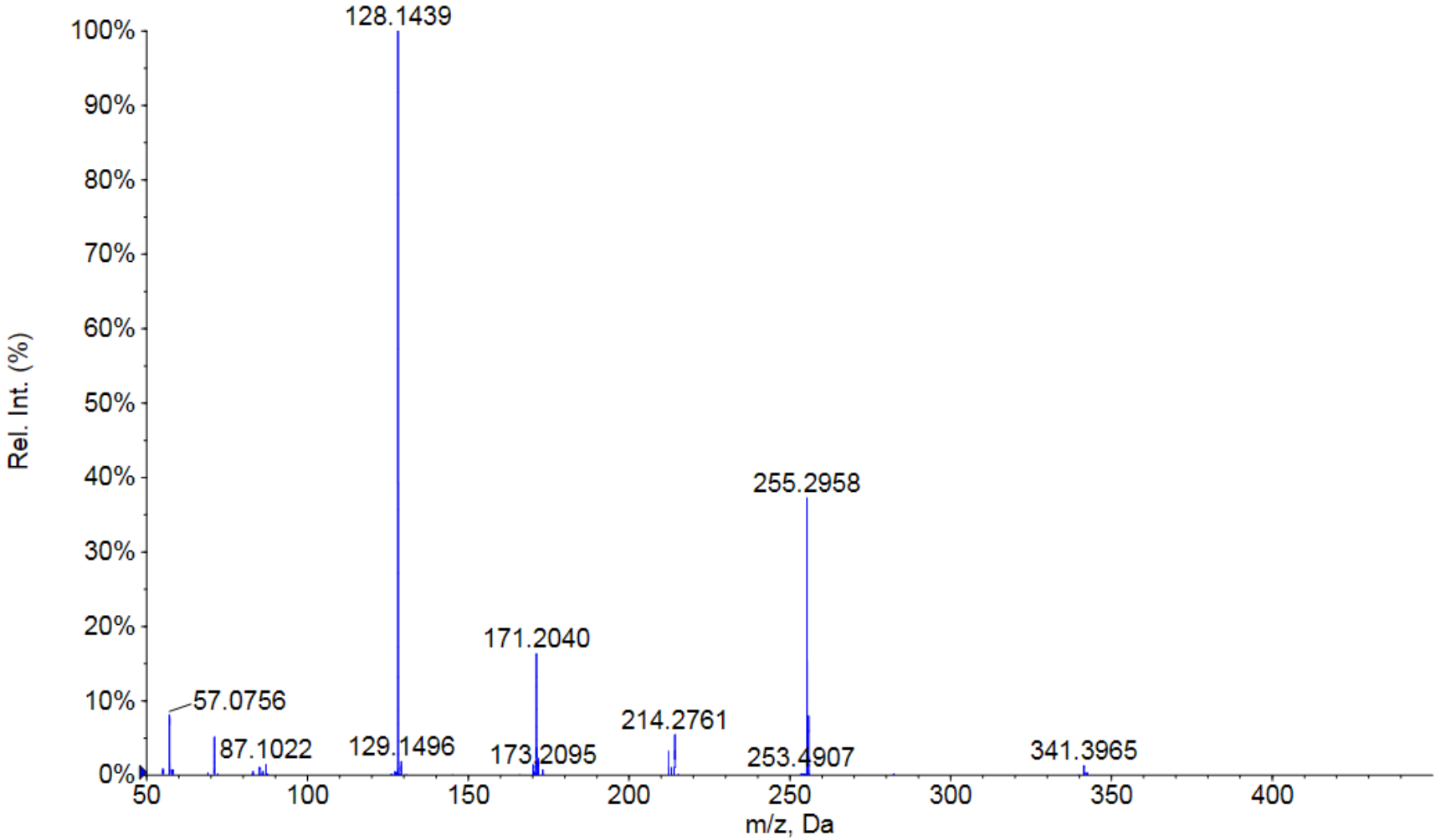

Appendix A Figure 4.2 A MS/MS spectra of G12-6 provided by an AB Sciex QSTAR XL qToF-MS

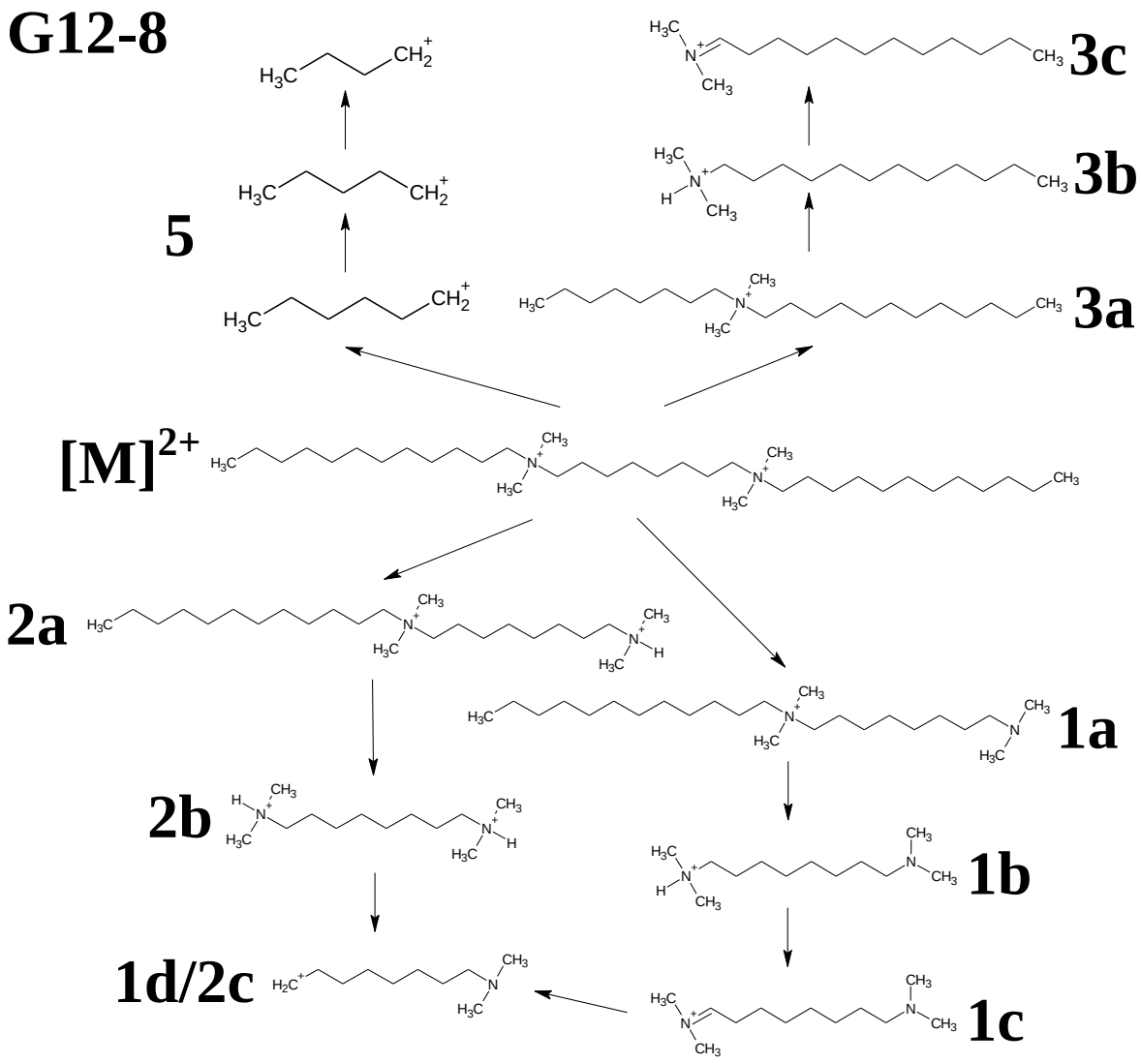

Appendix A Figure 5.1 Fragmentation pattern of G12-8

Appendix A Table 5 G12-8 gemini surfactant fragment ions (m/z)

$[M]^{2+}$	1a	1b	1c	1d	2a	2b	2c	3a	3b	3c	4	5
269.3	369.4	201.1	199.2	156.1	185.2	101.1	156.1	310.3	214.2	212.2		85.1 → 57.07

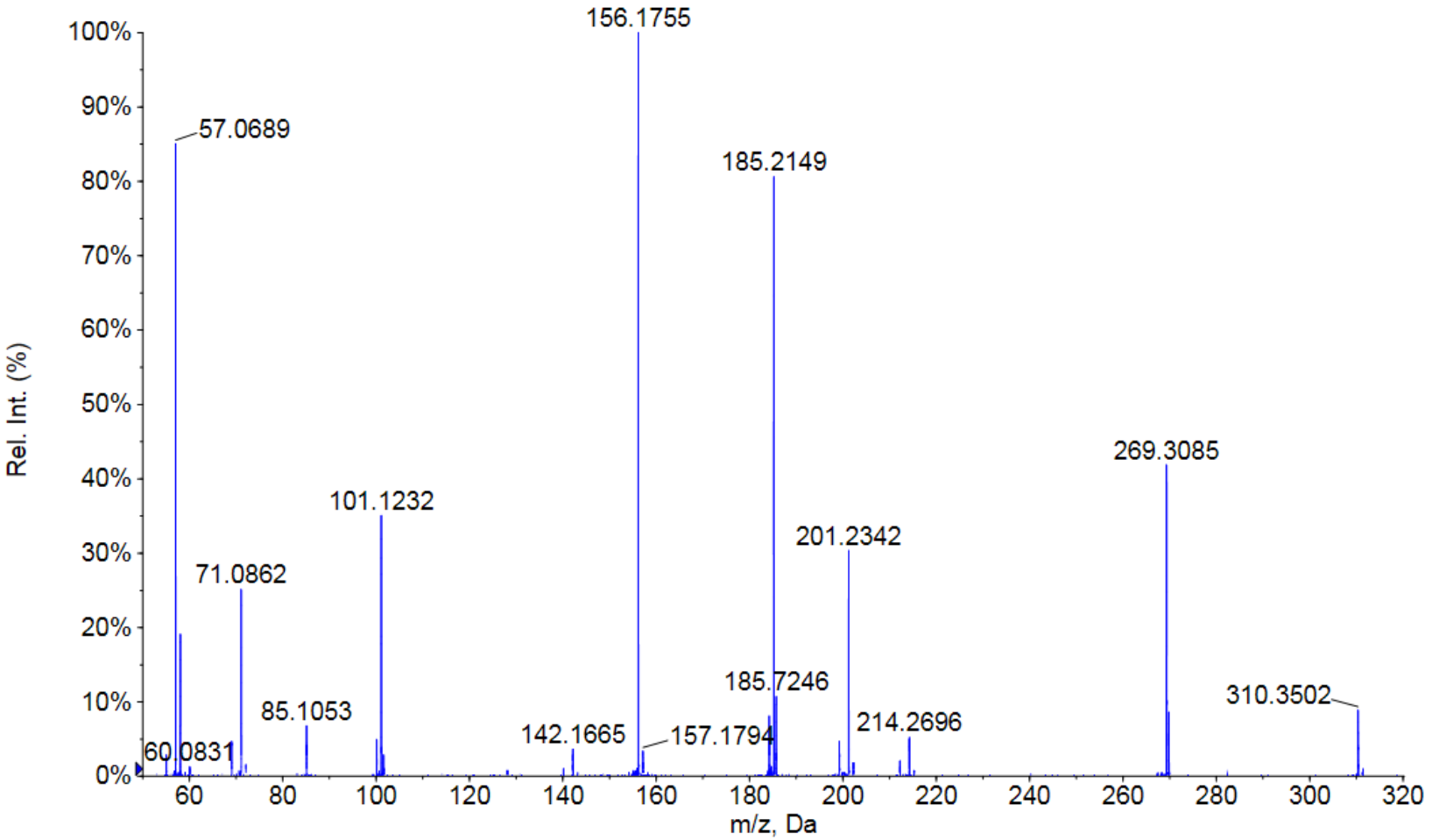

Appendix A Figure 5.2 A MS/MS spectra of G12-8 provided by an AB Sciex QSTAR XL qToF-MS

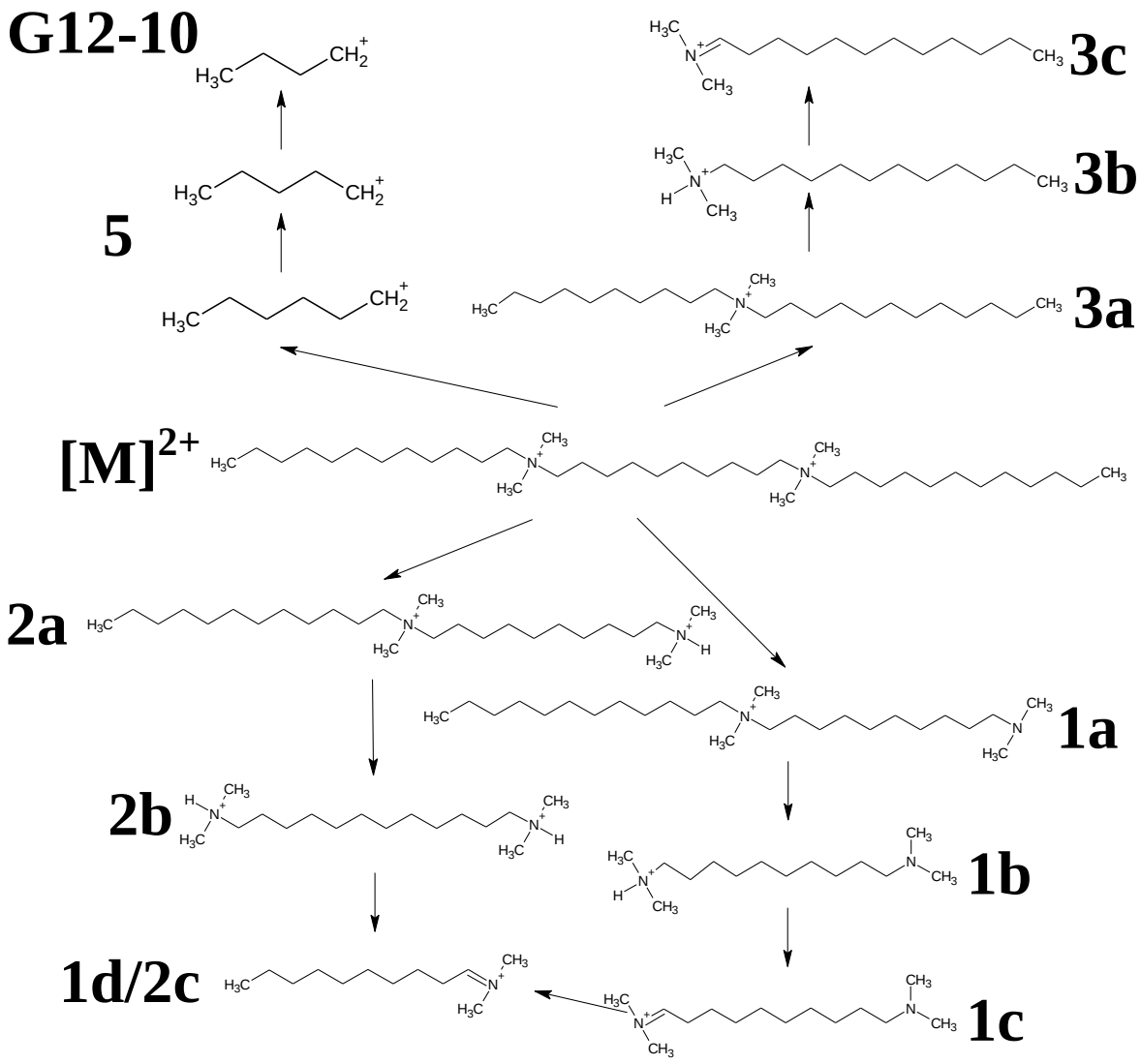

Appendix A Figure 6.1 Fragmentation pattern of G12-10

Appendix A Table 6 G12-10 gemini surfactant fragment ions (m/z)

$[M]^{2+}$	1a	1b	1c	1d	2a	2b	2c	3a	3b	3c	4	5
283.3	397.4	229.2	227.2	184.2	199.2	115.1	184.2	352.4	214.2	212.2		85.1 → 57.07

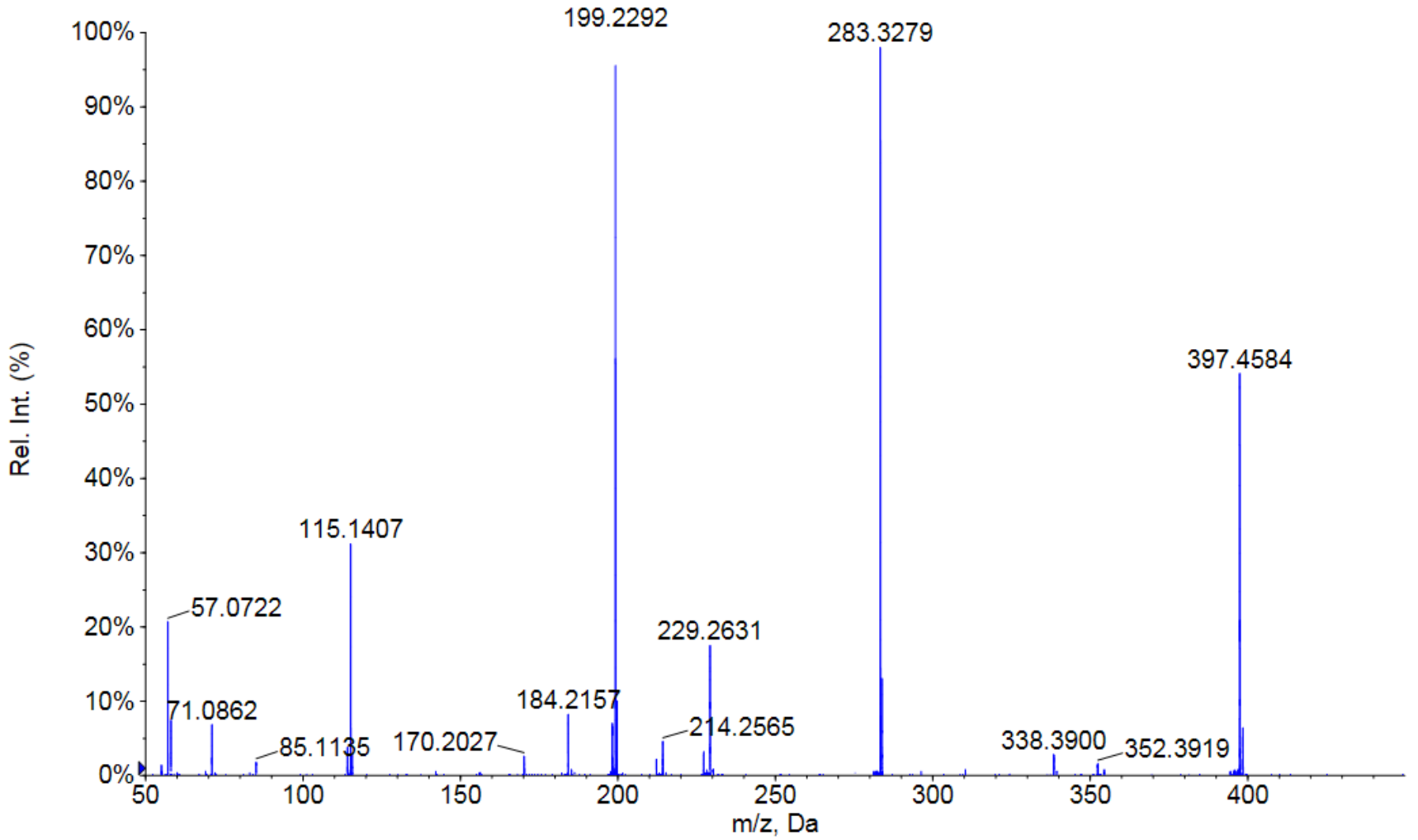

Appendix A Figure 6.2 A MS/MS spectra of G12-10 provided by an AB Sciex QSTAR XL qToF-MS

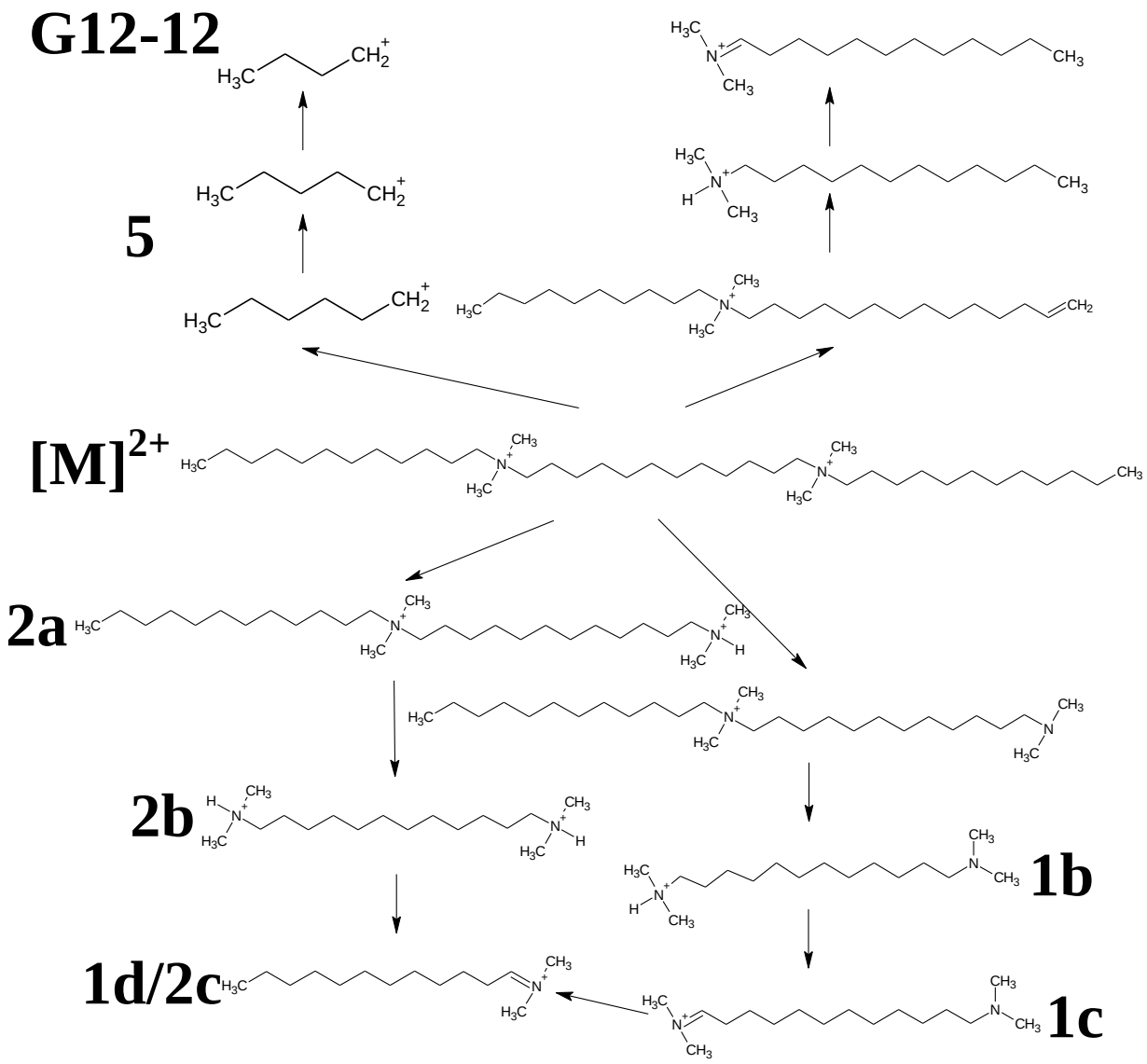

Appendix A Figure 7.1 Fragmentation pattern of G12-12

Appendix A Table 7 G12-12 gemini surfactant fragment ions (m/z)

$[M]^{2+}$	1a	1b	1c	1d	2a	2b	2c	3a	3b	3c	4	5
297.3	425.4	257.3	255.2	212.2	213.2	129.1	212.2	380.4	214.2	212.2		85.1 → 57.07

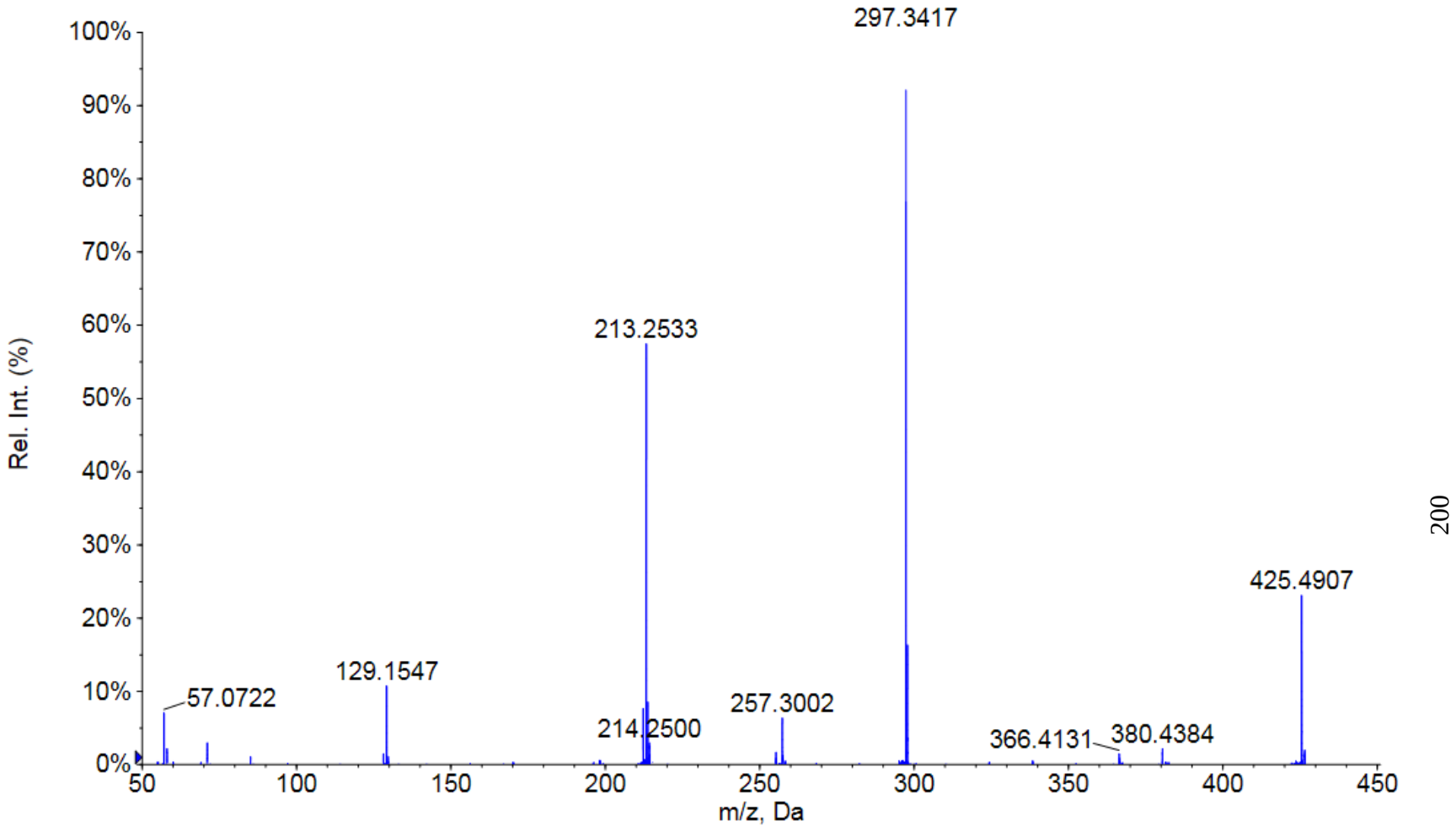

Appendix A Figure 7.2 A MS/MS spectra of G12-12 provided by an AB Sciex QSTAR XL qToF-MS

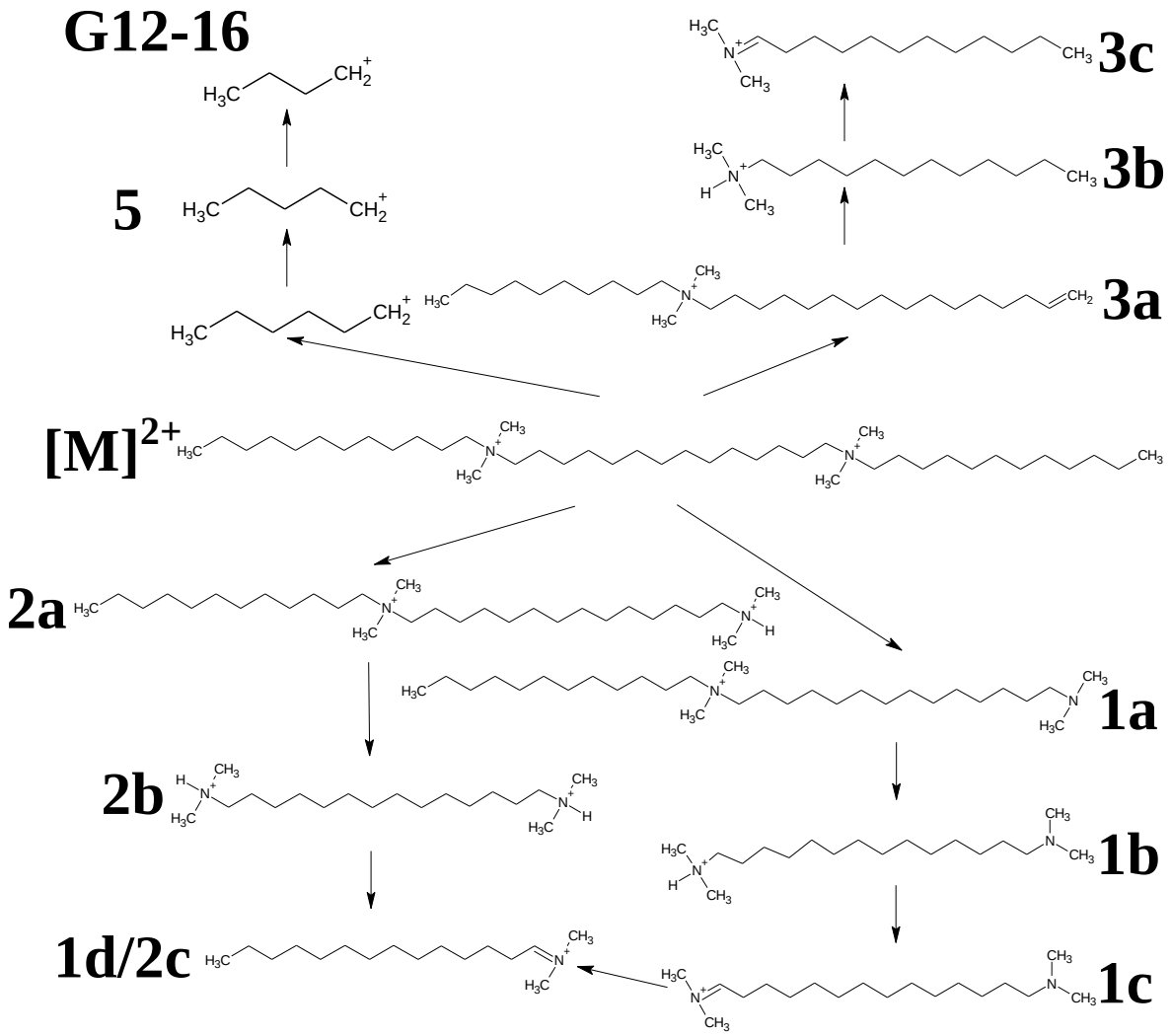

Appendix A Figure 8.1 Fragmentation pattern of G12-16

Appendix A Table 8 G12-16 gemini surfactant fragment ions (m/z)

$[M]^{2+}$	1a	1b	1c	1d	2a	2b	2c	3a	3b	3c	4	5
325.3	481.5	313.3	311.3	268.3	241.2	157.1	268.3	436.4	214.2	212.2		85.1 → 57.07

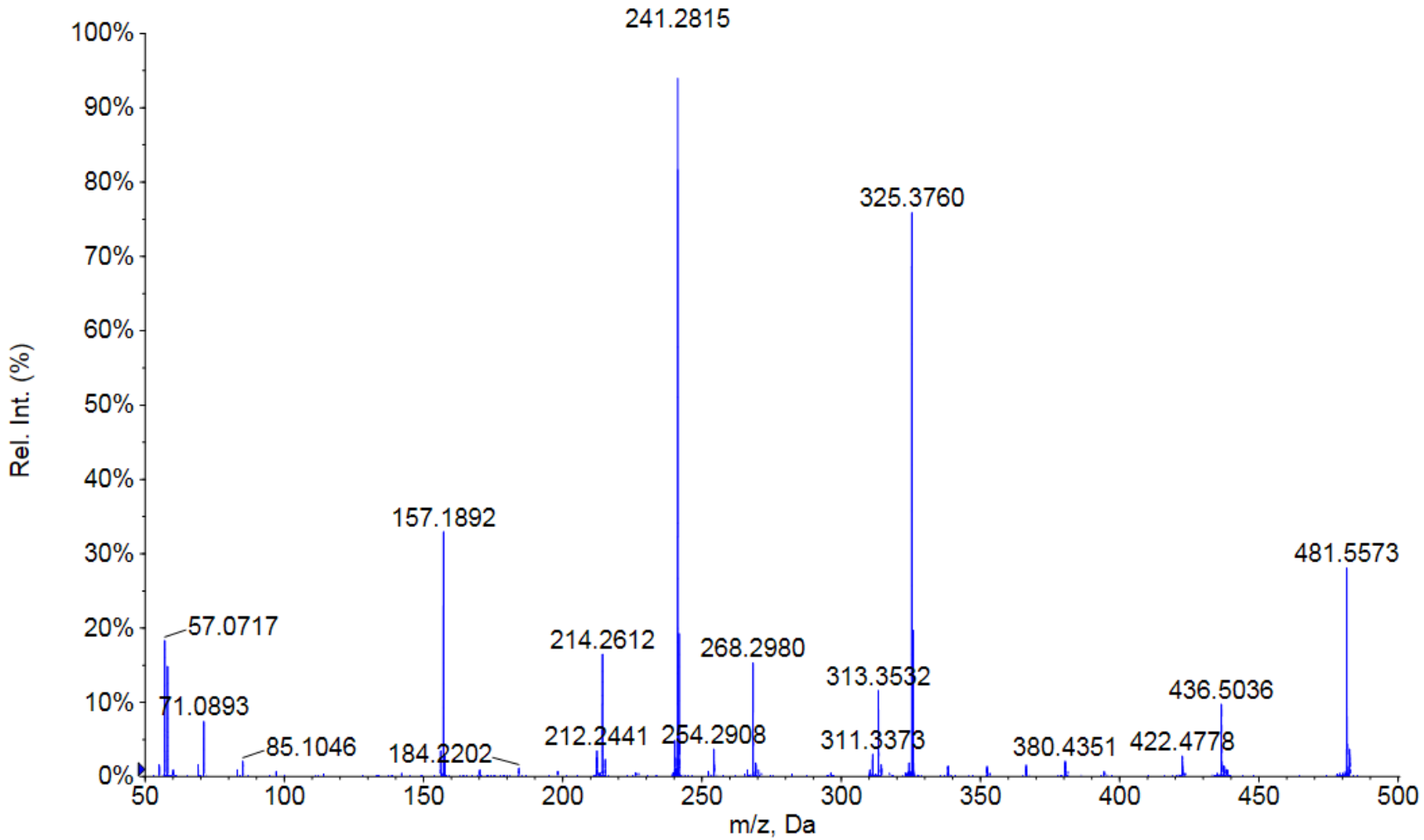

Appendix A Figure 8.2 A MS/MS spectra of G12-16 provided by an AB Sciex QSTAR XL qToF-MS

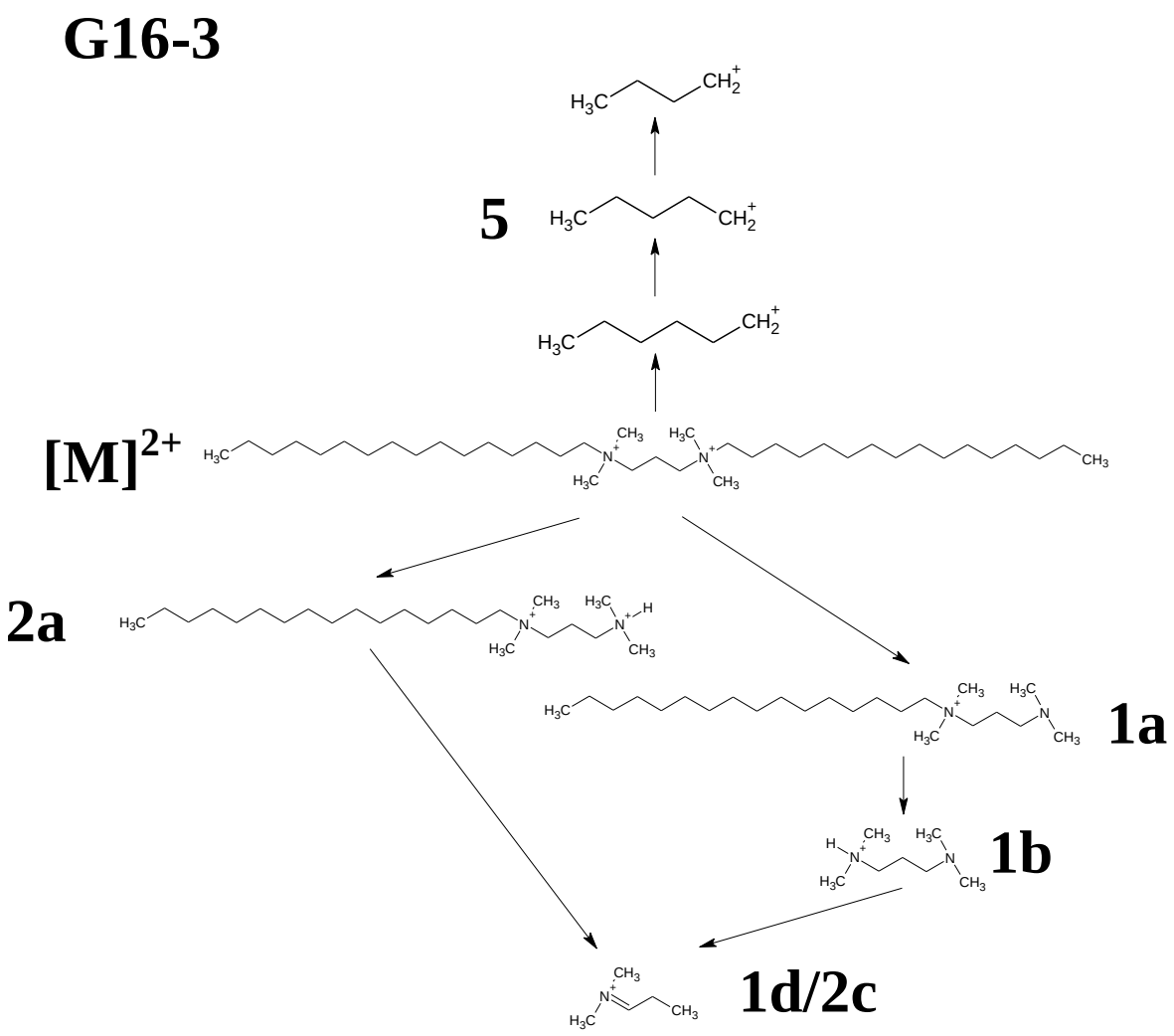

Appendix A Figure 9.1 Fragmentation pattern of G16-3

Appendix A Table 9 G16-3 gemini surfactant fragment ions (m/z)

$[M]^{2+}$	1a	1b	1c	1d	2a	2b	2c	3a	3b	3c	4	5
290.3	355.4	131.1		86.1	178.2		86.1					85.1 → 57.07

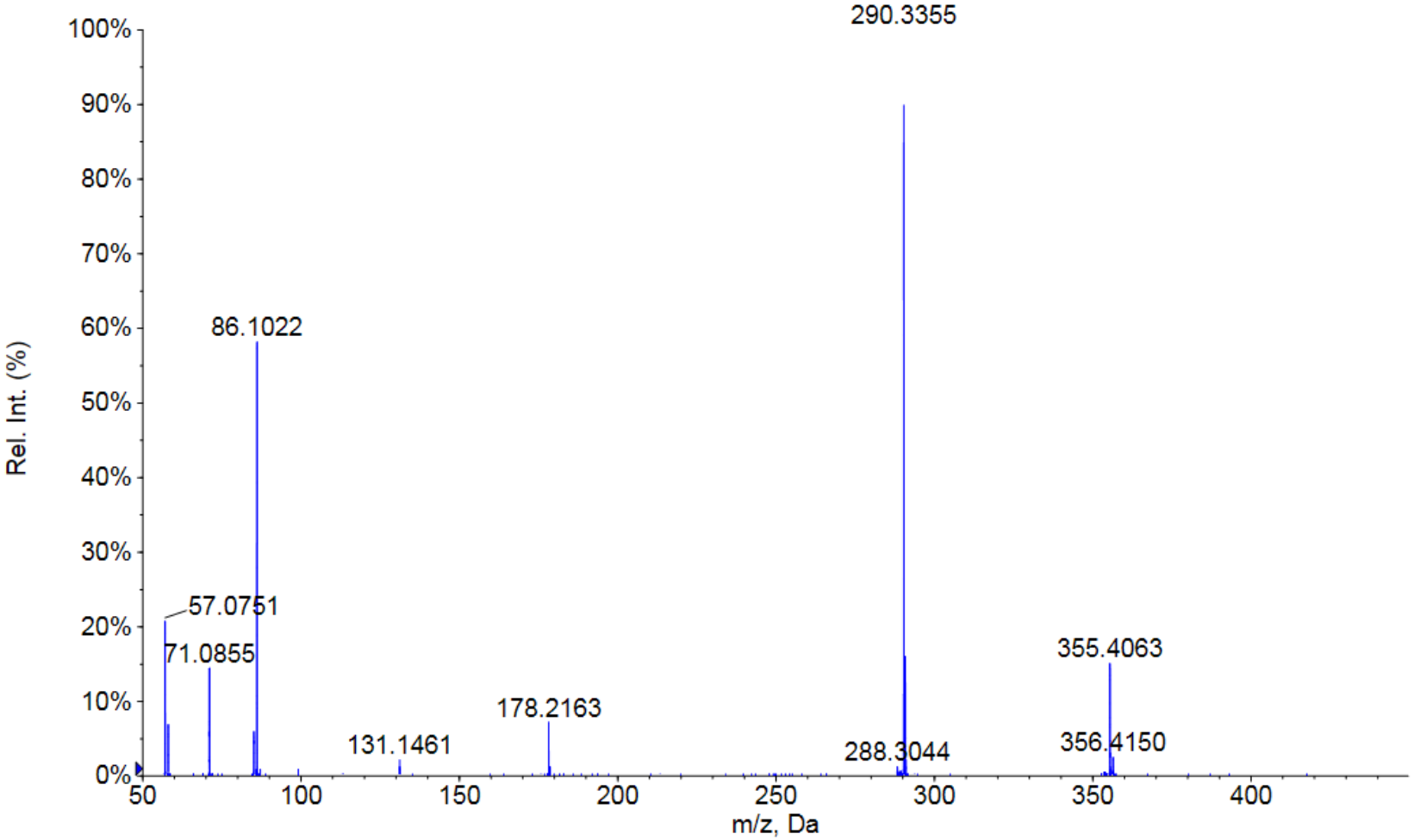

Appendix A Figure 9.2 A MS/MS spectra of G16-3 provided by an AB Sciex QSTAR XL qToF-MS

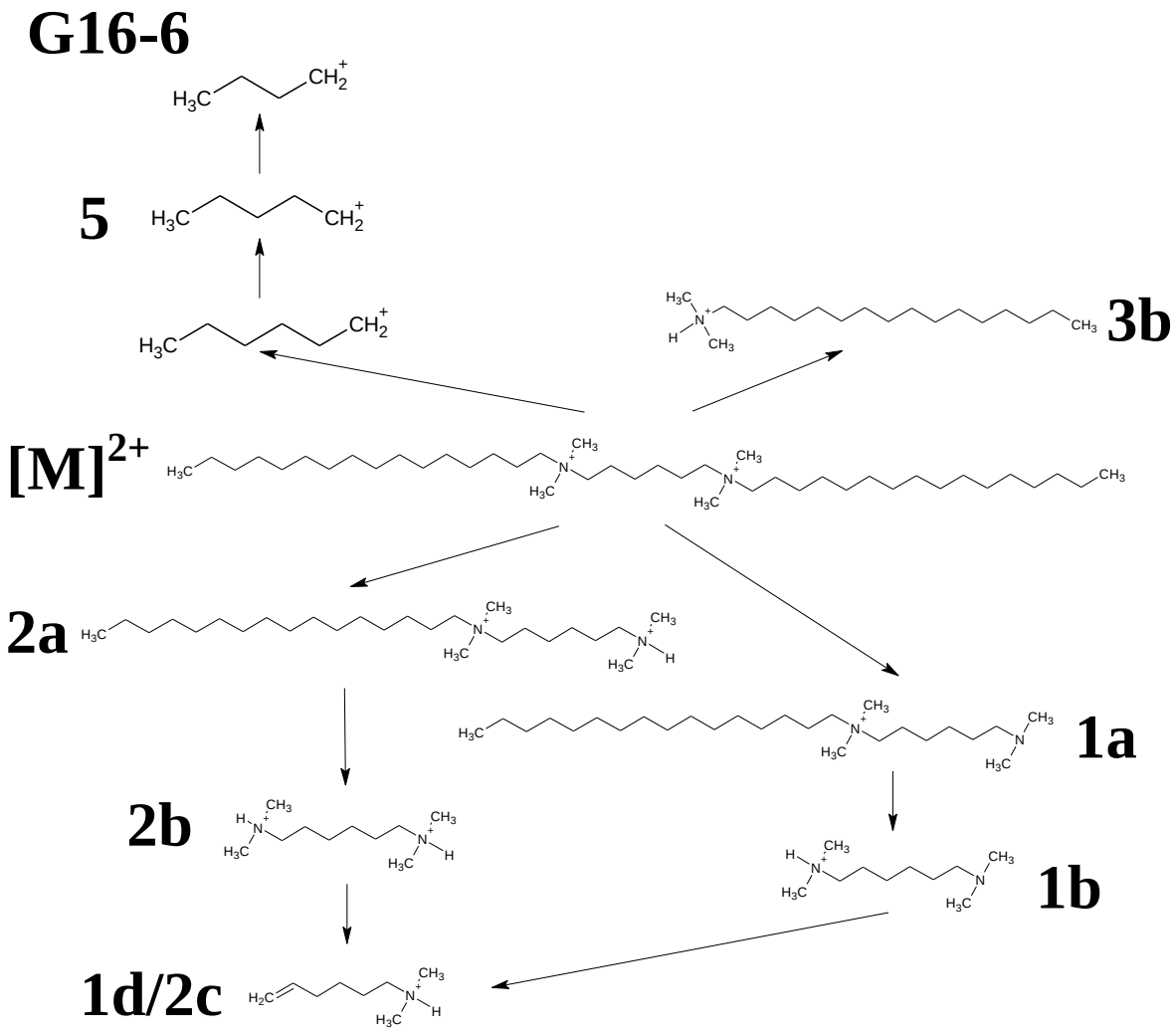

Appendix A Figure 10.1 Fragmentation pattern of G16-6

Appendix A Table 10 G16-6 gemini surfactant fragment ions (m/z)

$[M]^{2+}$	1a	1b	1c	1d	2a	2b	2c	3a	3b	3c	4	5
311.41	379.34	173.42		128.19	199.21	87.03	128.19		270.33			85.1 → 57.07

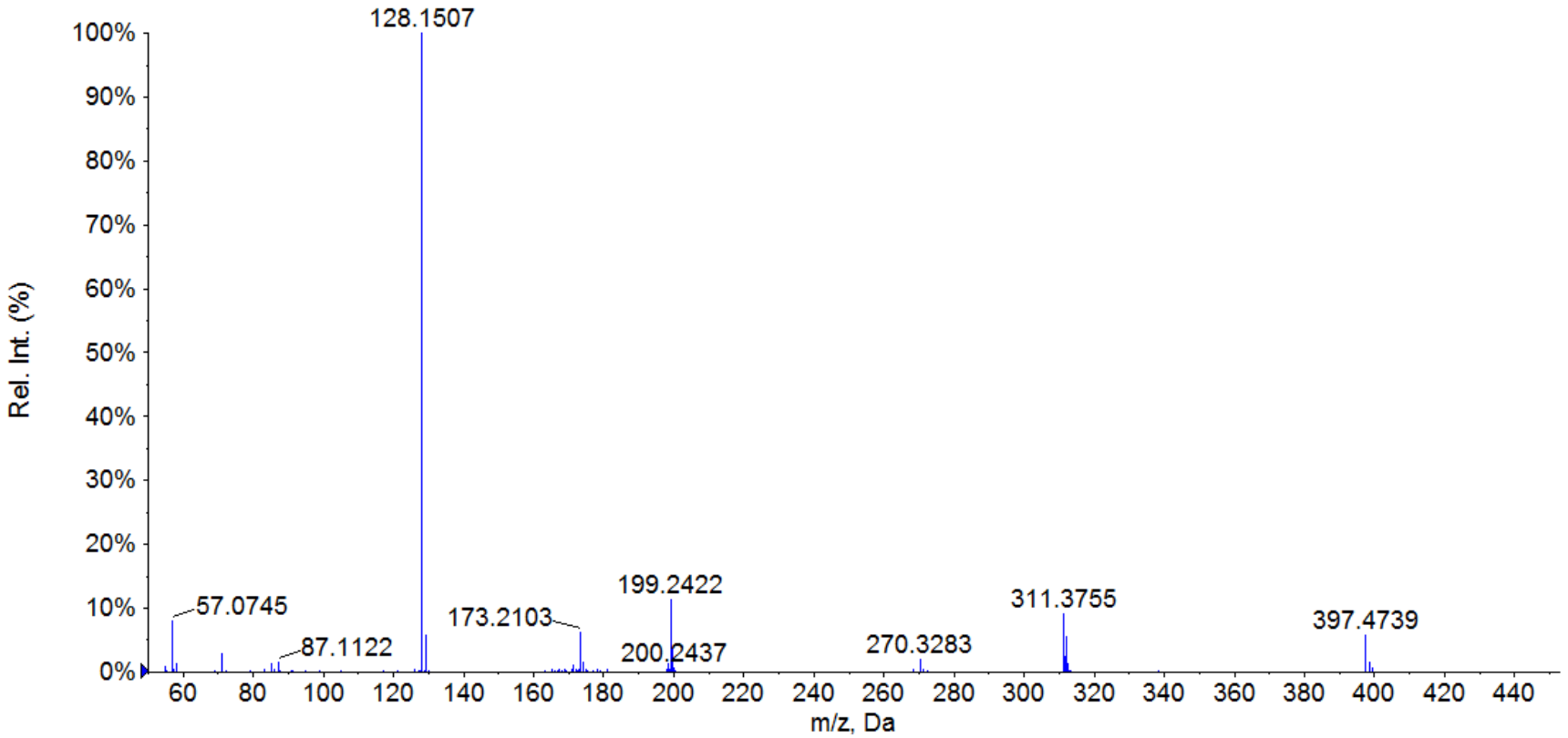

Appendix A Figure 10.2 A MS/MS spectra of G16-6 provided by an AB Sciex QSTAR XL qToF-MS

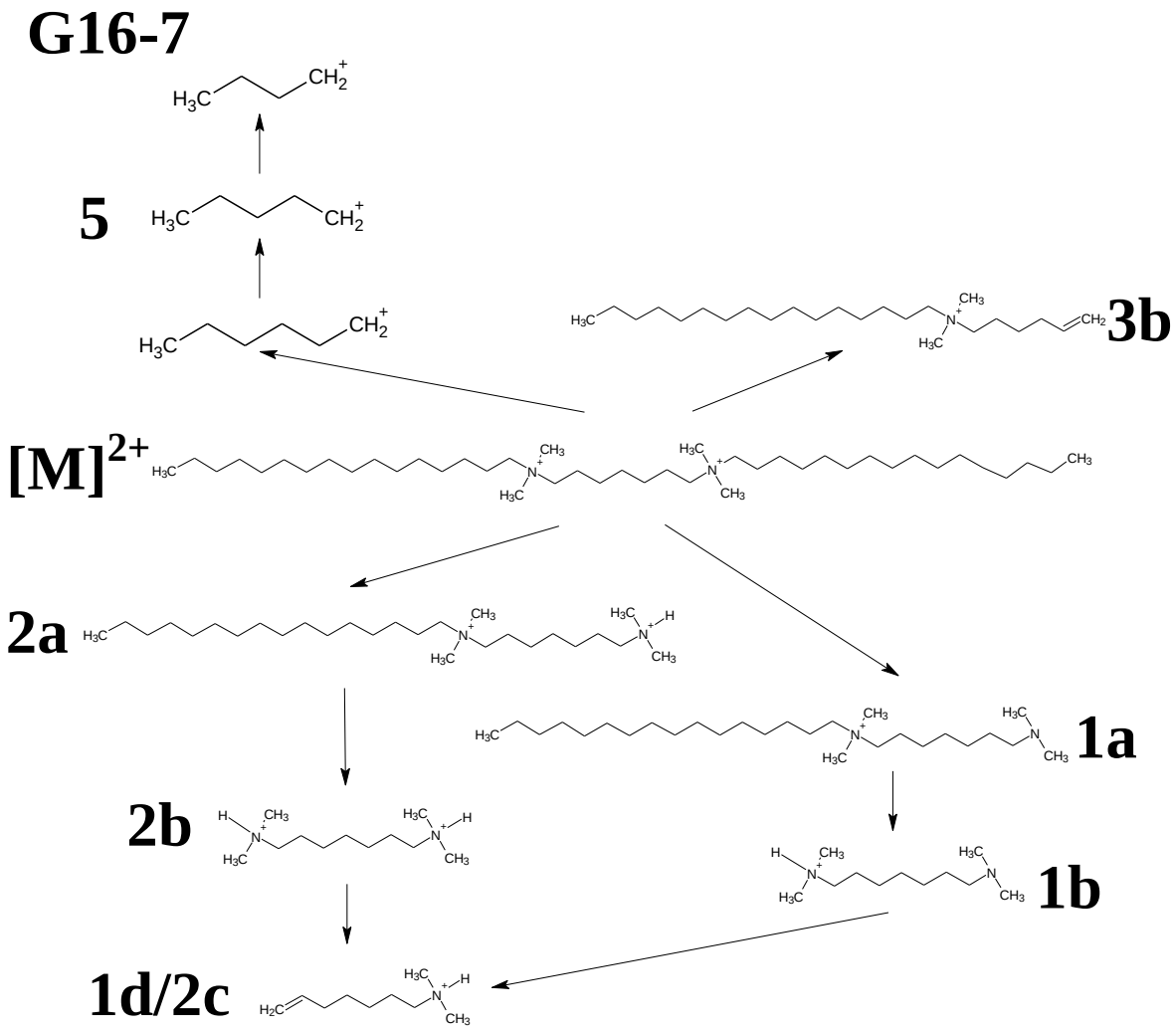

Appendix A Figure 11.1 Fragmentation pattern of G16-7

Appendix A Table 11 G16-7 gemini surfactant fragment ions (m/z)

$[M]^{2+}$	1a	1b	1c	1d	2a	2b	2c	3a	3b	3c	4	5
318.39	411.34	187.36		144.57	206.25	94.03	144.57	352.43				85.1 → 57.07

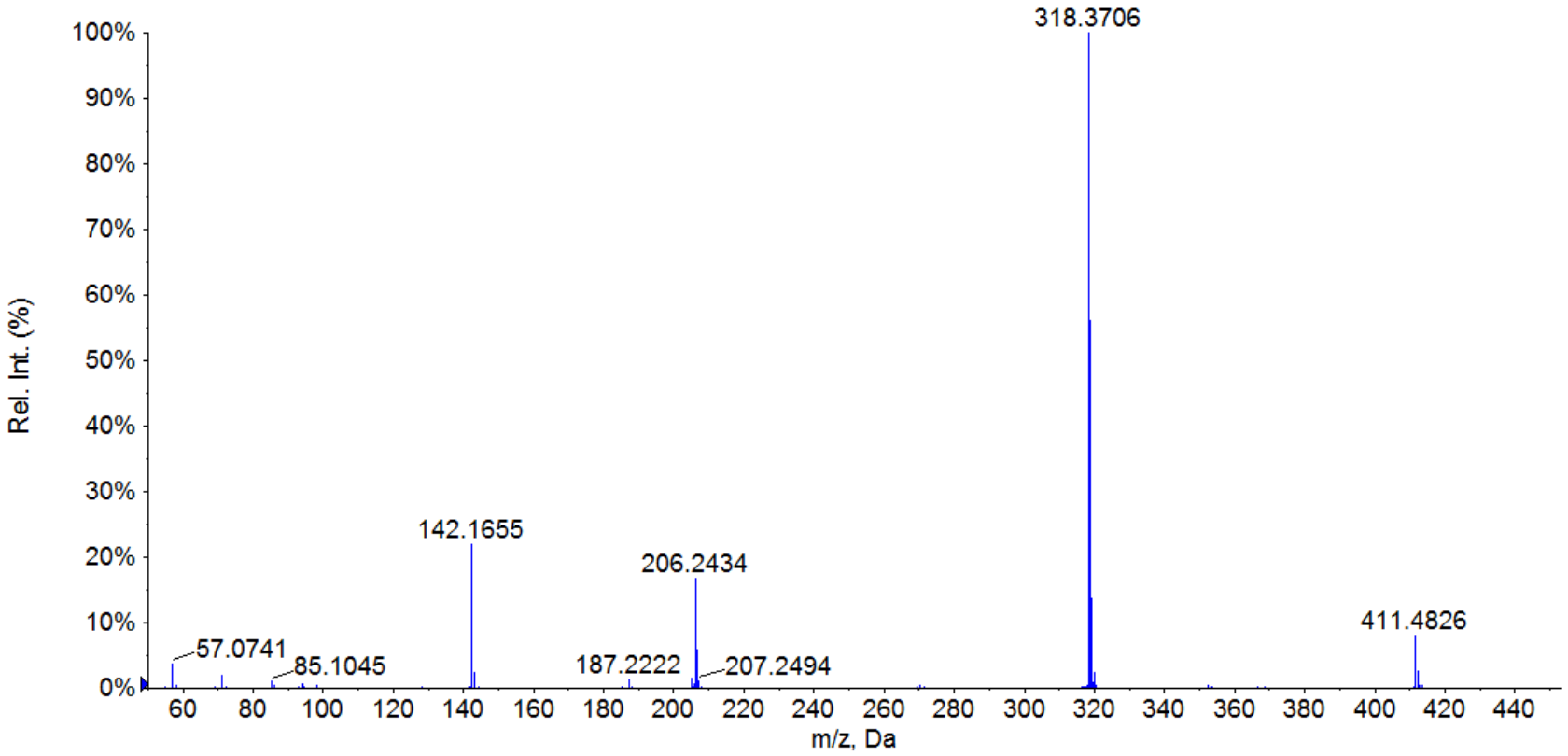

Appendix A Figure 11.2 A MS/MS spectra of G16-7 provided by an AB Sciex QSTAR XL qToF-MS

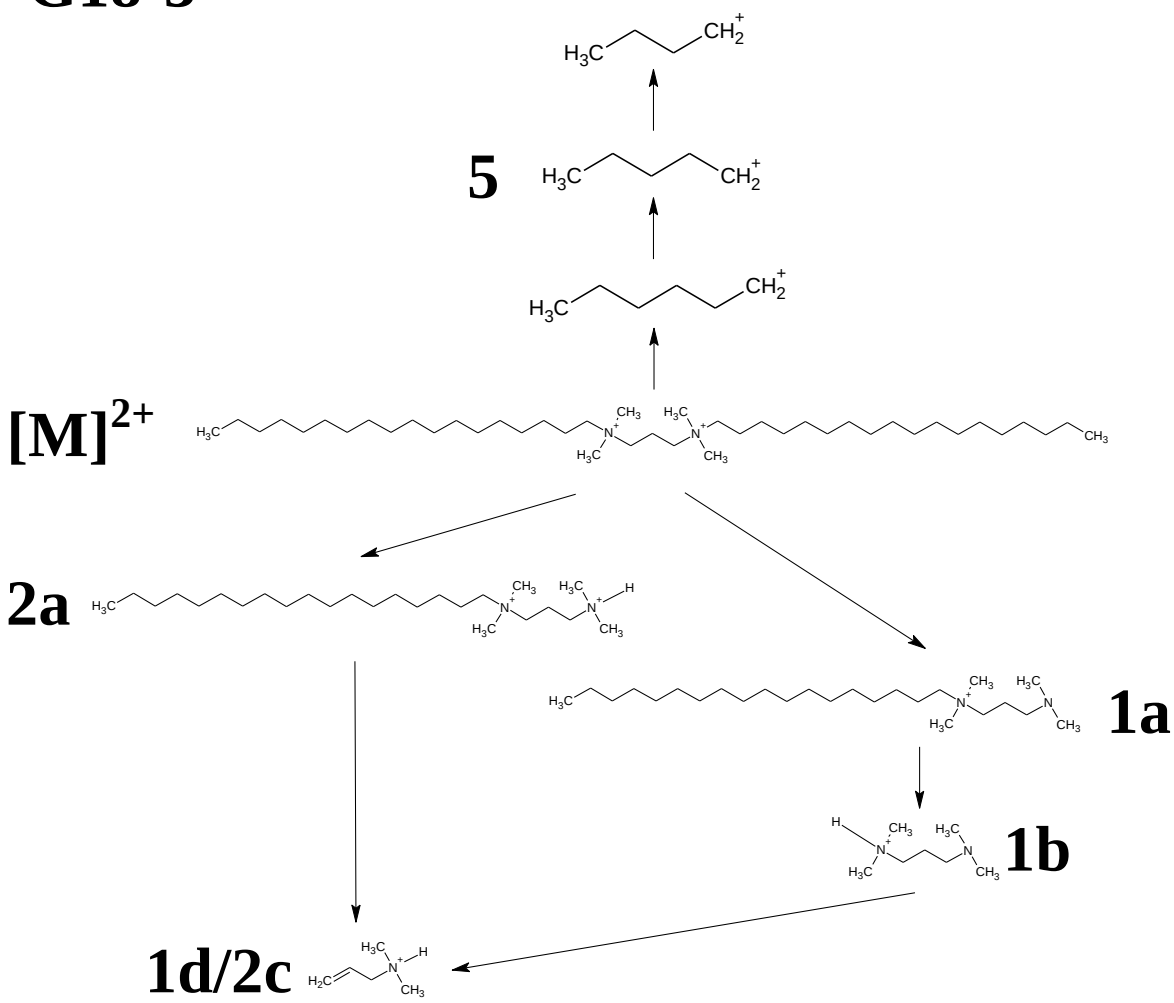

Appendix A Figure 12.1 Fragmentation pattern of G18-3

Appendix A Table 12 G18-3 gemini surfactant fragment ions (m/z)

$[M]^{2+}$	1a	1b	1c	1d	2a	2b	2c	3a	3b	3c	4	5
318.38	383.45	131.16		86.1	192.23		86.1					85.1 → 57.07

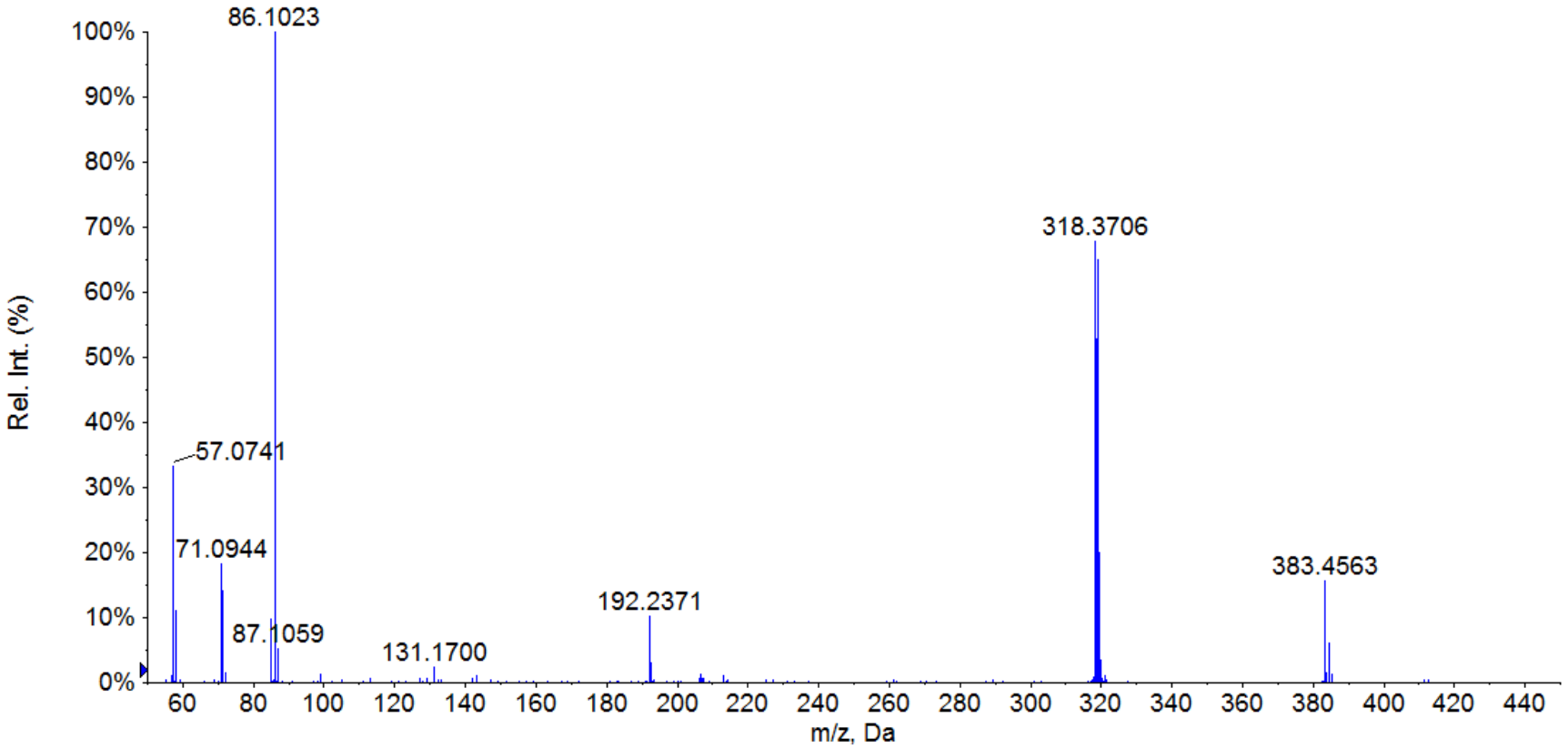

Appendix A Figure 12.2 A MS/MS spectra of G18-3 provided by an AB Sciex QSTAR XL qToF-MS

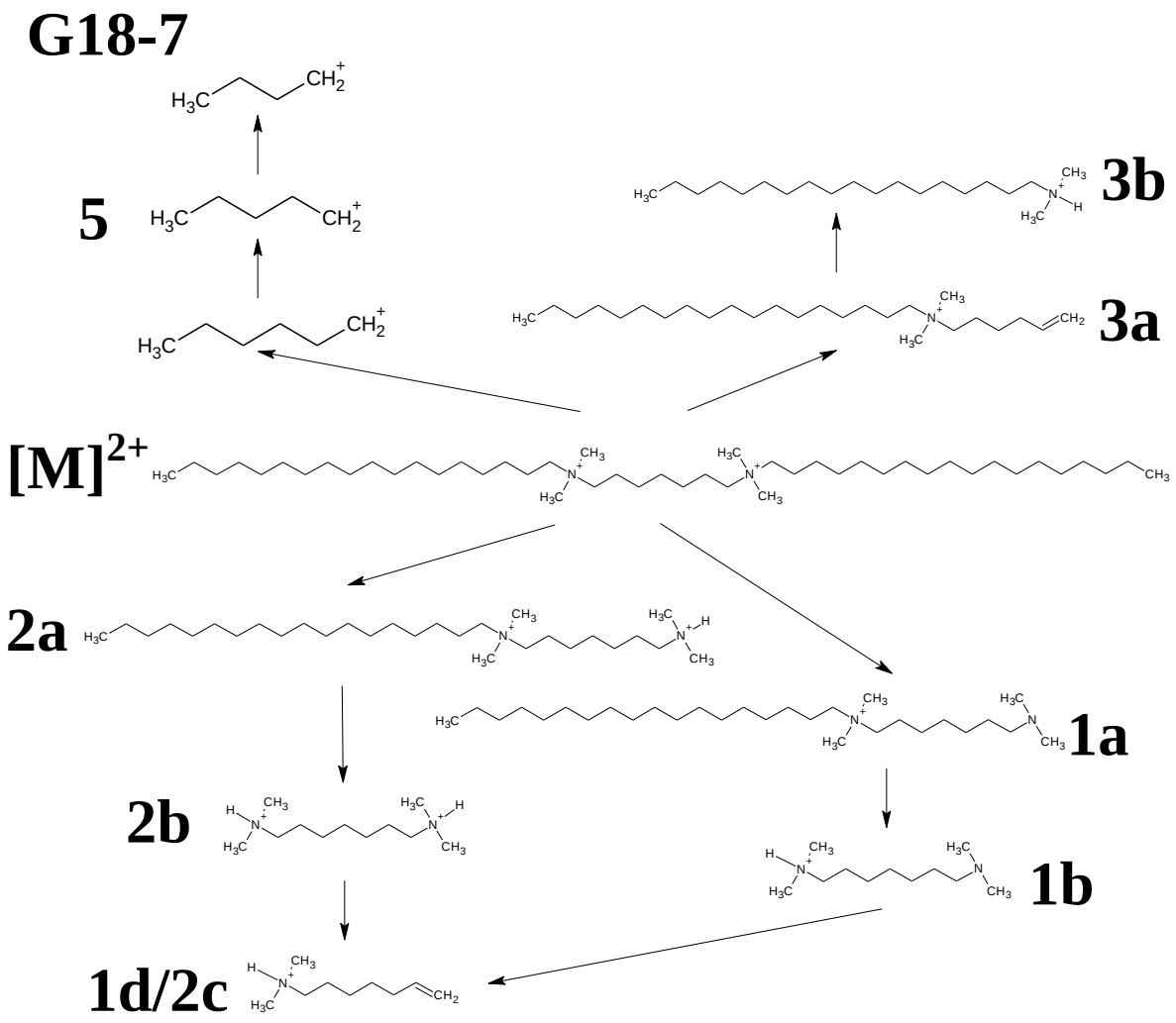

Appendix A Figure 13.1 Fragmentation pattern of G18-7

Appendix A Table 13 G18-7 gemini surfactant fragment ions (m/z)

$[M]^{2+}$	1a	1b	1c	1d	2a	2b	2c	3a	3b	3c	4	5
346.41	439.51	187.22		142.17	220.26	94.12	142.17	380.44	297.97			85.1 → 57.07

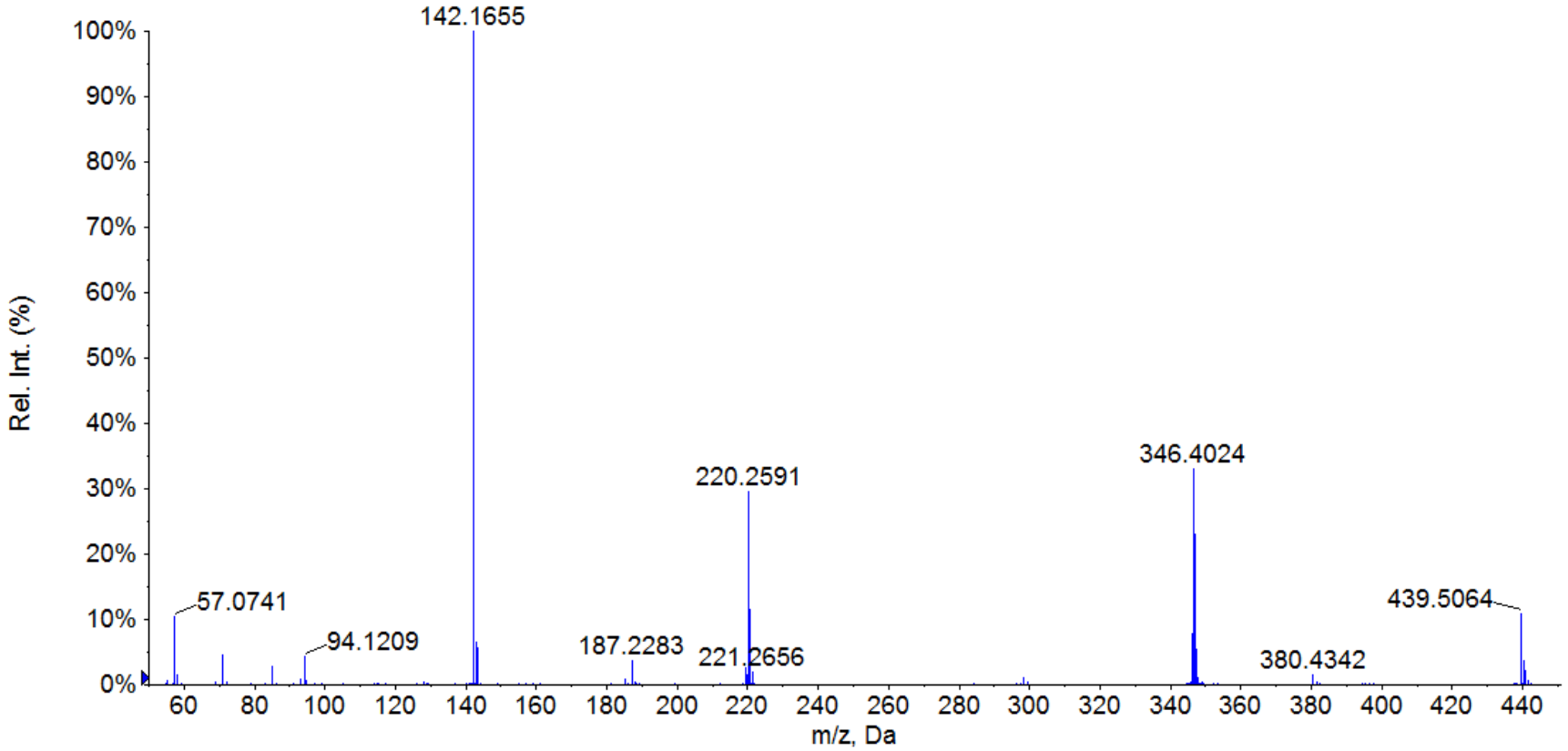

Appendix A Figure 13.2 A MS/MS spectra of G18-7 provided by an AB Sciex QSTAR XL qToF-MS

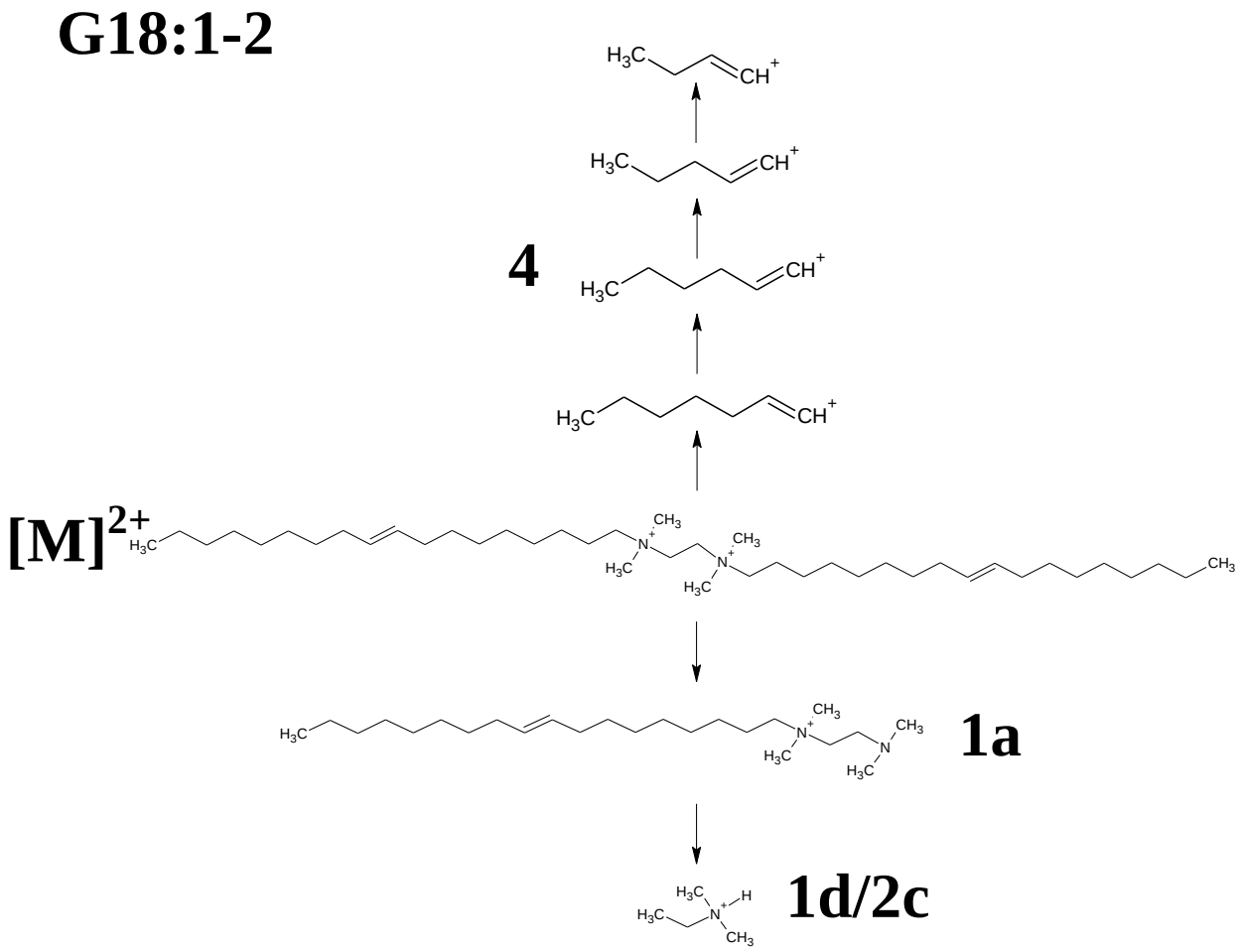

Appendix A Figure 14.1 Fragmentation pattern of G18:1-2

Appendix A Table 14 G18:1-2 gemini surfactant fragment ions (m/z)

$[M]^{2+}$	1a	1b	1c	1d	2a	2b	2c	3a	3b	3c	4	5
309.3	367.4			72.0			72.0				97.1→55.06	

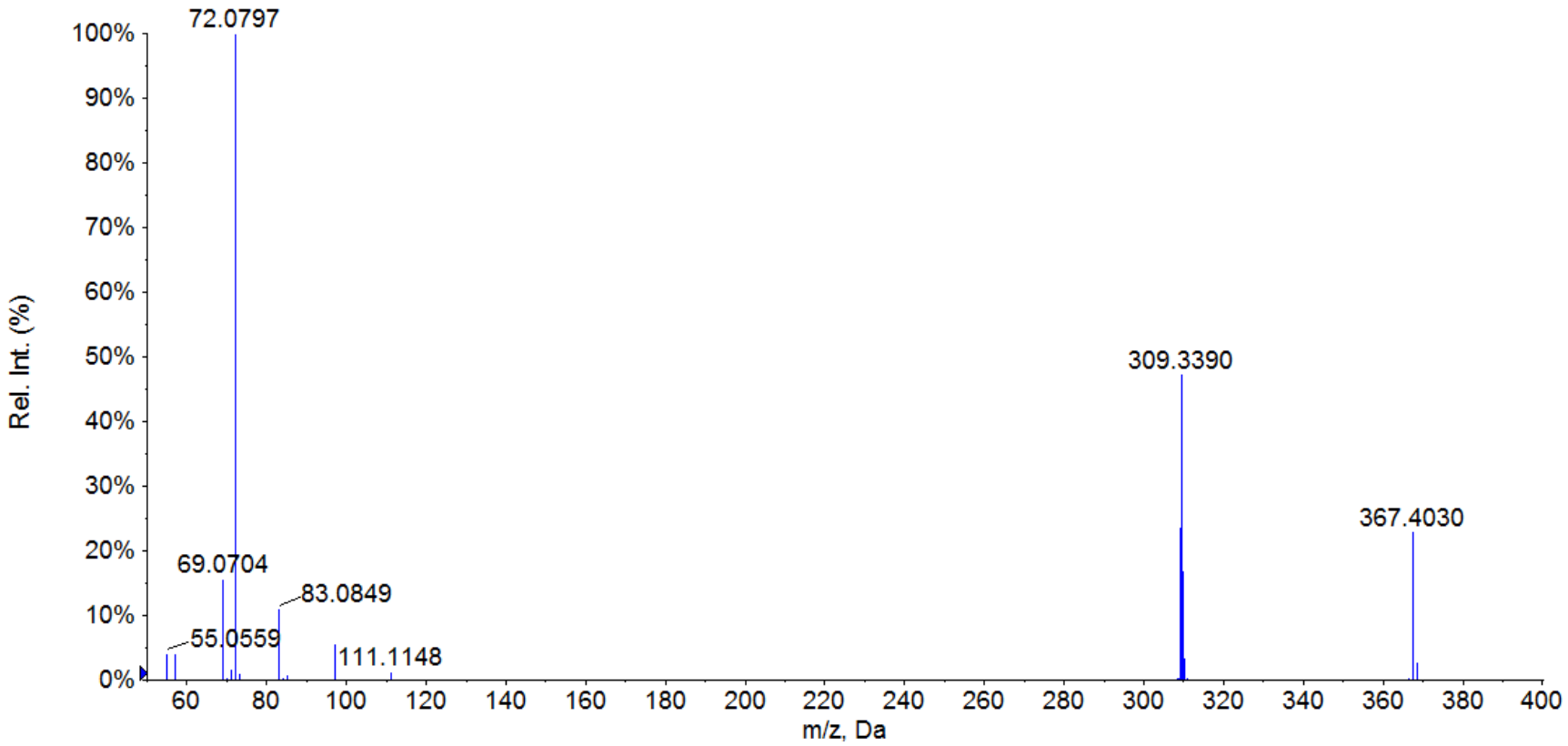

Appendix A Figure 14.2 A MS/MS spectra of G18:1-2 provided by an AB Sciex QSTAR XL qToF-MS

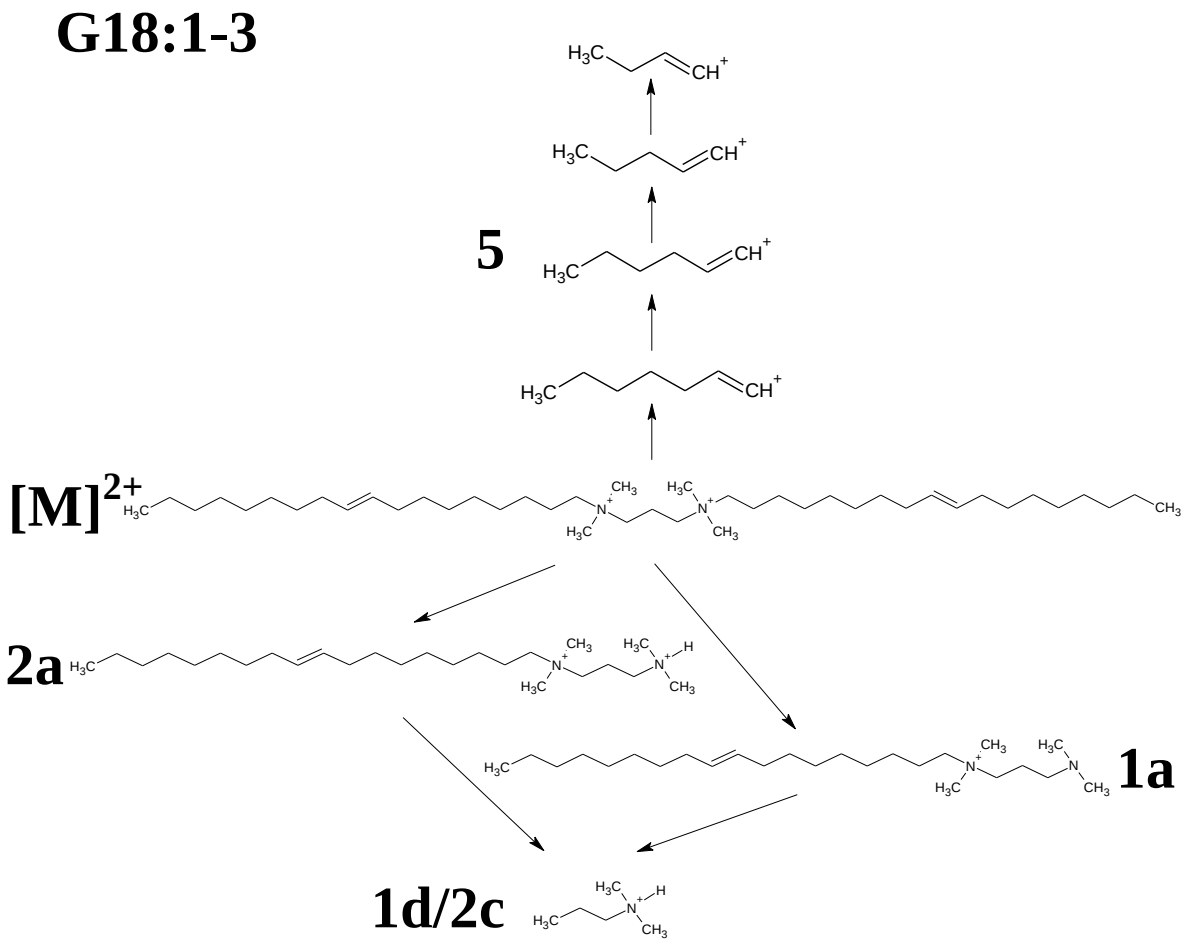

Appendix A Figure 15.1 Fragmentation pattern of G18:1-3

Appendix A Table 15 G18:1-3 gemini surfactant fragment ions (m/z)

$[M]^{2+}$	1a	1b	1c	1d	2a	2b	2c	3a	3b	3c	4	5
316.35	381.43			86.1	191.35		86.1				97.1→55.06	

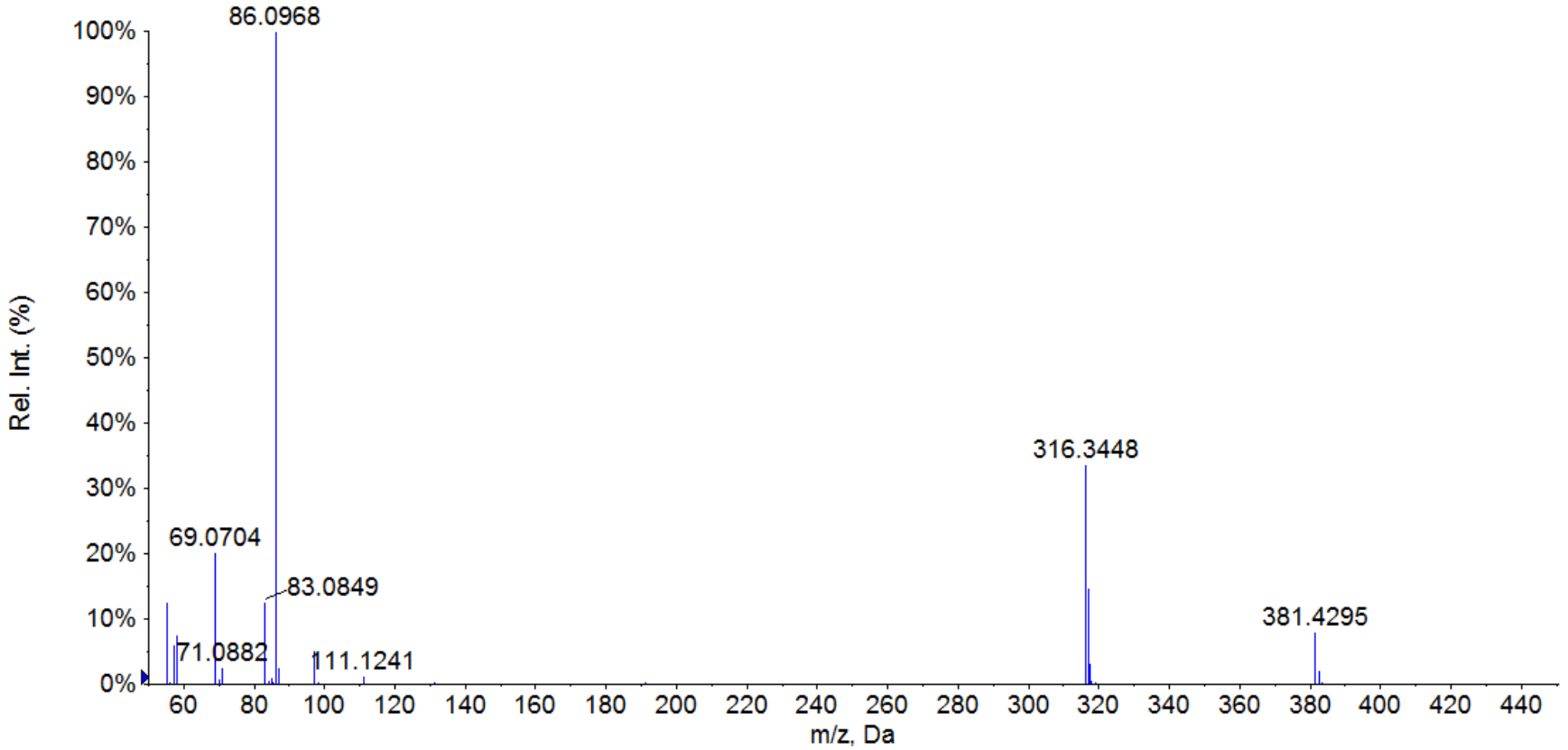

Appendix A Figure 15.2 A MS/MS spectra of G18:1-3 provided by an AB Sciex QSTAR XL qToF-MS

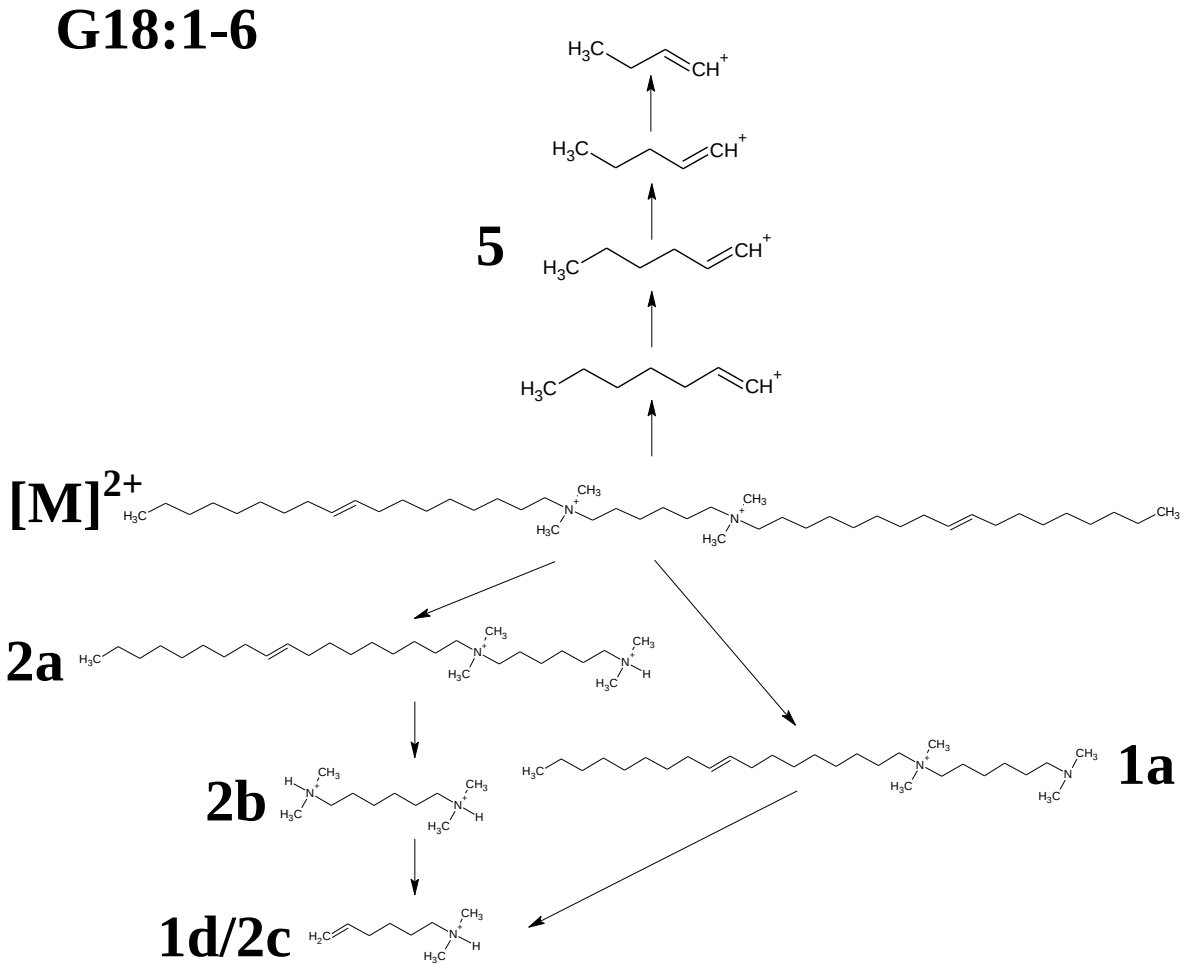

Appendix A Figure 16.1 Fragmentation pattern of G18:1-6

Appendix A Table 16 G18:1-6 gemini surfactant fragment ions (m/z)

$[M]^{2+}$	1a	1b	1c	1d	2a	2b	2c	3a	3b	3c	4	5
337.38	423.48			128.15	212.25	211.24	128.15				97.1→55.06	

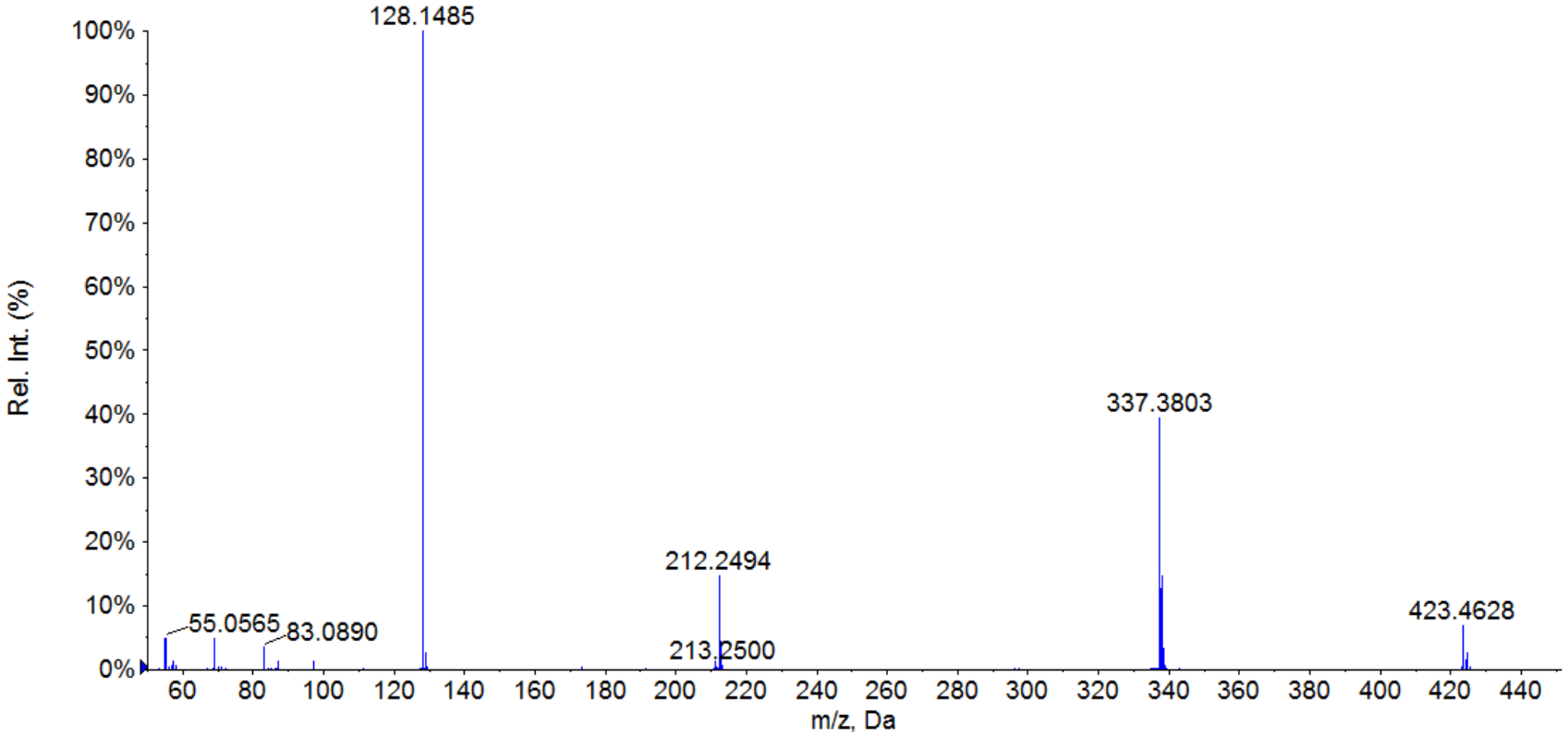

Appendix A Figure 16.2 A MS/MS spectra of G18:1-6 provided by an AB Sciex QSTAR XL qToF-MS

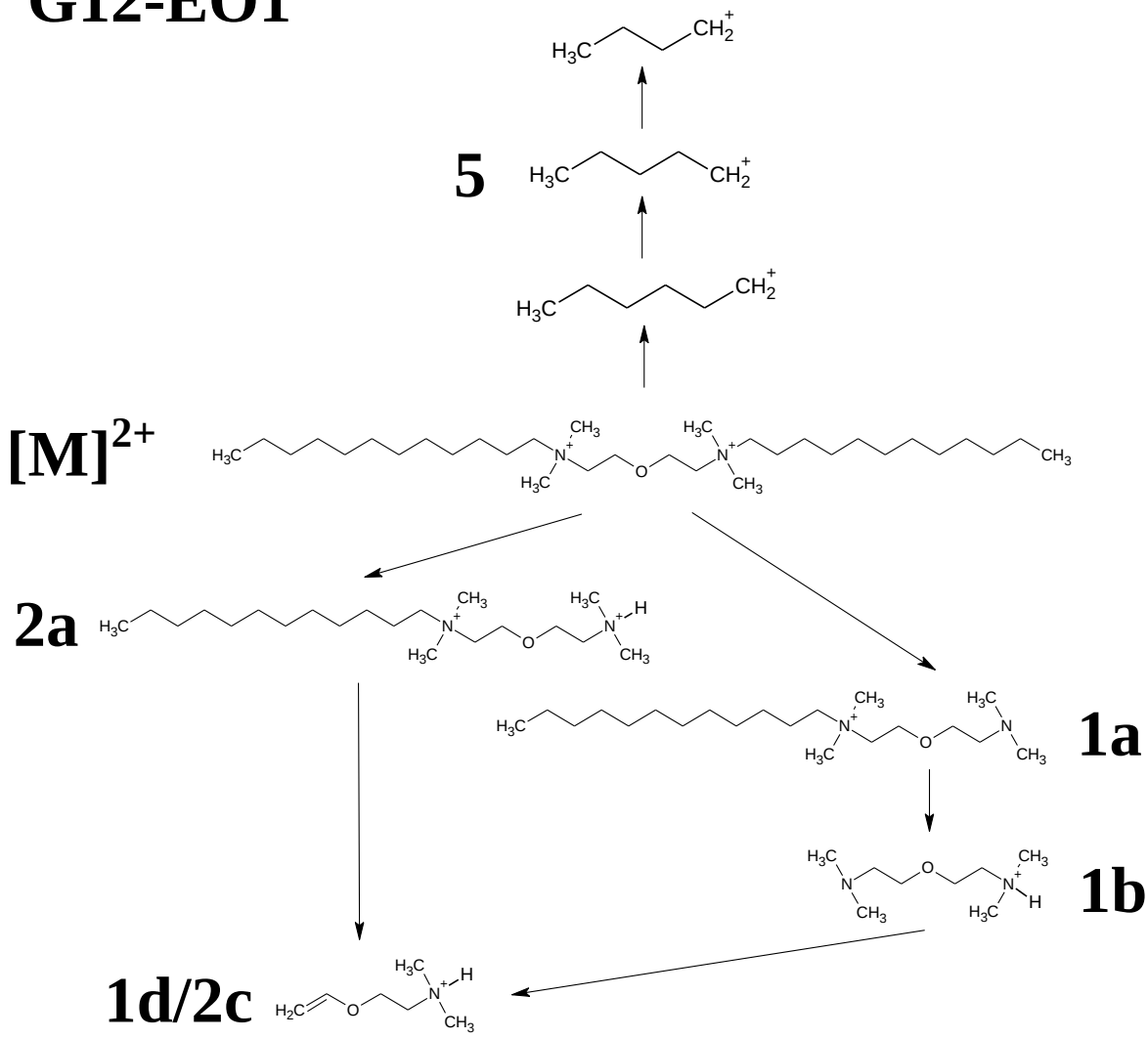

Appendix A Figure 17.1 Fragmentation pattern of G12-EO1

Appendix A Table 17 G12-EO1 gemini surfactant fragment ions (m/z)

$[M]^{2+}$	1a	1b	1c	1d	2a	2b	2c	3a	3b	3c	4	5
249.28	329.37	161.21		116.11	165.19		116.11					85.1 → 57.07

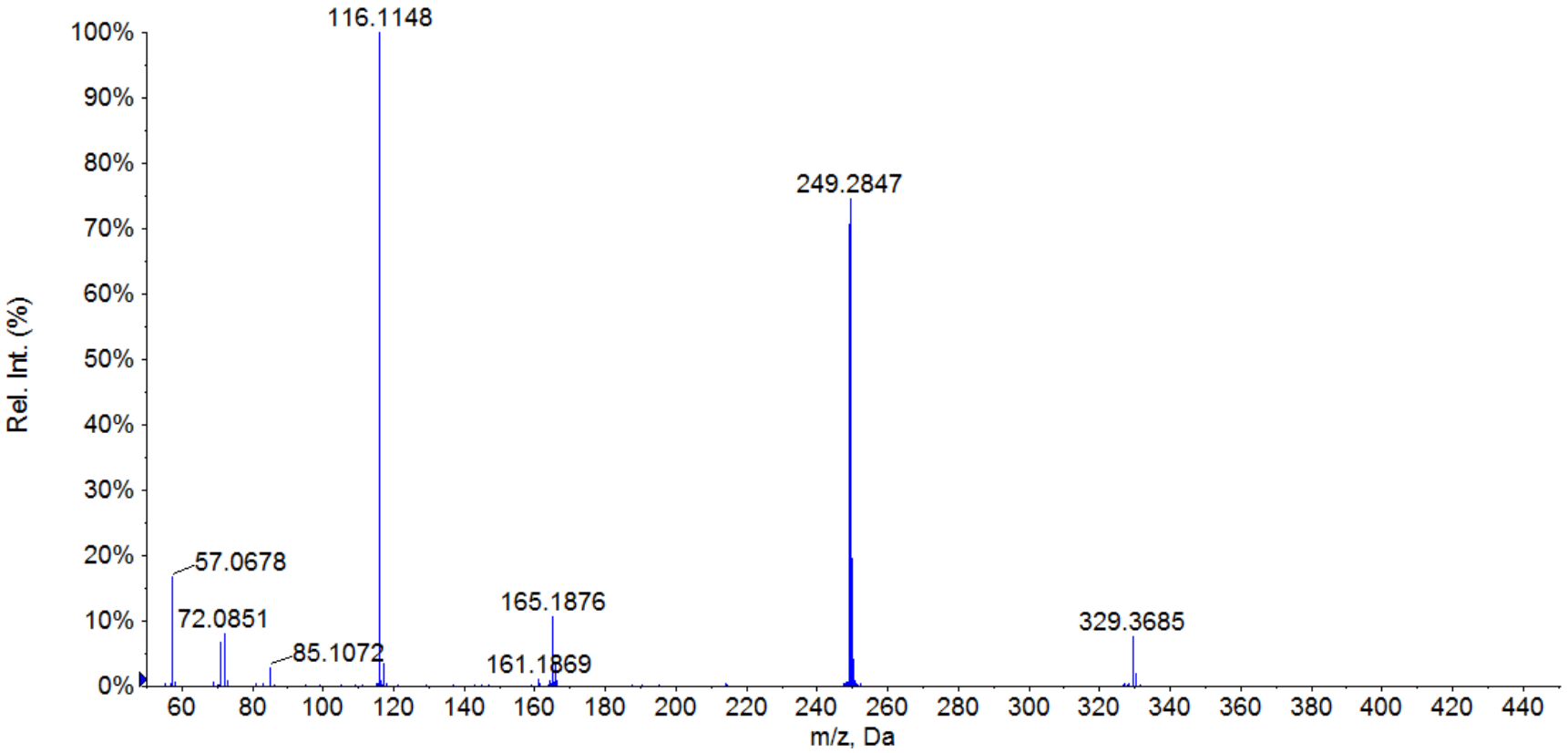

Appendix A Figure 17.2 A MS/MS spectra of G12-EO1 provided by an AB Sciex QSTAR XL qToF-MS

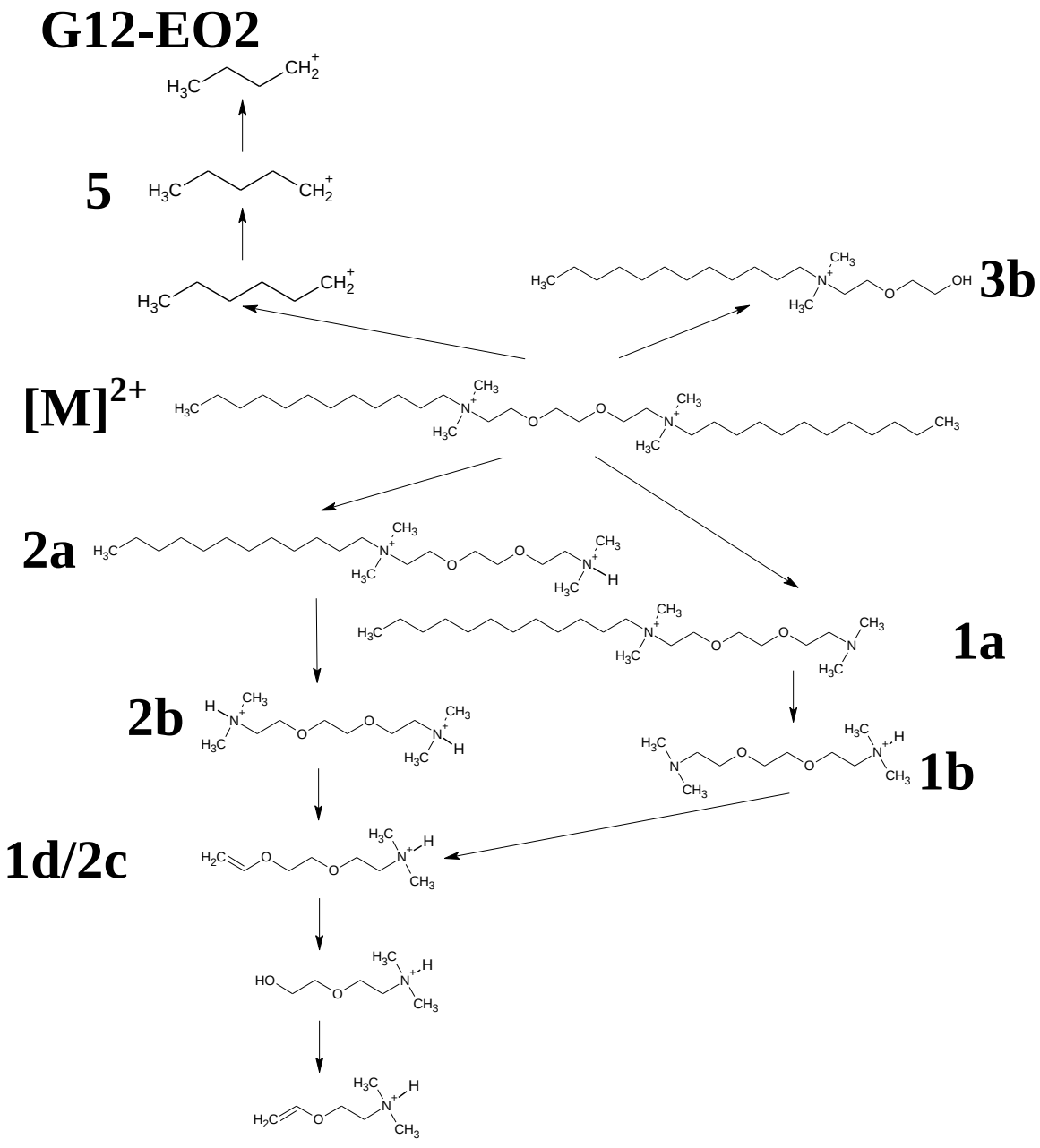

Appendix A Figure 18.1 Fragmentation pattern of G12-EO2

Appendix A Table 18 G12-EO2 gemini surfactant fragment ions (m/z)

$[M]^{2+}$	1a	1b	1c	1d	2a	2b	2c	3a	3b	3c	4	5
271.3	373.39	205.2		160.14	187.2	103.11	160.14	314.32				85.1 → 57.07

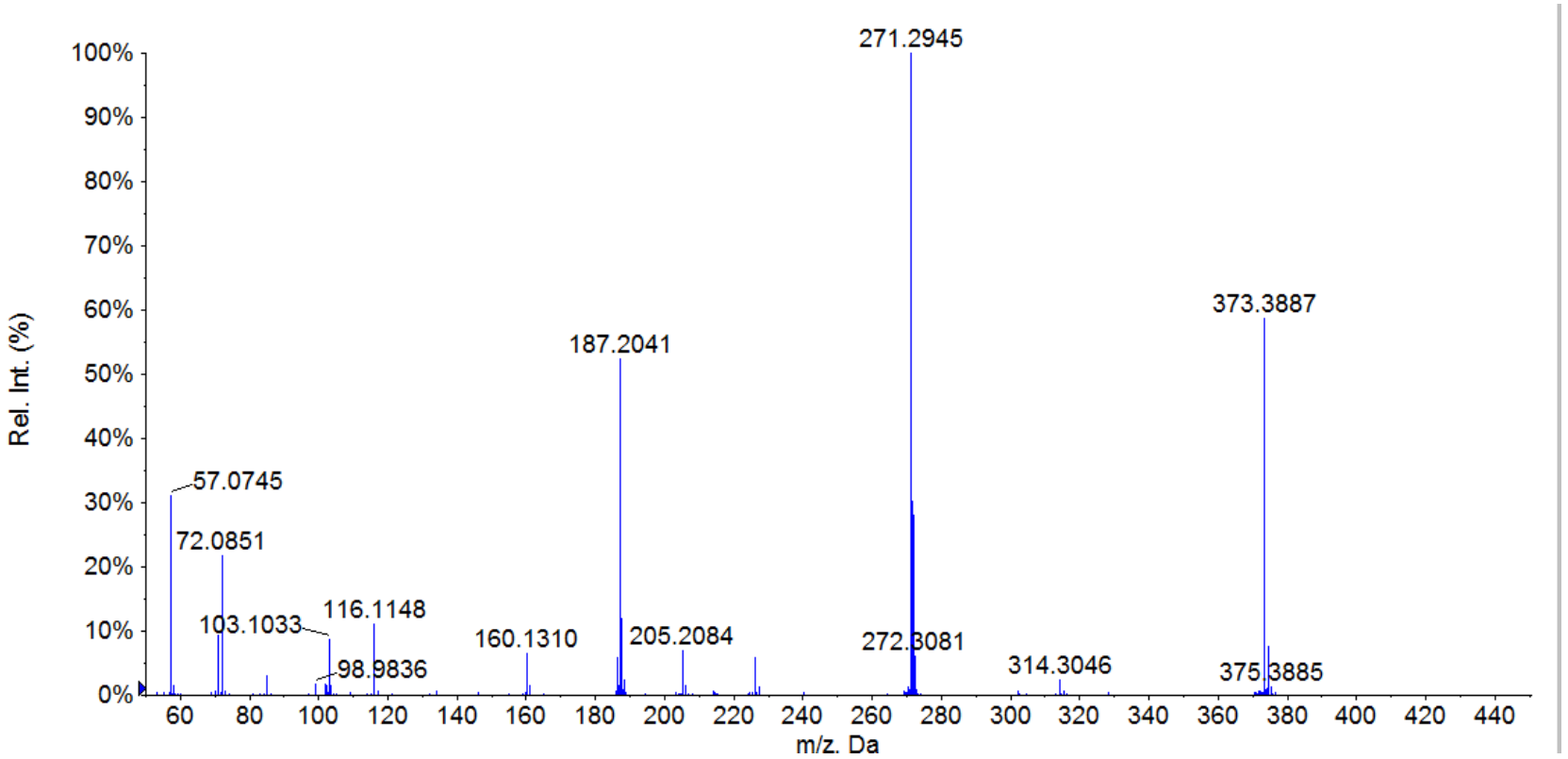

Appendix A Figure 18.2 A MS/MS spectra of G12-EO2 provided by an AB Sciex QSTAR XL qToF-MS

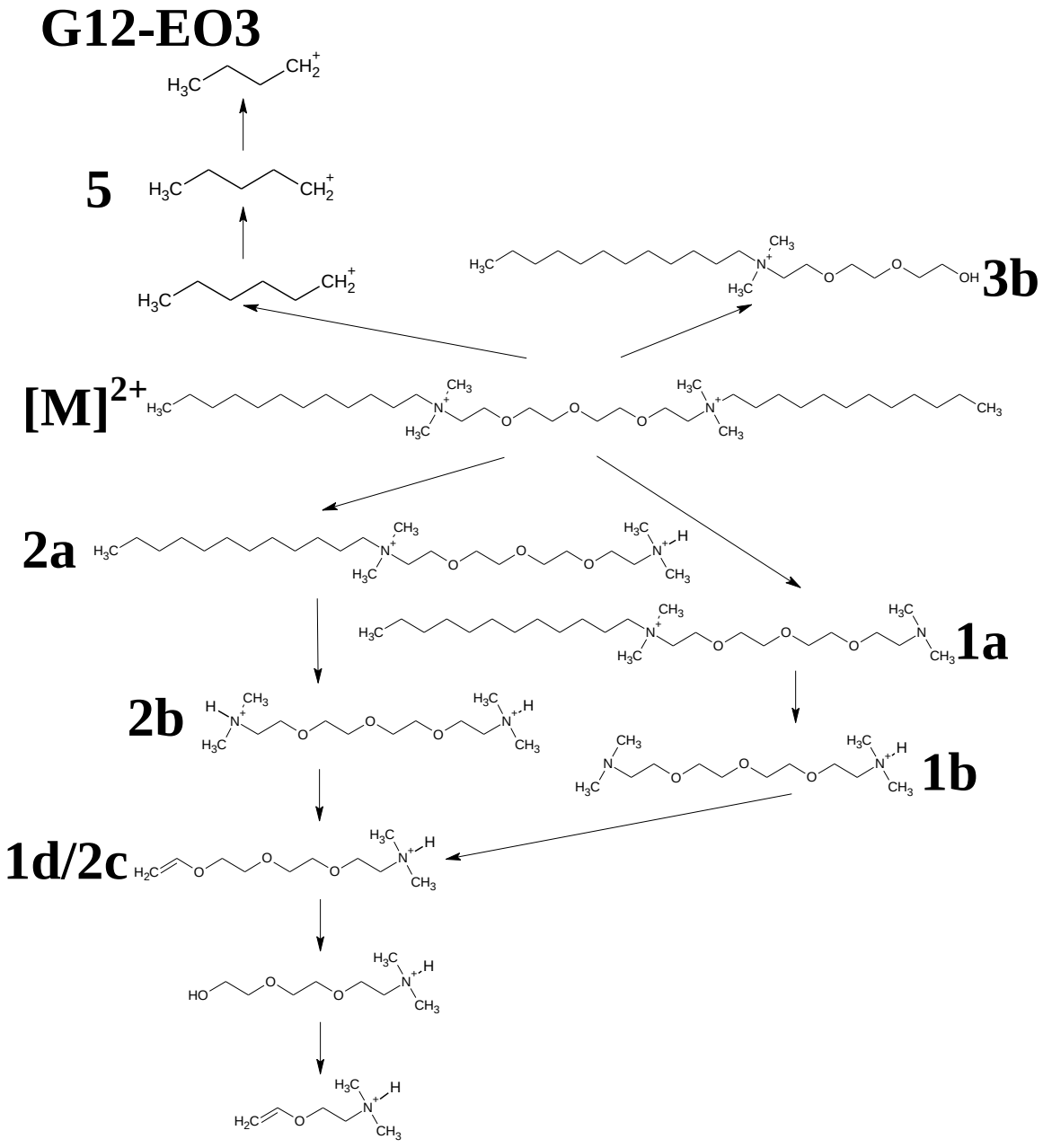

Appendix A Figure 19.1 Fragmentation pattern of G12-EO3

Appendix A Table 19 G12-EO3 gemini surfactant fragment ions (m/z)

$[M]^{2+}$	1a	1b	1c	1d	2a	2b	2c	3a	3b	3c	4	5
293.31	417.42	249.23		204.16	209.22	125.12	204.16	346.35				85.1 → 57.07

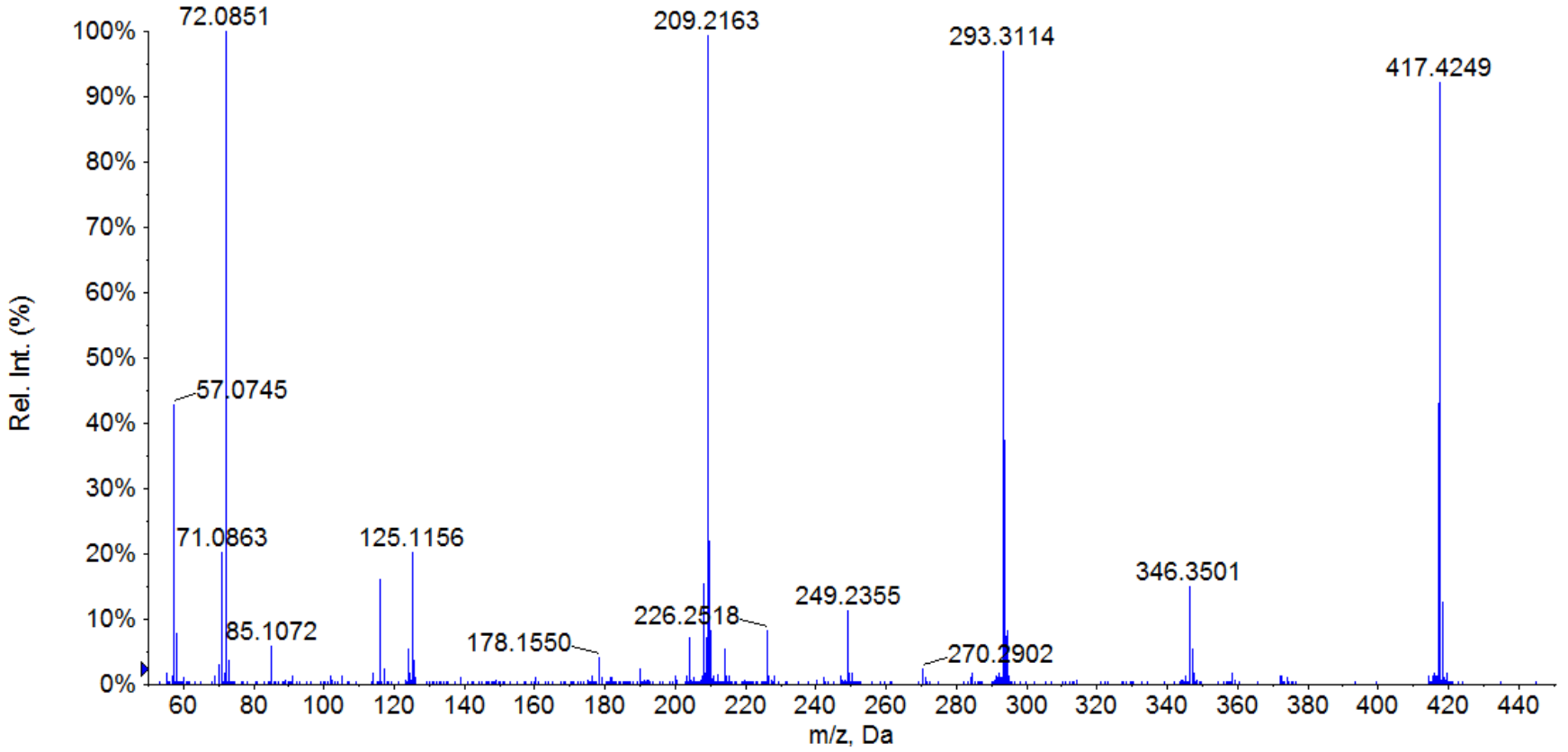

224

Appendix A Figure 19.2 A MS/MS spectra of G12-EO3 provided by an AB Sciex QSTAR XL qToF-MS

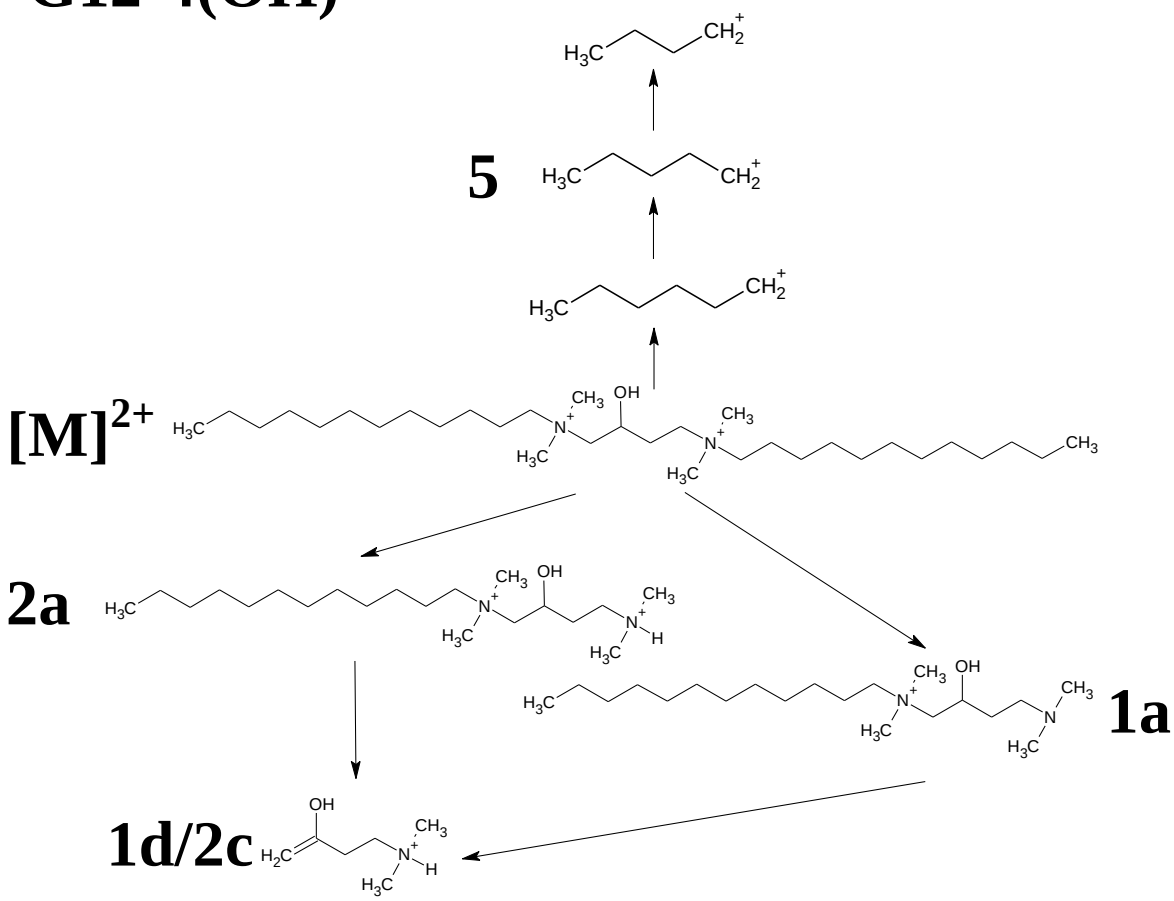

Appendix A Figure 20.1 Fragmentation pattern of G12-4(OH)

Appendix A Table 20 G12-4(OH) gemini surfactant fragment ions (m/z)

$[M]^{2+}$	1a	1b	1c	1d	2a	2b	2c	3a	3b	3c	4	5
249.29				116.11	165.19		116.11					85.1 → 57.07

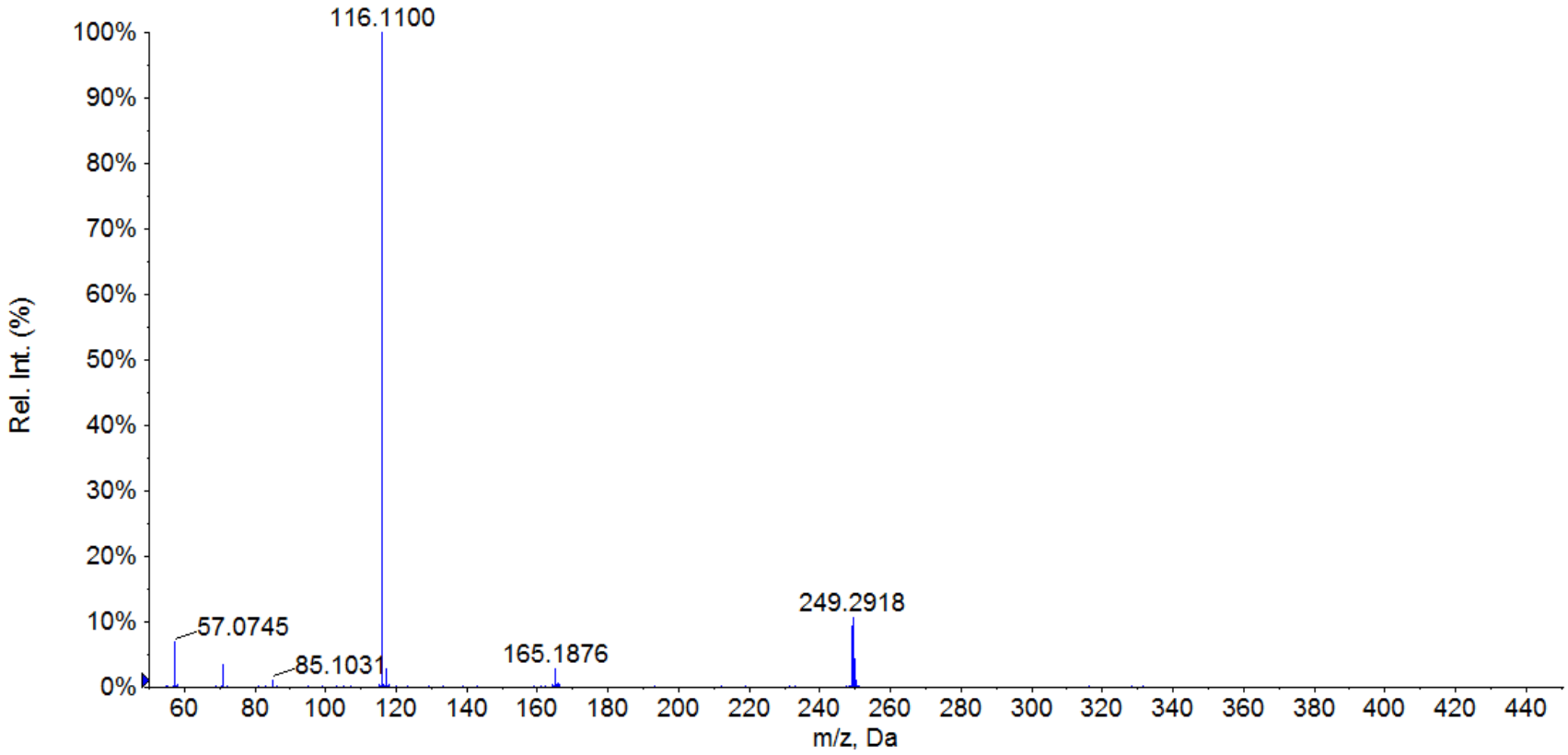

Appendix A Figure 20.2 A MS/MS spectra of G12-4(OH) provided by an AB Sciex QSTAR XL qToF-MS

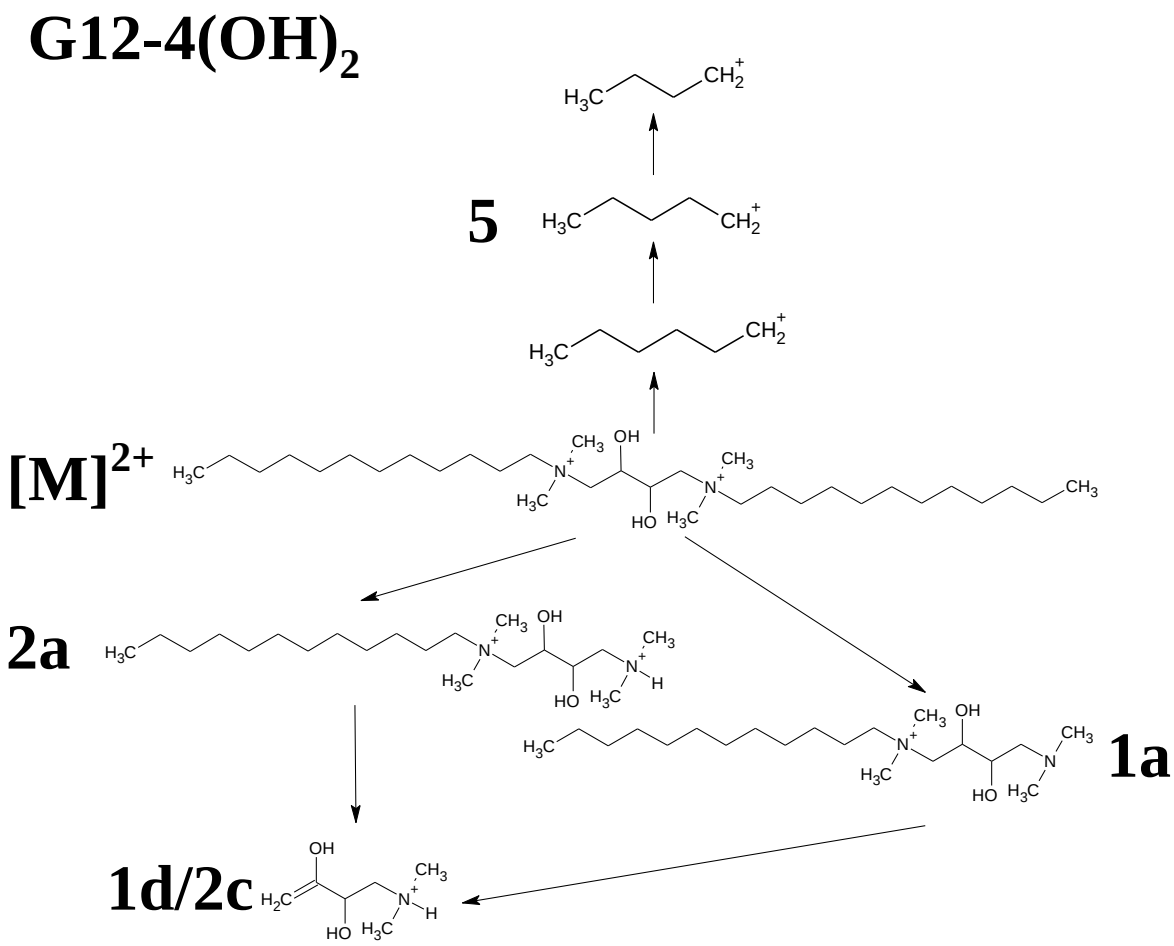

Appendix A Figure 21.1 Fragmentation pattern of G12-4(OH)$_2$

Appendix A Table 21 G12-4(OH)$_2$ gemini surfactant fragment ions (m/z)

$[M]^{2+}$	1a	1b	1c	1d	2a	2b	2c	3a	3b	3c	4	5
257.28	345.23			132.11	173.19		132.11					85.1 → 57.07

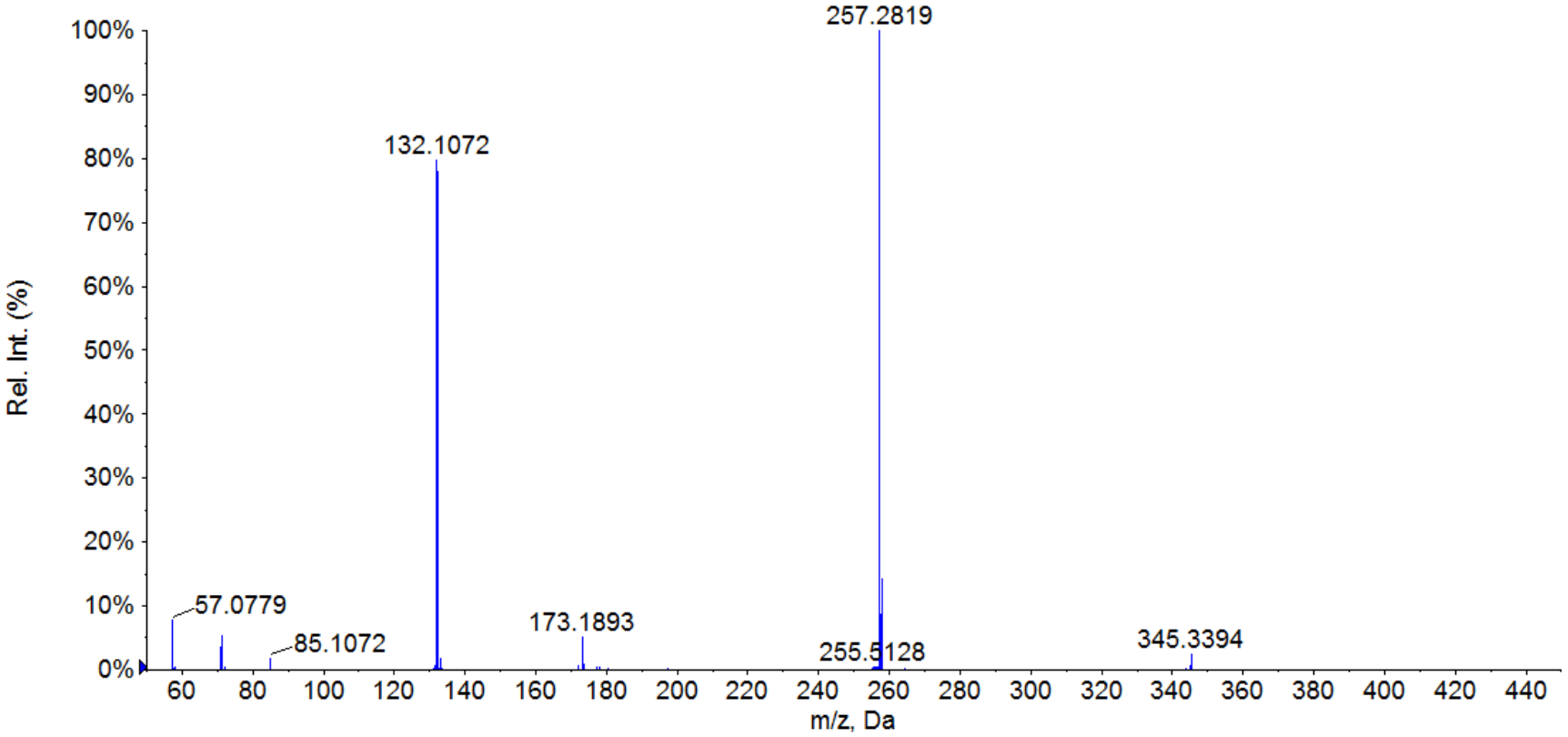

Appendix A Figure 21.2 A MS/MS spectra of G12-4$(OH)_2$ provided by an AB Sciex QSTAR XL qToF-MS

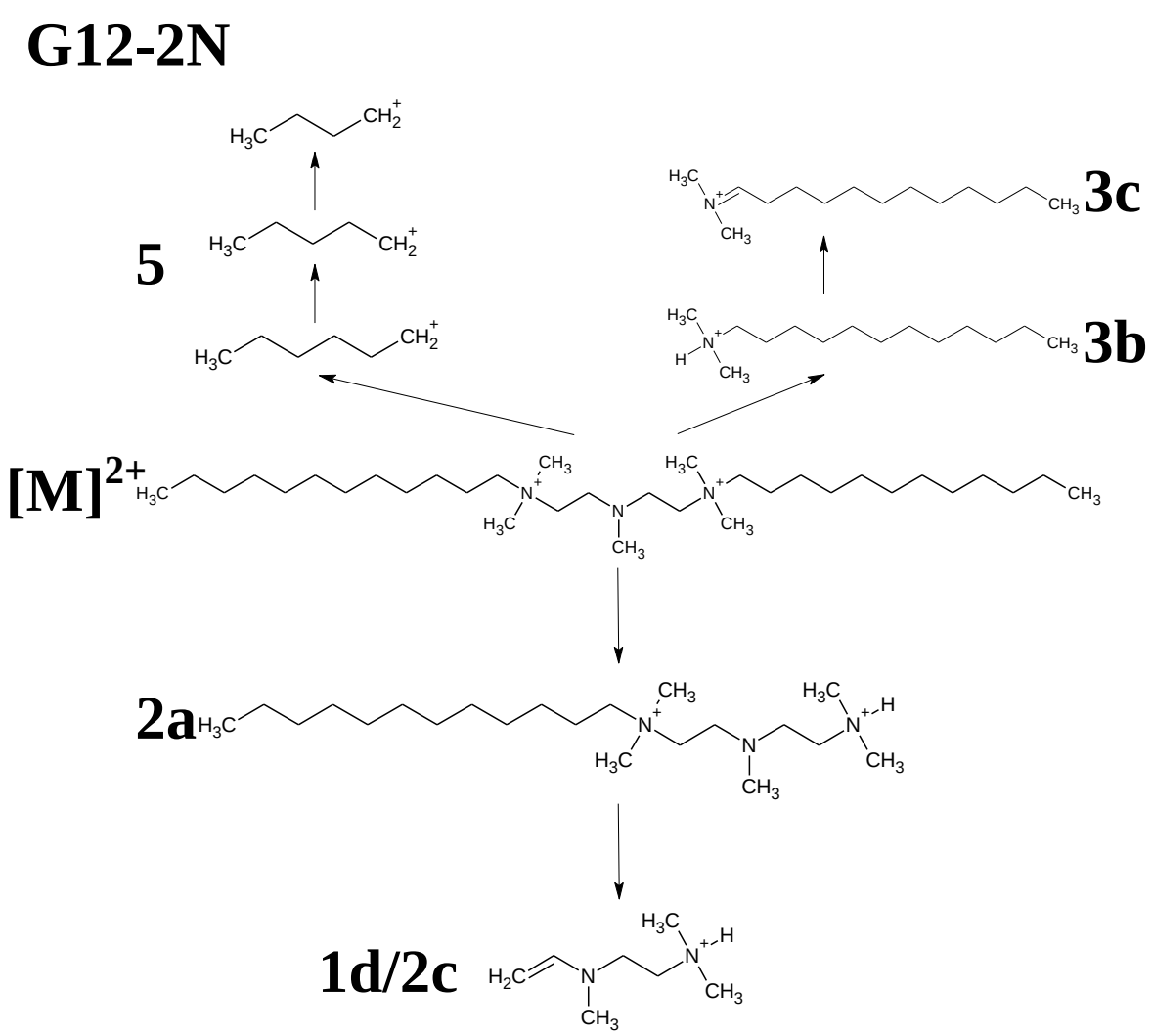

Appendix A Figure 22.1 Fragmentation pattern of G12-2N

Appendix A Table 22 G12-2N gemini surfactant fragment ions (m/z)

$[M]^{2+}$	1a	1b	1c	1d	2a	2b	2c	3a	3b	3c	4	5
255.8				129.14	171.71		129.14		214.26	212.25		85.1 → 57.07

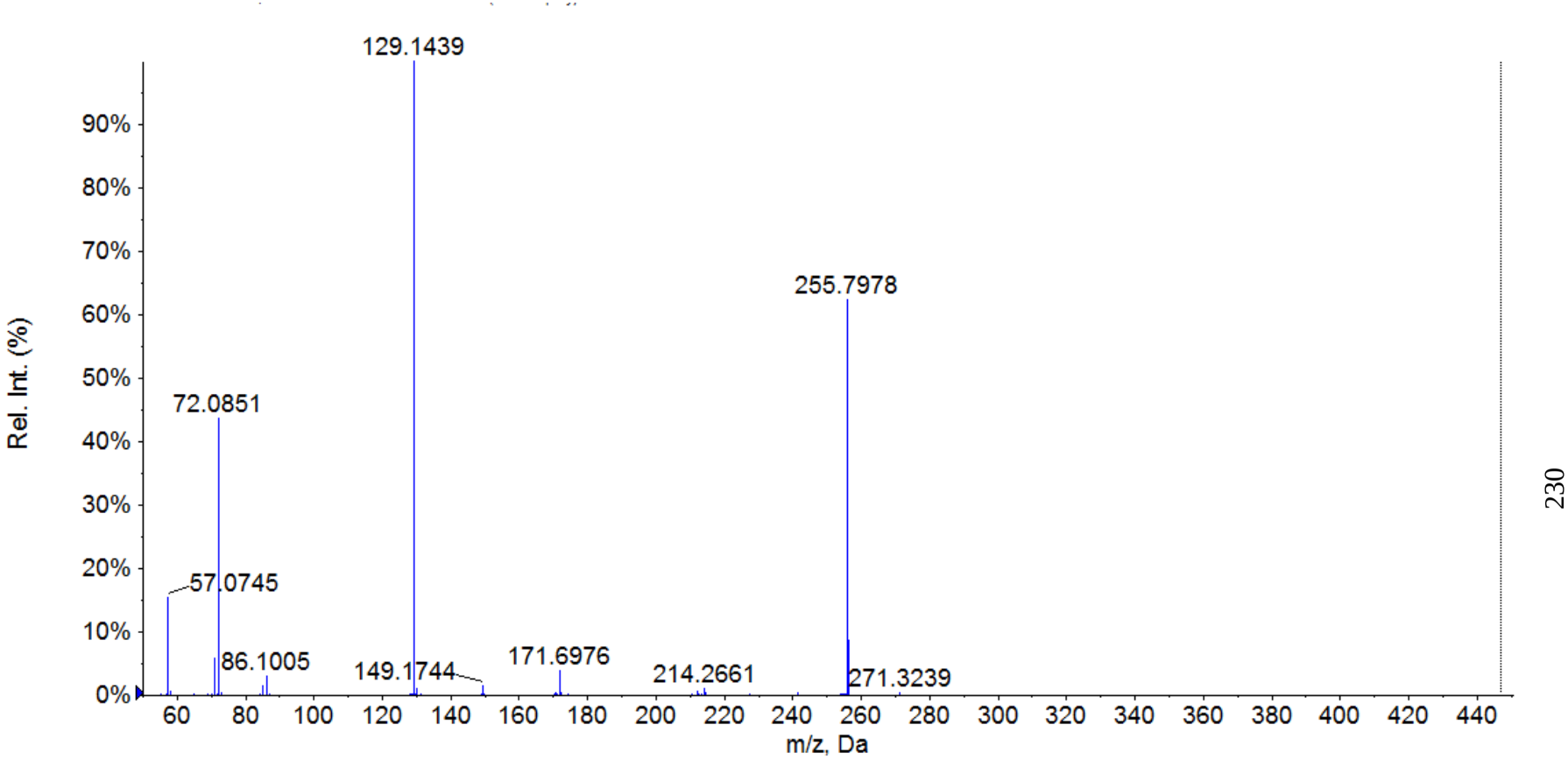

Appendix A Figure 22.2 A MS/MS spectra of G12-2N provided by an AB Sciex QSTAR XL qToF-MS

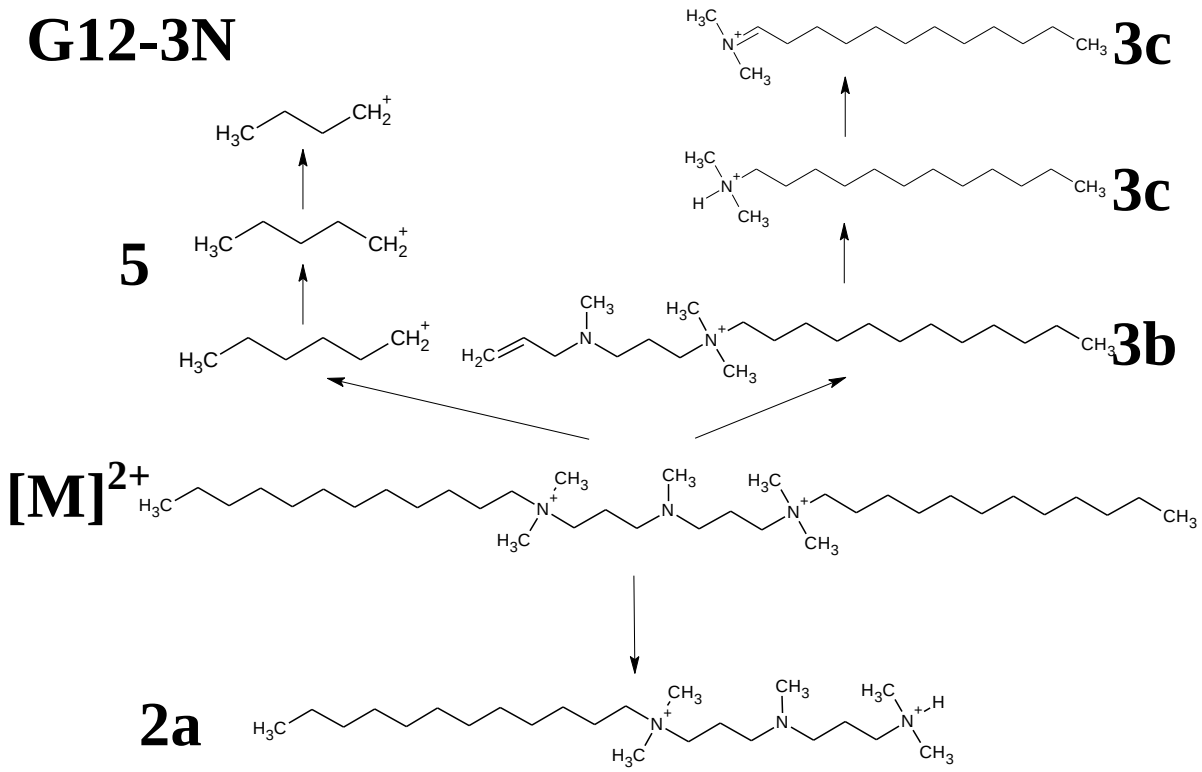

Appendix A Figure 23.1 Fragmentation pattern of G12-3N

Appendix A Table 23 G12-3N gemini surfactant fragment ions (m/z)

$[M]^{2+}$	1a	1b	1c	1d	2a	2b	2c	3a	3b	3c	4	5
269.72					185.72			284.32	214.26	212.25		85.1 → 57.07

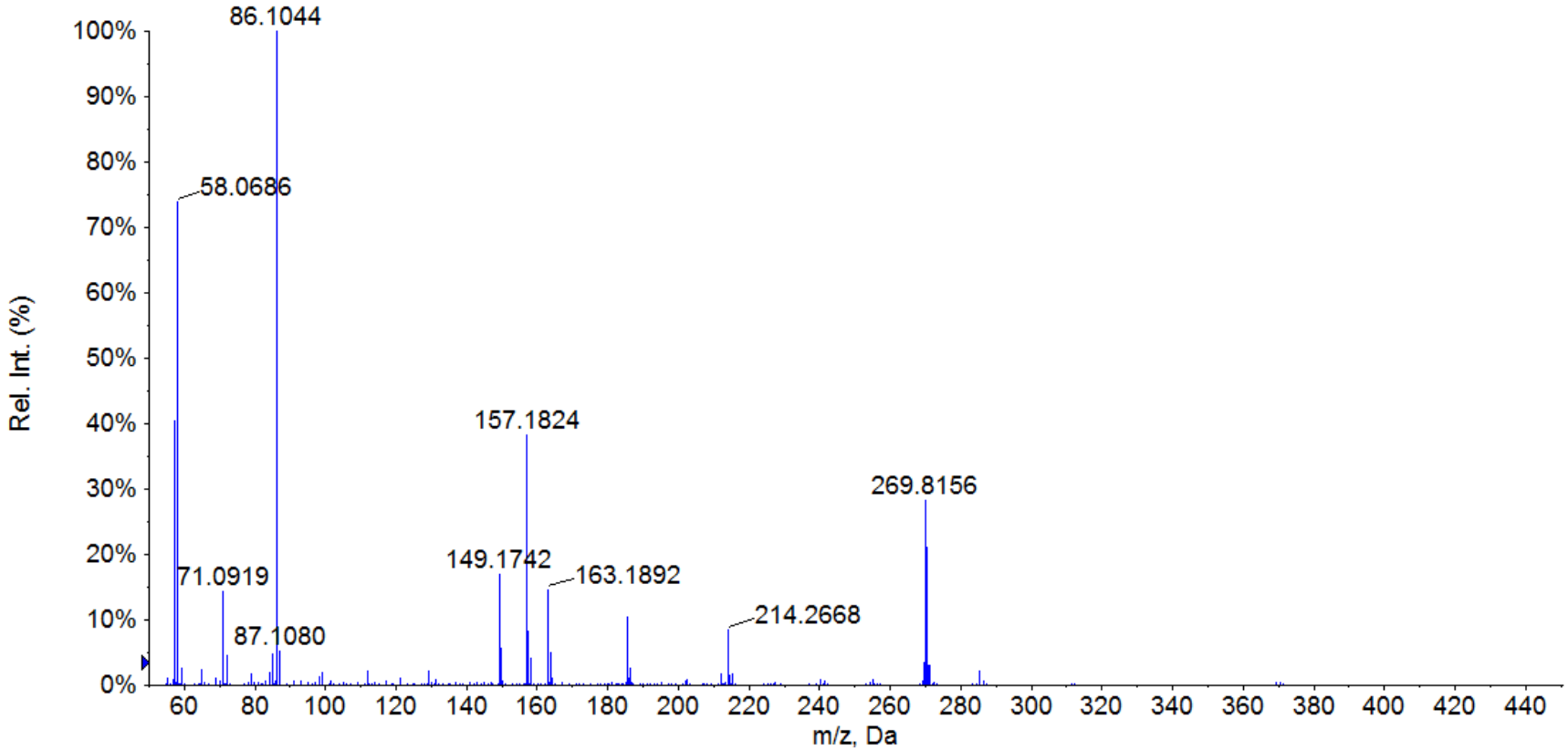

AppendixA Figure 23.2 A MS/MS spectra of G12-3N provided by an AB Sciex QSTAR XL qToF-MS

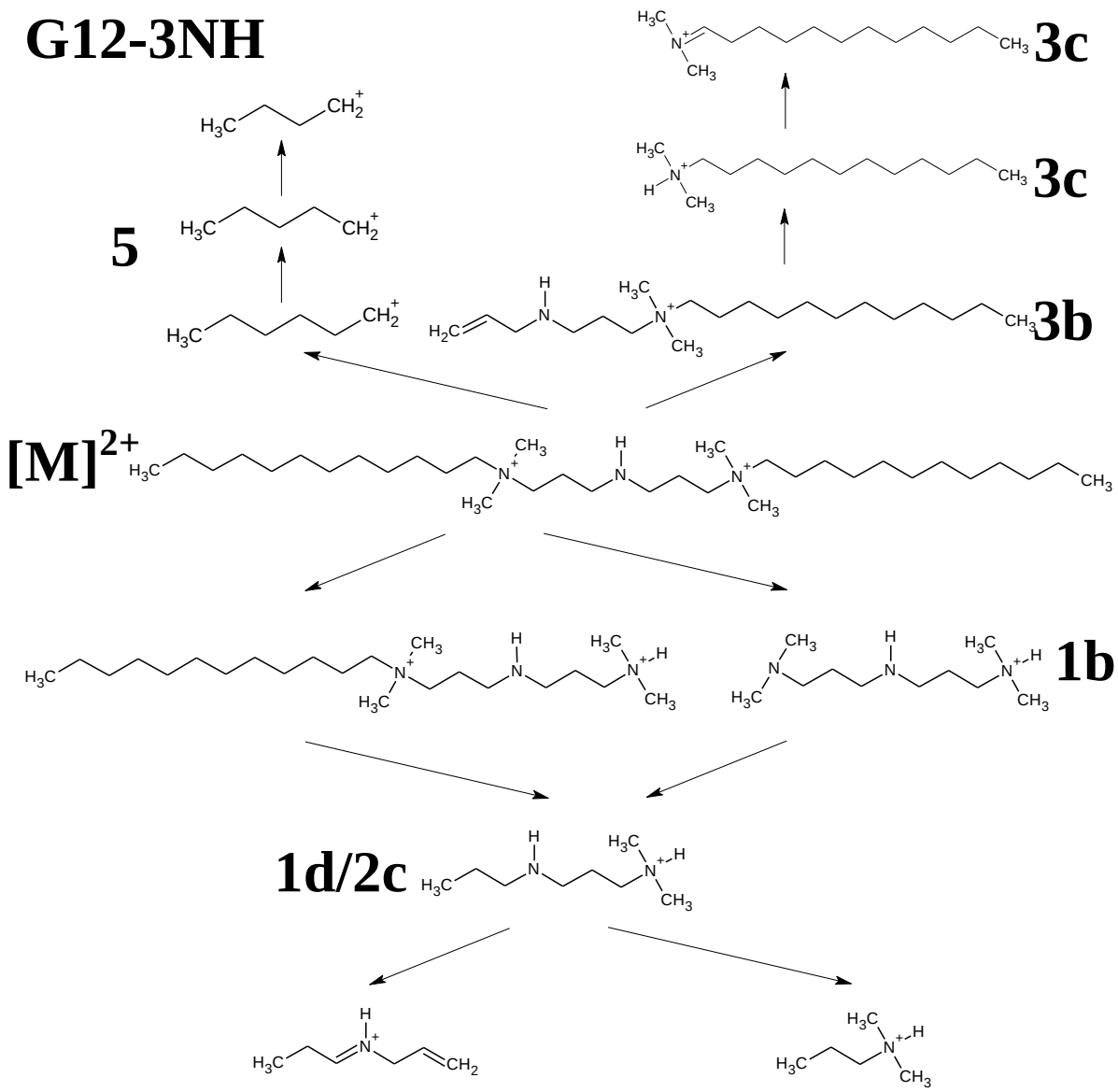

Appendix A Figure 25.1 Fragmentation pattern of G12-3NH

Appendix A Table 25 G12-3 gemini surfactant fragment ions (m/z)

$[M]^{2+}$	1a	1b	1c	1d	2a	2b	2c	3a	3b	3c	4	5
262.82		188.23		143.17	178.72		143.17	271.32	214.27	212.25		85.1 → 57.07

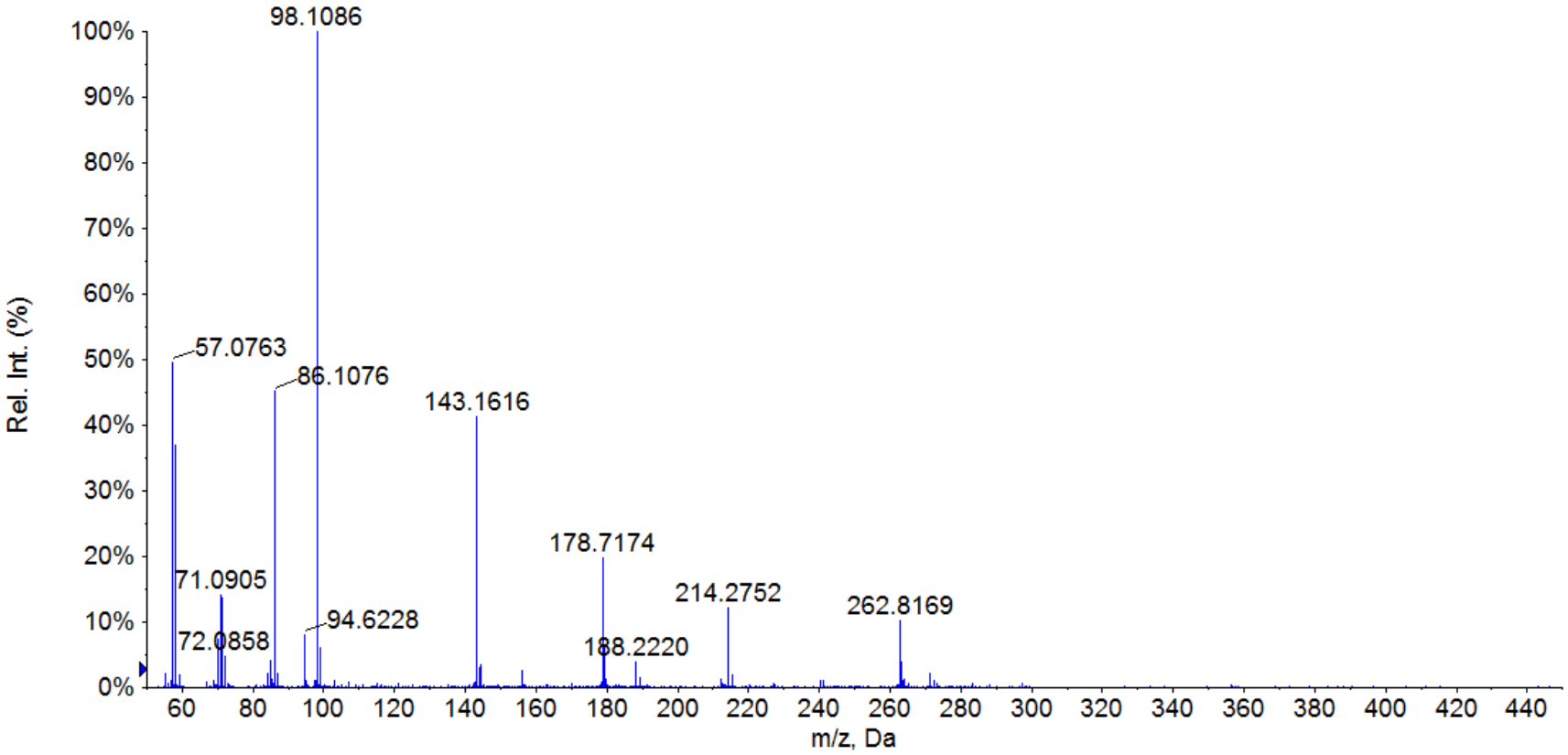

Appendix A Figure 25.2 A MS/MS spectra of G12-3NH provided by an AB Sciex QSTAR XL qToF-MS

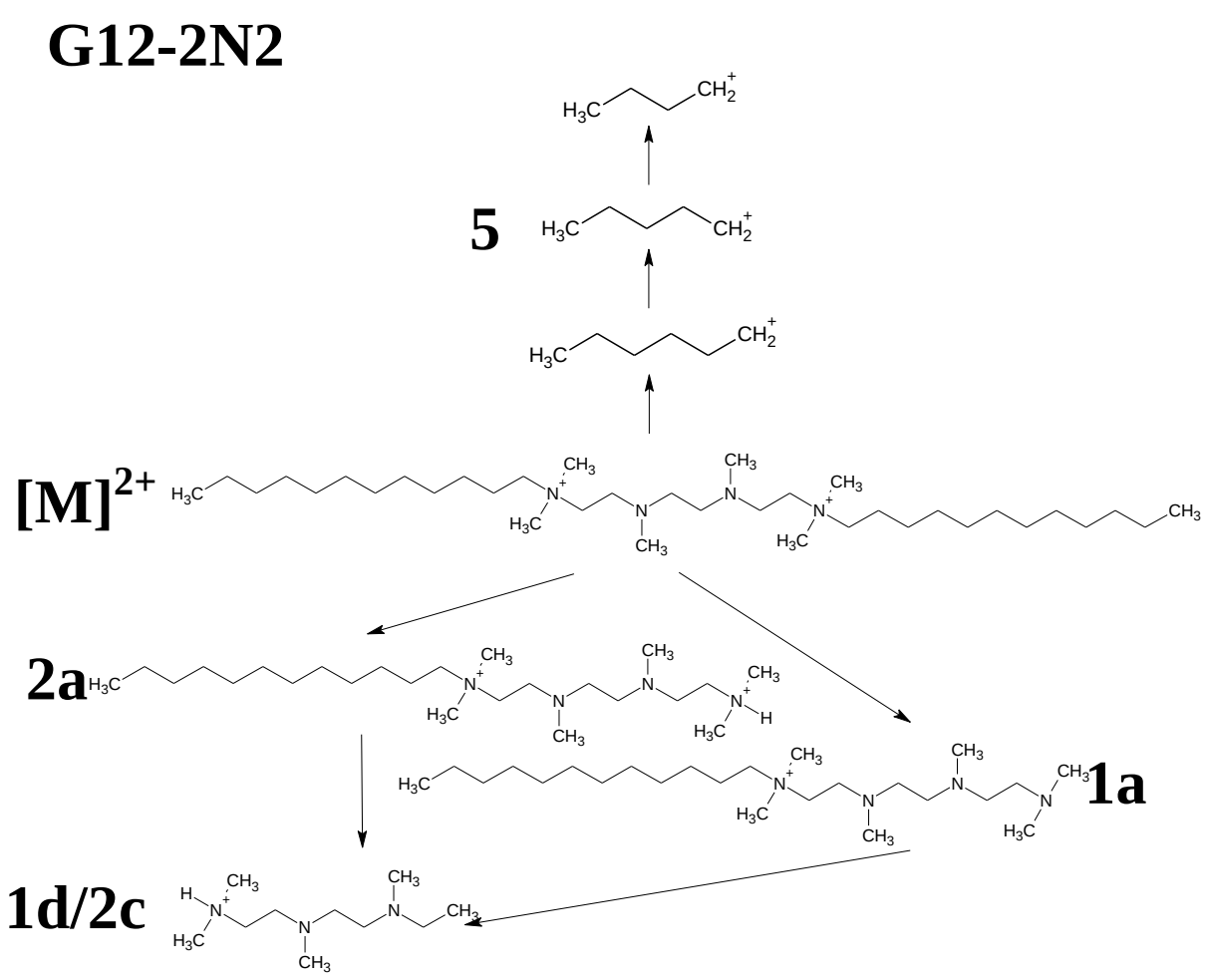

Appendix A Figure 26.1 Fragmentation pattern of G12-2N2

Appendix A Table 26 G12-2N2 gemini surfactant fragment ions (m/z)

$[M]^{2+}$	1a	1b	1c	1d	2a	2b	2c	3a	3b	3c	4	5
284.33	423.48			129.15	212.25		149.17					85.1 → 57.07

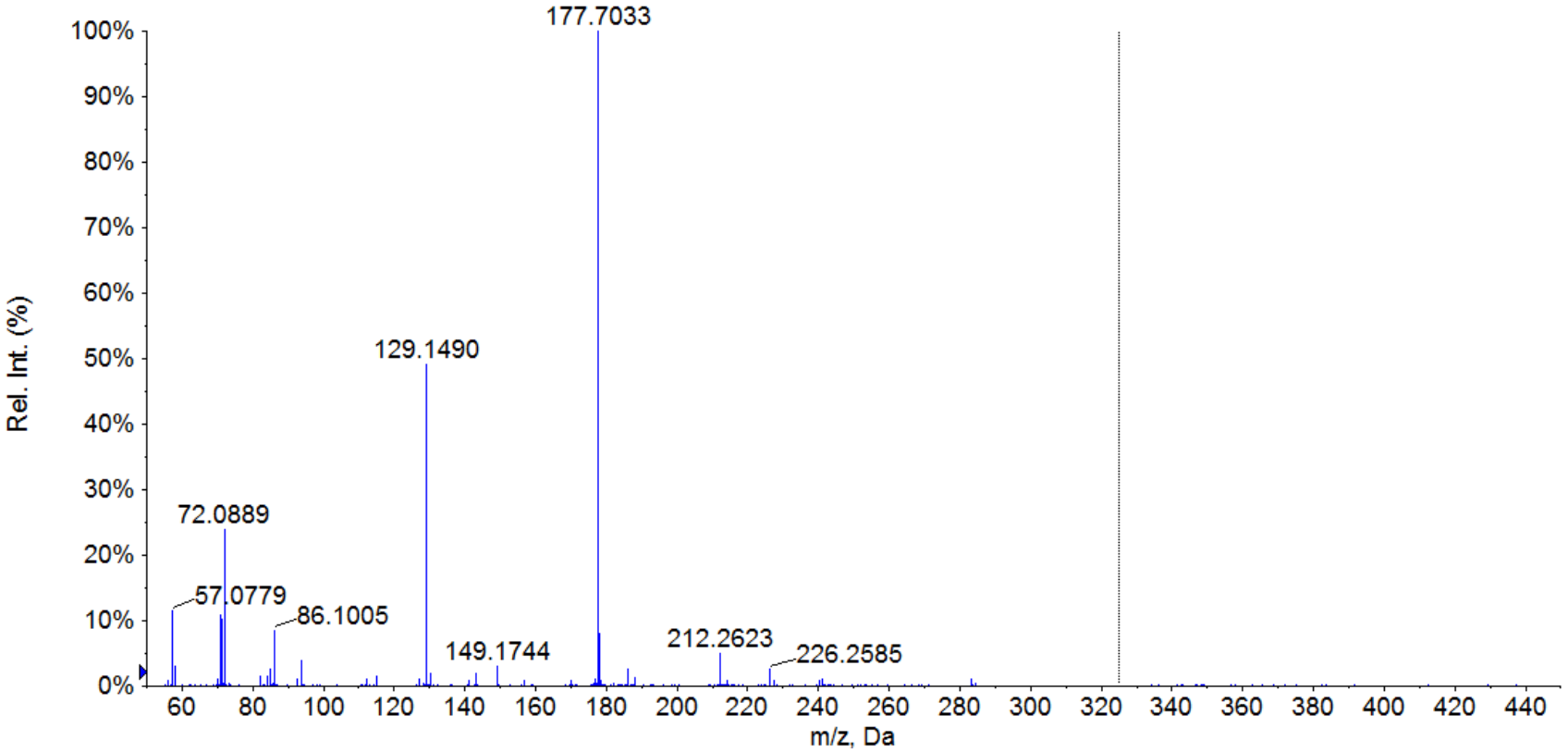

Appendix A Figure 26.2 A MS/MS spectra of G12-2N2 provided by an AB Sciex QSTAR XL qToF-MS

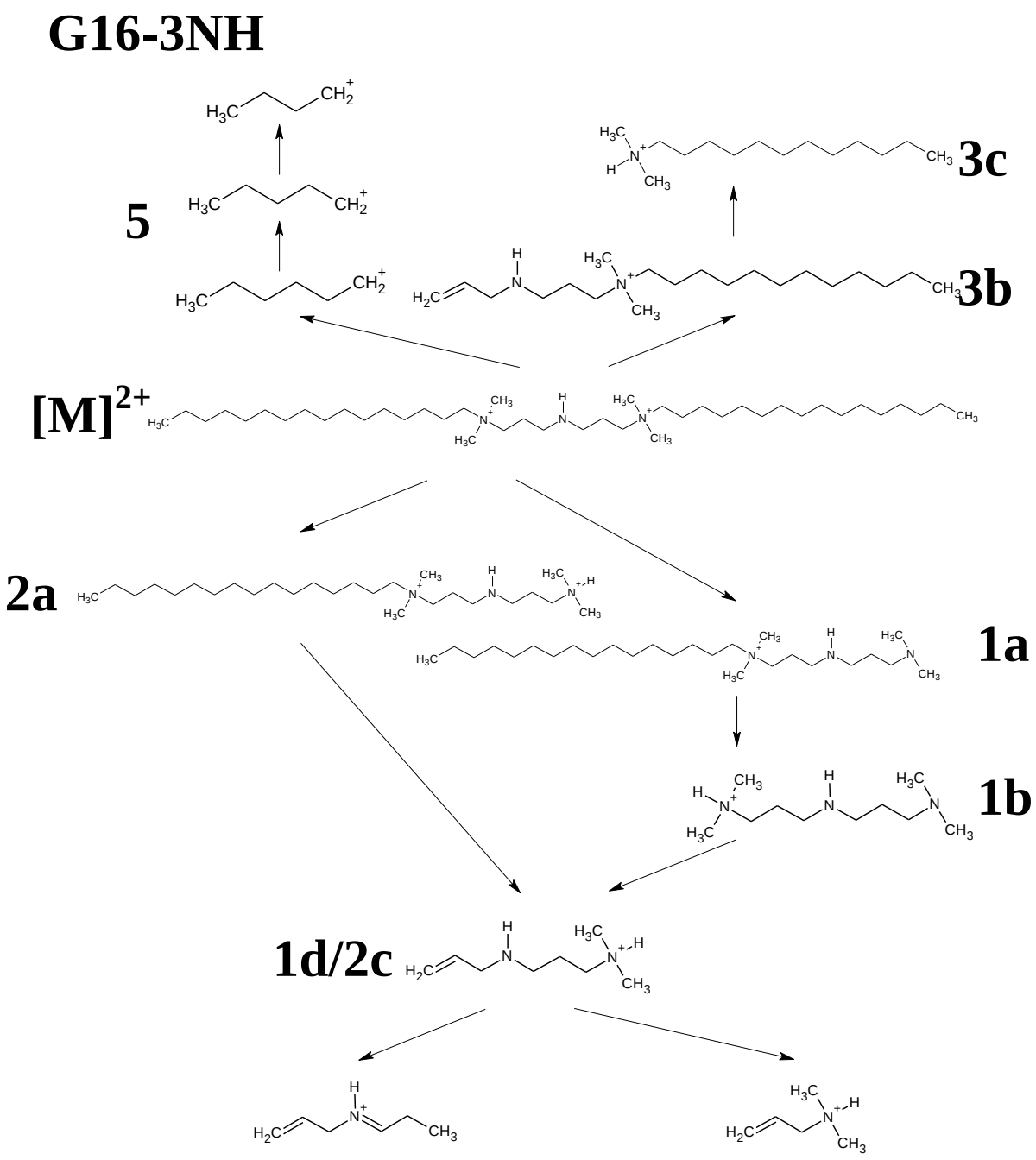

Appendix A Figure 27.1 Fragmentation pattern of G16-3NH

Appendix A Table 27 G16-3NH gemini surfactant fragment ions (m/z)

$[M]^{2+}$	1a	1b	1c	1d	2a	2b	2c	3a	3b	3c	4	5
318.87	412.47	188.22		143.17	206.74		143.17	327.38	270.32			85.1 → 57.07

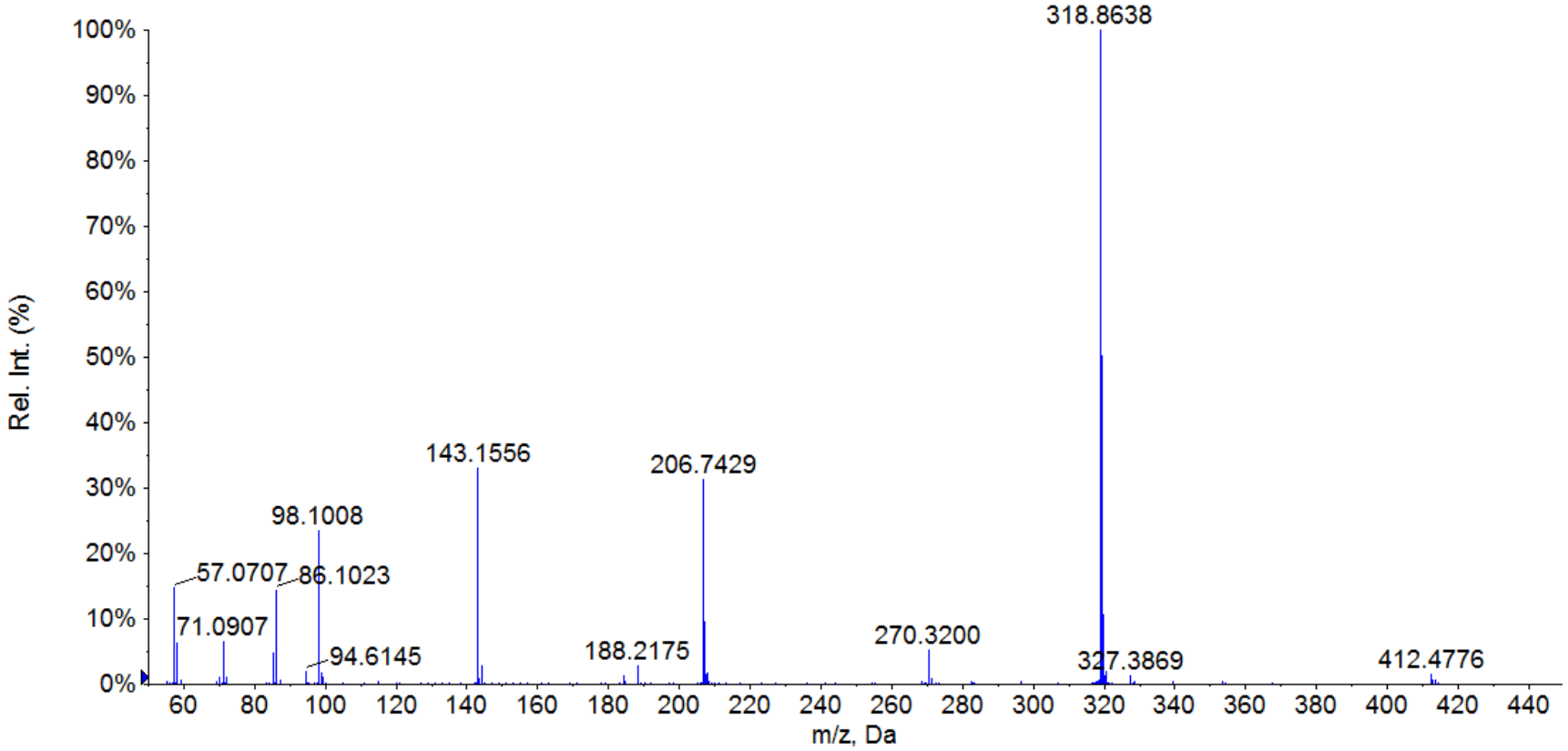

Appendix A Figure 27.2 A MS/MS spectra of G16-3NH provided by an AB Sciex QSTAR XL qToF-MS

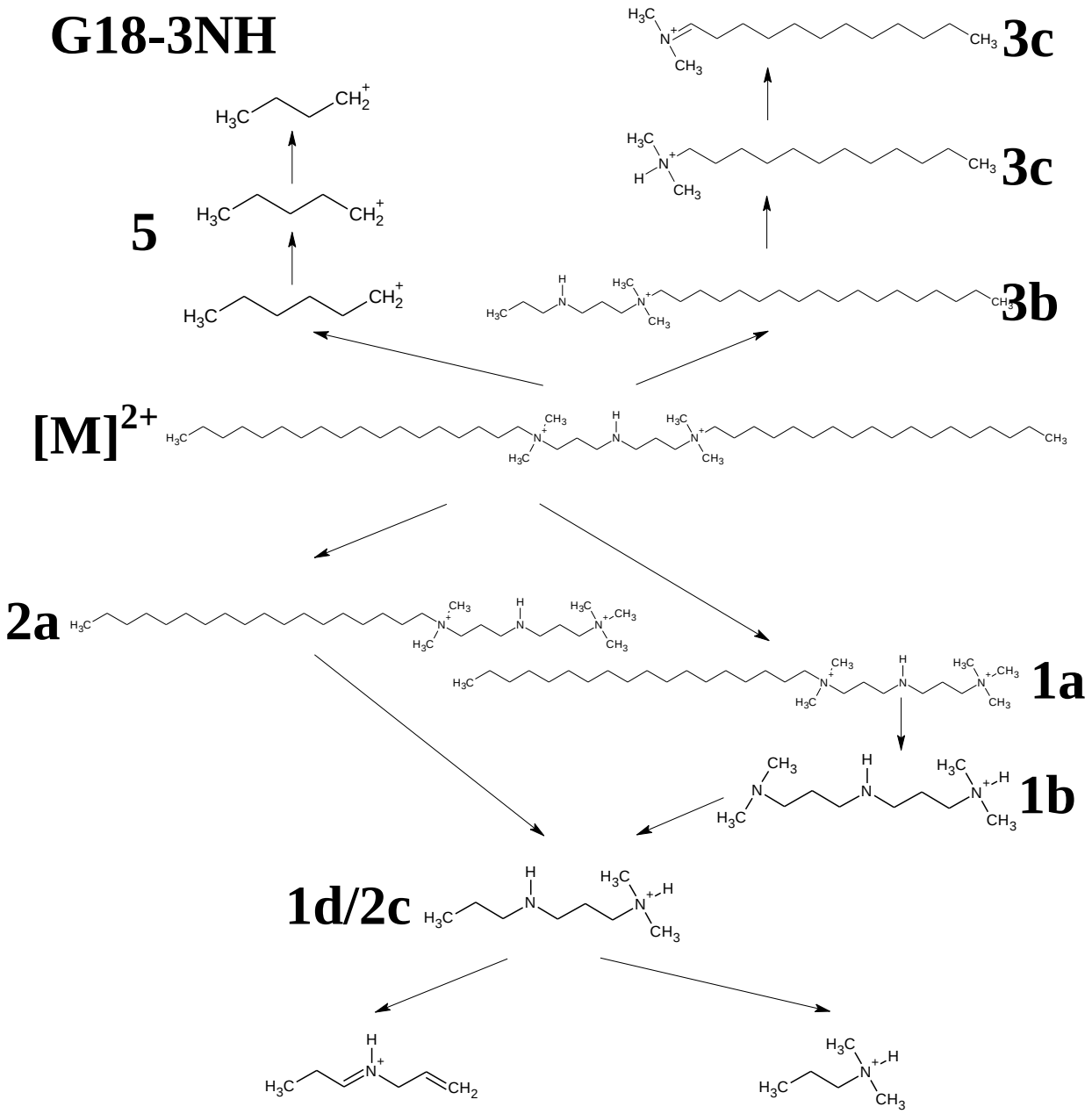

Appendix A Figure 28.1 Fragmentation pattern of G18-3NH

Appendix A Table 28 G18-3NH gemini surfactant fragment ions (m/z)

$[M]^{2+}$	1a	1b	1c	1d	2a	2b	2c	3a	3b	3c	4	5
346.89	439.5	188.21		143.15	220.74		143.15	397.45	297.96			85.1 → 57.07

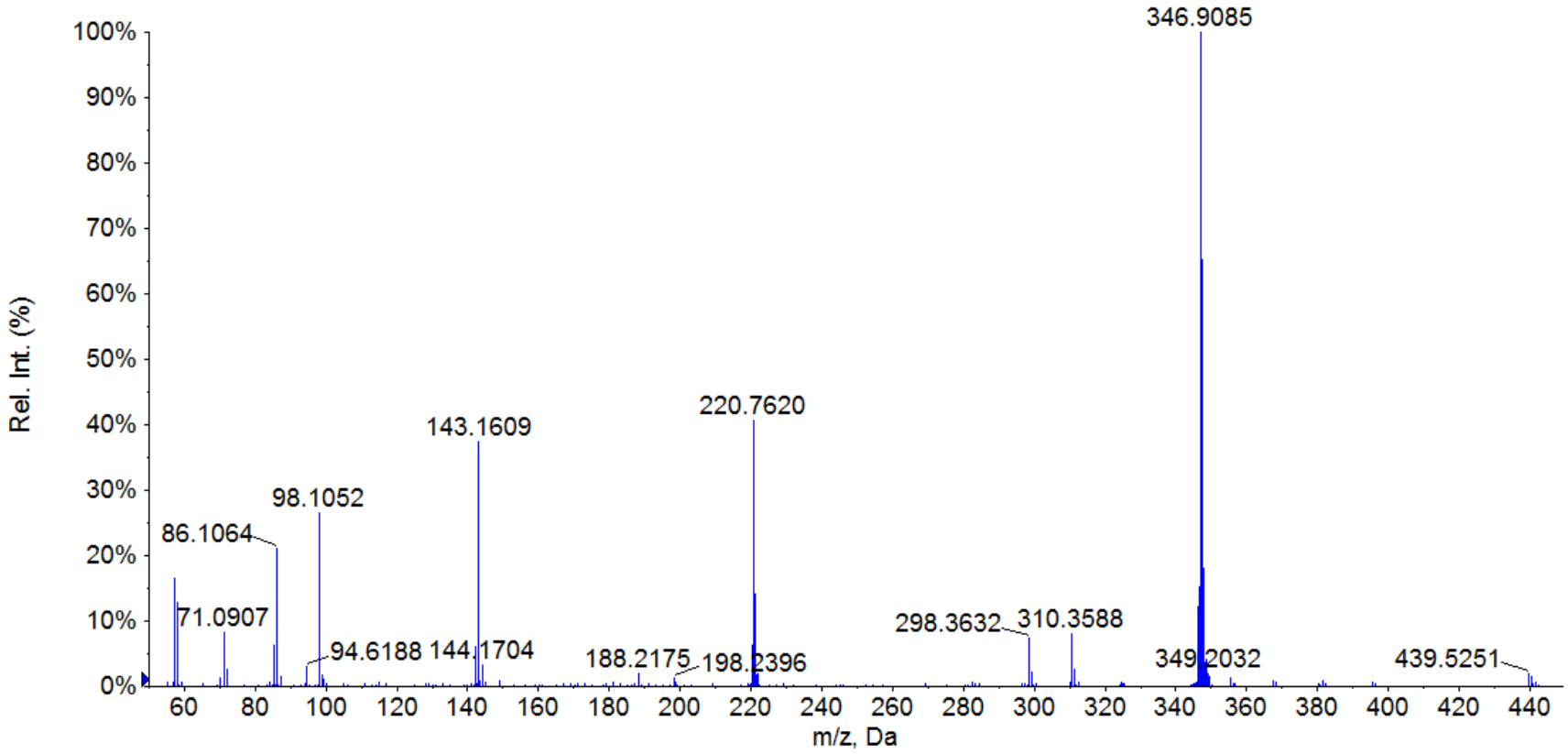

Appendix A Figure 28.2 A MS/MS spectra of G18-3NH provided by an AB Sciex QSTAR XL qToF-MS

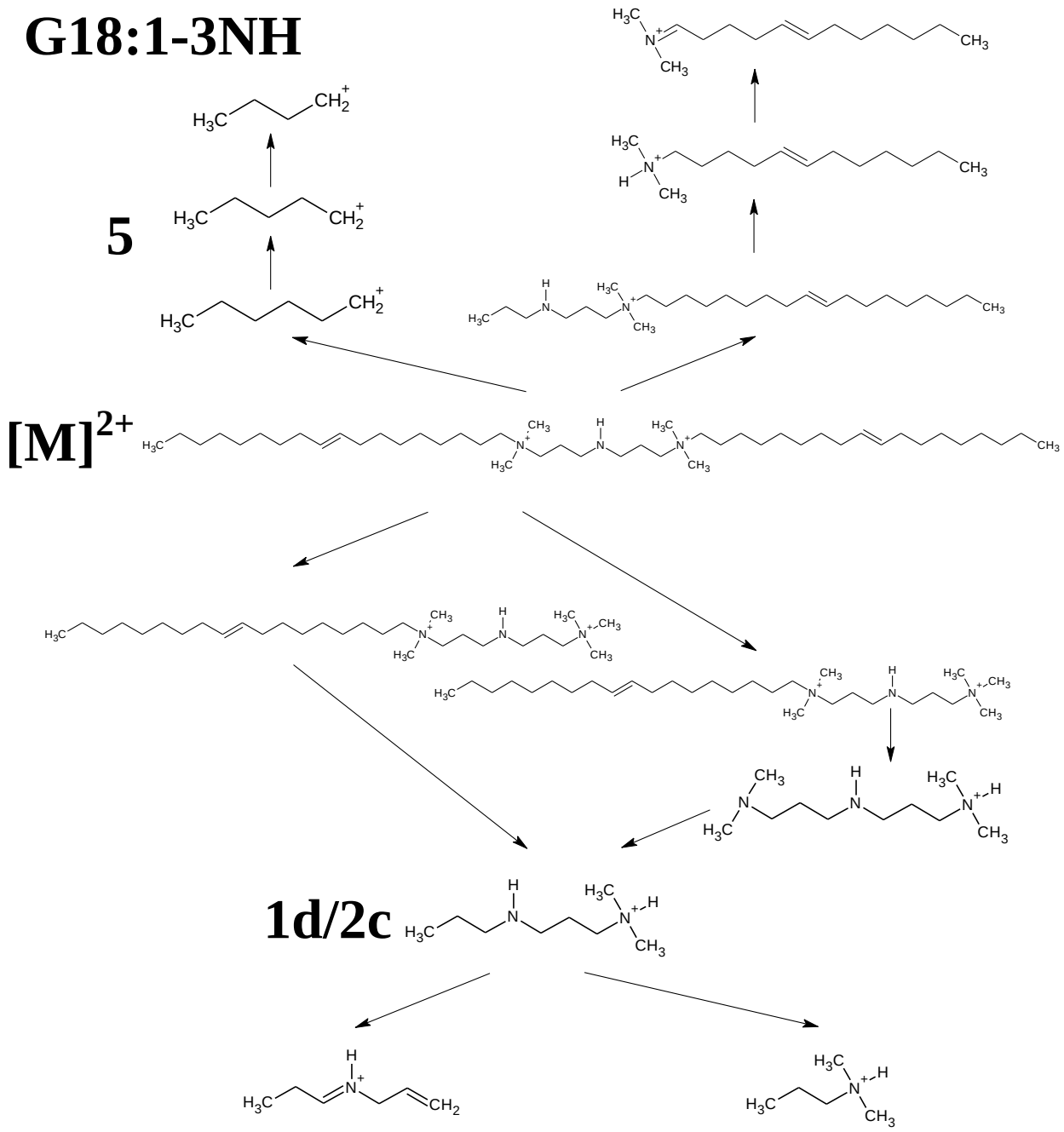

Appendix A Figure 29.1 Fragmentation pattern of G18:1-3NH

Appendix A Table 29 G18:1-3NH gemini surfactant fragment ions (m/z)

$[M]^{2+}$	1a	1b	1c	1d	2a	2b	2c	3a	3b	3c	4	5
344.88	438.5	188.21		143.15	219.74		143.15	395.44	295.33		97.1→55.06	

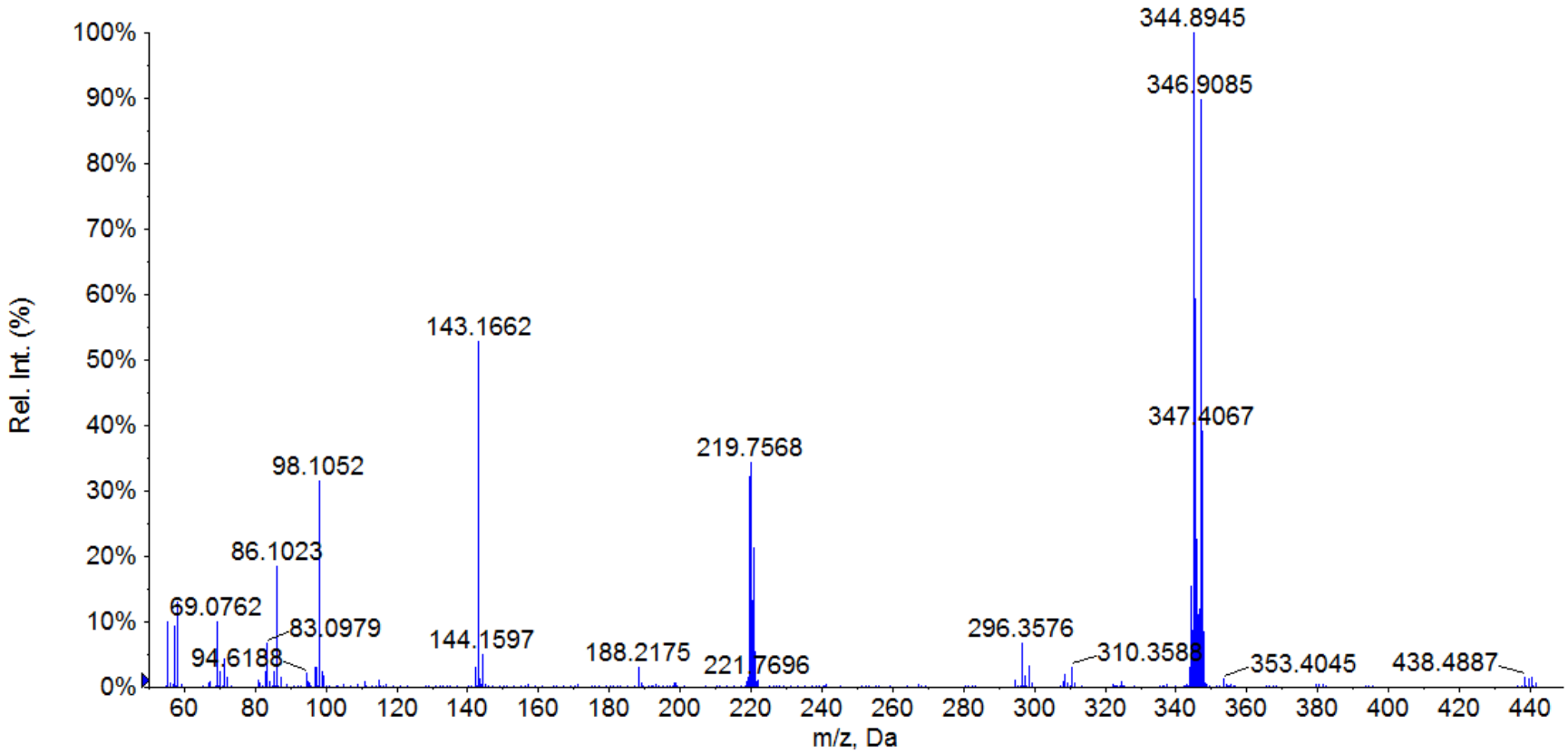

Appendix A Figure 29.2 A MS/MS spectra of G18:1-3NH provided by an AB Sciex QSTAR XL qToF-MS

APPENDIX B
Liquid chromatography method development

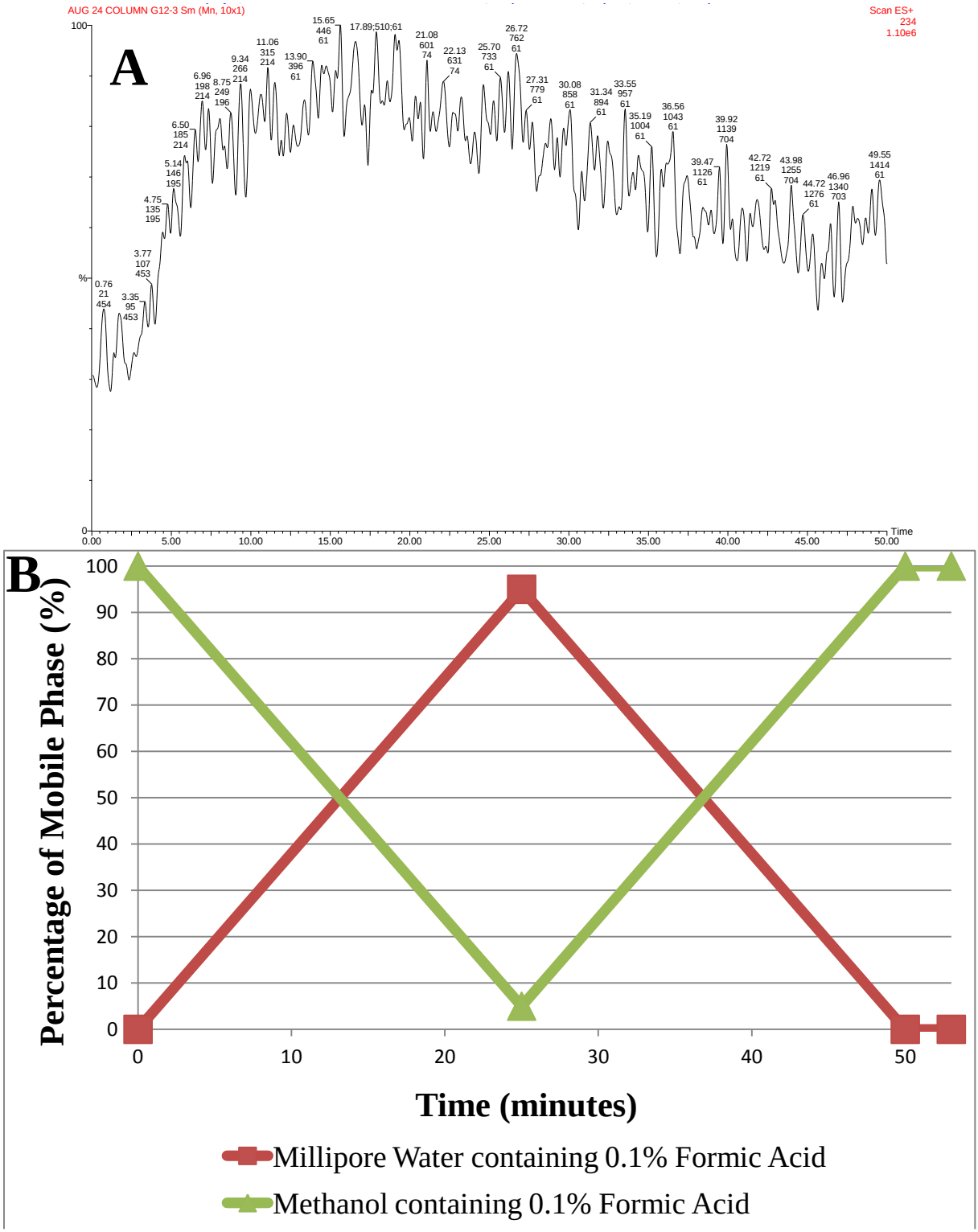

Appendix B Figure 1 Analysis of 100 µM G16-3 on an Alltech Allsphere C18 (150x2.1 mm, 3 µ) (A) following a 50 µL loop-injection and gradient LC analysis (B)

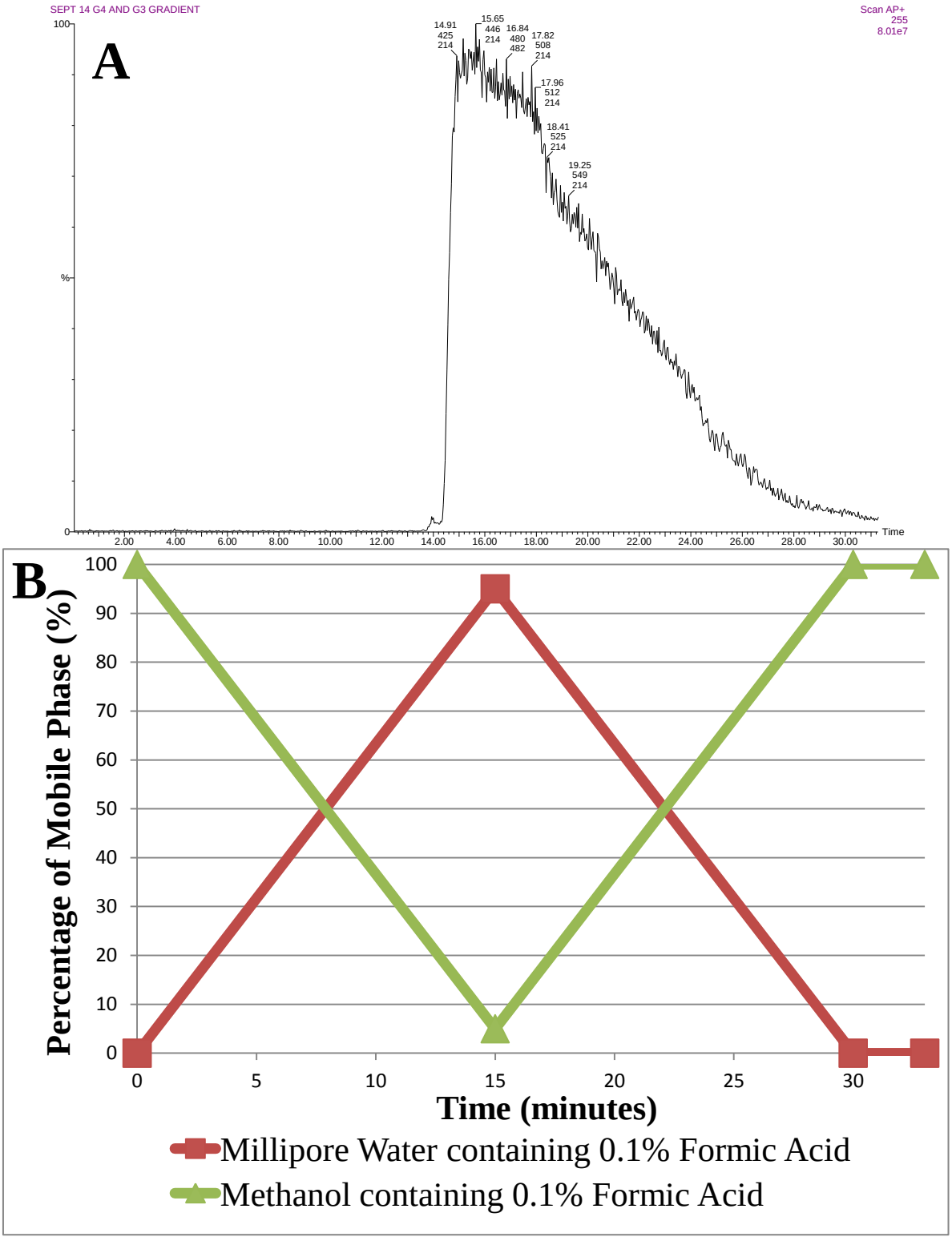

Appendix B Figure 2 Analysis of 100 µM G16-3 on an Vydac 214 TP C4 (50x4.6 mm, 5 µ) (A) following a 50 µL loop-injection and gradient LC analysis (B)

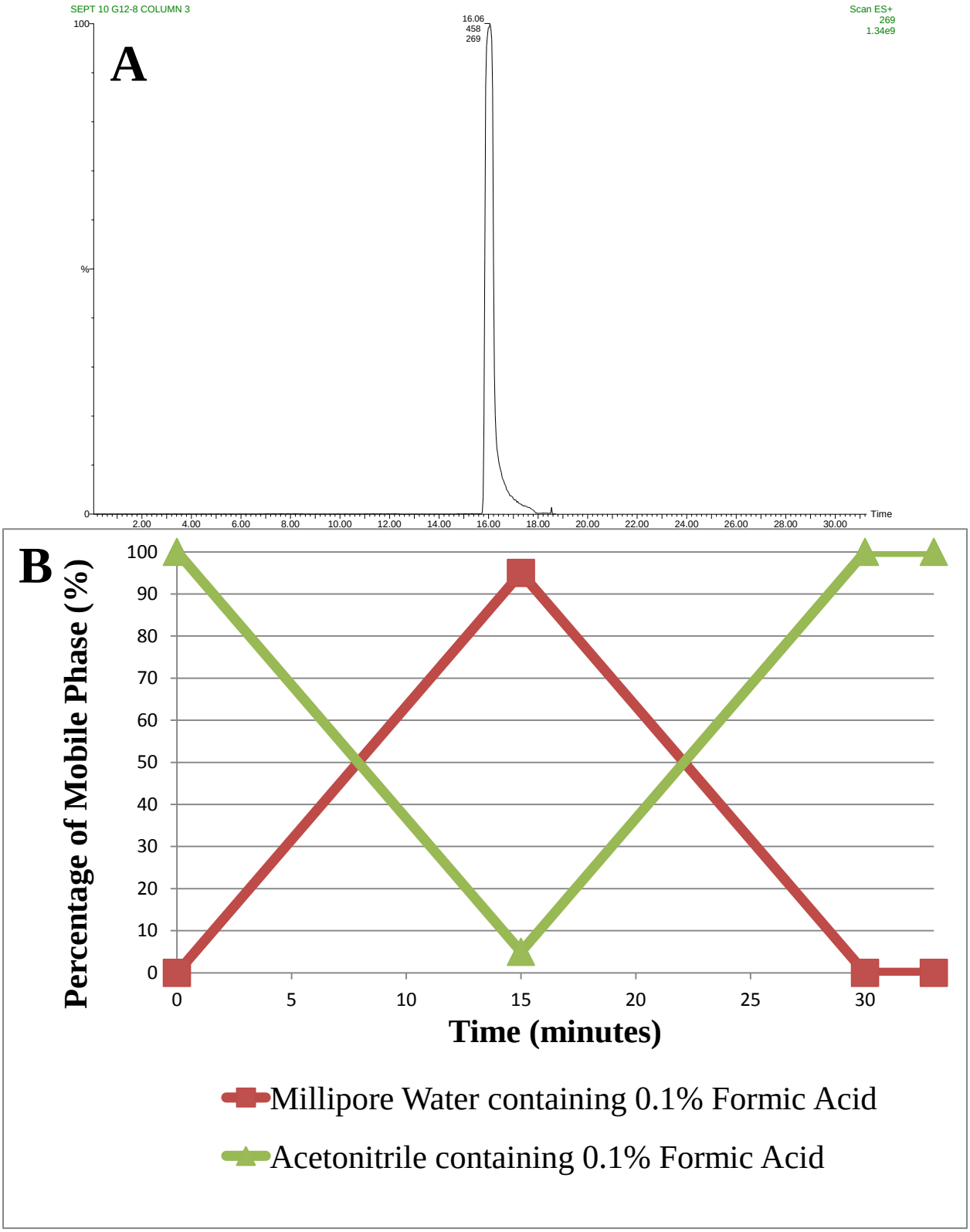

Appendix B Figure 3 Analysis of 100 µM G16-3 on an Phenomenex Luna CN (240x4.6 mm, 5 µ) (A) following a 50 µL loop-injection and gradient LC analysis (B)

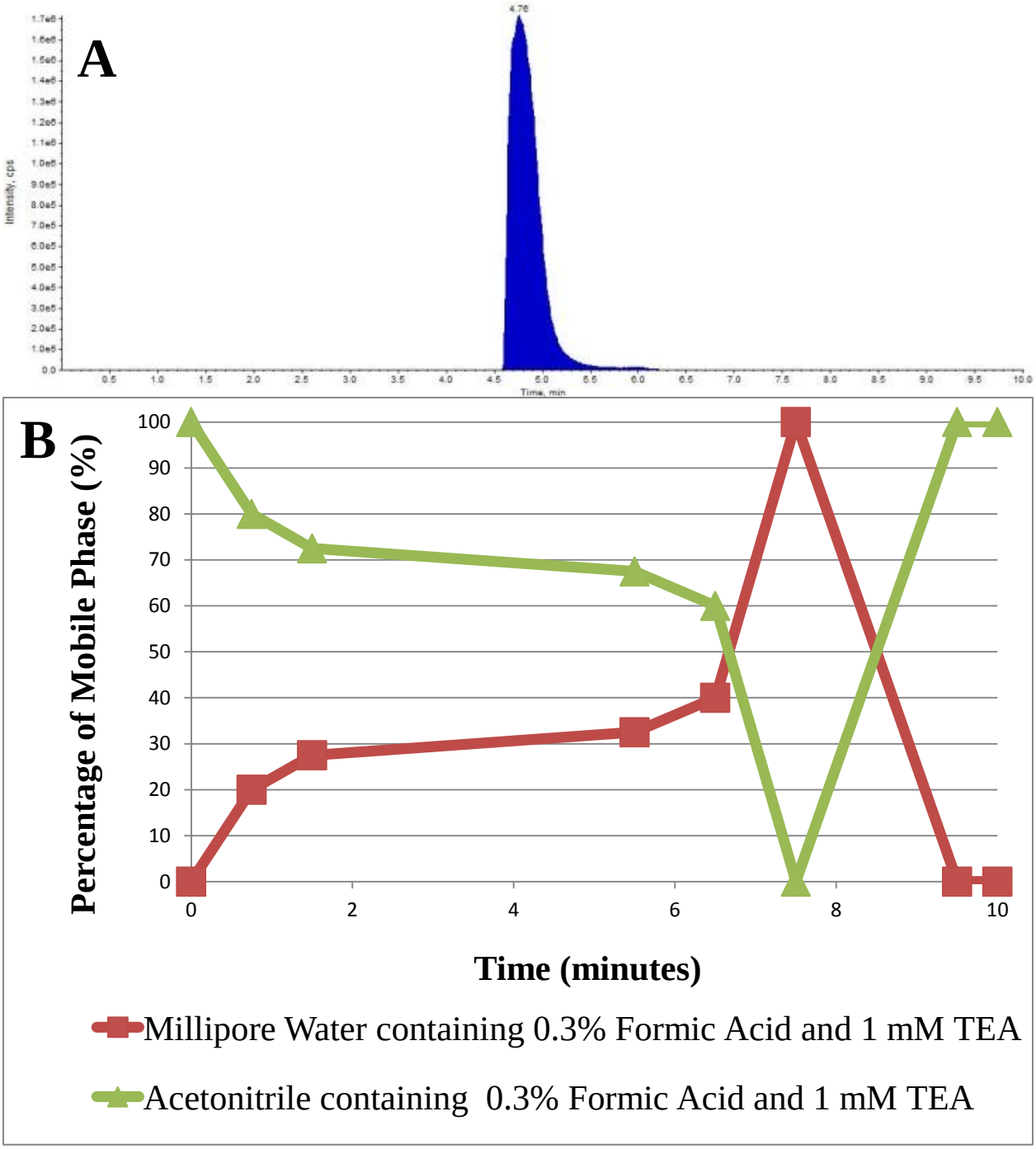

Appendix B Figure 4 Analysis of 100 µM G16-3 on an Aglient Eclipse CN column (100 x 2.1 mm with 3, 5 µ) (A) following a 10 µL loop-injection and gradient LC analysis (B)

APPENDIX C
Development of a liquid:liquid extraction method for G16-3

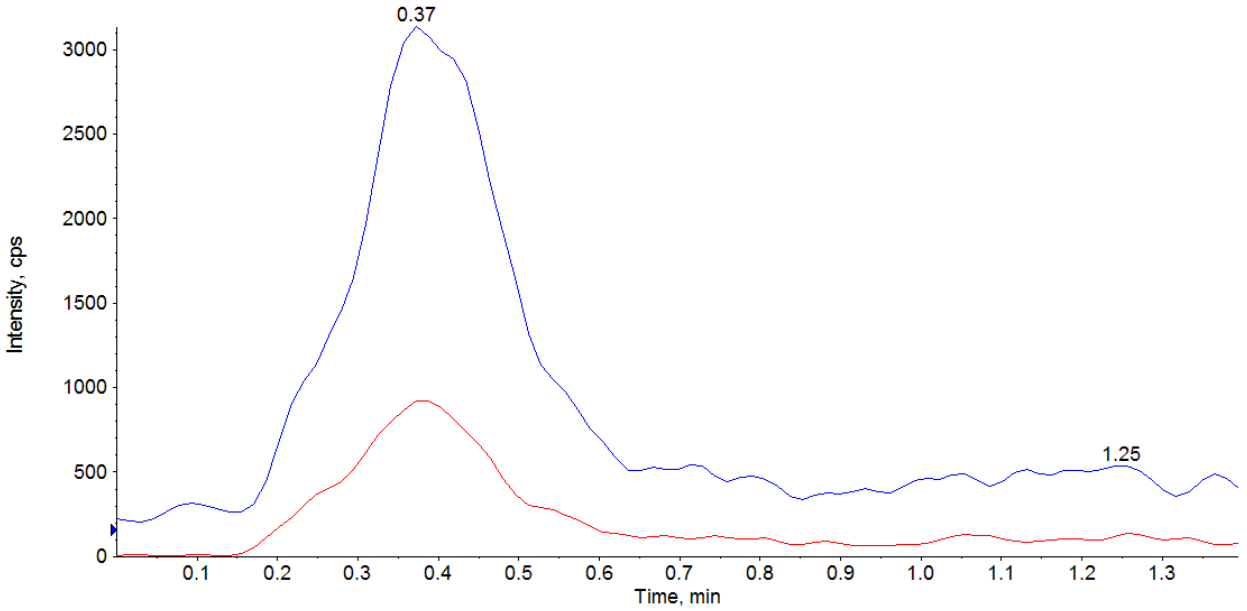

Appendix Figure C.1 FC-LR-MS/MS analysis of 0.500 µM concentration of G16-3 (*m/z* 290 → 86 [blue] & 355 [red]) following a methanol protein precipitation from PAM212 cell lysate. A 200 µL sample of PAM212 cell lysate was vortexed with 200 µL of methanol and 7.5 µL of the solution was in analyzed using the FC-LR-MS/MS method.

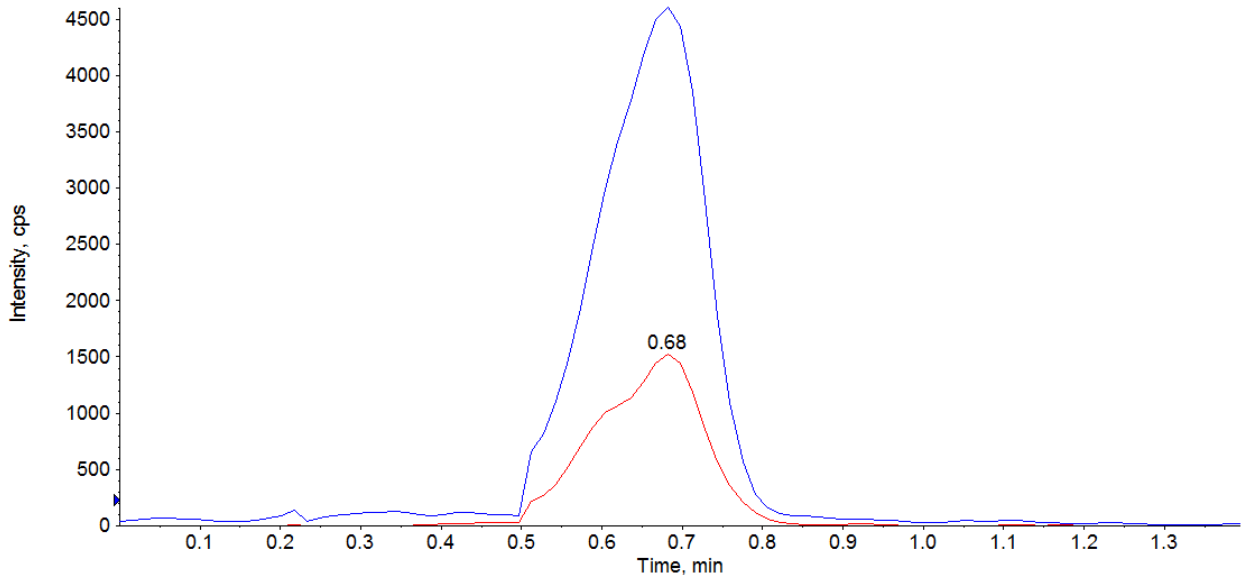

Appendix Figure C.2 FC-LR-MS/MS analysis of 0.500 µM concentration of G16-3 (*m/z* 290 → 86 [blue] & 355 [red]) following an octanol liquid:liquid extraction from PAM212 cell lysate. A 200 µL sample of PAM212 cell lysate was vortexed with 200 µL of octanol and 7.5 µL of the octanol phase was in analyzed using the FC-LR-MS/MS method.

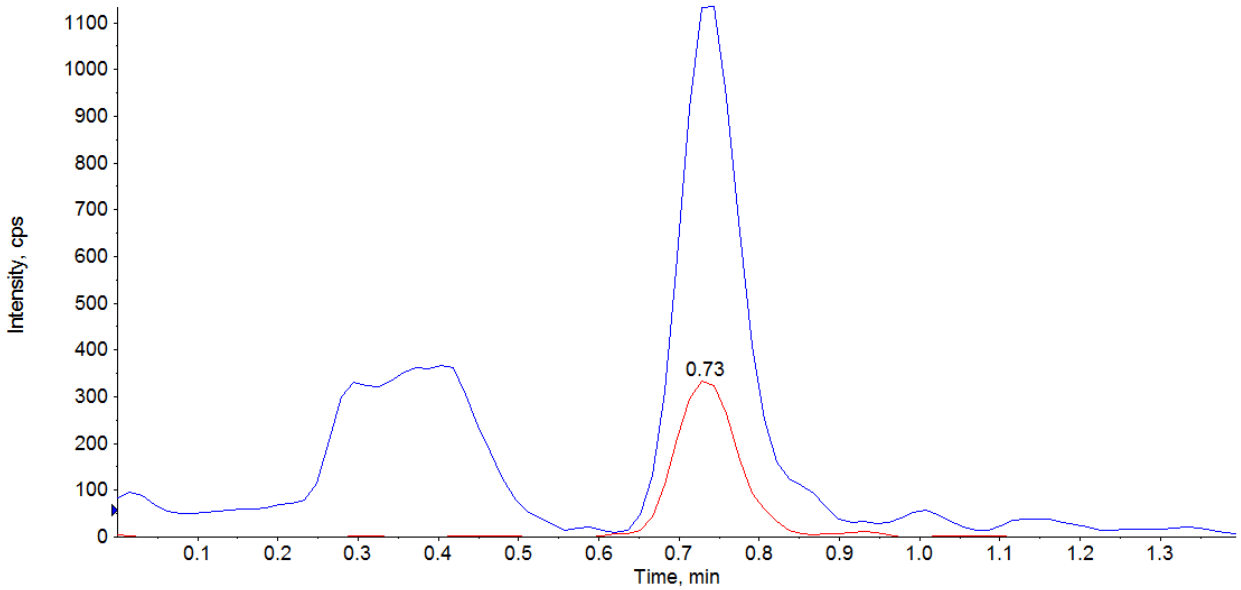

Appendix Figure C.3 FC-LR-MS/MS analysis of 0.500 µM concentration of G16-3 (*m/z* 290 → 86 [blue] & 355 [red]) following a hexane liquid:liquid extraction from PAM212 cell lysate. A 200 µL sample of PAM212 cell lysate was vortexed with 200 µL of hexane. A 175 µL volume of the hexane phase was removed, dried down under nitrogen gas, reconstituted in 175 µL of methanol and 7.5 µL of the methanol phase was analyzed.

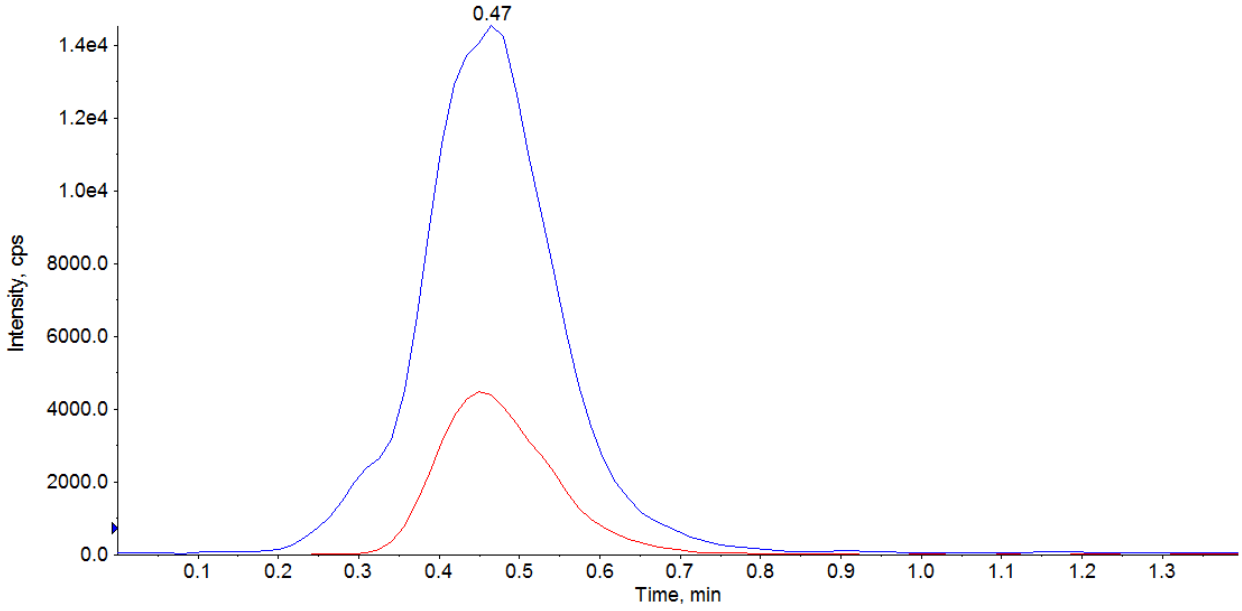

Appendix Figure C.4 FC-LR-MS/MS analysis of 0.500 µM concentration of G16-3 (*m/z* 290 → 86 [blue] & 355 [red]) following a toluene liquid:liquid extraction from PAM212 cell lysate. A 200 µL sample of PAM212 cell lysate was vortexed with 200 µL of tolune. A 175 µL volume of the toluene phase was removed, dried down under nitrogen gas, reconstituted in 175 µL of methanol and 7.5 µL of the methanol phase was analyzed.

APPENDIX D
Supplemental figures for chapter 5

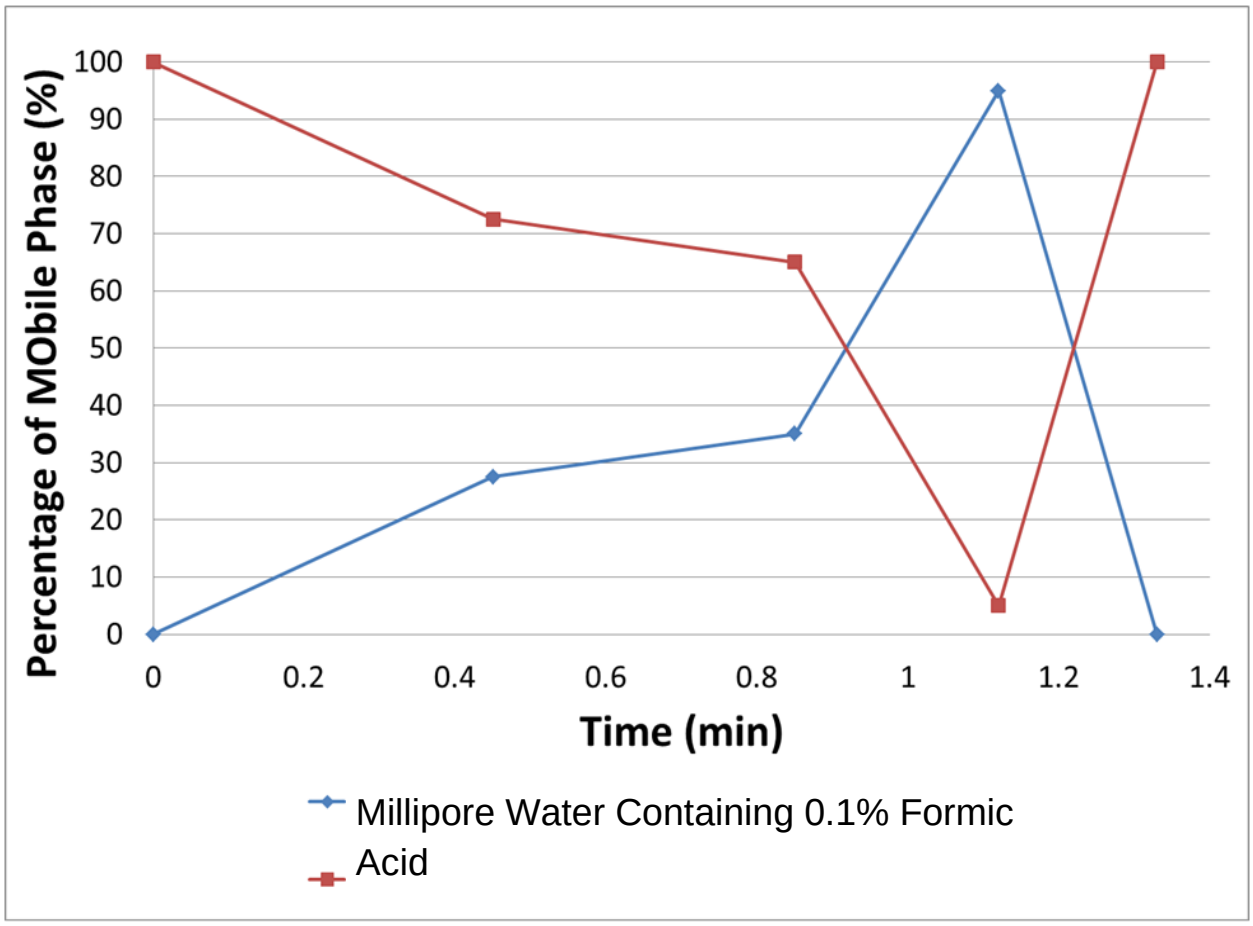

Appendix D Figure 1 Chromatographic conditions utilized for the FC-HR(LR)-MS(/MS) analysis of diquaternary ammonium gemini surfactants, G16-3 and $G16D_{66}$-3

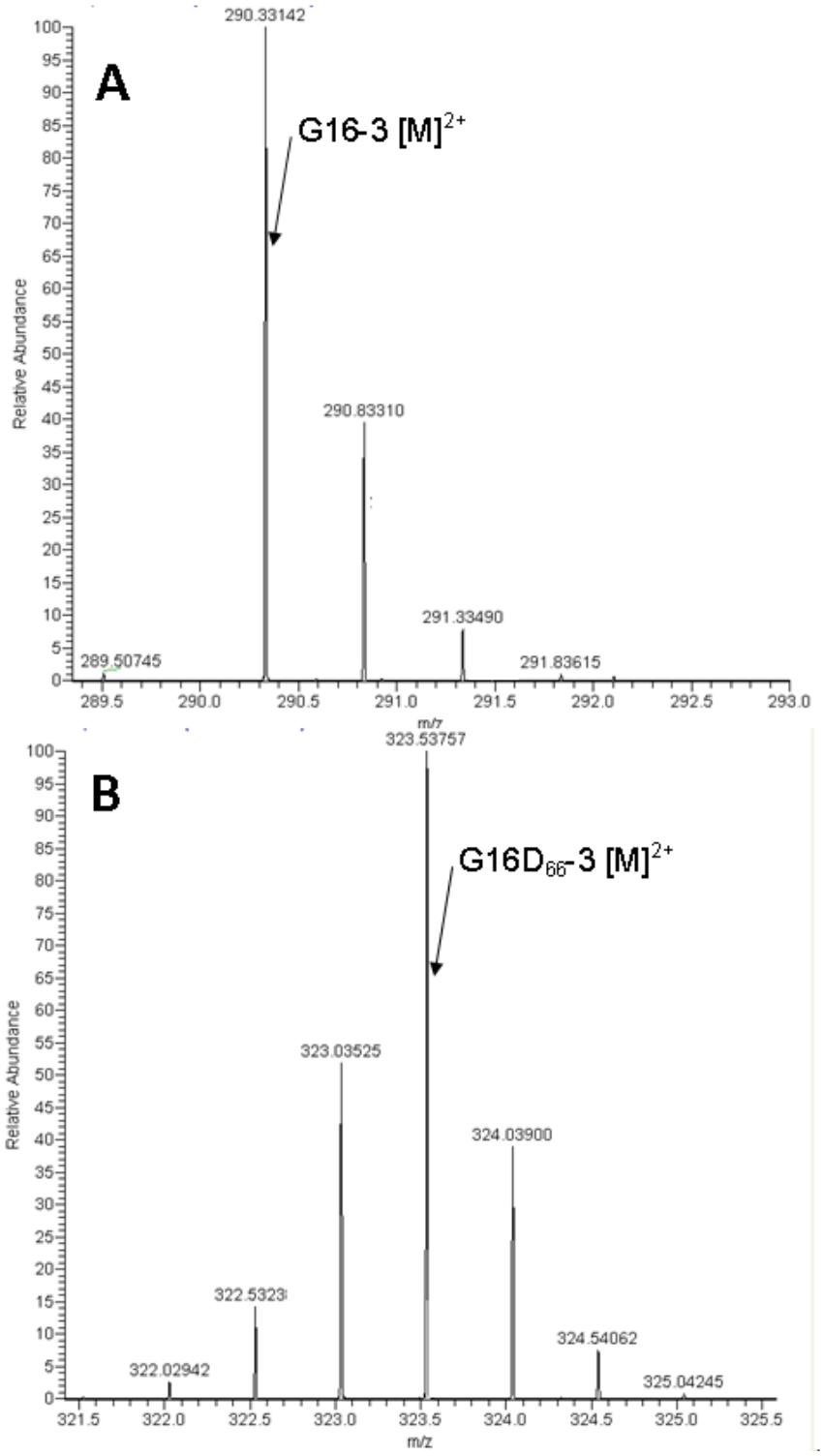

Appendix D Figure 2 Regions of the Thermo Scientific Orbitrap mass spectra that highlight the m/z distribution of G16-3 (A) and $G16D_{66}$-3 (B). Extracted ion chromatographs were obtained for G16-3 by selecting *m/z* of 290.331 (A) and $G16D_{66}$-3 by selecting *m/z* of 323.538 (B).

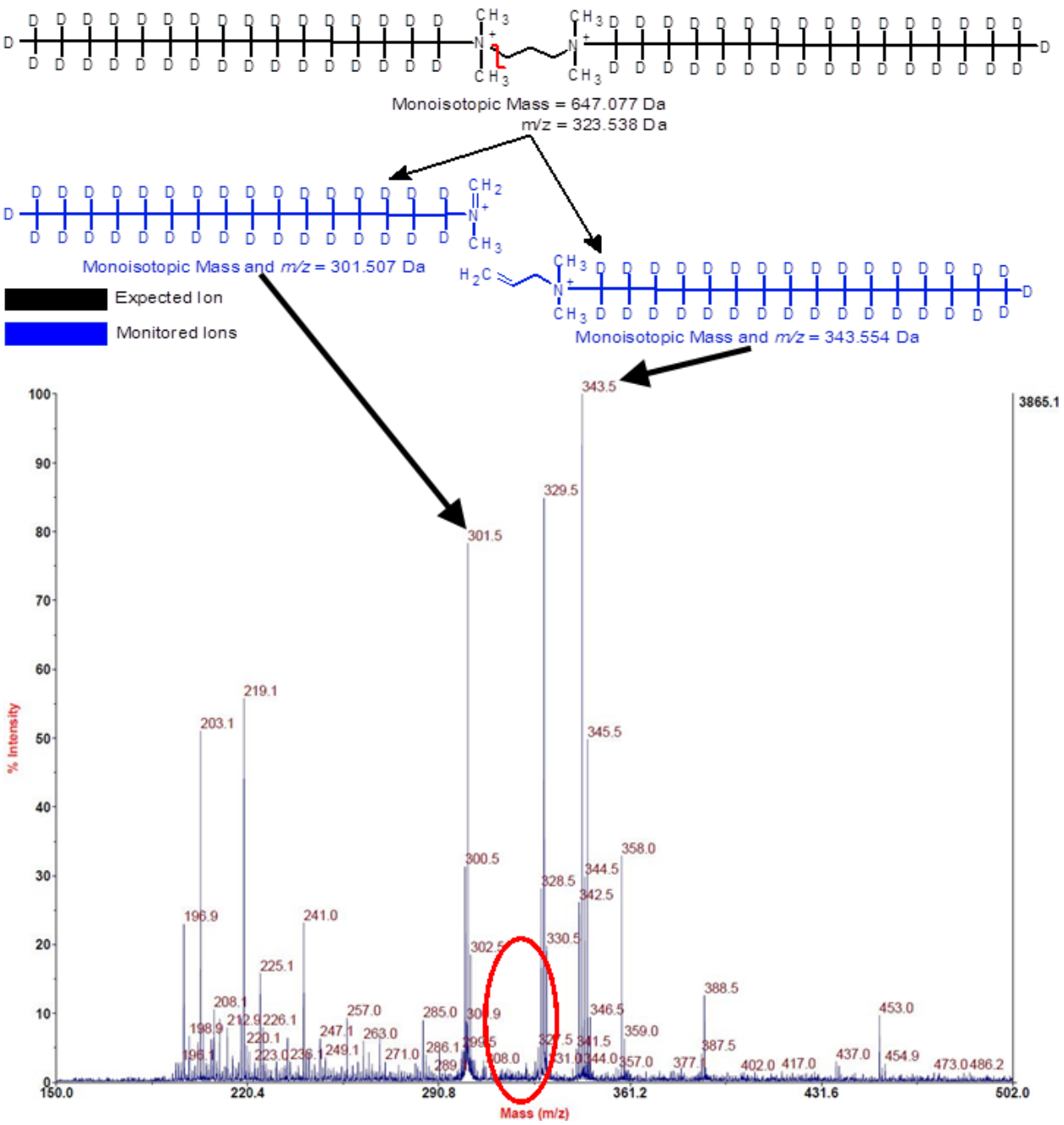

Appendix D Figure 3 Fragmentation of G16D$_{66}$-3 (323.589 *m/z)* into two ions of 343.554 *m/z* and 301.507 *m/z* during MALDI-MS analysis. No precursor ion was observed at the expected *m/z* value for G16D$_{66}$-3 ([M]$^{2+}$ = *m/z* 323.54)

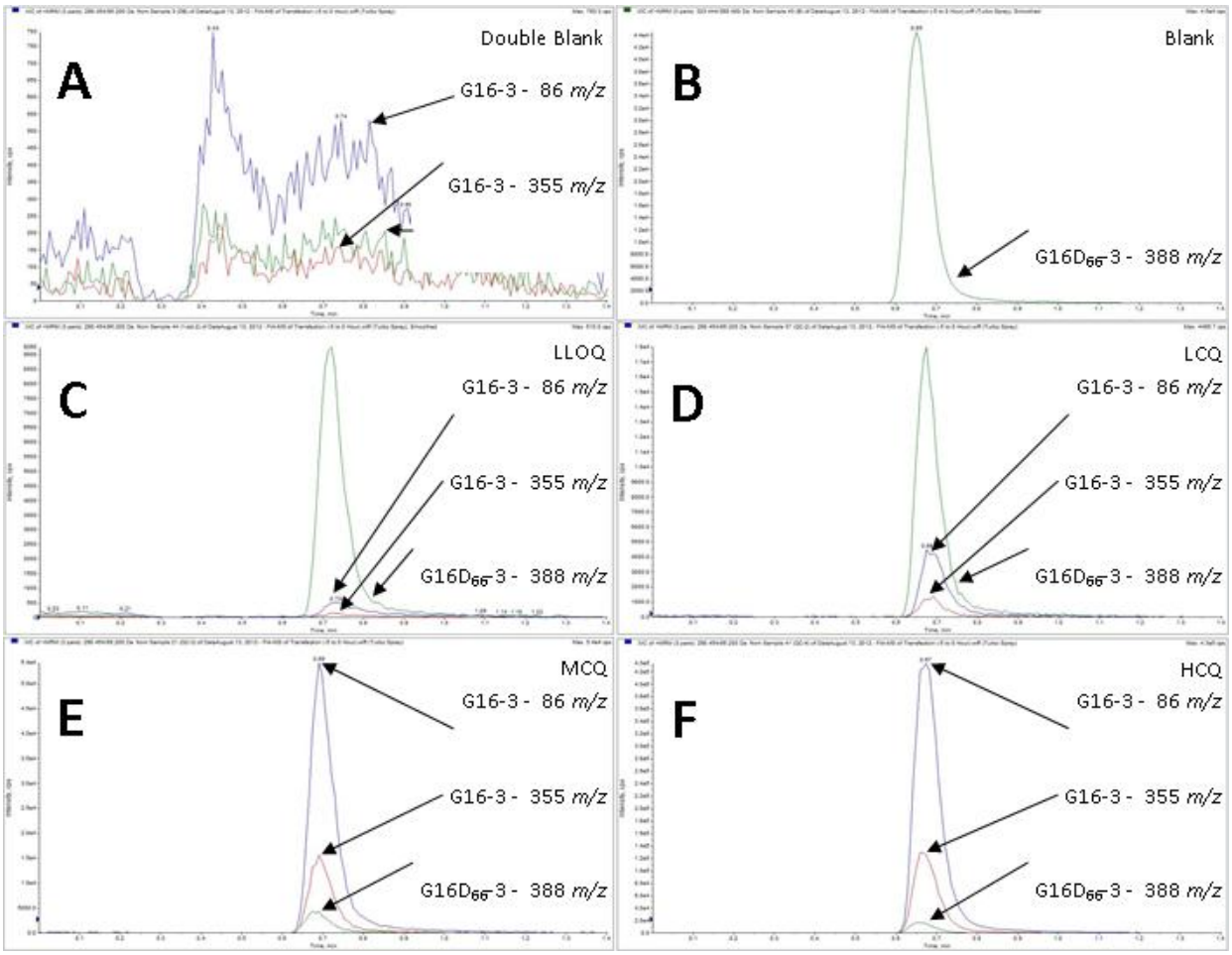

Appendix D Figure 4 During FC-LR-MS/MS analysis a low level of interference was observed within the PAM212 cell lysate for both G16-3 and $G16D_{66}$-3 (A). The internal standard $G16D_{66}$-3 did not interfere with the analysis of G16-3 (B). Representative chromatographs of the LLOQ (C), LCQ (D), MCQ (E) and HLOQ (F) peaks.

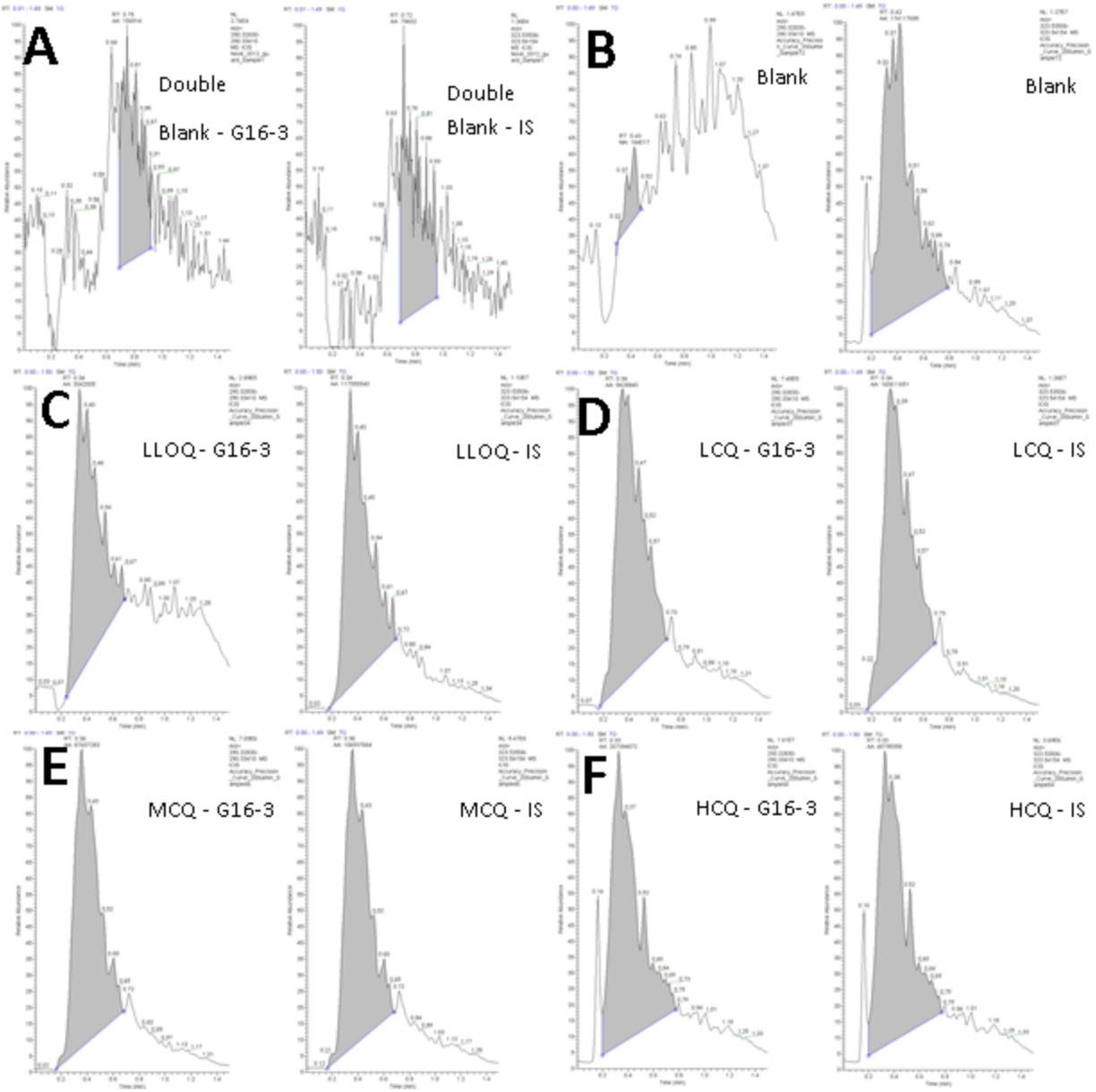

Appendix D Figure 5 Observed interference for both G16-3 ($[M]^{2+}$ = *m/z* 290.33) and $G16D_{66}$-3 ($[M]^{2+}$ = *m/z* 323.54) during FC-HR-MS analysis within the PAM212 cell lysate (A).The internal standard $G16D_{66}$-3 did not interfere with FC-MS analysis of G16-3 (B). Representative chromatographs of the LLOQ (C), LCQ (D), MCQ (E) and HLOQ (F) peaks.

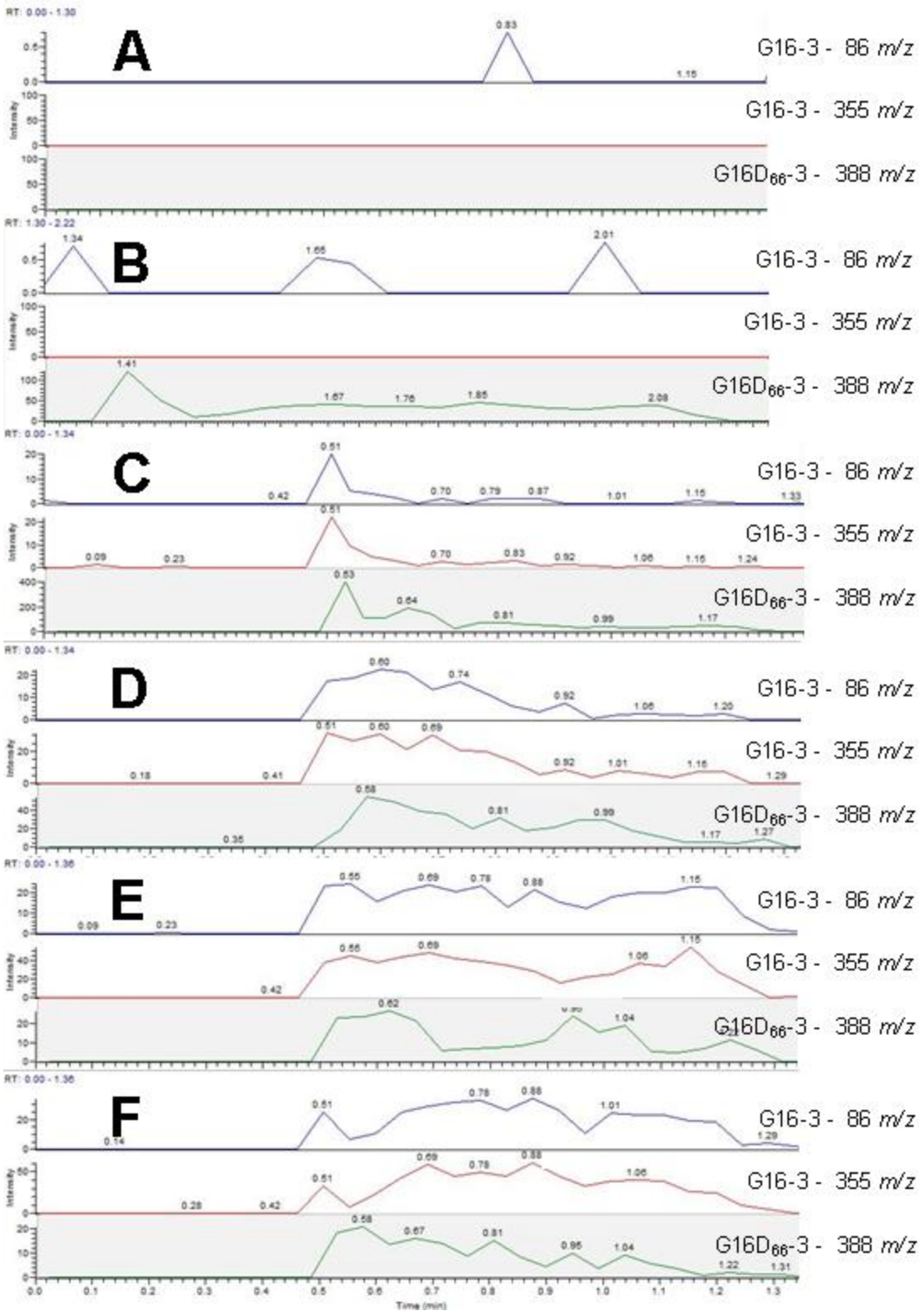

Appendix D Figure 6 During DESI-LR-MS/MS analysis no interference was observed within the PAM212 cell lysate for either G16-3 and $G16D_{66}$-3 (A). The internal standard $G16D_{66}$-3 did not interfere with the analysis of G16-3 (B). Representative chromatographs of the LLOQ (C), LCQ (D), MCQ (E) and HLOQ (F) peaks.

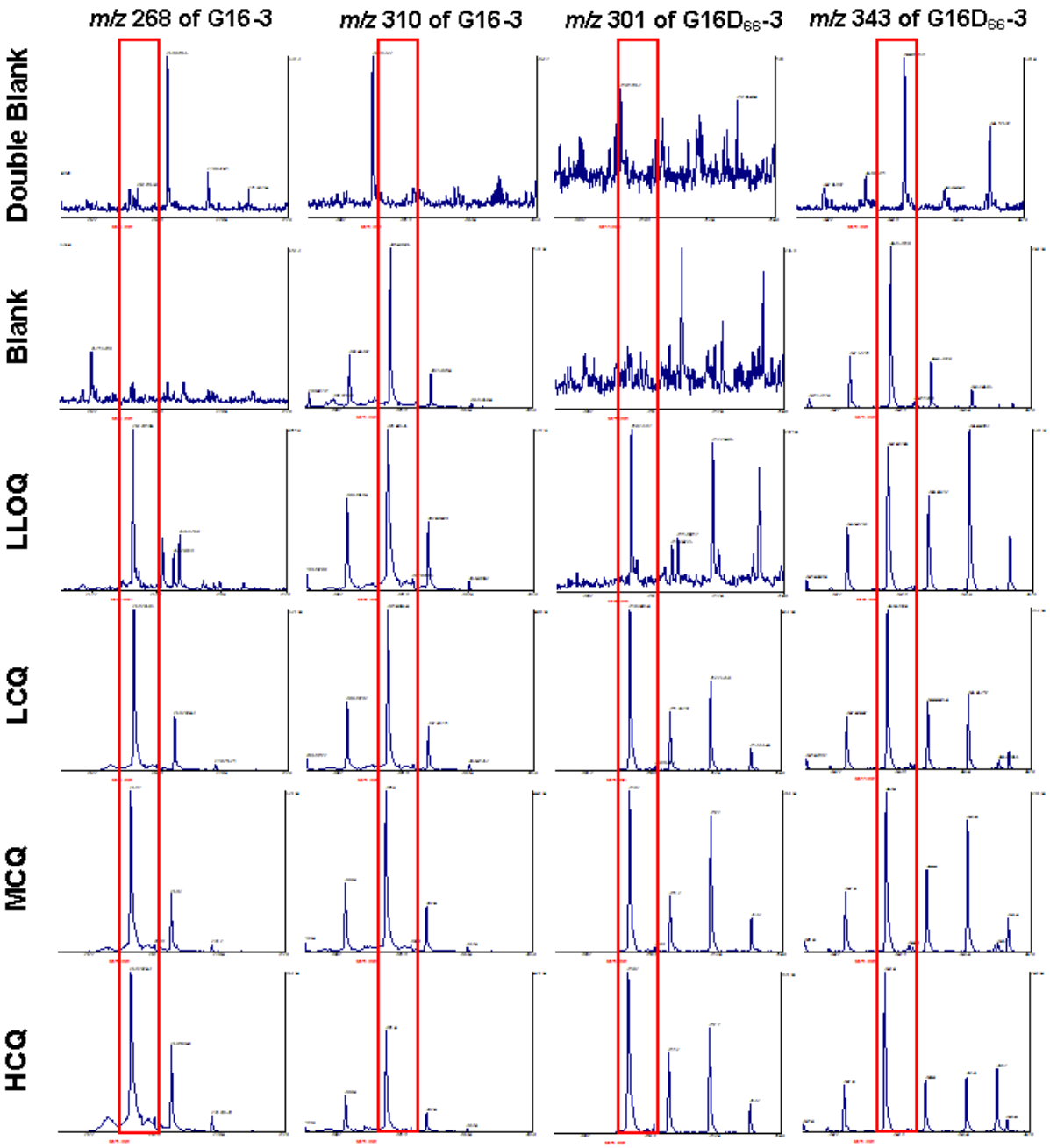

Appendix D Figure 7 MALDI-HR-MS analysis of G16-3 and $G16D_{66}$-3 saw no interference being observed within the PAM212 cell lysate for the double blank samples. The internal standard $G16D_{66}$-3 did not interfere with the analysis of G16-3 within the blank sample. Representative chromatographs of the LLOQ, LCQ, MCQ and HLOQ spectrum peaks which exhibited smooth peak shape and isolation from neighboring peaks.

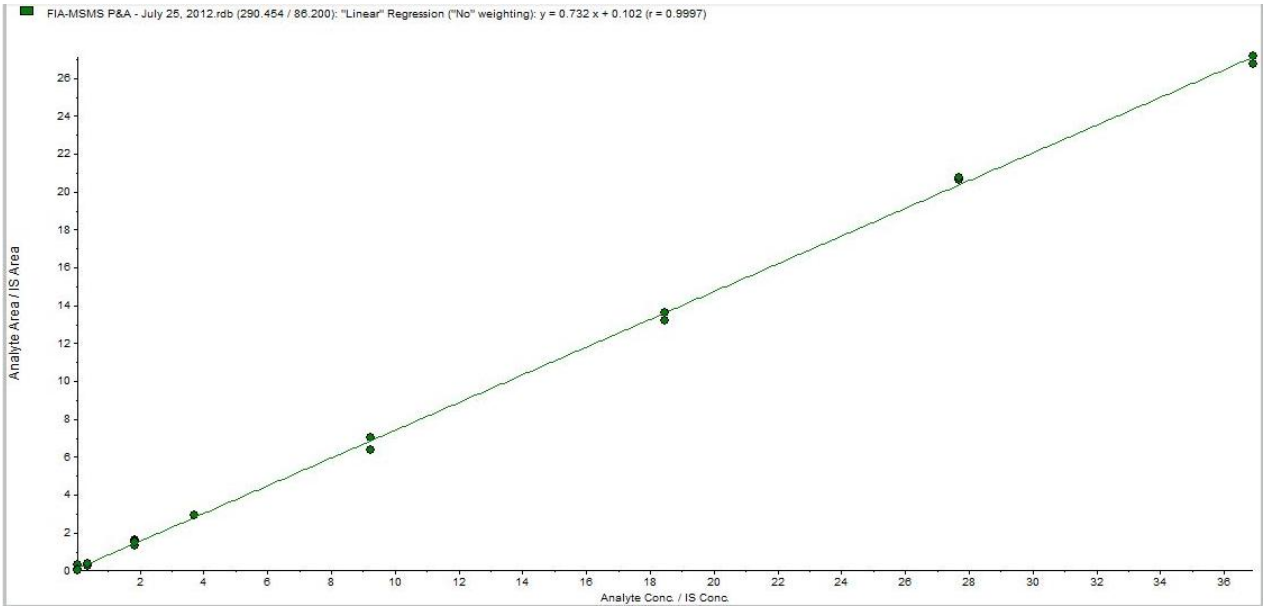

Appendix D Figure 8 Linear range of G16-3 within PAM212 cell lysate was assessed to be between 0.037-37.5 μM for FC-LR-MS/MS using a QTRAP 4000 instrument (G).

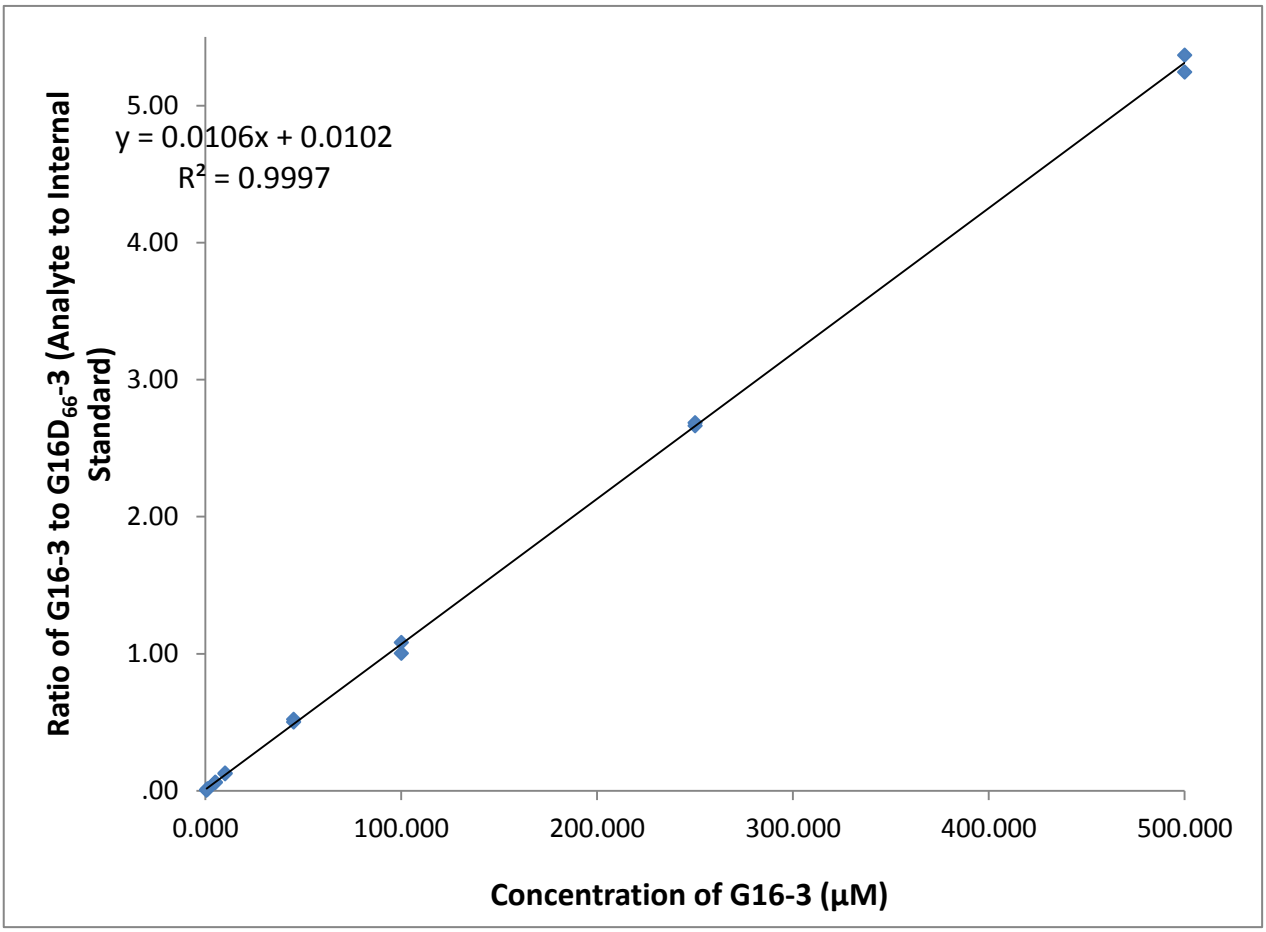

Appendix D Figure 9 Linear range of G16-3 within PAM212 cell lysate was assessed to be between 1.0000-500.00 μM for FC-HR-MS using an LTQ Orbitrap instrument (G).

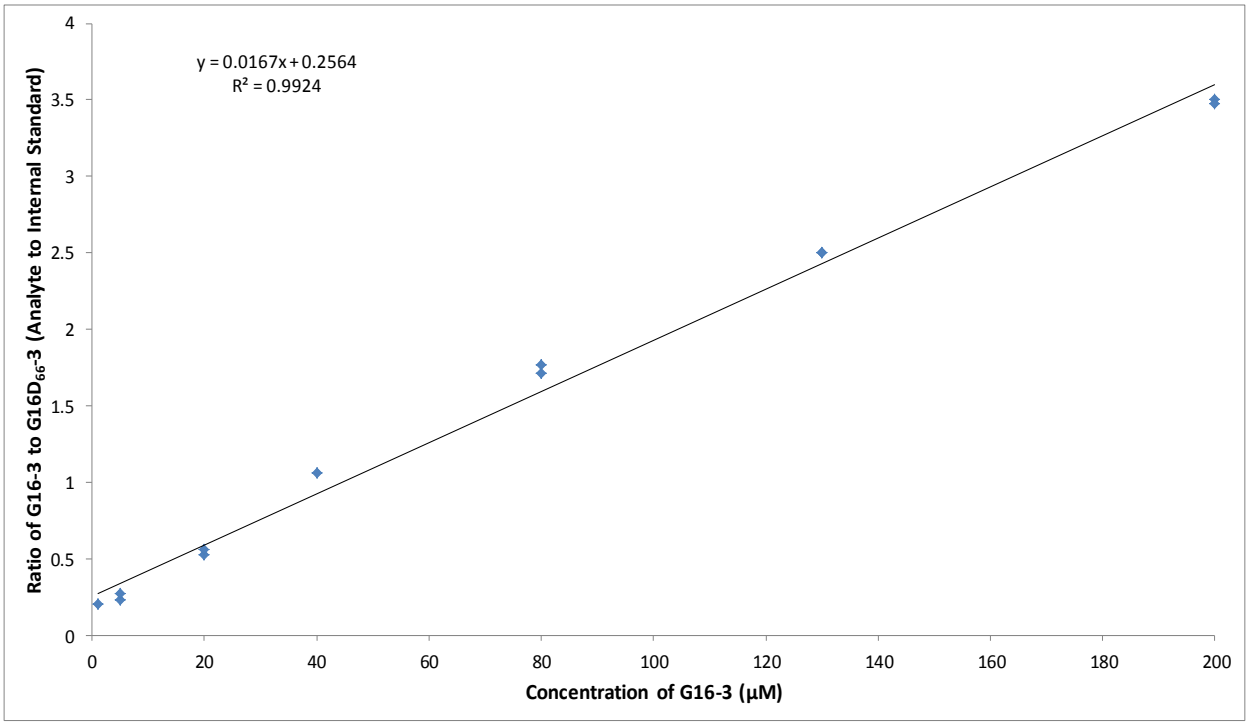

Appendix D Figure 10 Linear range of G16-3 within PAM212 cell lysate was assessed to be between 1.000-2000 µM for DESI-LR-MS/MS using a LCQ Fleet Ion Trap MS^n (G).

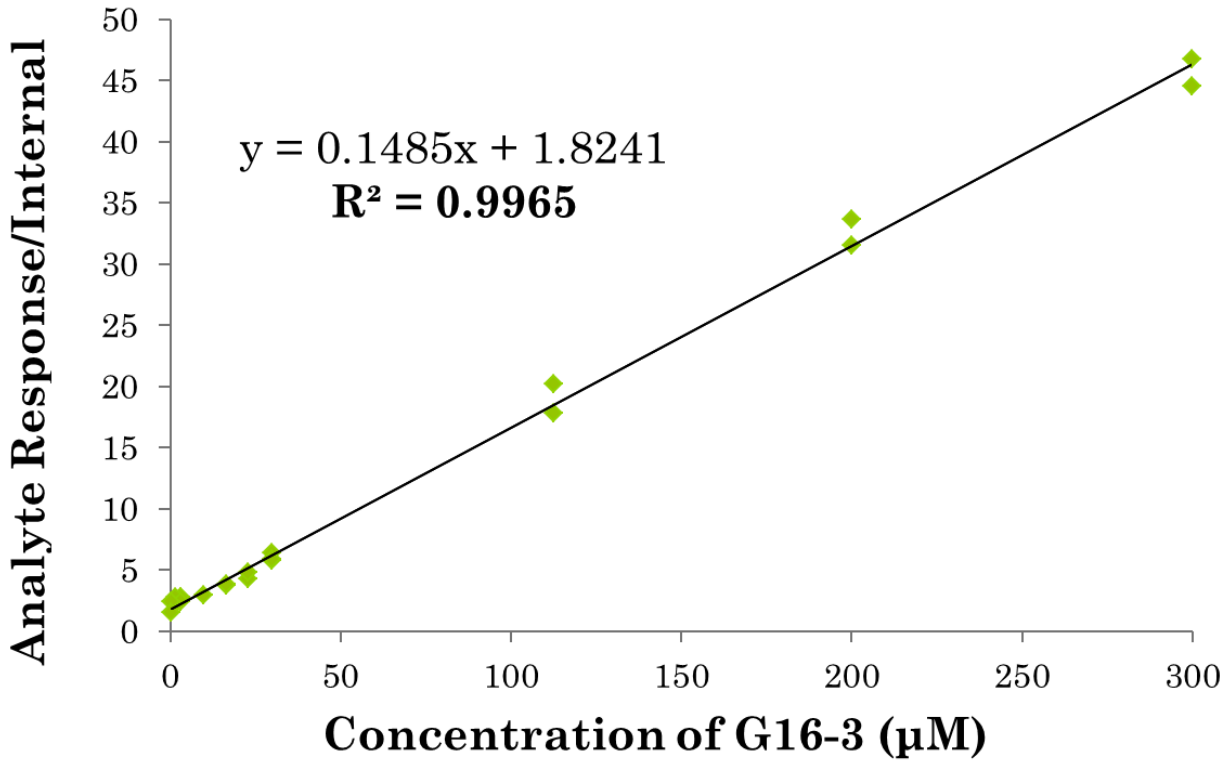

Appendix D Figure 11 Linear range of G16-3 within PAM212 cell lysate was assessed to be between 0.037-37.5 µM for MALDI-HR-MS using a AB Sciex MALDI-ToFToF 4800 instrument.

APPENDIX E
Supplemental table for chapter 5

Appendix E Table 1 Intra-day Assay of Precision and Accuracy for G16-3 using FC-LR-MS/MS in PAM212 Cell Lysate [6 replicates for each analysis day at each concentration]

Quality Control	Analysis Day	Observed Concentration (mean±SD, μM)			Accuracy	Precision
LLQC	1	0.0405	±	0.0099	109.6	18.0
	2	0.0387	±	0.0062	104.5	11.9
	3	0.0409	±	0.0018	109.1	2.6
LQC	1	0.986	±	0.056	98.2	5.6
	2	1.02	±	0.018	102.1	1.6
	3	0.983	±	0.057	98.0	5.8
MQC	1	10.2	±	0.7	101.6	6.5
	2	10.9	±	0.2	108.9	1.9
	3	10.1	±	0.6	100.7	5.6
LQC	1	38.1	±	2.2	95.6	5.7
	2	39.7	±	0.5	98.8	1.5
	3	38.7	±	1.9	96.7	4.8

Appendix E Table 2 Inter-day Assay of Precision and Accuracy for G16-3 using FC-LR-MS/MS in PAM212 Cell Lysate [18 replicates at each concentration]

Quality Control	Observed Concentration (mean±SD, μM)			Accuracy	Precision
LLQC	0.0399	±	0.0054	107.8	10.8
LQC	0.998	±	0.043	99.4	4.4
MQC	10.4	±	0.5	103.7	4.7
HQC	38.9	±	1.5	96.9	4.0

Appendix E Table 3 Intra-day Assay of Precision and Accuracy for G16-3 using FC-HR-MS in PAM212 Cell Lysate [6 replicates for each analysis day at each concentration]

Quality Control	Analysis Day	Observed Concentration (mean±SD, μM)			Accuracy	Precision
LLQC	1	1.08	±	0.096	89.7	8.9
	2	1.05	±	0.145	104.6	13.9
	3	1.11	±	0.063	110.7	5.7
LQC	1	2.56	±	0.11	102.3	4.5
	2	2.69	±	0.30	107.5	11.5
	3	2.68	±	0.21	107.3	7.8
MQC	1	53.2	±	1.3	106.4	2.4
	2	53.9	±	1.2	107.7	2.3
	3	53.7	±	2.2	107.3	4.1
LQC	1	393	±	21	98.3	5.3
	2	356	±	27	89.0	7.6
	3	409	±	16	102.2	4.0

Supplemental Table 4 - Inter-day Assay of Precision and Accuracy for G16-3 using FC-HR-MS in PAM212 Cell Lysate [18 replicates at each concentration]

Quality Control	Observed Concentration (mean±SD, μM)			Accuracy	Precision
LLQC	1.08	±	0.10	101.7	9.5
LQC	2.64	±	0.21	105.7	7.9
MQC	53.6	±	1.6	107.1	2.9
HQC	386	±	21	96.5	5.6

Appendix E Table 5 Intra-day Assay of Precision and Accuracy for G16-3 using DESI-LR-MS/MS in PAM212 Cell Lysate [6 replicates for each analysis day at each concentration]

Quality Control	Analysis Day	Observed Concentration (mean±SD, μM)			Accuracy	Precision
LLQC	1	1.09	±	0.20	108.8	17.9
	2	1.02	±	0.11	102.3	10.7
	3	1.01	±	0.18	97.3	18.2
LQC	1	7.33	±	0.73	97.8	9.9
	2	7.60	±	0.57	96.6	7.4
	3	8.05	±	1.08	110.3	13.4
MQC	1	103	±	5	103.0	4.3
	2	92.1	±	13.2	92.1	14.4
	3	109	±	7	108.7	6.7
LQC	1	183	±	19	101.7	10.1
	2	177	±	6	88.5	3.6
	3	180	±	8	99.0	4.6

Appendix E Table 6 Inter-day Assay of Precision and Accuracy for G16-3 using DESI-LR-MS/MS in PAM212 Cell Lysate [18 replicates at each concentration]

Quality Control	Observed Concentration (mean±SD, μM)			Accuracy	Precision
LLQC	1.04	±	0.17	102.8	15.6
LQC	7.66	±	0.75	101.6	10.2
MQC	101	±	10	101.5	8.5
HQC	180	±	11	96.4	6.1

Appendix E Table 7 Intra-day Assay of Precision and Accuracy for G16-3 using MALDI-HR-MS in PAM212 Cell Lysate [6 replicates for each analysis day at each concentration]

Quality Control	Analysis Day	Observed Concentration (mean±SD, μM)			Accuracy	Precision
LLQC	1	0.445	±	0.031	111.2	7.1
	2	0.395	±	0.023	98.5	5.9
	3	0.410	±	0.075	100.8	18.5
LQC	1	27.5	±	1.0	98.9	3.5
	2	26.7	±	3.2	97.1	12.1
	3	30.7	±	2.1	111.5	6.7
MQC	1	150	±	6	100.0	4.1
	2	153	±	10.	85.4	6.5
	3	146	±	6	97.6	4.2
LQC	1	382	±	21	99.4	5.6
	2	395	±	19	97.4	4.7
	3	411	±	21	107.0	5.2

Appendix E Table 6 Inter-day Assay of Precision and Accuracy for G16-3 using MALDI-HR-MS in PAM212 Cell Lysate [18 replicates at each concentration]

Quality Control	Observed Concentration (mean±SD, μM)			Accuracy	Precision
LLQC	0.414	±	0.035	103.5	10.5
LQC	28.3	±	2.1	102.5	7.5
MQC	150.	±	7	94.4	4.9
HQC	396	±	21	101.3	5.2

Appendix E Table 9 Precision and Accuracy for 24 Hour Stability Assay (25 °C) of G16-3 in PAM212 Cell Lysate [6 replicates at each concentration]

Quality Control	Analysis Type	Observed Concentration (mean±SD, µM)			Accuracy	Precision
FC-LR-MS/MS	LQC	1.07	±	0.14	106.4	13.0
	MQC	10.6	±	0.6	105.2	5.3
	HQC	37.8	±	0.7	94.4	2.1
FC-HR-MS	LQC	2.34	±	0.17	93.7	7.3
	MQC	53.1	±	0.1	106.2	1.1
	HQC	406	±	20	101.4	4.8
DESI-LR-MS/MS	LQC	8.06	±	0.60	107.5	7.4
	MQC	96.5	±	3.6	96.5	3.8
	HQC	184	±	18	102.4	9.7
MALDI-HR-MS	LQC	27.3	±	1.7	99.2	6.4
	MQC	144	±	8	95.8	5.5
	HQC	374	±	4	97.4	1.1

Appendix E Table 10 Precision and Accuracy for 24 Hour Stability Assay (4 °C) of G16-3 in PAM212 Cell Lysate [6 replicates at each concentration]

Quality Control	Analysis Type	Observed Concentration (mean±SD, µM)			Accuracy	Precision
FC-HR-MS	LQC	2.40	±	0.21	96.2	8.8
	MQC	53.3	±	2.3	106.6	4.3
	HQC	424	±	14	105.9	3.4

Appendix E Table 11 Precision and Accuracy for Freeze Thaw Stability Assay of G16-3 in PAM212 Cell Lysate [6 replicates at each concentration]

Quality Control	Analysis Type	Observed Concentration (mean±SD, µM)			Accuracy	Precision
FC-LR-MS/MS	LQC	1.15	±	0.11	114.2	9.4
	MQC	10.9	±	0.2	109	2
	HQC	38.9	±	0.8	97.1	2
FC-HR-MS	LQC	2.60	±	0.07	104.1	2.9
	MQC	53.5	±	1.3	106.9	2.5
	HQC	380.	±	16	95.1	4.3
DESI-LR-MS/MS	LQC	7.36	±	0.61	91.6	8.2
	MQC	95.5	±	11.6	95.5	12.2
	HQC	175	±	12	97.2	7
MALDI-HR-MS	LQC	26.2	±	3.4	97.9	12.8
	MQC	142	±	2.2	96.6	1.5
	HQC	384	±	5.3	100.0	1.4

Appendix E Table 12 Precision and Accuracy for 60 Day Stability (-20 °C) Assay of G16-3 in PAM212 Cell Lysate [6 replicates at each concentration]

Quality Control	Analysis Type	Observed Concentration (mean±SD, µM)			Accuracy	Precision
FC-LR-MS/MS	LQC	1.01	±	0.02	100.2	2.2
	MQC	10.1	±	0.3	101	2.8
	HQC	41.3	±	1.2	103.1	3
FC-HR-MS	LQC	2.53	±	0.15	101.3	5.8
	MQC	52.1	±	1.0	104.2	1.8
	HQC	395	±	15	95.7	3.9
DESI-LR-MS/MS	LQC	7.21	±	0.34	96.1	4.7
	MQC	106	±	5	102.9	4.3
	HQC	182	±	8	101	4.4

Appendix E Table 13 Precision and Accuracy for 60 Day Stability (25 °C) Assay of G16-3 in PAM212 Cell Lysate [6 replicates at each concentration]

Quality Control	Analysis Type	Observed Concentration (mean±SD, μM)			Accuracy	Precision
FC-LR-MS/MS	LQC	1.09	±	.14	108.7	9.6
	MQC	10.8	±	0.9	106.7	7.6
	HQC	39.2	±	2.0	97.9	5.1
MALDI-HR-MS	LQC	27.3	±	1.4	99.2	5.2
	MQC	148	±	5	98.4	3.4
	HQC	410.	±	18	106.69	4.5

APPENDIX F

Evaluation of fast liquid chromatography High-field asymmetric waveform ion mobility spectrometry tandem mass spectrometry for the quantification of G16-3

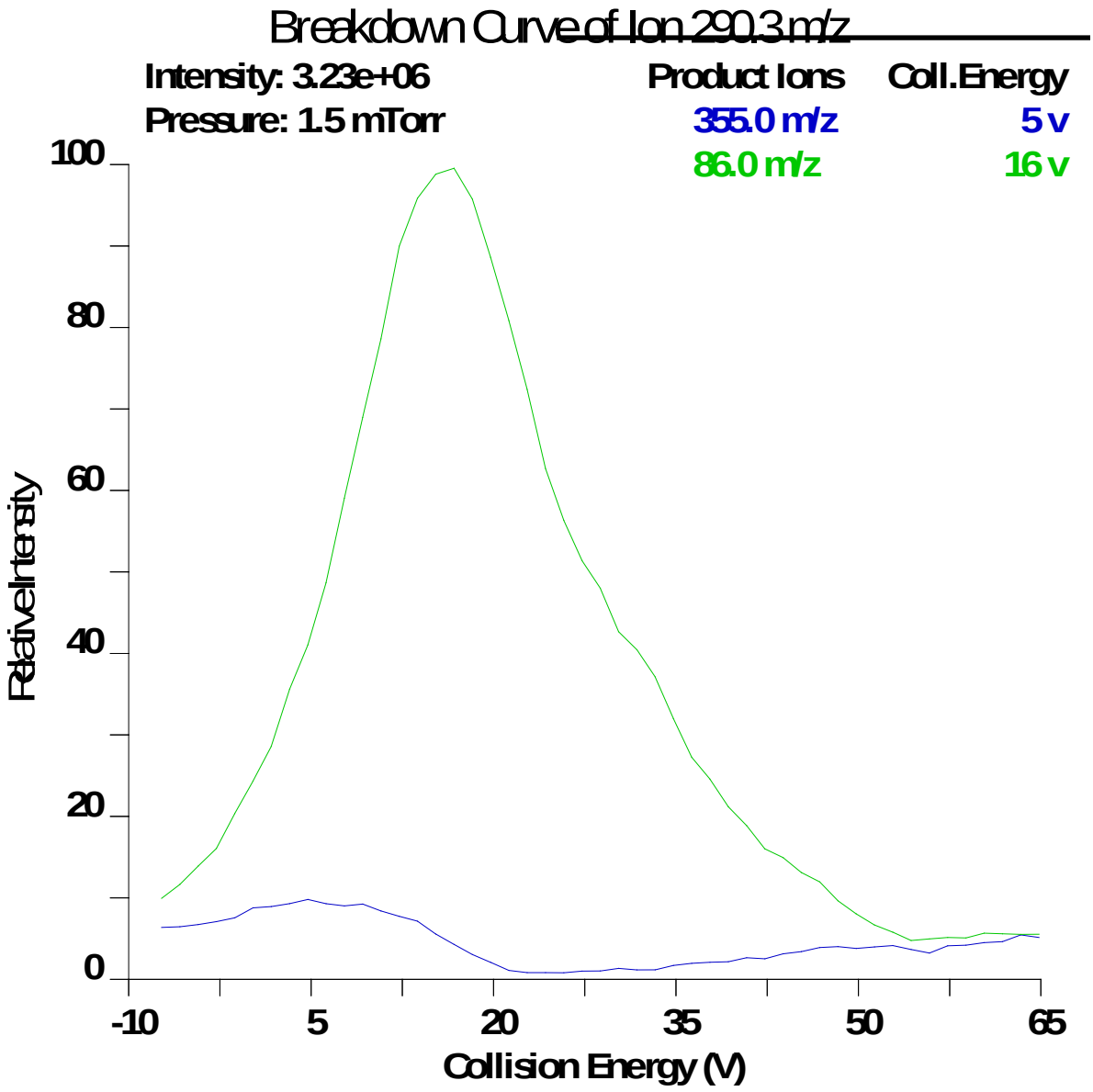

Appendix F Figure 1 Optimization of ESI and MS/MS parameters for G16-3 on a Thermo Scientific TSQ Quantum MS instrument resulted in a spray needle voltage of +5 V and collision energies of 5 V (*m/z* 290 → *m/z* 355*)* and 16 V (*m/z* 290 → *m/z* 86*)*

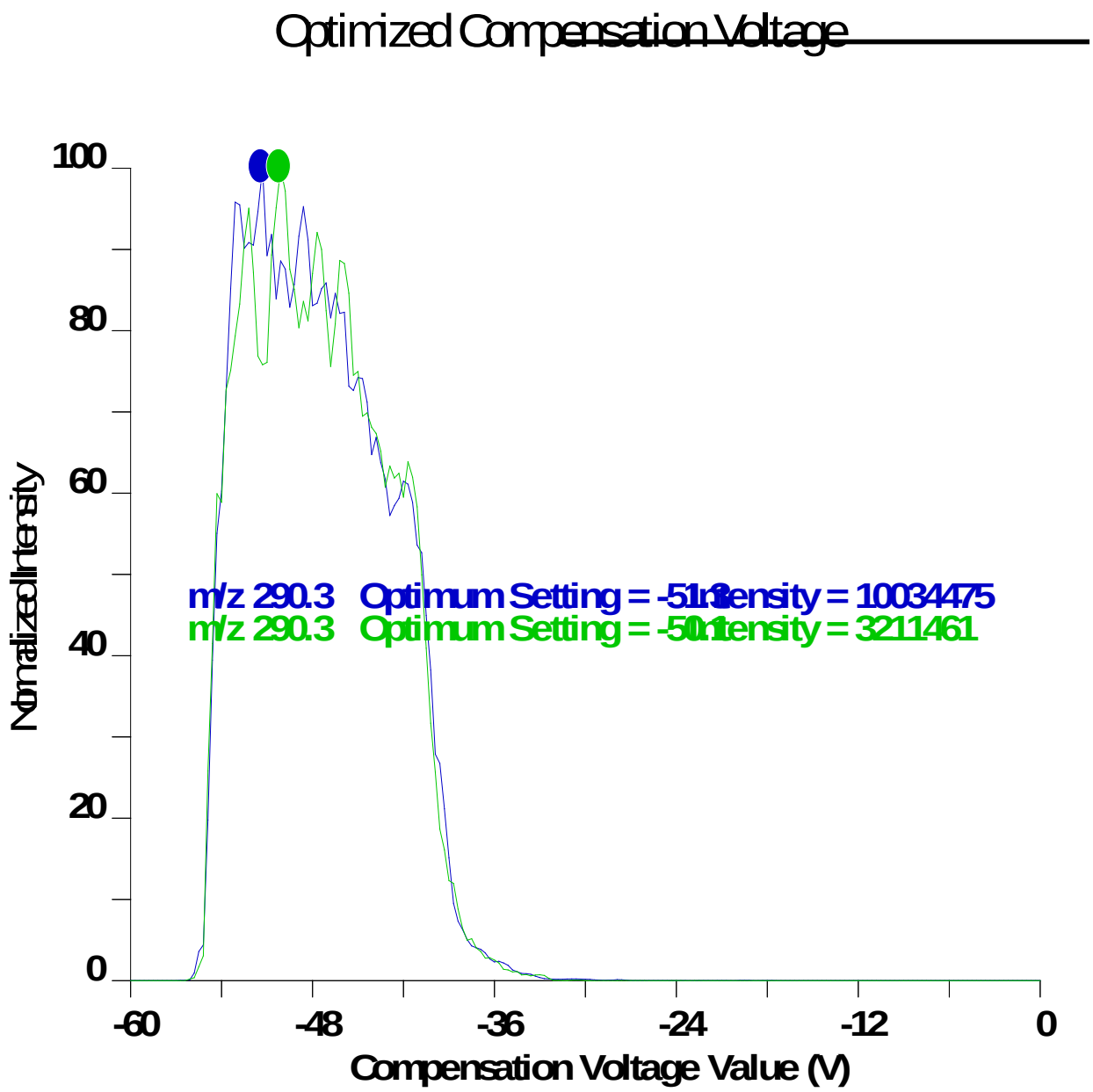

Appendix F Figure 2 Optimization of FAIMS parameters for the analysis of G16-3 on a FAIMS Thermo Scientific TSQ Quantum MS instrument applied a dispersion voltage of -5000V and spray voltage of 4000V in an environment of 50% helium; no dopant was utilized. Compensation voltages were assessed as -51 V (*m/z* 290 → *m/z* 355*)* and -50 V (*m/z* 290 → *m/z* 86*)*

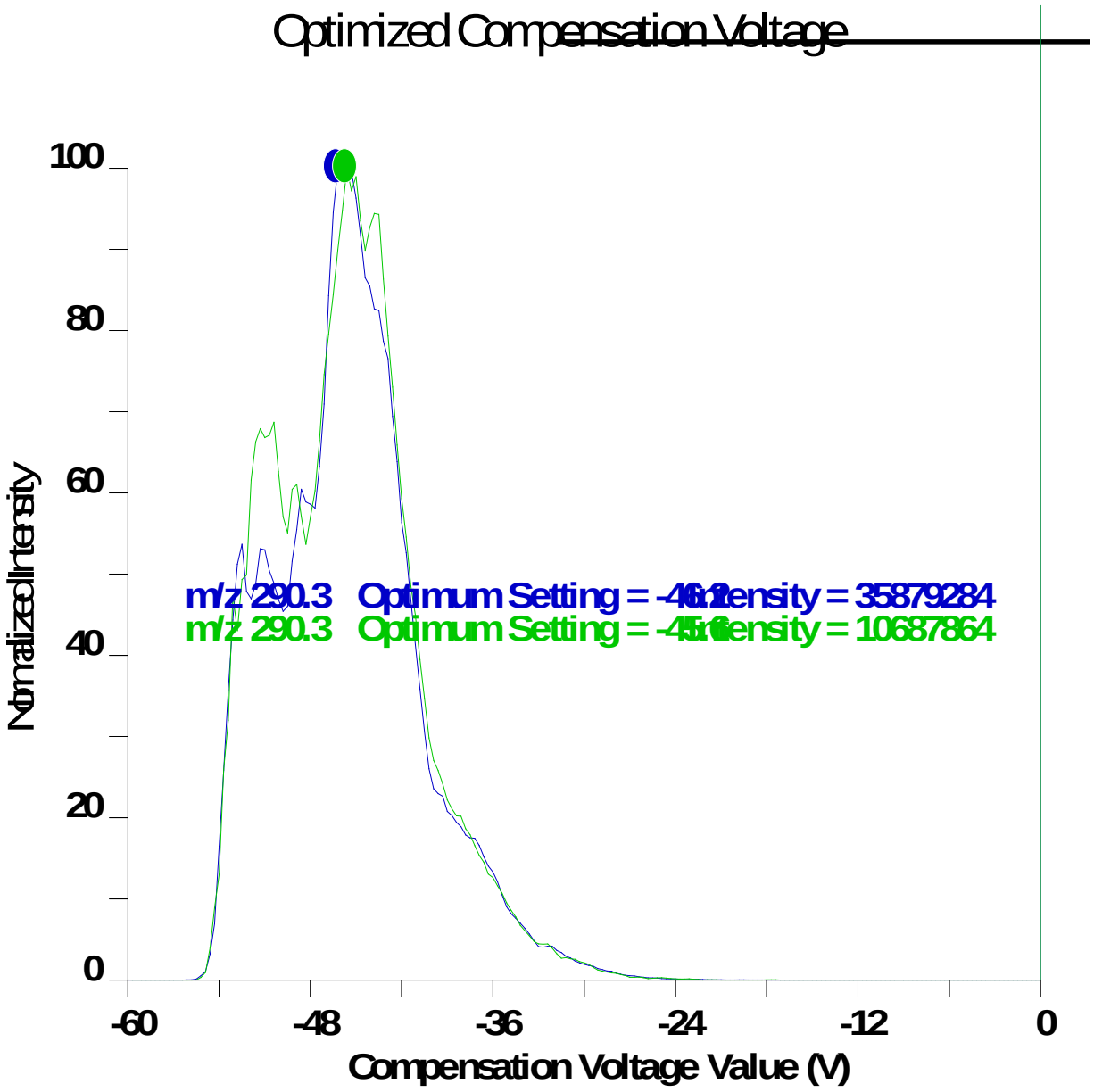

Appendix F Figure 3 Optimization of FAIMS parameters for the analysis of G16-3 on a FAIMS Thermo Scientific TSQ Quantum MS instrument applied a dispersion voltage of -5000V and spray voltage of 4200V in an environment of 50% helium; no dopant was utilized. Compensation voltages were assessed as -51 V (*m/z* 290 → *m/z* 355*)* and -50 V (*m/z* 290 → *m/z* 86*)*

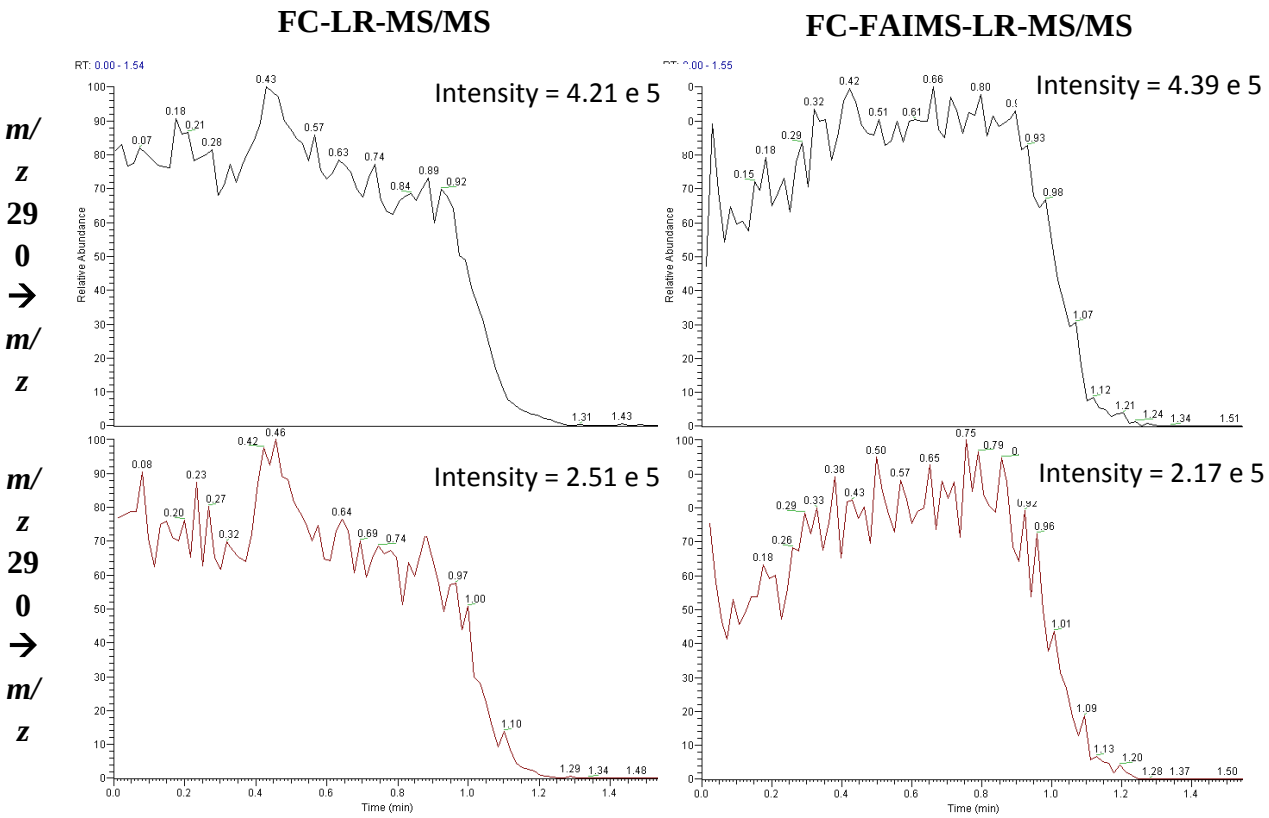

Appendix F Figure 4 A comparison of FC-LR-MS/MS and FC-FAIMS-LR-MS/MS analysis of blank PAM212 cellular lysate. The profiles and intensities of the chromatographs for both FC-LR-MS/MS and FC-FAIMS-LR-MS/MS are similar to one another.

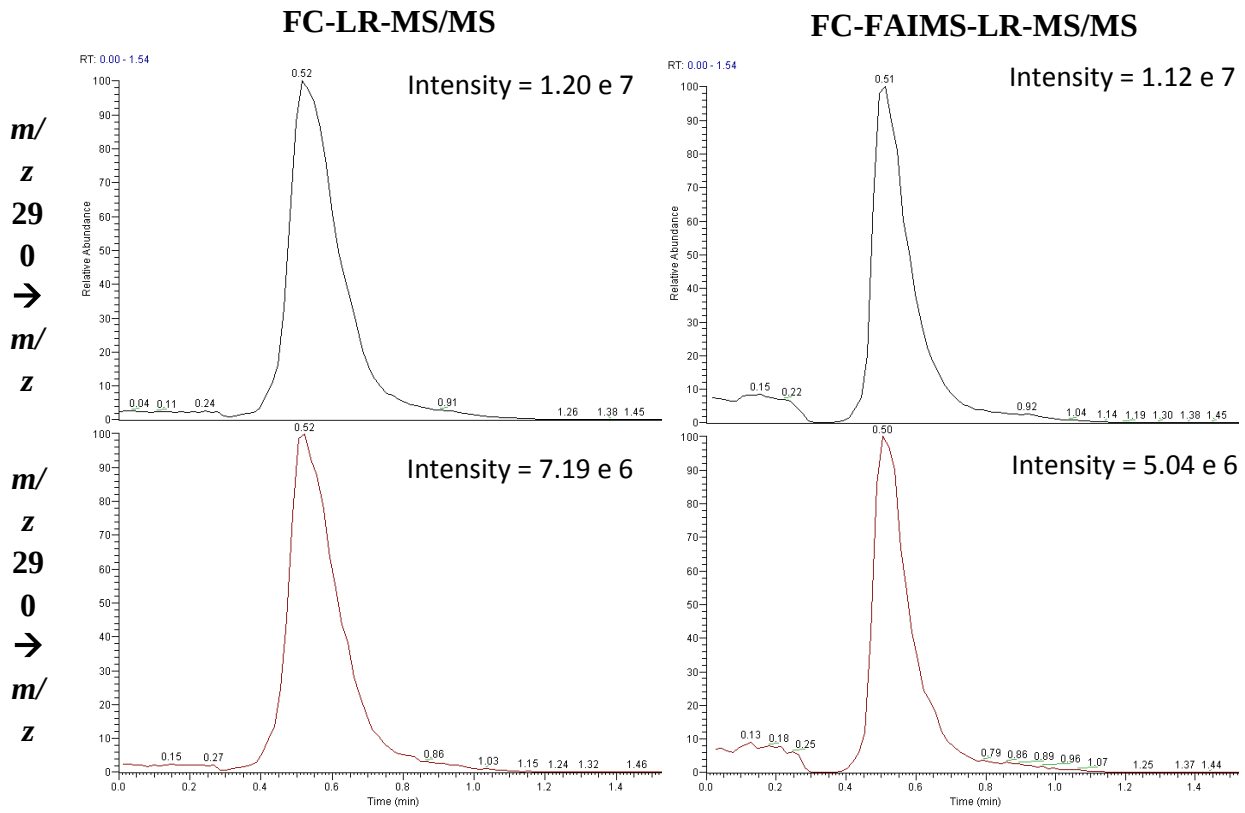

Appendix F Figure 4 A comparison of FC-LR-MS/MS and FC-FAIMS-LR-MS/MS analysis of PAM212 cellular lysate spiked with 200 µM G16-3. The profiles and intensities of the chromatographs for both FC-LR-MS/MS and FC-FAIMS-LR-MS/MS are similar to one another.

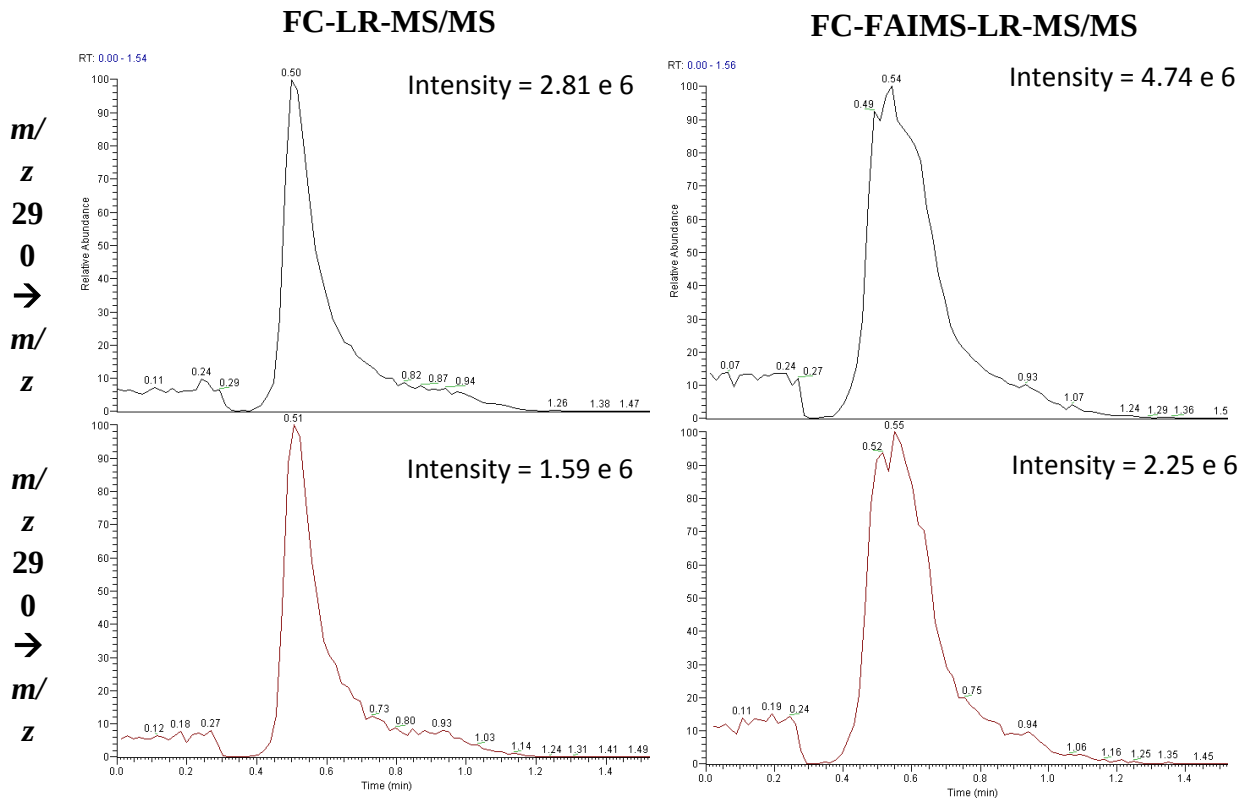

Appendix F Figure 4 A comparison of FC-LR-MS/MS and FC-FAIMS-LR-MS/MS analysis of PAM212 cellular lysate spiked with 200 nM G16-3. The profiles and intensities of the chromatographs for both FC-LR-MS/MS and FC-FAIMS-LR-MS/MS are similar to one another.